Isolation and Characterisation of Novel Glycosaminoglycan-like Polysaccharides Derived from Marine Molluscs with Antiproliferative activity

Abdullah Faisal K Aldairi

Submitted in Partial Fulfilment of the requirements for the Degree of Doctor of Philosophy

School of Environment and Life Sciences
University of Salford, Manchester, UK

2019

Contents

List of figures

List of tables

Abbreviations

2D	Two-dimension
ALL	Acute lymphoid leukaemia
AML	Acute myeloid leukaemia
AS	Acharan sulphate
Asn	Asparagine
B-ALL	B-lymphocyte acute lymphoblastic leukaemia
B-cell	B-lymphocyte
B-DNF	Brain-derived neurotrophic factor
BSA	Bovine serum albumin
CD	Cluster of differentiation
CDK	Cyclin dependent kinase
CE	Crude extract
CLL	Chronic lymphoid leukaemia
cm	Centimeter
CML	Chronic myeloid leukaemia
COSY	Correlation spectroscopy
CS	Chondroitin sulphate
CS-A	Chondroitin sulphate-A
CS-B	Chondroitin sulphate-B
CS-C	Chondroitin sulphate-C
CS-D	Chondroitin sulphate-D
CS-E	Chondroitin sulphate-E
CS-K	Chondroitin sulphate-K
CS-L	Chondroitin sulphate-L
CS-M	Chondroitin sulphate-M
CSPG	Chondroitin sulphate proteoglycan
D-	Dextro-rotary
DBA	Dibutylamine

DEAE	Diethylaminoethanol
DMSO	Dimethyl sulfoxide
DNA	Deoxyribonucleic acid
Dolichol-P	Dolichol-phosphate
DS	Dermatan sulphate
ECM	Extracellular matrix
EDTA	Ethylenediaminetetraacetic acid
EMA	European Medicines Agency
ER	Endoplasmic reticulum
EXTL-1	Exostosin-like-1
EXTL-2	Exostosin-like-2
EXTL-3	Exostosin-like-3
F1	Fraction 1
F2	Fraction 2
F3	Fraction 3
F4	Fraction 4
F5	Fraction 5
F6	Fraction 6
FBS	Foetal bovina serum
FDA	Food and drug administration
FGF	Fibroblast growth factor
FGFR	Fibroblast growth factor receptor
FITC	Fluorescein isothiocyanate
FPLC	Fast performance liquid chromatography
FT-IR	Fourier transform infrared spectroscopy
Fuc	Fucose
Fuc*p*	Fucopyranose
G_1	Growth phase $_1$
G_2	Growth phase $_2$
GAG	Glycosaminoglycan
Gal	Galactose
GalA	Galacturonic acid

GalNAc	N-acetylated-galactosamine
$GalNH_2$	Galactosamine
GC-MS	Gas chromatography coupled with mass spectrometry
GDP	Guanosine diphosphate
Glc	Glucose
GlcA	Glucuronic acid
GlcNAc	N-acetyle-glucosamine
GlcNAcT-I	N-acetyl-glucosaminyl-transferase-I
GlcNAcT-II	N-acetyl-glucosaminyl-transferase-II
GlcNAcT-IV	N-acetyl-glucosaminyl-transferase-IV
GlcNAcT-IX	N-acetyl-glucosaminyl-transferase-IX
GlcNAcT-V	N-acetyl-glucosaminyl-transferase-V
GlcNAcT-Vb	N-acetyl-glucosaminyl-transferase-Vb
GlcNAcT-VI	N-acetyl-glucosaminyl-transferase-VI
$GlcNH_2$	Glucosamine
GRIL	Glycan reductive isotope labelling
GPI	Glycosylphosphatidylinositol
h	Hour
HA	Hyaluronan
HAS	Hyaluronan synthase
HAS-A	Hyaluronan-synthase-A
HAS-B	Hyaluronan-synthase-B
HAS-C	Hyaluronan-synthase-C
HAS-D	Hyaluronan-synthase-D
HSC	Hematopoietic stem cells
Hexose	Monosaccharide with six-carbons
HIF	Hypoxia induced transcription factor
HPAEC-PAD	High-pH anion-exchange chromatography coupled with pulsed amperometric detection
HS	Heparan sulphate
HSPG	Heparan sulphate proteoglycan
HSQC	Heteronuclear single quantum correlation

Hyal-1	Hyaluronidase -1
Hyal-2	Hyaluronidase-2
Hyal-3	Hyaluronidase-3
IC_{50}	Half maximal inhibitory concentration
IdoA	Iduronic acid
IU	International unit
kDa	Kilo-dalton
KS	Keratan sulphate
KSPG	Keratan sulphate proteoglycan
L-	Levo-rotary
LC-MS	Liquid Chromatography coupled with mass spectrometry
M	Molar
Man	Mannose
Mg	Milligram
MHz	Megahertz
Min	Minutes
mIU	Milli international unit
mL	Milliliter
mm	Millimeter
mM	Millimolar
MWCO	Molecular weight cut-off
NA	N-acetylated
NaCl	Sodium chloride
NADP	Nicotinamide adenine dinucleotide phosphate
NaOAc	Sodium acetate
NaOH	Sodium hydroxide
nM	Nanomolar
NMR	Nuclear magnetic resonance spectroscopy
NS	N-sulphated
^{o}C	Degree Celsius
OST	Oligosaccharide transferase
P	Phosphate group

PAPS	3’-Phosphoadenosine 5’-Phosphosulfate
PBS	Phosphate buffer saline
PDGF	Platelet derived growth factor
PE	Purified extract
PEF-1	Purified extract fraction-1
PEF-2	Purified extract fraction-2
Pentose	Monosaccharide with 5-carbon
PG	Proteoglycan
PI	Propidium iodide
pmol	Picomole
r-ER	Rough Endoplasmic reticulum
RHAMM	Receptor for hyaluronan mediated motility
RNA	Ribonucleic acid
rpm	Round per minutes
S	Synthesis phase
Ser	Serine
sER	Smooth endoplasmic reticulum
Sulf-1	Sulphatase-1
Sulf-2	Sulphatase-2
T-ALL	T-lymphocyte acute lymphoblastic leukaemia
Tetrose	Monosaccharide with 4-carbon
Thr	Threonine
TMS	Tetramethylsilane
TOCSY	Total correlation spectroscopy
Triose	Monosaccharide with 3-carbon
UDP	Uridine diphosphate
UMP	Uridine monophosphate
VEGF	Vascular endothelial growth factor
Xyl	Xylose
Δ	Delta

Acknowledgement

I owe my deepest gratitude to my supervisor Dr. David Pye for his guidance, and without his encouragement and support this study would hardly been completed. I express my warmest gratitude to my research colleagues and ELS staff for their support during my studies. I also would like to acknowledge Glycotechnology Core Resource, San Diego, California, USA, for their collaboration as well as Dr Matthew Cliff for his ultimate help in analysing my samples (NMR facilities, Manchester institute of biotechnology, University of Manchester, UK).

I would acknowledge Umm Al-Qura University and the ministry of higher education of Saudi Arabia for giving me this scholarship and a special thanks to Professor Adel Asiri for his support. My deepest appreciation is expressed to my mother, my sisters, my wife and my wonderful daughters (Hala and Lana) and all family and friends, especially (Feras Maslokh) for their support through the whole years.

DECLARATION

I declare that this thesis, which I submit to the University of Salford as partial fulfilment of the requirements for a Degree of Doctor of Philosophy, is a presentation of my own research work. Wherever contributions of others are involved, every effort is made to indicate this clearly with due reference to the literature and acknowledgement of collaborative research. The content of this thesis has not been submitted for a higher degree at this or any other university. Part of the work presented in this thesis has been published.

Aldairi, A., Ogundipe, O. and Pye, D., 2018. Antiproliferative activity of glycosaminoglycan-like polysaccharides derived from marine molluscs. *Marine drugs*, *16*(2), p.63.

MDPI

Article

Antiproliferative Activity of Glycosaminoglycan-Like Polysaccharides Derived from Marine Molluscs

Abdullah Faisal Aldairi, Olanrewaju Dorcas Ogundipe and David Alexander Pye *

School of Environment and Life Sciences, Cockcroft Building, University of Salford, Manchester M5 4WT, UK; A.Aldairi@edu.salford.ac.uk (A.F.A.); dorcasogundipe14@gmail.com (O.D.O.)

* Correspondence: d.pye@salford.ac.uk; Tel.: +44-(0)161-295-470

Received: 10 January 2018; Accepted: 12 February 2018; Published: 15 February 2018

Abstract

Although various anticancer therapeutic tools have been launched, such as immunotherapy and targeted therapy, newly developed drugs with antiproliferative/cytotoxic effects are still in demand; hence, newly discovered anticancer drugs with an improved pharmacological profile are needed to overcome drug resistance of cancer cells. This study focused on identifying and characterising novel polysaccharides isolated from the common cockle (*Cerastoderma edule*) with antiproliferative activity, using the cetylpyridinium chloride precipitation method. Marine polysaccharides have exhibited *in-vitro* potent antiproliferative activity, leading to induced apoptotic cellular death in three cancer cell lines, which are chronic myelogenous leukaemia, relapsed acute lymphoblastic leukaemia and mesothelioma of the pleural cavity with asbestos exposure. Structural analysis has confirmed the presence of glycosaminoglycan-like polysaccharides in cockle extracts with potent antiproliferative activity, which are susceptible to three classes of heparinase enzymes, which has not been seen previously, but not to chondroitinase enzymes. Cockle polysaccharide purification using anion-exchange chromatography has generated six peaks (1-6); however, only fraction 5 exhibited antiproliferative activity, which was determined to be susceptible to heparinase enzymes. Surprisingly, some sequence of resistance to heparinase was observed within cockle polysaccharide chains; therefore, a new type of marine-derived heparan sulphate/heparin-like polysaccharide with potent anticancer properties was suggested, as none of the mammalian glycosaminoglycans exhibited antiproliferative activity on cancer cell lines. Overall, the final structural characterisation did confirm the presence of fucosylated polysaccharide, *N*- and *O*-linked glycans, in addition to HS-like structures. These various chains made creating the final judgment about cockle polysaccharide structural elucidation very challenging because of sample complexity.

1. General introduction

A cell is an organism's smallest functional unit. They have different shapes and functions, but basic cellular structure is common in all cells. Mammalian cells are composed of an extracellular plasma membrane that encloses the cytoplasm and cellular contents from the extracellular compartments. The cytoplasm contains cellular organelles, which make up the cells internal structure, including the nucleus, the endoplasmic reticulum, the mitochondria, the Golgi apparatus, and other cellular vesicles. Depending on the type of cell, these cellular organelles perform specific cellular functions (Figure 1).

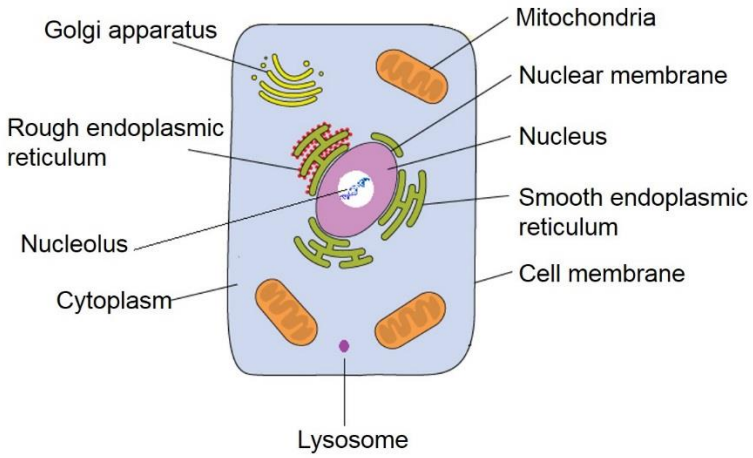

Figure 1. Schematic diagram shows the cell strcuture.

Briefly, the cell membrane is composed of lipids and proteins, and it is essential for normal cellular function, as it acts as a barrier that regulates the movements of substances to and from cells. The nucleus is separated from the cellular cytoplasm by a lipid bilayer membrane known as the nuclear envelope. Inside the nucleus, there is a fine structure known as deoxyribonucleic acid (DNA), which carries all genetic information, as the nucleus has the machinery to assemble the cells ribonucleic acid (RNA), which is released through nuclear envelope pores, in a process called gene expression to synthesise new protein. The mitochondria are the energy providers for cellular functions such as cell growth and motility. Mitochondria have outer and inner membranes. The outer membrane is smooth and regular, whereas the inner membrane is folded.

The endoplasmic reticulum (ER) is an extended system around the nucleus that is found next to the nuclear membrane. The ER can be classified according to its shape into rough endoplasmic reticulum (rER) and smooth endoplasmic reticulum (sER). Ribosomes are attached to the rER, which makes it important in protein synthesis as well as the addition of carbohydrates to proteins. On the other hand, the sER is responsible for the synthesis of lipids, hormones and storing calcium. The Golgi apparatus is composed of three flattened membranous sacs that are involved in a carbohydrate and protein modification process known as glycosylation. The Golgi apparatus is composed of three main faces: *cis*-face, *cisternae*, and *trans*-face. The Golgi apparatus also has an extended ER function, where transported vesicles pinch off the ER and fuse in the *cis*-Golgi before secretion; then, the Golgi modifies the protein and carbohydrate in *cisternae* and releases them as secretory vesicles to the *trans*-face to the plasma membrane. Finally, the cell membrane has bound vesicles that are important to cellular function, such as lysosomes and peroxisomes. Lysosomes have hydrolytic enzymes that recycle cellular contents or materials have been taken up by endocytosis. Peroxisomes contain several different enzymes involved in various metabolic reactions, especially in energy metabolism. In addition, a peroxisome can utilise cellular hydrogen peroxide in oxidation reactions or eliminate it via its enzymes (Pocock et al., 2013).

The extracellular matrix (ECM) is a network of proteins and fibres that are critical for normal cellular function. The ECM has various key functions, such as mechanical support for cellular integrity, control of cellular proliferation, basement membrane scaffolding for tissue renewal, and making the boundary between the epithelium and connective tissues. The ECM has two basic domains: the interstitial matrix and the basement membrane. The interstitial matrix is the area between cells to support cellular integrity, which mainly consists of fibres, collagen, and proteoglycans. The basement membrane is a specialised form of ECM which is highly condensed and organised layer around the epithelium and other cells that can do a specific biological function (Bosman and Stamenkovic, 2003).

1.1. The chemical constituents of the body

Multicellular organisms consist of 70% water, and the rest is a mixture of organic compounds. The organic and inorganic compounds consist largely of four major elements, oxygen, carbon, hydrogen, and nitrogen, which are combined to make a huge number of various biomolecules, such as carbohydrates, proteins, fat, minerals, and nucleic acids (Figure 2) (Pocock et al. 2013).

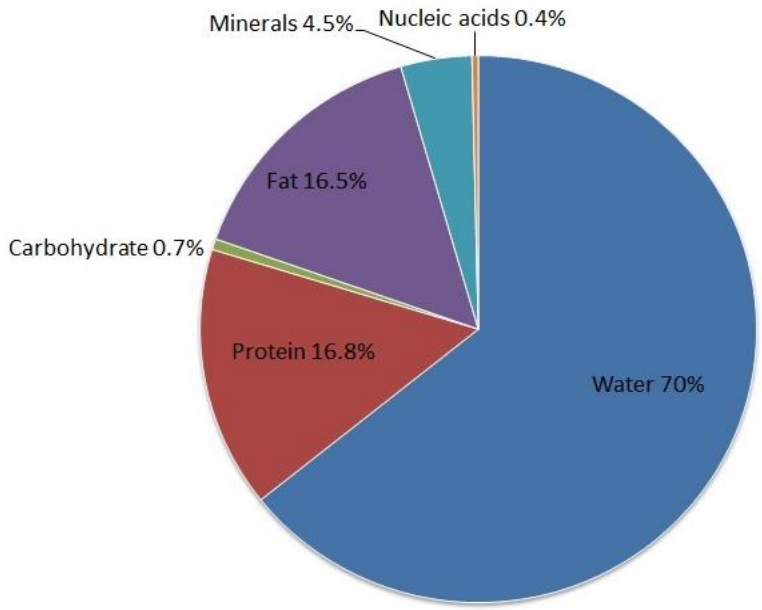

Figure 2. The distribution of biomolecules in multicellular organisms. Water contributes about 70% of the living organism biomolecule, followed by proteins (16.8%), fats (16.5%), minerals (4.5%), carbohydrates (0.7%) and nucleic acids (0.4%) (Pocock et al., 2013)

1.1.1. Carbohydrates

Carbohydrates are the main source of energy. Carbohydrates consist of three basic elements, carbon, oxygen, and hydrogen, with the empirical formula $(CH_2O)_n$. Simple carbohydrates can be found freely in the blood, and complex carbohydrates are found attached to proteins or lipids. There are three classes of carbohydrates based on its chain length, which are monosaccharides, oligosaccharides, and polysaccharides (Nelson, Lehninger and Cox, 2008).

1.1.1.1. Monosaccharides

Monosaccharides are the simplest form of carbohydrates, which can be found in linear or ring forms. Monosaccharides are composed of three-carbons (known as triose), four-carbons (tetrose), five-carbons (pentose), and six-carbons (hexose). In carbohydrate chemistry, when a carbon atom is double-bonded with an oxygen atom, that will form a carbonyl group, whose location can classify monosaccharides as either aldehydes or ketones. In aldehydes, the carbonyl group is at one end of the monosaccharide structure; by contrast, in ketones, the carbonyl group is present at any other position. For instance, glucose is an aldehyde, and fructose is a ketone (Figure 3). In addition, monosaccharides have chiral

carbon, which is defined as carbon that is attached to four different atoms or functional groups. Monosaccharides structural configuration can be in either a dextro-rotary (D) or levo-rotary (L) isomer. In linear form, when the hydroxyl group on the bottom of chiral carbon is pointing to the right side, this is the D-configuration. In contrast, if the hydroxyl group on the bottom of the chiral carbon is pointing to the left side, this is the L-configuration (Bertozzi and Rabuka, 2009).

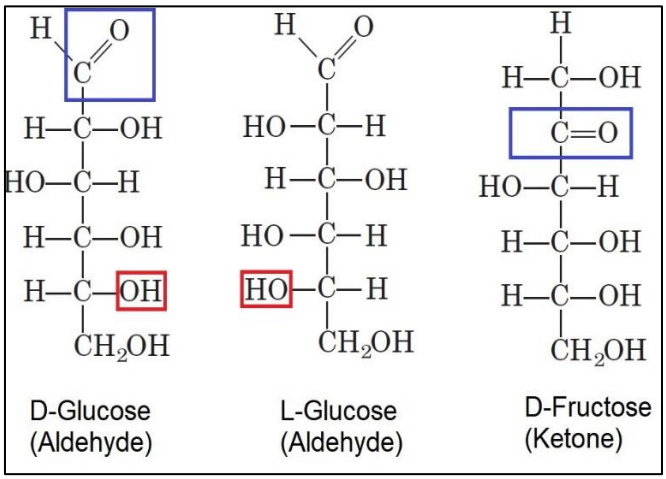

Figure 3. Monosaccharides structural differences as aldehydes (glucose) or ketones (fructose) are assigned in blue colour, in addition to the difference in D- and L-configuration in glucose as an example in red colour (Nelson, Lehninger and Cox, 2008).

1.1.1.2. Oligosaccharides

Oligosaccharides are composed of small number of monosaccharides in ring form. Oligosaccharides are made up of short chains of monosaccharides attached with glycosidic linkages. Indeed, when two monosaccharides are attached together, they will form disaccharides (double sugars). These two monosaccharides are attached together via glycosidic linkage; for instance, lactose is composed of one galactose and one glucose attached together via glycosidic linkage (Figure 4). According to the glycosidic linkage type, molecules will have different structural properties and biological functions. Glycosidic linkage is formed between the anomeric carbon and a hydroxyl group from the attached compound; this will generate either α- or β-glycosidic linkages in ring form, resulting in pyranose or furanose forms. Pyranose is defined as a six-membered ring of five carbons and one oxygen, by contrast, furanose is defined as five-member ring of four carbons and one oxygen (Bertozzi and Rabuka, 2009; Pastrana and Jauregi, 2017).

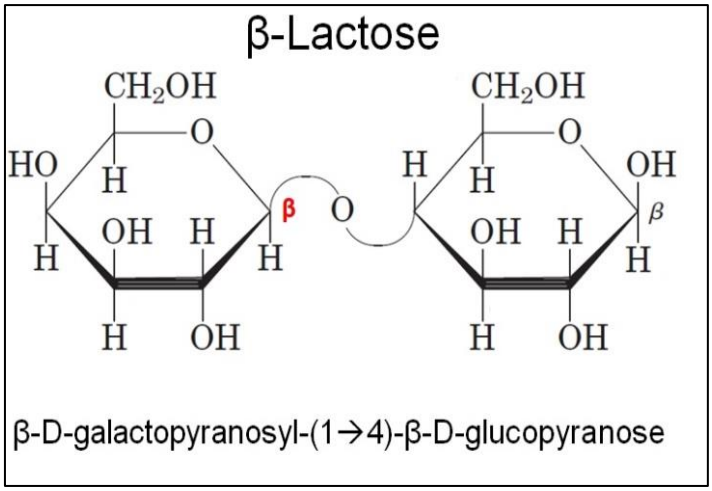

Figure 4. Lactose chemical structure as an example of disaccharide. It is composed of galactopytanose attached to glucopyranose via β-glyosidic linkage (Nelson, Lehninger and Cox, 2008).

1.1.1.3. Polysaccharides

Polysaccharides consist of long branched or unbranched chains of up to thousands of monosaccharides attached together via α-/β- glycosidic bonds. Polysaccharides differ from each other by their monosaccharide building blocks, chain length, branching point, and type of linkage (Figure 5). Amylose and amylopectin polysaccharides are examples that show some of polysaccharides' features. Amylose is composed of a chain of unbranched polymers of glucose (500–20,000 units) attached together via α (1→4) glycosidic linkages. In contrast, amylopectin is composed of a branched glucose polymer chain (2,000–200,000 units) attached together via α (1→4) and α (1→6) glycosidic linkages (Nelson, Lehninger and Cox, 2008).

Additionally, polysaccharides can be classified according to their monosaccharide building blocks into homo-polysaccharides and hetero-polysaccharides, which can combine any other polysaccharide features such as branching or unbranching, chain length and both types of glycosidic linkages. Homo-polysaccharides simply consist of only one type of monosaccharide along the chain. One example is glycogen, which is composed of repeating glucose units. In contrast, hetero-polysaccharides consist of more than one type of monosaccharide along the chain—for example, heparan sulphate, which consists of repeating glucosamine and uronic acid units (Figure 6) (Nelson, Lehninger and Cox, 2008).

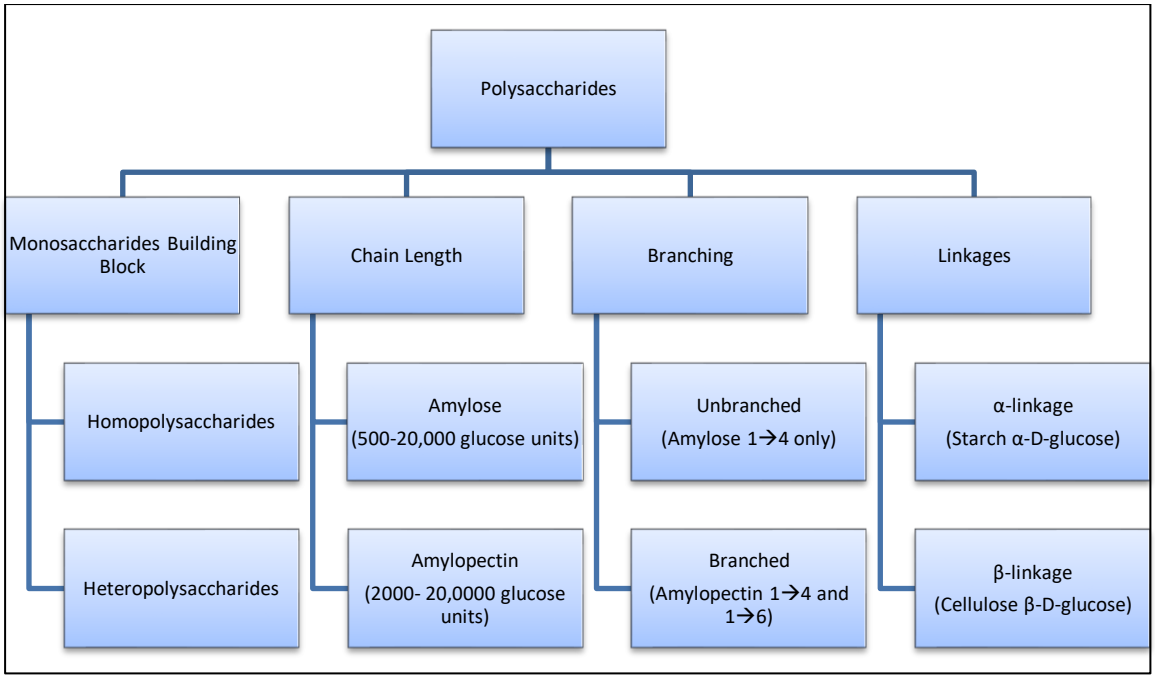

Figure 5. Demonstrate the main features that can be found in polysaccharide chain

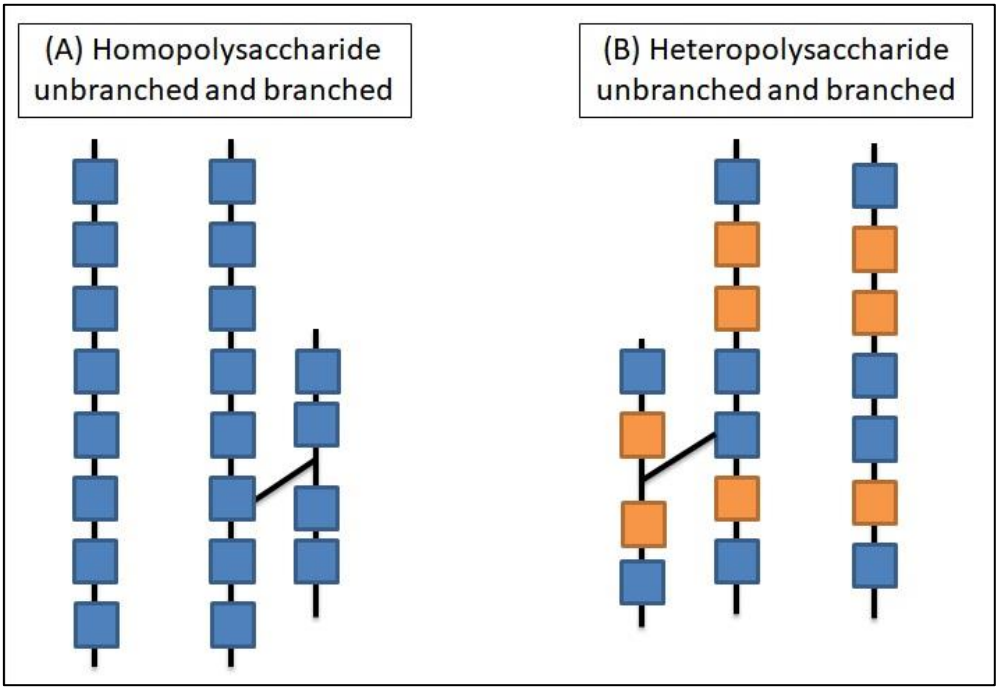

Figure 6. Schematic diagram showing polysaccharides classification according to monosaccharide building blocks, as homo-polysaccharide chain (A) that consists of repeating units of only one type monosaccharide or hetero-polysaccharide chain (B), which consist of more than one monosaccharide along the chain. Both (A) and (B) can have different chain lengths, glyosidic linkages, branching or unbranching features (Nelson, Lehninger and Cox, 2008).

1.1.1.3.1. Glycoconjugates

Glycoconjugates are a type of polysaccharides composed of more than 10 monosaccharides covalently attached to non-carbohydrate structures such as proteins and lipids via glycosidic linkages. There are several monosaccharides in nature that have the ability to conjugate with non-carbohydrates to form glycoconjugates (Table 1). Glycoconjugates can be classified into different categories according to their non-carbohydrate molecule, such as glycolipids, glycoproteins, and proteoglycans. Glycolipids are defined as carbohydrate chains attached to lipids. Glycoproteins are defined as carbohydrate chains attached to polypeptide chains. Proteoglycans are a subclass of glycoproteins, which a particular type of amino-sugars, known as glycosaminoglycan, is attached to protein chains (Bertozzi and Rabuka, 2009).

Table 1. Most common monosaccharides that can bind to a non-carbohydrate moiety to form glycoconjugates (Varki and Sharon, 2009).

Monosaccharide	**Structure**	**Example**
Pentoses	Five-carbon	D-xylose
Hexoses	Six-carbon	D-glucose
Hexosamine	Hexose with an amino group at C-2	Glucosamine
Deoxyhexose	Six-carbon hexose without hydroxyl group at C-6	L-fucose
Uronic acids	Hexose with negatively charged carboxylate group at C-6	Glucuronic acid
Sialic acids	Nine-carbon	N-acetylneuraminic acid

1.2. Glycosaminoglycans

Glycosaminoglycans (GAGs) are a group of long, unbranched hetero-polysaccharides consisting of repeated disaccharide units of uronic acid covalently attached to hexose-sugar

via glycosidic bonds. GAG structures are very diverse, and their synthesis is not template based, like that of proteins. What is more, each monosaccharide can acquire several structural modifications via various enzymes, which give GAGs their vast structural heterogeneity. For instance, a GAG chain can be composed of long polysaccharide chain with different glycosidic linkages between each monosaccharide, as well as the addition of various possible functional groups, as sulphates at different points. All these structural modifications give GAGs their structural heterogeneity and wide range of biological functions (Nelson, Lehninger and Cox, 2008).

GAGs can be freely released or attached to core proteins to form glycoconjugates known as proteoglycans (PGs), these are found in the extracellular matrix, on the cell surface, and intracellularly. GAGs are covalently attached to the core protein polypeptides via N- or O-linkages by a process known as protein glycosylation. N-linked GAGs are usually attached to the core protein via asparagine (Asn) residues in the consensus peptide sequence Asn-X-Ser/Thr; where X represents any amino acid; (Ser) represent serine and (Thr) represent threonine. These N-linked glycans can be divided into three main classes: hybrid, complex, and high-mannose glycans. On the other hand, O-linked glycans are usually attached to the hydroxyl group of Ser or Thr residues on core protein polypeptides (Figure 7) (Esko, 1991; Yayon et al., 1991; Nelson, Lehninger and Cox, 2008; Sarrazin, Lamanna and Esko, 2011).

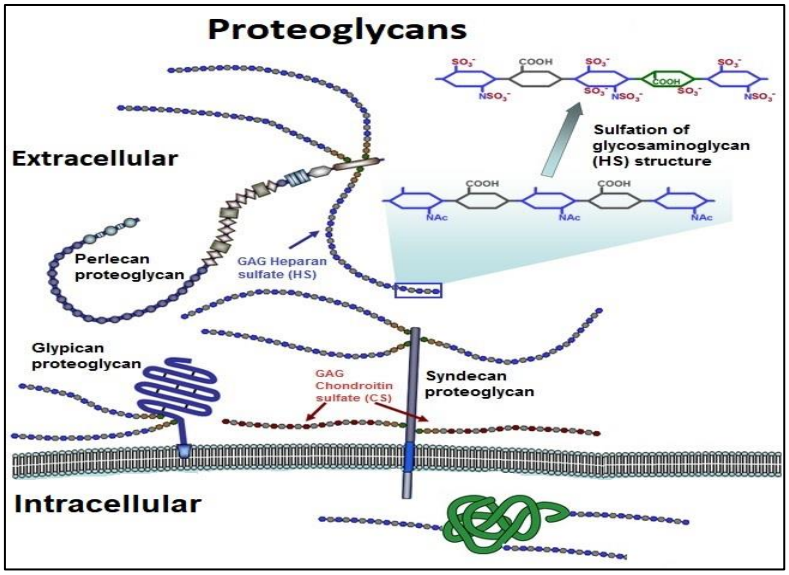

Figure 7. Schematic diagram showing GAGs attached to different core proteins at different locations.

1.2.1. Glycosaminoglycan biosynthesis

GAGs can be biosynthesised from different forms of monosaccharide, such as hexosamines and uronic acids. Hexosamine sugars consist of hexose-sugar structure with an amine group replacing the hydroxyl group at carbon-2, and uronic acid is composed of hexose-sugar, where the hydroxyl group at carbon-6 is oxidised to form a carboxylate. Both biosynthesis pathways are crucial for GAGs biosynthesis and are therefore it's been discussed below.

1.2.1.1. Hexosamine biosynthesis pathway

Hexosamines are composed of six-carbon sugar structures with an amine group attached to carbon-2. They are biosynthesised in cells via breakdown of polysaccharides to monosaccharides to be used as precursors in GAG synthesis. Glucose (Glc) will be used as an example to illustrate the synthesis of glucosamine ($GlcNH_2$) (Figure 8). Initially, Glc carbon-6 is phosphorylated to glucose-6-phosphate by hexokinase enzyme; then, the glucose-6-phosphate is converted to fructose-6-phosphate via phosphohexose isomerase enzyme. Next, the fructose-6-phosphate is converted to glucosamine-6-phosphate by a rate-limiting enzyme known as glutamine-fructosamine transferase; this enzyme converts glutamine, which is used as an amino group donor, into glutamate, resulting in the formation of glucosamine-6-phosphate. After that, the glucosamine-6-phosphate is converted to N-acetyl-glucosamine-6-phosphate by glucosamine-6-phosphate-N-acetyl transferase, which transfers the acetyl group from acetyl-CoA to glucosamine-6-phosphate C-2, resulting in N-acetyl-glucosamine-6-phosphate. Afterwards, this N-acetyl-glucosamine-6-phosphate is converted to N-acetyl-glucosamine-1-phosphate by phosphoacetyl-glucosamine mutase. Finally, the N-acetyl-glucosamine-1-phosphate is converted to uridine diphosphate (UDP)-N-acetyl-glucosamine by UDP-N-acetylglucosamine pyrophosphorylase. This UDP-N-acetyl-glucosamine can be converted to UDP-N-acetyl-galactosamine by UDP-galactose-4-epimerase, which can be used as a precursor for synthesising GAGs, when required (Schleicher and Weigert, 2000).

1.2.1.2. Uronic acids biosynthesis pathway

Uronic acids are derived from hexose-sugars—for example, Glc, galactose (Gal), and mannose (Man)—where the hydroxyl group at C-6 of the hexose-sugar is oxidized to a carboxyl group to form uronic acids, such as glucuronic acid (GlcA), galacturonic acid

(GalA), or mannuronic acid (Figure 8). GlcA biosynthesis occurs in many cells, starting with the phosphorylation of Glc by hexokinase transferase to glucose-6-phosphate, which is then converted to glucose-1-phosphate by phosphoglucomutase enzyme; then, glucose-1-phosphate is converted to UDP-glucose by UDP-glucose pyrophosphorylase. Oxidation of the hydroxyl group at C-6 of the UDP-glucose by UDP-glucose dehydrogenase leads to the formation of UDP-glucuronic acid. This UDP-glucuronic acid is used as a substrate for GAG synthesis (Dutton, 1966). GlcA can be further modified to L-iduronic acid (L-IdoA) by epimerization of glucuronic acid via D-glucuronyl C5-epimerase enzyme, which is the key enzyme in converting GlcA to L-IdoA (Li, 2010).

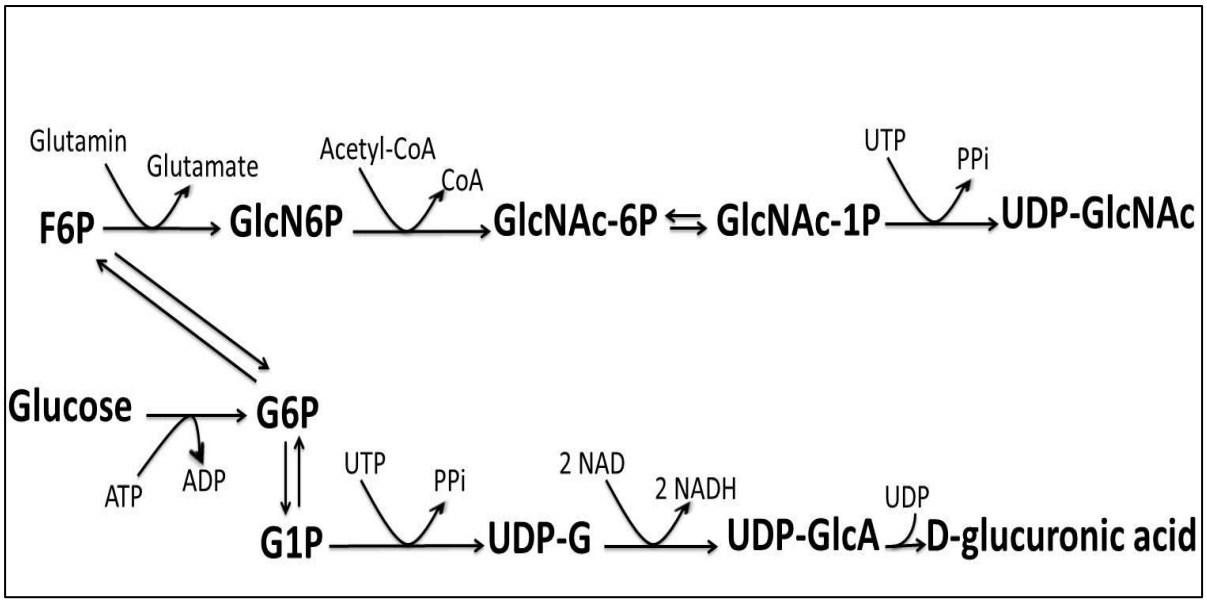

Figure 8. Schematic diagram demonstrates an example of the biosynthesis pathway of glucosamine or glucuronic acid from glucose.

1.3. Core protein glycosylation

Protein glycosylation is defined as the addition of sugar molecules to the polypeptide sequence of the core protein in order to determine a specific cellular function. Glycosylation results in the attachment of different types of monosaccharides to a core protein backbone. The glycosylation process is non–template-driven, so the addition of a particular saccharide sequence to the chain is random, thus making the structure of these PGs very diverse.

Proteins are targeted for various biological functions, so they can be modified according to cell function as well as extracellular secretions. The core protein is synthesised in the rER, then transported via vesicles to the Golgi apparatus, where glycosylation process

takes place (Esko et al., 1987; Stanley, Schachter and Taniguchi, 2009). However, Prydz and Dalen (2000) suggested that the chain could start earlier in the rER.

Principally, protein glycosylation requires various monosaccharides to be used as saccharide donors, for example, hexoses, hexosamines and uronic acids. These substrates are synthesised in the cytosol and attached to UDP as derivative precursors such as UDP-GlcNAc, UDP-GlcA, UDP-Xyl, and UDP-Glc. These substrates from endogenous or exogenous origins enter the Golgi via antiporter channels from the cytosol to be available for protein glycosylation (Figure 9) (Hirschberg, Robbins and Abeijon, 1998).

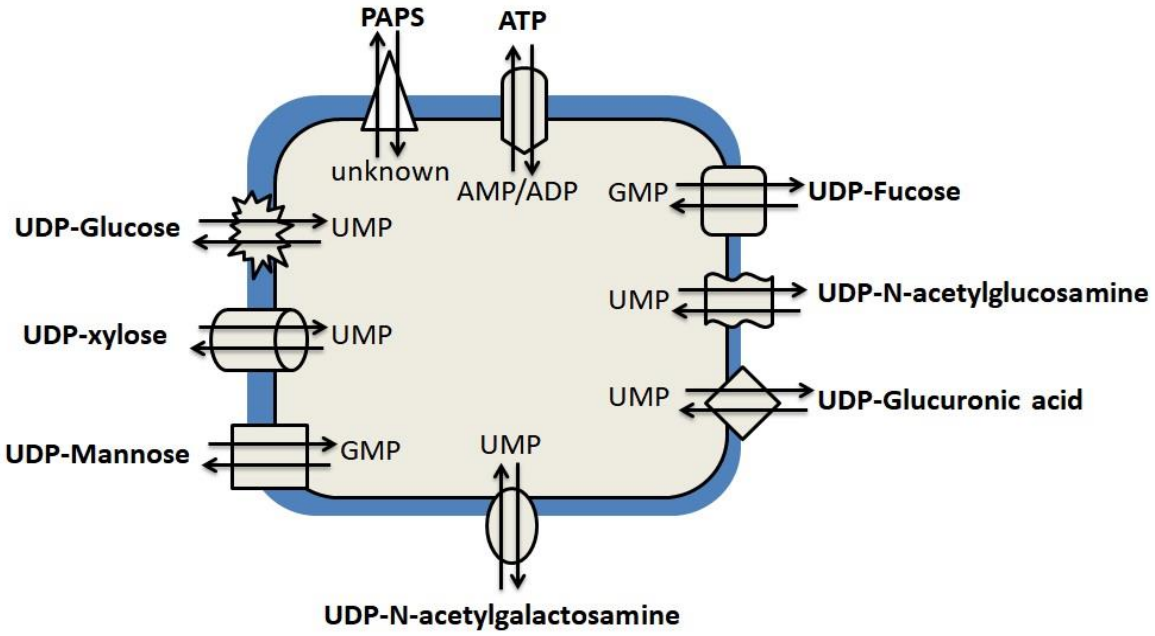

Figure 9. Schematic diagram shows the antiporter mechanism of monosaccharides and the phosphate donor 3′-phosphoadenosine 5′-phosphosulphate (PAPS) precursors in Golgi apparatus membrane. As the transporters are functionally like antiporters, except for PAPS, the antiporter is unknown (Hirschberg, Robbins and Abeijon, 1998).

In the Golgi, protein glycosylation takes place in three consecutive phases—chain initiation, chain polymerisation, and chain modification. Chain initiation starts by enzymatic transfer of the sugar residues to the polypeptide residues of the core protein, which results in either N-linked or O-linked glycans. Next, the chain is elongated by various enzymes that add more monosaccharides, such as hexosamines and uronic acids. Finally, the chain acquires multiple modifications, resulting in non–template-driven modifications that gives GAGs their unique structure (Figure 10). This process is highly dependent on the cell type and the type of GAG that is required for the biological function (Hassell, Kimura and Hascall, 1986).

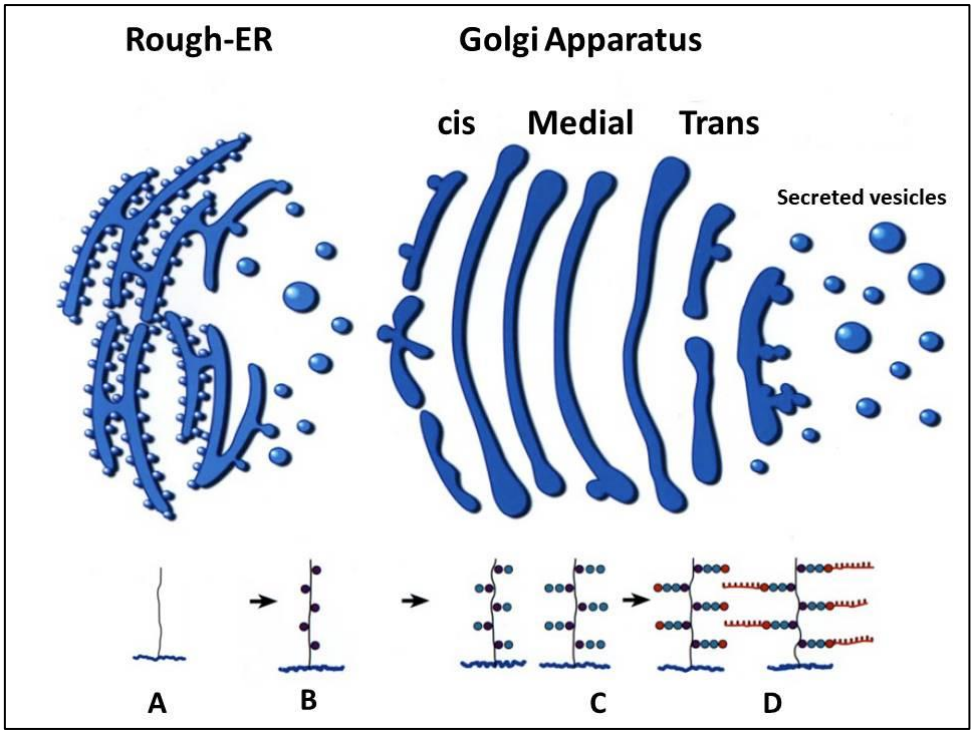

Figure 10. Schematic diagram of protein glycosylation process: (A) Represents the core protein formation in the endoplasmic reticulum. (B) The initial addition of saccharides to the polypeptide residues of the core protein that can be added from the rER or Golgi apparatus, following by chain elongation (C) and chain modification (D). Finally, according to the cell-type, the fully synthesised glycosylated core protein can be secreted to its location (Silbert, 1966).

1.3.1. N-linked glycan

If a carbohydrate sequence attaches to the polypeptide residues of core protein via N-glyosidic linkages, this conjugation is known as an N-linked glycan. This process starts in the rER surface via a process known as the Dolichol-phosphate pathway, followed by addition of the sugar sequence to the Asn residues in the core protein sequence. Afterwards, this glycoconjugated sequence travels to the *cis*-Golgi, where the first step of sequence modification takes place, which is known as sequence early modifications. Then this early modified sequence travels to the *medial*-Golgi where further modifications take place, which is known as sequence late modification. Finally, before secretion to its final destination, the mature sequence is able to travel to *trans*-Golgi for its final decorations/modifications such as addition of chain branches, sulphate groups and sialic acids among other decorations (Figure 11) (Stanley, Schachter and Taniguchi, 2009).

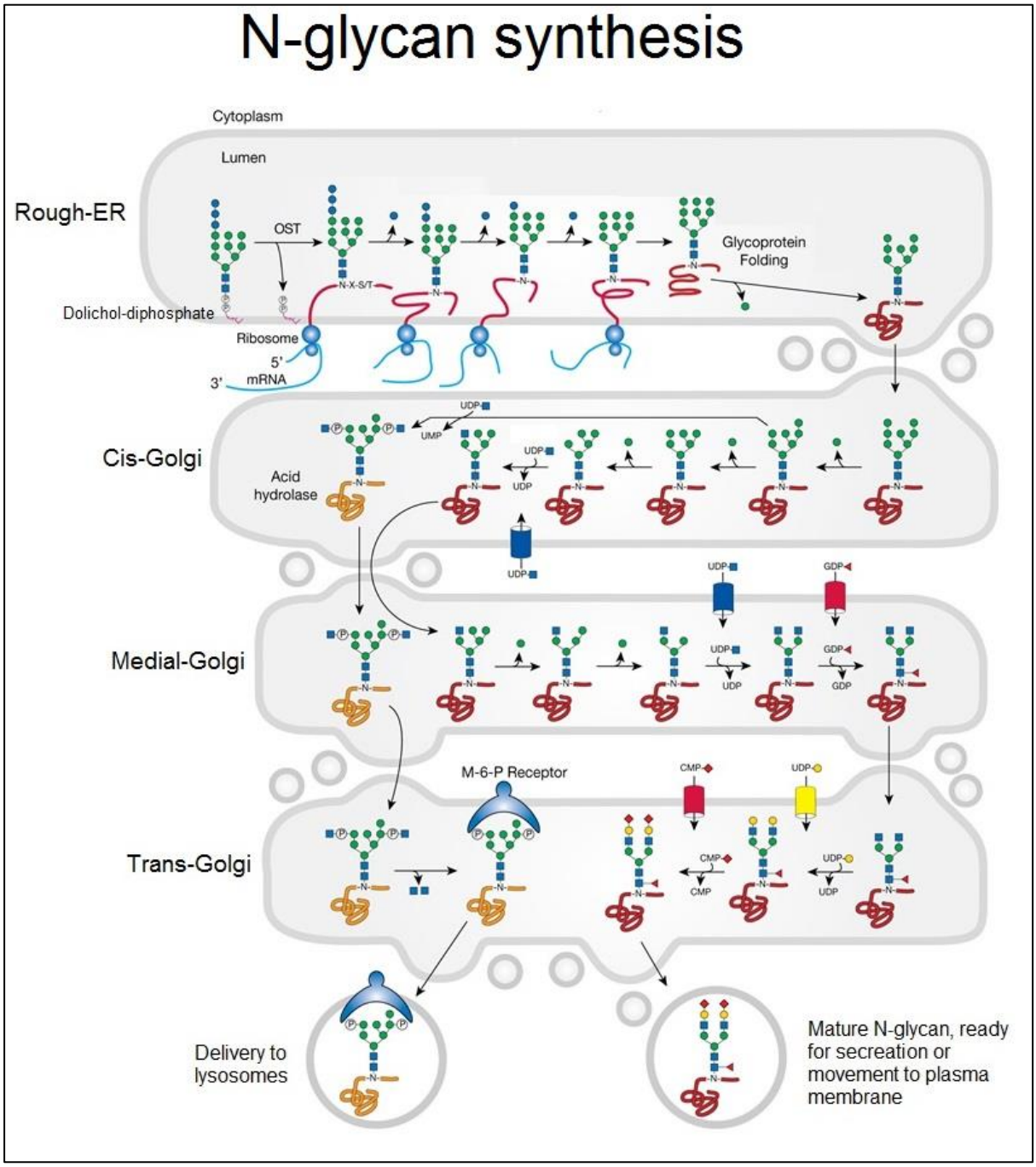

Figure 11. Schematic diagram showing N-linked glycan biosynthesis following Dolichol-phosphate pathway (Stanley, Schachter and Taniguchi, 2009).

1.3.1.1. Dolichol precursor formation

N-linked glycans are synthesised through the Dolichol-phosphate pathway. Dolichol is a poly-isoprenol lipid compound, which is composed of five-carbon isoprene units with a

phosphate group (Figure 12). The N-glycan synthesis process starts in the rER, where Dolichol-phosphate is facing the cytoplasm to allow the addition of different sugar precursors to Dolichol-phosphate (Dolichol-P), for instance, UDP-N-acetylglucosamine (UDP-GlcNAc).

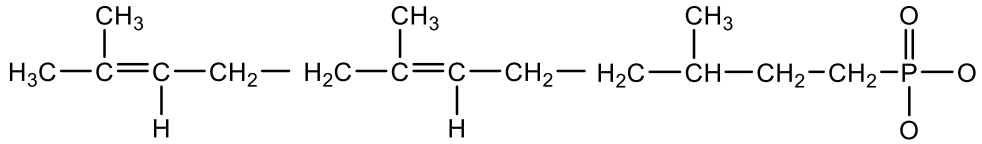

Figure 12: Dolichol-phosphate chemical structure that is composed of multiple isoprene monomers that can reach 19 units in mammalian cells (Stanley, Schachter and Taniguchi, 2009).

This step is catalysed by GlcNAc-1-phosphotransferase, which transfers GlcNAc-1-P from UDP-GlcNAc, resulting in an attached GlcNAc-phosphate unit to the sequence from its UDP precursor, as Dolichol-P-P-GlcNAc, followed by addition of another GlcNAc unit to become Dolichol-P-P-GlcNAc-GlcNAc. This is followed by the addition of five Man residues from its guanosine diphosphate (GDP) precursor, which leads to formation of the sequence of a Dolichol diphosphate high-mannose structure, as [Dolichol-di-phosphate-$GlcNAc_{(2)}$-$Man_{(5)}$]. Afterwards, this Dolichol high-mannose structure is translocated to face the rER lumen by an enzyme known as flippase.

Then, four additional Man residues, which are donated from Dolichol-P-Man, by the action of mannosyltransferases, and three Glc residues are donated from Dolichol-P-Glc by glucosyltransferases. Those Man and Glc units are formed in the cytoplasm from GDP-Man and UDP-glucose, respectively, transferred to Dolichol-phosphate and flipped to the rER lumen. Finally, after the addition of these sugar residues, Dolichol-diphosphate will be mature to be act as an N-glycan precursor, which acquires this formula [Dolichol-P-P-$GlcNAc_{(2)}$-$Man_{(9)}$-$Glc_{(3)}$] (Figure 13).

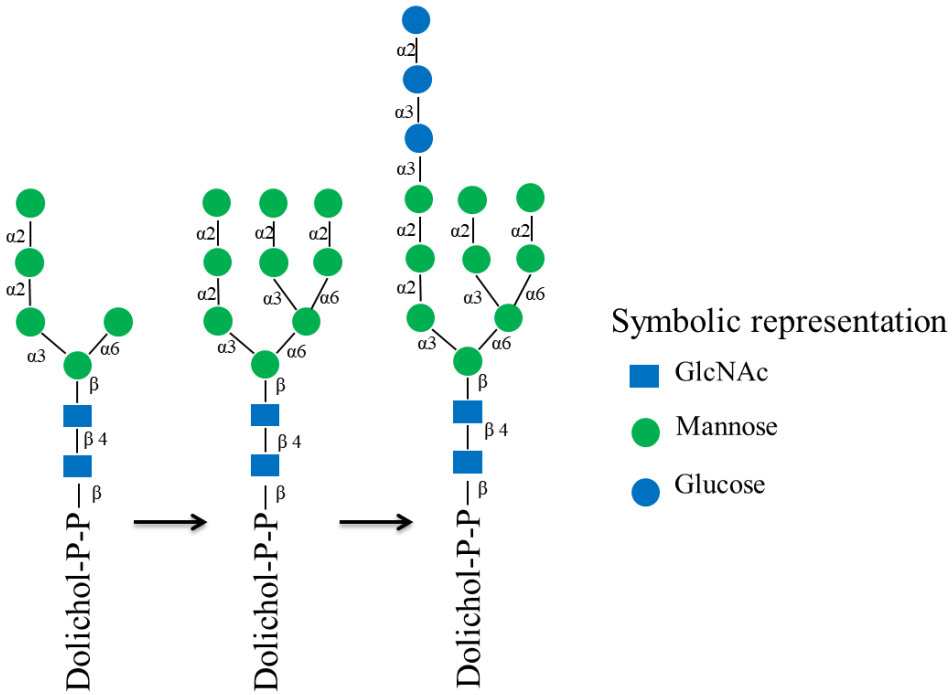

Figure 13: Schematic diagram showing synthesis of [Dolichol-P-P-GlcNAc$_{(2)}$-Man$_{(5)}$] after flipping to the rER lumen, followed by chain elongation by addition of 4 Man residues as well as 3 Glc units after several chain modifications as a result of [Dolichol-P-P-GalNAc$_{(2)}$-Man$_{(9)}$-Glc$_{(3)}$] (Stanley, Schachter and Taniguchi, 2009).

1.3.1.2. N-glycan precursor addition to the polypeptide sequence

N-glycan precursor [Dolichol-P-P-GlcNAc$_{(2)}$-Man$_{(9)}$-Glc$_{(3)}$] is ready to be attached to the polypeptide region of Asn-X-Ser/Thr via N-glycosidic linkage. Oligosaccharyltransferase (OST) enzyme will catalyse the cleavage of the sugar sequence to release it from Dolichol-P-P, resulting in covalent bonds between sugar complex and Asn [Asn-GlcNAc$_{(2)}$-Man$_{(9)}$-Glc$_{(3)}$].

1.3.1.3. Early-sequence modifications

Early-sequence modifications start by removing most of the sugar residues from the polypeptide sequence and prepare the sequence to be transferred to the *cis*-Golgi via vesicles. The process begins with the removal of Glc residues by the action of α-glucosidases-I and II, which remove one terminal Glc α(1→2) and two inner Glc α(1→3), respectively. After the removal of glucose residues [Asn-GlcNAc$_{(2)}$-Man$_{(9)}$], an additional ER enzyme called α-mannosidase-I is responsible for removing one terminal Man unit α(1→2) before the

sequence pass through *cis*-Golgi as [Asn-GlcNAc$_{(2)}$-Man$_{(8)}$]. Most N-glycans that pass through the *cis*-Golgi can be further modified. In the *cis*-Golgi, further removal of the remaining glucose and Man residues by endo-α-mannosidase (1→2) results in [Asn-GlcNAc$_{(2)}$-Man$_{(5)}$], however, Man inhibitors might inhibit the removal of all mannose residues, which result in uncompleted chain that cannot be modified any further. At this stage, three types of N-glycans can be formed: oligomannose and hybrid and complex glycans (Figure 14). Oligomannose will not undergo further modifications, whereas hybrid and complex glycans will be further modified (Stanley, Schachter and Taniguchi, 2009).

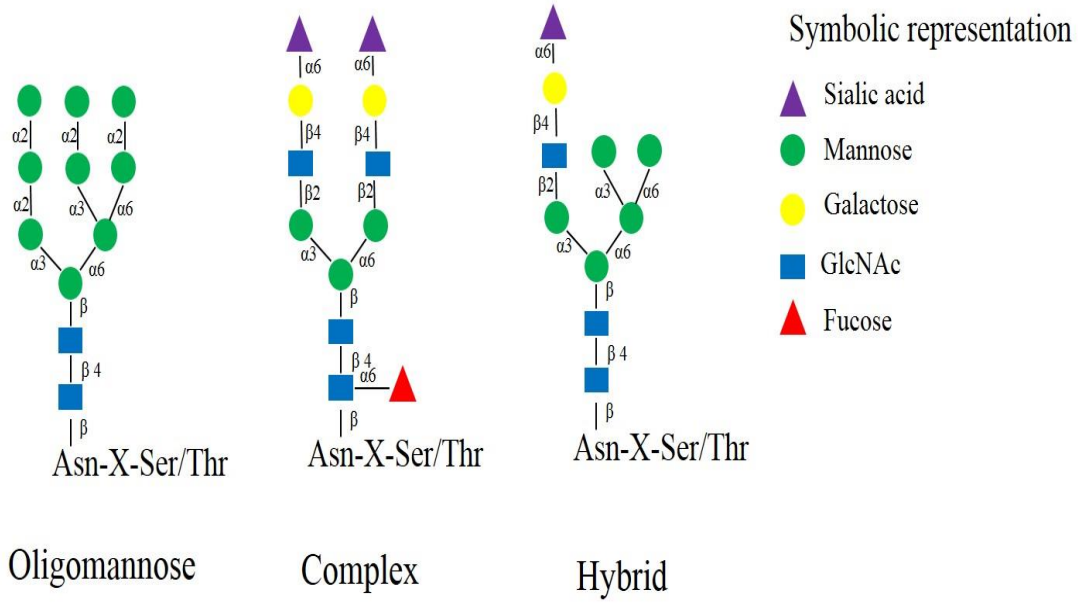

Figure 14. Schematic diagram shows three possible modified glycan structures, namely oligomannose, complex and hybrid (Stanley, Schachter and Taniguchi, 2009).

1.3.1.4. Late-sequence modifications

In the *cis*-Golgi, the addition of GlcNAc to the Man α(1→3) by the action of N-acetyl-glucosaminyl transferase-I (GlcNAcT-I) catalyses the addition of GlcNAc to the sequence of [Asn-GlcNAc$_{(2)}$-Man$_{(5)}$], resulting in [Asn-GlcNAc$_{(2)}$-Man$_{(5)}$-GlcNAc]. This sequence is crucial for further modifications on the sequence in the *medial*-Golgi, which modifies the chain to form hybrid or complex glycans. In the *medial*-Golgi, immediately following this step, the majority of N-glycans containing terminal α(1→3) and α(1→6) Man will be trimmed by α-mannosidase-II enzyme to yield [Asn-GlcNAc$_{(2)}$-Man$_{(3)}$-GlcNAc].

Afterwards, additional GlcNAc will be added to the sequence by N-acetyl-glucosaminyl transferase-II (GlcNAcT-II) to yield [Asn-$GlcNAc_{(2)}$-$Man_{(3)}$-$GlcNAc_{(2)}$]. This final sequence is responsible for the formation of complex N-glycans. On the other hand, terminal α(1-6) and α(1-3) mannoses on the N-glycan sequence remain intact or incomplete action of α-mannosidase-II will result in generating the hybrid N-glycan structure [Asn-$GlcNAc_{(2)}$-$Man_{(4)}$-GlcNAc] (Stanley, Schachter and Taniguchi, 2009).

1.3.1.5. Trans-Golgi modification

In the *Trans*-Golgi, N-glycans will acquire various chain branches. Initially, complex N-glycans can acquire additional GlcNAc branches at C-4 of core Man α(1→3) and at C-6 of core Man α(1→6) by the action of N-acetyl-glucosaminyl transferase-IV (GlcNAcT-IV) and N-acetyl-glucosaminyl transferase-V (GlcNAcT-V), respectively. In addition to these two enzymes N-acetyl-glucosaminyl transferase-IX (GlcNAcT-IX), N-acetyl-glucosaminyl transferase-Vb (GlcNAcT-Vb) can catalyse the addition of GlcNAc to C-6 of core Man α(1→6), and to C-6 of the core Man α(1→3). Another possible branching point can be found in both complex and hybrid N-glycans with the addition of GlcNAc to β-Man by the action of GlcNAcT-III. These enzymes can result in highly branched and complex N-glycan structures, which can have further sequence modifications (Stanley, Schachter and Taniguchi, 2009).

The second possible modification to the sequence can be the addition of different sugar residues to the sequence. For example, fucose can be added to the GlcNAc adjacent to the Asn. Fucosylation occurs by an enzyme fucosyl-transferase-III, which catalyse the addition of fucose α(1→3) and/or fucosyl-transferase-VIII, which catalyses the addition of fucose α(1→6). In plants, fucose can only be added to the α(1→3) GlcNAc adjacent to the Asn, in contrast, invertebrates can acquire both fucose in both linkages α(1→3) as well as α(1→6). Furthermore, xylose (Xyl) can be added to the sequence by the action of xylosyl-transferase, which catalyses the addition of Xyl α(1→2) to the core β-Man. Thirdly, chain elongation can be achieved by addition of β-linked Gal building blocks [-3 Gal β(1→4)GlcNAc β1-] known as N-acetyllactosamine. (Stanley, Schachter and Taniguchi, 2009).

Finally, the most important part of N-glycans is known as chain decorations. Chain decorations can be achieved by the addition of sialic acid, fucose, a sulphate group, and α-linked GalNAc. Chain decoration features α-linkages that would facilitate glycan presentation

and interaction with various lectins, as this feature is shared with O-linked glycans (Stanley, Schachter and Taniguchi, 2009).

1.3.2. O-linked glycan

O-linked glycan chains are initiated in the Golgi apparatus, in contrast to N-linked glycans which initiate its chain in the rER. O-linked glycans do not require Dolichol-diphosphate to initiate its chain; in addition, there is no particular sugar sequence to be transferred to the amino acid residues. However, the addition of sugars to the O-linked chain heavily depends on the cell-type, which has the specific sugar transferase enzymes to transfer it to the amino acid residues. O-glycans are linked to the core protein commonly via Ser or Thr residues, which make it very challenging to analyse and predict within the sequence (Steen et al., 1998).

Different sugar residues can attach to the core protein to initiate the proteoglycan sequence. For instance, O-Xyl can be the first monosaccharide attached to the hydroxyl group of Ser or Thr by the action of Xyl-transferase, which catalyses the addition of a Xyl residues from its UDP-Xyl precursor to Ser or Thr, resulting in the first glycosylation of the core protein as Ser-O-β-Xyl. Then, the chain will be elongated and modified according to cell type and the required proteoglycan (Brockhausen, Schachter and Stanley, 2009).

1.4. Glycosaminoglycan classification

The literature has distinguished six types of GAGs based on their repeating disaccharide units: heparan sulphate (HS), heparin, chondroitin sulphate (CS), dermatan sulphate (DS), keratan sulphate (KS), and hyaluronan (Rabenstein, 2002). Hyaluronan is structurally linked to GAGs; however, it is not bound to a core protein as a side chain; hence, it is not considered a proteoglycan (Höök et al., 1984).

1.4.1. HS

HS is biosynthesised in almost all mammalian cells with molecular weight 10–70 kDa, and it is found both on the cell surface and in the extracellular matrix. The most common repeating disaccharide building block is thought to be [GlcA (1→4) $GlcNH_2$], chemically formulated as [→4 β-D-GlcA (1→4) α-D-GlcNAc (1→]. Although the HS chain can acquire different structural modifications at different position, the GlcA is usually found

non-sulphated, and the $GlcNH_2$ is mainly N-acetylated. Other typical modifications include the epimerisation of GlcA to IdoA and the addition of the sulphate groups in a number of positions (Rabenstein, 2002; Köwitsch, Zhou and Groth, 2018).

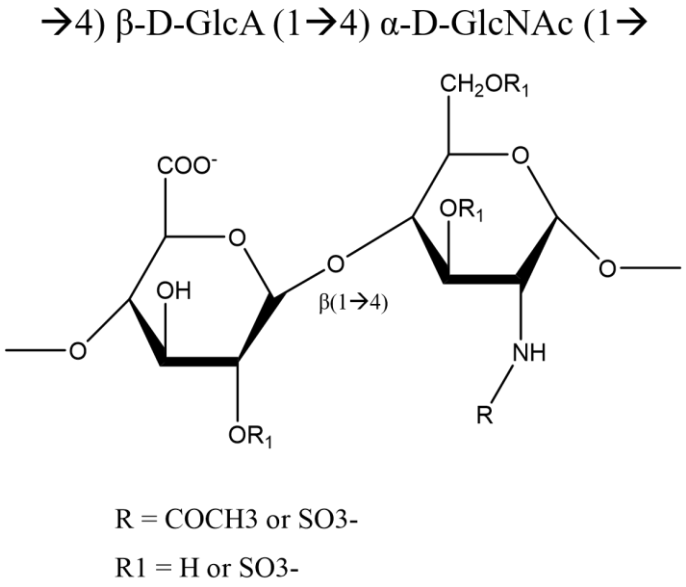

Figure 15. HS common disaccharide structure. During the modification phase, GlcA can acquire sulphate group at C-2, while $GlcNH_2$ can acquire sulphate group at C-3 and/or C-6 and the amino group (C-2) can be sulphated or acetylated, depending of cell function (Höök et al., 1984).

1.4.1.1. HS biosynthesis pathway

The HS chain is biosynthesised in the Golgi apparatus as a long polymer (50–200 disaccharide units) in three consecutive phases: chain initiation, chain polymerisation, and chain modification. The chain initiation phase starts by the addition of the basic tetrasaccharide linkers which are Xyl, two Gal residues, and GlcA—to the Ser/Thr residues of the core protein via O-linkage. Four enzymes are involved in this process, which are Xylose-transferase, galactose-transferase-I, galactose-transferase-II, and glucuronic-acid-transferase-I (Figure 16) (Rabenstein, 2002). Xylose-transferase enzyme catalyses the addition of Xyl from UDP-Xyl to the serine residues via O-linkages; then, two Gal residues are added by galactose-transferase-I β(1→4) and galactose-transferase-II β(1→3); and finally, GlcA is added by the action of glucuronyltransferase-I enzyme β(1→3) (Prydz and Dalen, 2000).

Subsequently, chain polymerisation starts with the addition of the first GlcNAc α(1→4) by GlcNAc-transferase-I, which control HS-GAG synthesis, followed by the

addition of GlcA α(1→4) by an exotoxin like glycosyltransferase-3 (EXTL3). Next, the chain is extended by the addition of various GlcA and GlcNAc from their corresponding UDP-precursors to make the disaccharide building blocks of HS by the action of the copolymerase enzymes transmembrane glycosyltransferase EXT1 and EXT2. After the HS chain is extended, it is ready for the modification phase, which gives HS its unique structure (Lin, 2004).

The chain modification phase undertakes a series of adjustments and modifications to the whole sequence, including deacetylation, acetylation, sulphation, and epimerization. N-deacetylase and N-sulphotransferase, which are a group of enzymes that catalyse the transfer of sulphate groups to their respective sites from the sulphate group universal donor PAPS, lead the removal of the acetyl group from GlcNAc and add a sulphate group to the free amino group, resulting in the generation of sulphated chain. Epimerization of GlcA by C-5 epimerase enzyme converts GlcA to IdoA. Further sulphation can take place at different positions of the chain via specific sulphotransferases (Lin, 2004).

The uronic acid can be further modified by O-sulphation at C-2 and/or C-3 as GlcA(2S/3S), in addition to the epimerised IdoA, which can acquire more sulphates at C-2/C-3. On the other hand, β-D-GlcNAc can be either acetylated or N-sulphated as (GlcNS). Both structures can acquire 6-O-sulphate to become GlcNAc(6S) or GlcNS(6S). However, only GlcNS(6S) can be further modified by the addition of 3-O-Sulphate to become GlcNS(3,6S) (Rabenstein, 2002). 3-O-Sulphation and/or 6-O-Sulphation of the GlcNAc occur via 3-O-Sulphotransferase and 6-O-Sulphotransferase, respectively (Blackhall et al., 2001; Rabenstein, 2002; Lin, 2004).

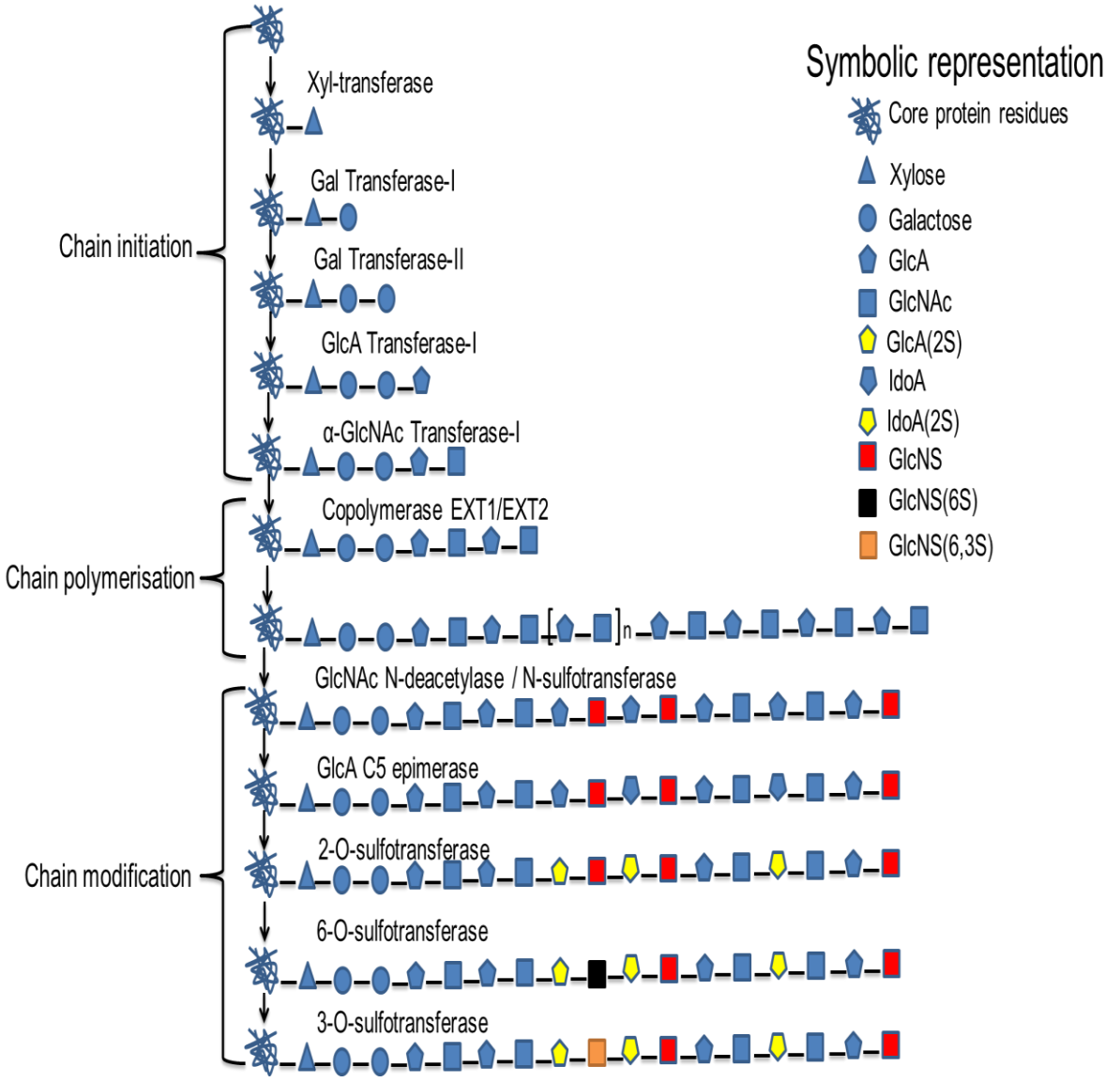

Figure 16. HS biosynthesis pathway in Golgi apparatus that follow HS three phases, namely chain initiation, chain polymerization and chain modification. HS chain starts by addition of tetrasaccharide linker, which is Xyl-Gal-Gal-GlcA, to Ser or Thr residues. Following chain polymerization, where addition of GlcA and $GlcNH_2$ to extend the HS chain. Finally, chain modification, where several possible modifications can take place to give HS its unique structure according to cell type, for instance, epimerisation, deacetylation, sulphation for both the GlcA/IdoA and the $GlcNH_2$ (Lin, 2004).

Lastly, HS chain modifications are highly dependent on the cellular function, so the HS chain varies along the proteoglycan in terms of HS chain length and sulphation patterns. HS chain modifications occur in clusters, which means the chain can be divided into different modified domains across the proteoglycan. These domains are referred to as N-sulphated (NS), N-acetylated (NA), and mixed domains (NA/NS). NS-domains are characterised by highly sulphated saccharides on both GlcA and $GlcNH_2$, the NA-domain is characterised by a

highly acetylated sequence, and NS/NA contains a mixture of variable sulphated and acetylated regions. All these variable domains are non–template-driven, which results in different HS chains, making HS chain sequencing very heterogeneous (Nelson, Lehninger and Cox, 2008; Esko, Kimata and Lindahl, 2009). Following successful assembly of the chain in the Golgi apparatus, cells secrete HS-PG to different locations, such as the cell membrane. Recently identified cell membrane endosulphatases can alter the HS chain on the cell membrane by removing 6-O-sulphate from $GlcNH_2$ residues (Lamanna, 2008).

1.4.2. Heparin

Heparin is biosynthesised in connective tissues in mast cells attached to a unique intracellular core protein known as serglycin (Volpi et al., 2014). When a mast cell is stimulated, it releases heparin by exocytosis, resulting in unfractionated heparin with molecular weight 12-15 kDa. The most common heparin disaccharide formula is [IdoA (1→4) $GlcNH_2$], chemically formulated as [→4) α-L-IdoA(2S) (1→4) α-D-GlcNS (1→], where IdoA is mostly sulphated at C-2, and $GlcNH_2$ is NS, with additional sulphate groups at C-3 and C-6 can be added to the chain (Figure 17). Hence, heparin is known to be more sulphated than HS and carry high negative charge along the chain (Sasisekharan and Venkataraman, 2000; Sasisekharan et al., 2002; Köwitsch, Zhou and Groth, 2018).

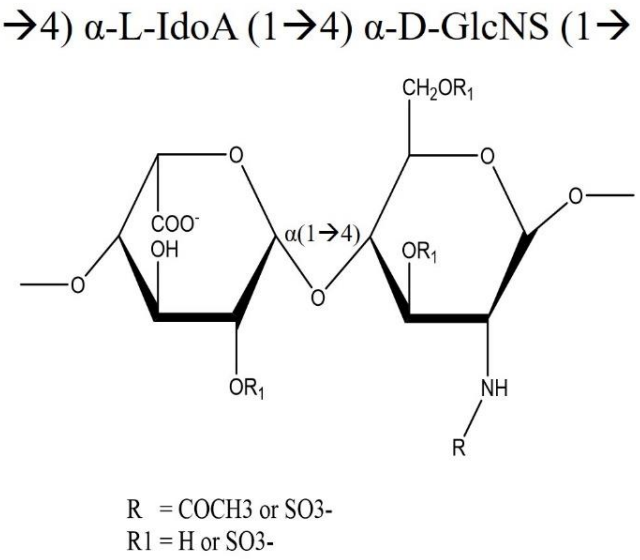

Figure 17. Heparin common disaccharide building blocks structure. During modification phase, IdoA can acquire a sulphate group at C-2, while $GlcNH_2$ can acquire sulphate group at C-3 and/or C-6, however, the amine group is more likely sulphated or to a lesser extend acetylated, depending on cell function (Höök et al., 1984).

1.4.2.1. Heparin biosynthesis pathway

Heparin is biosynthesised in the Golgi apparatus in a similar biosynthesis pathway to that of HS, including chain initiation, chain polymerisation, and chain modification. However, during chain modification, the heparin chain undergoes additional modifications by N-deacetylation and N-sulphation of the $GlcNH_2$, as well as more epimerisation by the C5-epimerase enzyme, leading to conversion of about 70% of the GlcA to IdoA. Hence, the heparin chain has a higher frequency of sulphated IdoA than HS (Sugahara and Kitagawa, 2002).

1.4.2.1.1. Enzymatic degradation of HS/heparin chain

HS and heparin are secreted to the ECM as fully synthesised chains. However, some chains are shed from the cell through proteolytic cleavage of the core protein and endocytosis enzymes such as heparinases. Heparinase enzymes are endoglycosidase enzymes that cleave the glycosidic bonds between $GlcNH_2$ (1→4) and uronic acid in both heparin and HS chains, resulting in unsaturated disaccharides with double bonds between C-4 and C-5 of the uronic acid (Figure 18). The heparinase gene in human chromosome 4 is known as HPSE, which is expressed by the lacrimal gland, lens, cornea, epithelium, and other tissues. Secreted heparinase is 508 amino acids long, with approximately 57.7 kDa (Zhang et al., 2010).

Heparinase was extracted from bacteria *Flavobacterium heparinum*, which releases enzymes that cleave both HS- and heparin-containing molecules. There are three classes of heparinase enzymes that can cleave heparin/HS α(1→4) glycosidic linkage, which are heparinase-I, heparinase-II and heparinase-III. Heparinase-I is highly specific to this sequence [α-D-GlcNS (1→4) β-D-GlcA(2S)/α-L-IdoA(2S)]. Heparinase-II is thought to be the only enzyme that can cleave the glycosidic linkage of [α-D-GlcN(S/Ac) (1→4) unsulphated or sulphated uronic acid]. Heparinase-III can hydrolyse the glycosidic linkage between [α-D-GlcNAc/(2S) (1→4) β-D-GlcA] (Linhardt et al., 1990).

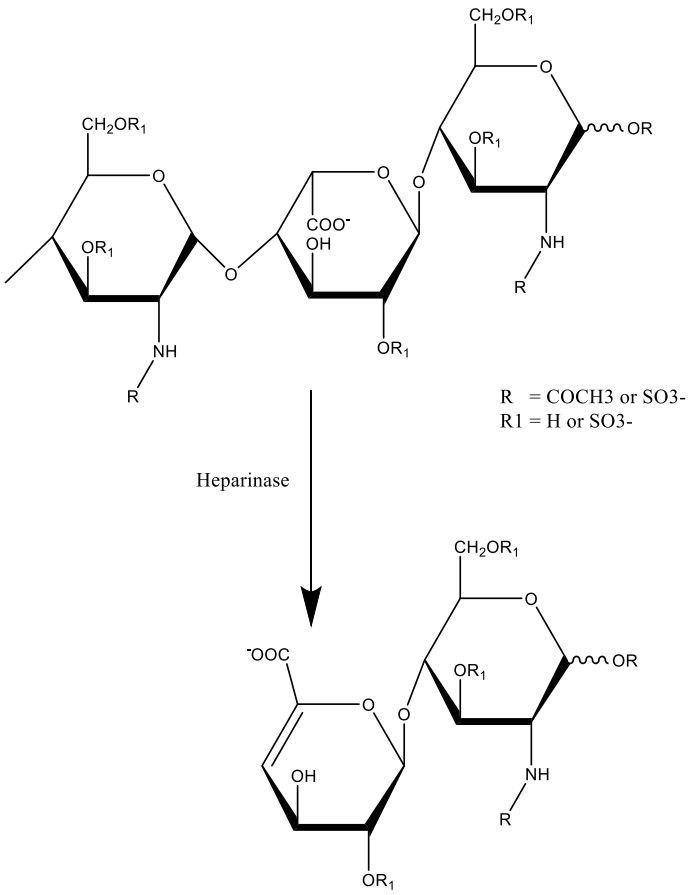

Figure 18. Heparinase reaction pathway. This figure shows the heparinase enzyme that catalase the elimination of polysaccharides containing heparin/HS α(1→4), resulting in unsaturated oligo- and disaccharides.

1.4.3. CS

CS is expressed in the cell membrane, intracellularly, and in the ECM. It can be found covalently bonded to the core protein to form CS-proteoglycan (CSPG). CS common repeating disaccharide units are composed of [GlcA (1→3) $GalNH_2$,], with chemical formula [→4 β-D-GlcA (1→3) β-D-N-GalNAc (1→] (Mizumoto, Yamada and Sugahara, 2015). In addition, the CS chain can acquire a high negative charge, as it can acquire several sulphates at different positions on both $GalNH_2$ and GlcA, in addition to the hydroxyl group on the GlcA (Figure 19) (Huang et al., 2003).

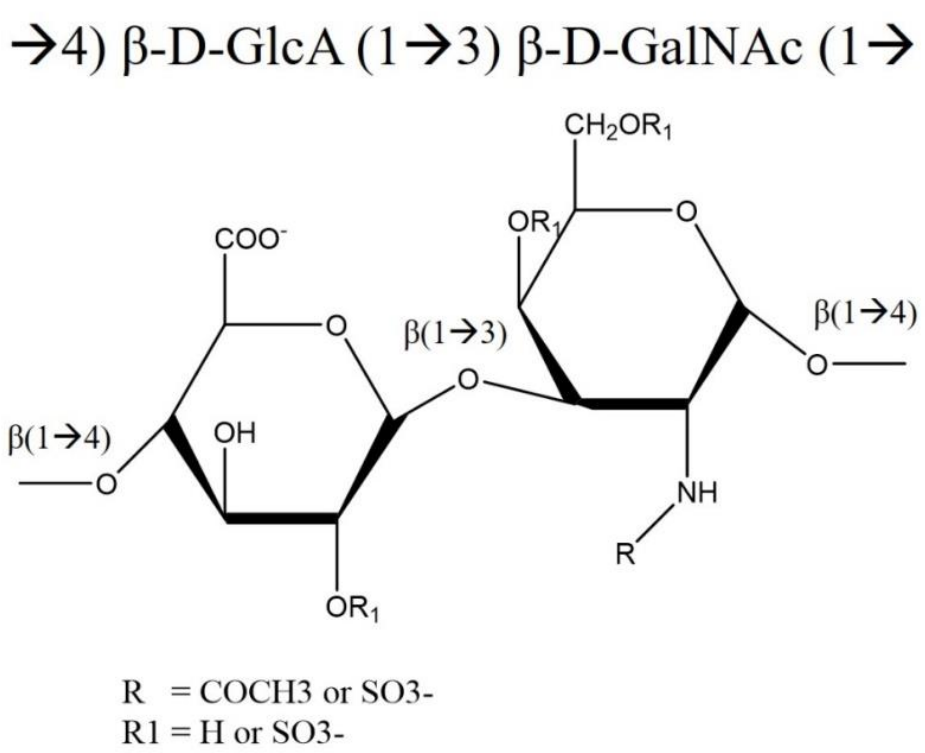

Figure 19. CS common disaccharide building block structure. During the modification phase, GlcA can acquire sulphate group at C-2, and $GalNH_2$ can acquire sulphate group at C-4 and/or C-6 and the amino group either can be sulphated or acetylated, depending on cell function (Höök et al., 1984).

1.4.3.1. CS biosynthesis pathway

Basically, the CS chain synthesis follows a similar synthesising pathway to HS and heparin; however, the CS chain is initiated by the addition of GalNAc to the tetrasaccharide linker region. After the addition of the tetrasaccharide linkers to the core protein sequence, β(1→4) *N*-acetylgalactosaminyltransferase-I and β(1→3) glucuronosyltransferase-II—which catalyse the addition of GalNAc and GlcA, respectively, from their UDP-precursors—create the CS backbone. Then, the CS chain undergoes polymerisations, which result in several forms of modified CS structures (Bülow and Hobert, 2006).

CS has been identified to have several isomers according to the disaccharide posttranslational modifications. Some CS isomers are common in mammals, and others are rare or not found in mammalian cells (Table 2). Common CS subtypes are CS-A, CS-B, CS-C, CS-D, and CS-E. CS-A is composed of [GlcA-GalNAc(4S)], and CS-C is composed of [GlcA-GalNAc(6S)]. CS-B can be distinguished from other CS isomers due to its

epimerization of the GlcA to IdoA [IdoA(2S)-GlaNAc(4S)/(6S)] (Lamari and Karamanos, 2006). CS-D structurally possess a disaccharides unit [GlcA(2S)-GalNAc(6S)] (Nadanaka et al., 1998). Finally, CS-E has repeated disaccharide structure units [GlcA-GalNAc(4,6S)] (Iwata, 1969).

The rarest CS posttranslational modifications have been identified in marine invertebrates, including CS-K, CS-L, and CS-M. CS-K was isolated from king crab cartilage (*Tachypleus tridentatus*), which has unique disaccharides that contain 2-O-sulphated or 3-O-sulphated GlcA and GalNS or GalNAc(4S) (Sugahara et al., 1996). CS-L has unique 3-O-sulphated GlcA, and $GalNH_2$ is acetylated with 6-O-sulphated structure [GlcA(3S)-GalNAc(6S)]. Finally, CS-M is characterised by 3-O sulphated GlcA, and the $GalNH_2$ is N-acetylated with 4-O-sulphated structure [GlcA(3S)-GalNAc(4S)] (Lamari and Karamanos, 2006).

According to Vieira & Mourão (1988), a novel marine sourced CS chain with branched fucose was discovered from sea cucumber *(holothurian)*, which was characterised as fucosylated-CS. Fucose is attached to the GlcA via $\alpha(1\rightarrow3)$ glycosidic linkage, which make CS resistant to certain CS-degrading enzymes (Pomin, 2015; Ustyuzhanina et al., 2015).

Table 2. Different CS isomers.

Chondroitin sulphate subtypes	Structure
CS-A	GlcA-GalNAc(4S)
CS-B	IdoA(2S)-GlaNAc(4S)/(6S)
CS-C	GlcA-GalNAc(6S)
CS-D	GlcA(2S)-GalNAc(6S)
CS-E	GlcA-GalNAc(4S,6S)
CS-K	GlcA(2S/3S)-GalN(S)/(4S)
CS-L	GlcA(3S)-GalNAc(6S)
CS-M	Glc(3S)-GalNAc(4S)

1.4.4. DS

DS is expressed in many cells, and it can be found in high quantities in the skin (Trowbridge and Gallo, 2002). The basic disaccharide building block is composed of [IdoA

(1→3) $GalNH_2$], chemically formulated as [→4 α-L-IdoA (1→3) β-D-GalNAc (1→] (Figure 20) (Sugahara et al., 2003). Although 80–90% of the DS chain's uronic acid is epimerised to IdoA by C-5 epimerase enzyme, DS is considered as subtype of CS. In addition, the DS chain can acquire sulphate group at different positions on both IdoA and $GalNH_2$, which makes it highly negatively charged (Figure 20).

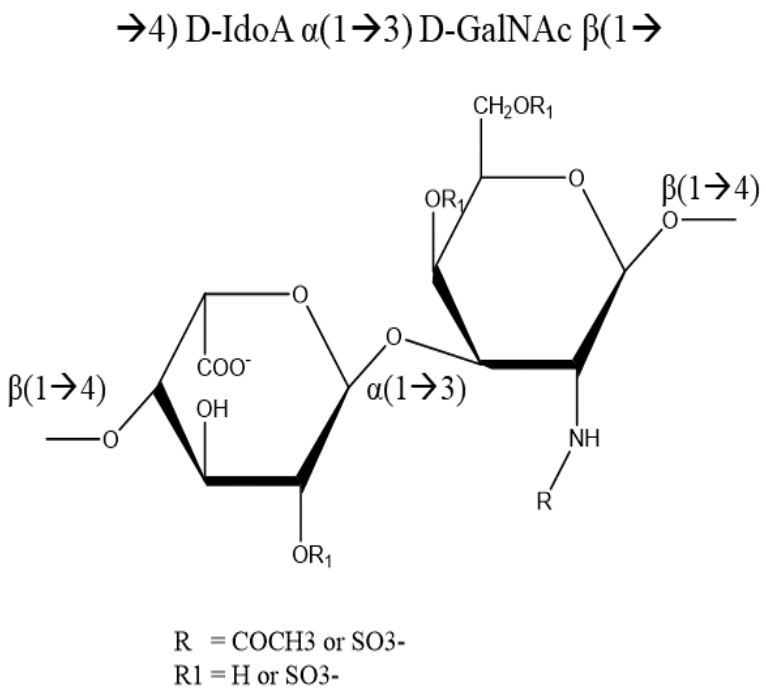

Figure 20. DS common disaccharide building blocks structure. During the modification phase, IdoA can acquire a sulphate group at C-2, and $GalNH_2$ can acquire a sulphate group at C-4 and/or at C-6 and the amino group (C-2) can be either acetylated or sulphated, depending on cell function (Höök et al., 1984).

1.4.4.1. Enzymatic degradation of CS/DS

Human chondroitin sulphatases are hydrolases enzymes, which are lysosomal and microsomal enzymes that can be found in various cells such as fibroblasts and leukocytes (Bond et al., 1997). These enzymes can hydrolyse CS-A, CS-B, and CS-C chains, resulting in the release of unsaturated disaccharides. In case of enzyme deficiency in humans, mainly CS and, to a lesser extent, DS and hyaluronic acid are accumulated in tissues (Linhardt et al., 2006).

A CS/DS degrading enzyme, known as chondroitinase-ABC, which is extracted from bacteria *Proteus Vulgars*. Chondroitinase-ABC is a broad-spectrum endoglycosidase that can

degrade chondroitin-4-sulphate (CS-A), dermatan sulphate (CS-B), chondroitin-6-sulphate (CS-C) and, to a lesser extent, hyaluronan. Chondroitinase-ABC can catalyse the elimination of polysaccharides containing a glycosidic linkage between [β-D-GalN (1→4) β-D-GlcA/-α-L-IdoA], resulting in unsaturated disaccharides (Figure 21) (Salyers and O'Brien, 1980; Huang et al., 2003).

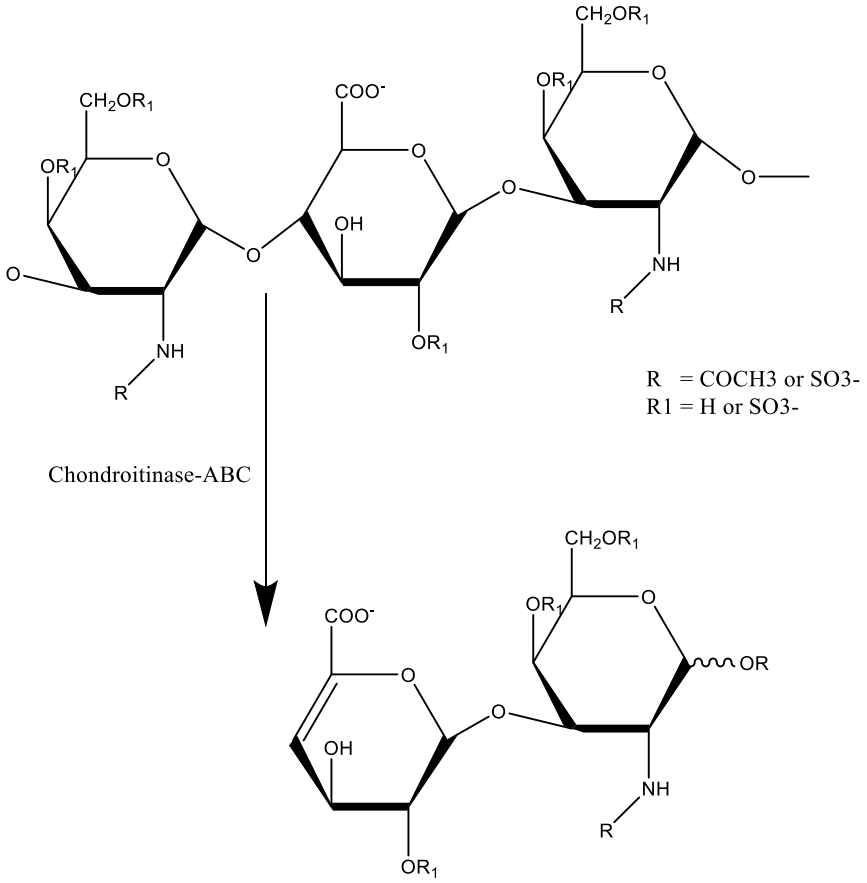

Figure 21. Chondroitinase-ABC reaction pathway. chondroitinase-ABC enzyme catalase the elimination of polysaccharides containing CS/DS chain β(1→4), resulting in unsaturated oligo- and disaccharides.

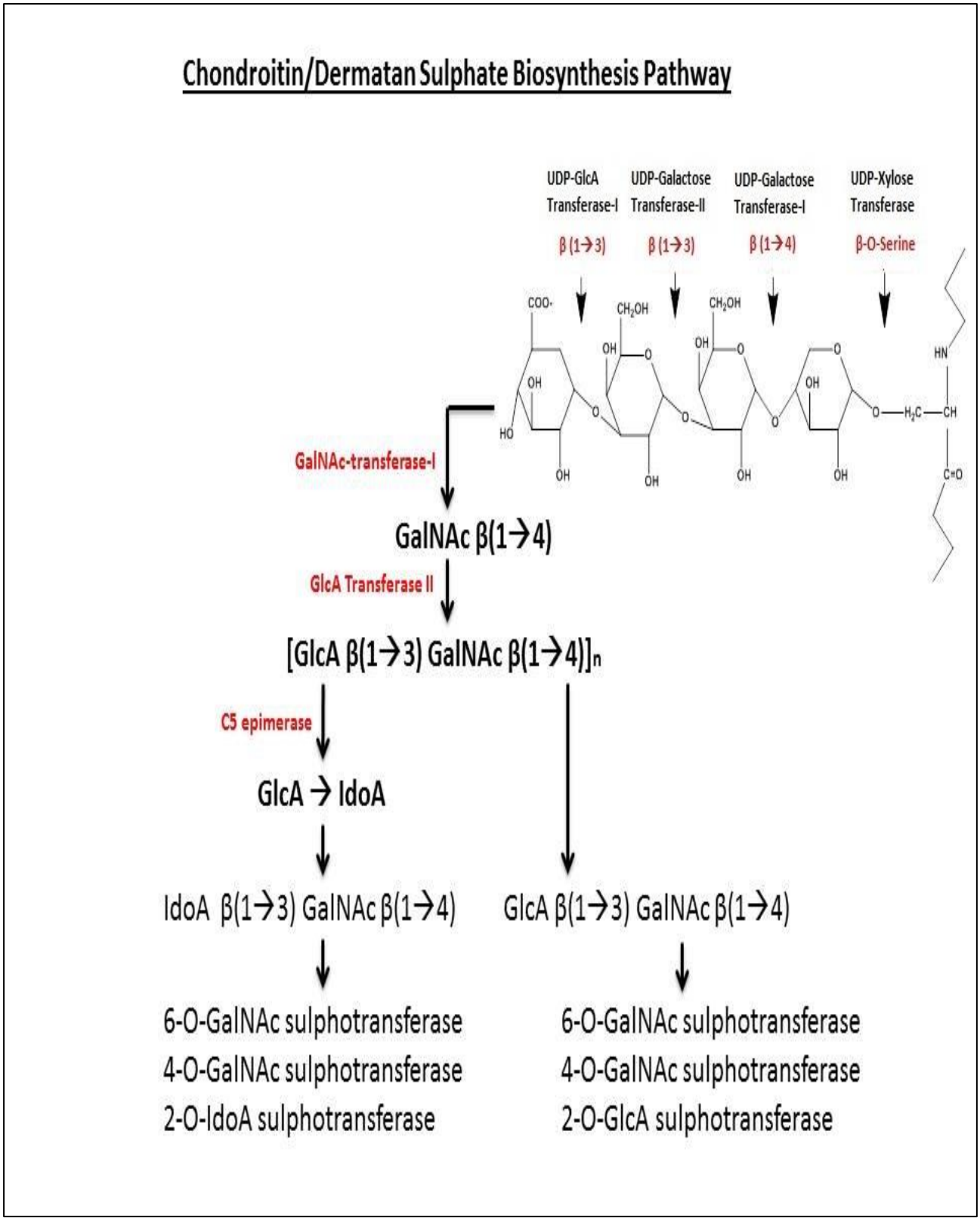

Figure 22. Schematic figure shows CS/DS biosynthesis pathway. Chain starts by addition of O-linked tetrasaccharides to Ser residues on the core protein. According to the cell type, specific enzymes catalyse the synthesis of either CS or DS.

1.4.5. KS

KS was first isolated from the cornea of a cow (Suzuki, 1939), then Meyer et al. (1953) isolated KS from bovine cornea, characterising it as keratosulphate, which refers to both sulphated disaccharide units of KS at Carbon-6. KS is a unique GAG type, as it lacks uronic acid residues on its basic structure, which consists of a linear polymer of repeated disaccharides of Gal and $GlcNH_2$ [→3) β-D-galactose (1→4) β-D-GlcNAc (1→] (Figure 23).

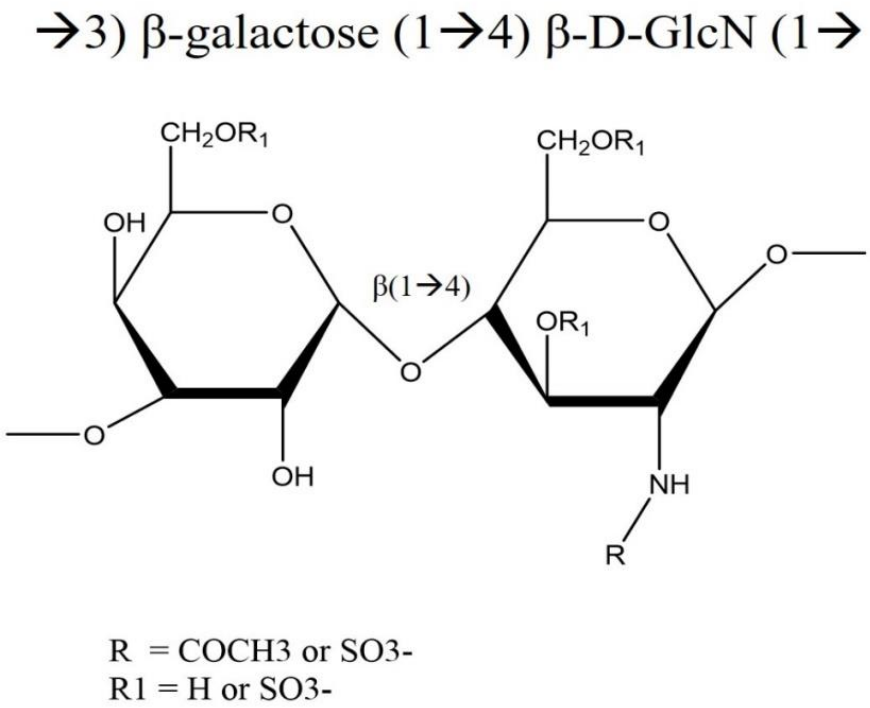

Figure 23. KS common disaccharide building blocks structure. During the modification phase, Gal can acquire sulphate group at C-6 and/or sialic acid at C-3, and $GlcNH_2$ can be capped with sialic acid at C-4, fucose at C-3 and/or sulphate group at C-4, C-6 and/or C-3 and the amino group (C-2) can be either acetylated or sulphated, depending on cell function. (Meyer et al., 1953; Funderburgh, 2000; Meininger et al., 2016).

1.4.5.1. KS classification and biosynthesis pathway

After the initial isolation of KS from bovine cornea, keratan sulphate proteoglycan (KSPG) was isolated from other tissues such as cartilage, which resulted in the discovery of various types of KS. Hence, KS was found to bind different core proteins in both N- and O-linked manners. As a consequence, KS was classified according to its linkages to the core protein into KS-I, KS-II, and KS-III (Krusius et al., 1986).

KS-I was first identified in the cornea as N-linked to the core protein via Asn residues, with molecular weight 20–25 kDa. The KS chain can acquire sulphate group on both GlcNAc and Gal anywhere on the chain. KS-I can be found non-sulphated, mono-sulphated, and di-sulphated by the action of sulphotransferases that catalyse the addition of sulphate groups (Esko, Kimata and Lindahl, 2009). KS-II is found in bovine articular cartilage, which has major disulphated pattern of sulphation, which act as cell surface ligands. It is found linked to the core protein, where the GalNAc is O-linked to Ser/Thr residues, in addition, Gal C-3 is usually capped with sialic acids, but GlcNAc C-3 can also be partially capped with sialic acids. Finally, KS-III was found to be O-linked to the core protein in the brain via mannose linked to Ser/Thr residues. Therefore, KS subtypes are not tissue-specific, it depends on the linkage structure (Funderburgh, 2000).

The KS chain can have variable length and sulphation patterns. Chain length is managed by the addition of sugar molecules to Gal and GlcNAc, resulting in chain branching and elongation or chain termination. This step depends on the cell type, and it is adapted in the *trans*-Golgi in addition to fucose and sialic acid as the chain's final decoration step (Stanley, Schachter and Taniguchi, 2009).

1.4.6. Hyaluronan

Hyaluronan is the simplest GAG type in terms of structure and modifications. It is composed of long unbranched and unmodified polysaccharide structure. Hyaluronan was originally called hyaluronic acid (Meyer and Palmer, 1934). Its basic repeating disaccharides is composed of GlcA (1→3) GlcNAc, which is chemically formulated as [→4 β-D-GlcA (1→3) β-D-GlcNAc (1→] (Figure 24).

Hyaluronan is not considered a PG for two reasons, firstly, it is not attached to the core protein as a sidechain (Almond, 2007); secondly, it is synthesised in the cytoplasm near the plasma membrane, which enables hyaluronan to polymerize more sugars and increase its mass, unlike other GAGs-related saccharides, (Fraser, Laurent and Laurent, 1997).

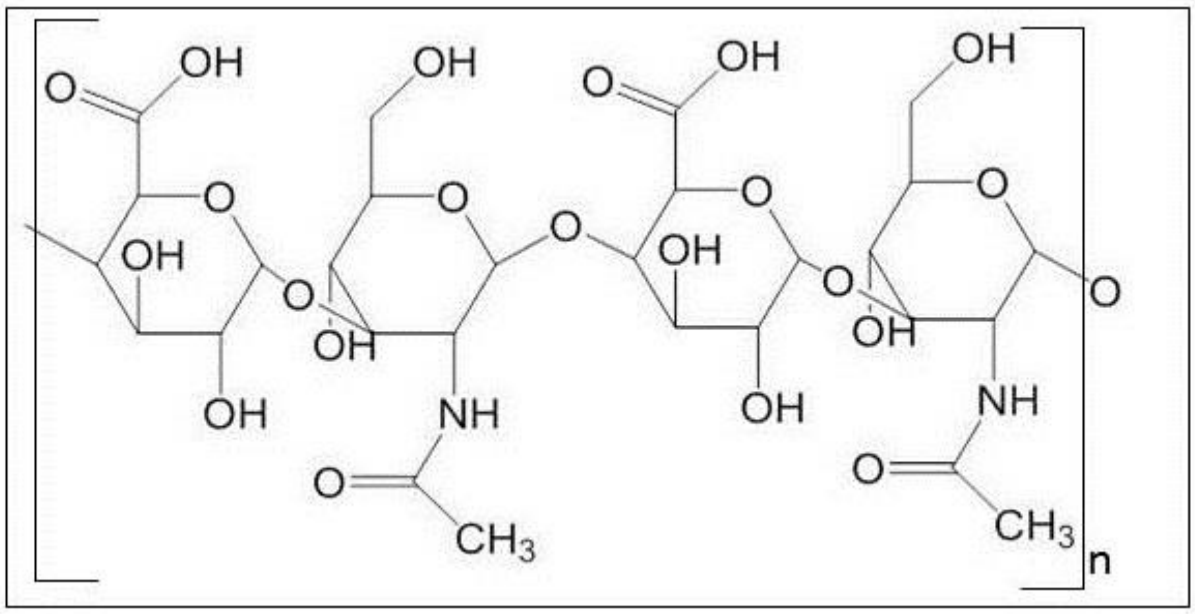

Figure 24. Hyaluronan saccharides structure, which is consist of long unbranched and unmodified GlcA-GlcNAc.

1.4.6.1. Hyaluronan biosynthesis pathway

Basically, hyaluronan is a unique type of glycan that differs from other GAGs because it is synthesized near the plasma membrane. Hyaluronan-synthase (HAS) is the enzyme that catalyses the addition of GlcNAc and GlcA from their UDP-substrates, resulting in the formation of hyaluronan building blocks (Figure 25). The HAS enzyme has four isoforms—HAS-A, HAS-B, HAS-C, and HAS-D. HAS-C is responsible for making UDP-Glc from glucose-1-phosphate; HAS-B encodes the hydrogenase enzyme to convert UDP-Glc to UDP-GlcA; HAS-D generates UDP-GlcNAc from UDP-glucosamine-1-phosphate and acetyl CoA. Finally, HAS-A encodes the synthesis of the hyaluronan chain by catalysing GlcNAc and GlcA from its precursors (Magee, Nurminskaya and Linsenmayer, 2001; Hascall and Esko, 2015).

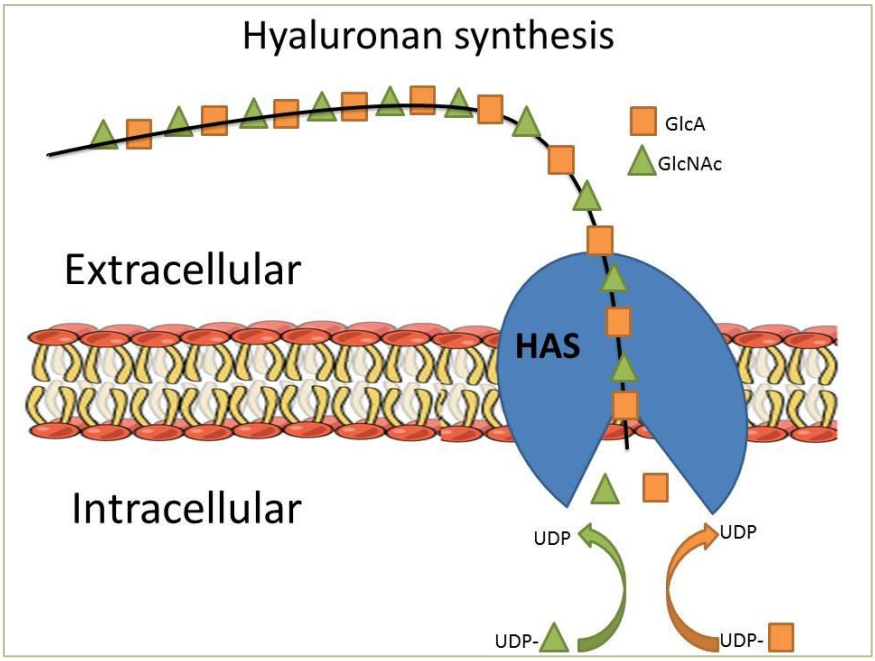

Figure 25. Schematic diagram of hyaluronan biosynthesis pathway by HAS enzyme family, where HAS is responsible for catalysing the addition of monosaccharides from their UDP-precursors. Then, hyaluronan is synthesized and maturated in the ECM (Hascall and Esko, 2015).

1.4.6.2. Hyaluronan degrading enzymes

Hyaluronan can be degraded to monosaccharides by enzymes known as hyaluronidases. The hyaluronidase gene (*HYAL*) expresses three enzymes: hyal-1, hyal-2, and hyal-3. Hyaluronan turnover mostly depends on cell type and can last up to one day. Degradation of hyaluronan can be achieved by either cellular endocytosis through CD44 or the lymph node. Hyal-2 is present on the cell membrane and degrades the hyaluronan chain into smaller fractions so fragments can enter the cell via endocytosis. In the cell, hyaluronan fragments are directed to the lysosome, as it has hyal-1, which can degrade fragments into monosaccharides via exoglycosidase enzymes such as β-glucuronidase and β-*N*-acetylglucosaminidase (Hascall and Esko, 2015).

1.5. Proteoglycans (PG)

Various cells can produce different types of PGs, which can be found secreted in the cytosol, bound to the cell membrane, on the basement membrane, or in the ECM. To date, serglycin is the only intracellular PG that has heparin and CS as glycoconjugates (Iozzo and Schaefer, 2015). Membrane-bound PGs have the ability to interact with various extracellular ligands. Extracellular PGs are thought to support cellular stability and function.

1.5.1. Secreted PG

The most well-known intracellular PG is known as serglycin (Bourdon et al., 1985). Serglycin PG carries highly sulphated GAGs, which can be assigned as intracellular PGs as well as secretory PGs that can secrete their contents into the ECM and onto the cell surface. Serglycin PGs can be found in various cells such as endothelial cells, haemopoietic cells, and pancreatic cells. GAGs have been found stored in granules in the mast cells, which contain heparin and to a lesser extent, CS-E; however, in monocytes and macrophages, they have been found freely existing without attachment to a protein core (Kolset and Tveit, 2008).

1.5.2. Basement membrane PGs

The basement membrane is one of the extracellular contents, and it plays an important role in maintaining haemostasis, modification of growth factor activity, and angiogenesis. On the basement membrane, there are several PGs such as collagen-XVIII, collagen-XV, perlecan, and agrin. Collagen-XVIII is expressed in cartilage, which belongs to the collagen family, and is characterised by the N-terminal region–triple-helical collagenous and non-collagenous domain–C-terminal region. HS can attach to collagen-XVIII via O-linked linkage on the non-collagenous region (Iozzo, 2005). Collagen-XV is expressed in many tissues except liver and brain cells. CS and HS can attach to its N-terminal non-collagenous domain (Amenta et al., 2005). Perlecan PG participates in cellular mitogenesis and adhesion, and it has HS attached via O-linkages (Iozzo, 2005).

1.5.3. Membrane-bound PGs

This type of PG comprises two large PG superfamilies—syndecan and glypican. The syndecan superfamily can be subdivided into four syndecan-members (1–4) characterised by a cytoplasmic domain, transmembrane region and an extracellular domain with G-protein coupled receptors that most likely have both HS and CS (Iozzo and Schaefer, 2015). Meanwhile, glypicans have six members (1–6) (Figure 26). According to Filmus et al. (2008), the glypican superfamily has the extracellular domain attached to the cell membrane via a glycosylphosphatidylinositol anchor (GPI) that acquires an HS chain (Sarrazin, Lamanna and Esko, 2011).

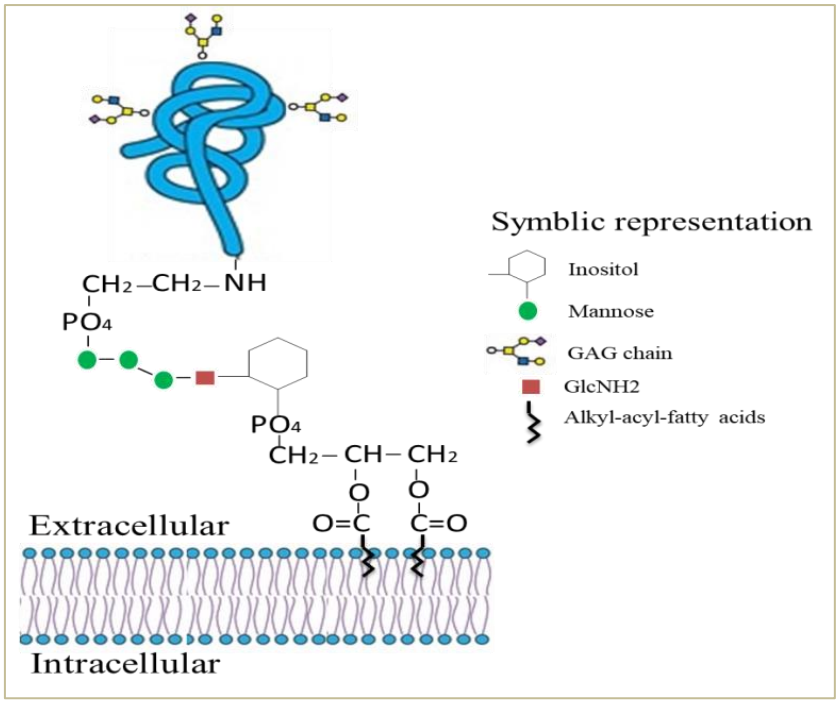

Figure 26. Schematic diagram showing membrane bound glypican PG via its GPI anchor.

1.5.4. Extracellular PGs

Extracellular PGs can be found in connective tissues. Their major function is to support the interstitial space between cells. Extracellular PGs can be subdivided into three superfamilies, namely lectican, leucine-rich, and testican. Lecticans can carry highly negatively charged GAGs such as CS and KS, and they can be subdivided into four PGs—aggrecan, versican, neurocan, and brevican.

Aggrecan PG has three regions: amino-terminal, central, and carboxyl-terminal. It is the major PG of the cartilage, which it supports by resisting compressional force as well as by retaining water. Leucine-rich PGs have a small molecular weight, about 40 kDa. This type of PG is known to help the organisation of collagen fibres in the cornea via their KS. Leucine-rich PGs can be subdivided into biglycan, decorin, fibromodulin, and lumican. Biglycan and decorin can carry two CS and DS. Fibromodulin has KS as a side chain, and it is expressed in tendons. Lumican can be found in the cornea and heart valves, and it carries KS (Yanagishita, 1993). Decorin has high binding ability to growth factors such as transforming growth factor β, and it can keep growth factors isolated in the ECM. Testican is an extracellular

proteoglycan, it can be subdivided into testican (1-3). Testicans are expressed in the thalamus and cerebrum. They can act as metalloproteinase inhibitors (Lee et al., 2018).

Table 3. Classification of proteoglycans based on their location (Iozzo and Schaefer, 2015).

Proteoglycan Location	**Classification**	**Predominant protein side chain**	**Predominant GAG**
Intracellular	Secretory granules	Serglycin	Hep/CS-E
Pericellular	Basement membrane	Perlecan Argin Collagen-XVIII Collagen-XV	HS HS HS CS/HS
Membrane-bound	Transmembrane GPI-Anchored	Syndecan (1-4) Glypican (1-6)	HS HS
Extracellular	Hyalectan lectican Small leucine rich PGs Spock	Aggrecan Versican Neurocan Bervican Biglycan Decorin Fibromodulin Lumican Testican	CS/KS CS CS CS CS DS KS KS HS

1.6. Glycosaminoglycan roles in normal cell physiological status

Generally, GAGs are known to have enormous structural heterogeneity, which can lead to several cellular and extracellular functions. GAGs' biological functions depend on the cell type and can vary from simple cellular function to cellular morphogenesis (Edgren et al., 1997). GAG-PGs have several structural and modulatory functions to maintain cellular organization, structure, and integrity. Extracellular PGs can protect polypeptides from non-specific proteolysis enzymes, and they can block antibody binding sites, in addition to storing several biologically important molecules such as growth factors. For example, the GAG chain can store heparin-binding growth factors near the cell that needs to be stimulated, which protects it from degradation and increases its life span (Varki and Gagneux, 2017). Furthermore, GAGs can increase PGs' affinity for extracellular ligands due to their negative charge and structural heterogeneity, acting as co-receptors for several soluble lectins such as enzymes, proteins, and growth factors (Mythreye and Blobe, 2009; Sarrazin, Lamanna and Esko, 2011). Stemming from this concept, GAGs can participate in various biological roles in cell development, adhesion, repair, wound healing, and coagulation (Wight, Heinegård and Hascall, 1991).

1.6.1. GAG's role in cellular development

Physiologically, GAGs are involved in normal cell development and growth, since they have high affinity to a wide range of growth factors. GAGs are thought to be the coupler between the cell membrane and the extracellular matrix via its PGs. This could be due to their structural diversity, which allows them to bind specifically to various extracellular lectins (Bernfield et al. 1999). GAG classes as HS, CS, KS, and hyaluronan have various roles in cellular development. According to Ornitz (2000), HSPG has a pivotal role in cellular development, as it plays a key role in activating fibroblast growth factors (FGFs) and their fibroblast growth factor receptors (FGFRs), which are known to regulate cellular development (Rabenstein, 2002; Stringer, 2006). HSPG contributes to the FGF-FGFR by accessing the complex's stability, sequestration, and activation (Ye et al., 2001). Yayon et al. (1991) clarified that FGFs essentially bind to surface HSPGs especially a specific highly sulphated HS sequence before binding to their FGFR to increase the complex's affinity and half-life.

HSPG interaction with FGF is a tightly regulated process which requires a specific HS sequence. As a consequence, altered HSPG structure, mutated HS synthesising enzymes, cells treated with HS degrading enzymes, or cells pre-treated with sulphation inhibitors might affect the FGF signalling pathway and the FGF-FGFR complex stability (Ornitz, 2000). Bullock et al. (1998) observed that mice with mutated 2-O-sulphotransferase enzymes had defective bone and kidney development, which could be due to a defective HS-FGF signalling pathway.

The literature has indicated a further role of GAGs during cellular morphogenesis, which is defined as the cellular developmental cascade that leads to the formation of well-organized and functional tissue, as reported in embryogenesis (Spooncer et al., 1983). Multiple elements participate in embryogenesis, such as signalling molecules and growth factors. It has been shown via animal studies that HSPG participates in embryogenesis, while a lack of HS alleles would result in developmental abnormalities. For instance, in mice with EXT1, which is an enzyme that extends GAG sequences, a hypomorphic allele has led to the development of skeletal muscle abnormalities (Bishop, Schuksz and Esko, 2007).

CS plays a key role in cellular development in conjunction with its PGs or as free GAG. As suggested by Shannon et al. (2003), CSPG plays an important role in supporting mammals' lung branching developments by interacting with growth factors. Indeed, lung cells treated with chondroitinase-ABC show inhibited lung branching, which supports the role of CSPG in this process. In addition, CS is involved in embryonic morphogenesis, as a mutated CS chain would result in growth abnormalities; for instance, the glycosyltransferase-I knockout gene in mouse oocytes has resulted in growth failure (Mikami and Kitagawa, 2013). Moreover, CS is considered to be the richest GAG-type in the central nervous system, where it can act as co-receptor to various growth factors such as brain-derived neurotrophic factor (B-DNF). CSPG's pattern of sulphation can affect its function, as reported in CS-A, which inhibits axonal regeneration after injury (Laabs et al., 2005), while CS-C appears to allow axonal regeneration (Mikami and Kitagawa, 2013). Thiele et al. (2004) emphasised that mutated chondroitin-6-sulphotransferase leads to the development of chondrodysplasia with spinal involvement.

It is also worth noting that hyaluronan has an important role during cell morphogenesis. High levels of hyaluronan have been observed in various proliferation and regeneration regions, as illustrated when mesenchymal stem cells migrate from the corneal

stroma to form the mature cornea, in atrioventricular cushion cells leading to the formation of heart valves, and in the embryonic brain ECM. Interestingly, hyaluronan concentration decreases after cellular differentiation and proliferation (Toole, 1997). In addition, hyaluronan causes swelling pressure on chondrocytes during bone development, resulting in bone growth, while in a bone erosion zone, CD44 has been observed to promote hyaluronan cellular endocytosis (Pavasant, Shizari and Underhill, 1994). During embryonic development, the ECMs of embryonic cells have a high amount of hyaluronan, which suggests that it plays an important role in embryonic development (Laurent, Laurent and Fraser, 1995).

1.6.2. GAGs' role in cellular adhesion

Cellular organisation defines a cell's overall final structure, which results from cellular interaction with various adhesion molecules. Cellular adhesion to the ECM is regulated by interaction of the adhesion molecules to maintain normal cellular physiological properties. Cellular adhesion molecules' major families are integrin, selectin, immunoglobulin, and cadherin. Cellular adhesion molecules' interaction with the ECM allows cells to attach to the ECM, detach from it, change shape, migrate, and divide. PGs can participate in adhesion process via the interaction between their GAG chains and the adhesion molecules and the ECM to maintain a cell's stability. For instance, the interaction between HSPG and the integrin can stimulate the cellular adhesion process (Wight, Kinsella and Qwarnström, 1992). On the other hand, Sage and Bornstein (1991) suggested that there are several PGs on the cell surface and on the cellular basement membrane, such as osteonectin and thrombospondin can interact with different extracellular elements, leading to release cells from the ECM and stimulating the cellular migration process. Furthermore, cellular migration also depends on the extracellular ligands and their interaction with the cellular GAGs. For example, cells upregulate their HSPG to facilitate cellular adhesion; by contrast, cells upregulate their surface CSPG to release cells from the ECM (Kinsella and Wight, 1986). In addition, hyaluronan would participate in cellular migration due to its physicochemical properties and its cell membrane receptor, known as receptor for hyaluronan mediated motility (RHAMM), which promotes cellular migration; therefore, cellular migration can be inhibited by hyaluronan degradation (Vigetti et al., 2014).

1.6.3. GAGs' role in wound healing and tissue repair

Tissue injury can be caused by trauma, heat exposure, cold exposure, or contact with chemical agents, amongst other factors. Wounds can be defined as damage to the normal physiological and anatomical structure and/or function of cells, which can be as simple as epithelial skin injury or as serious as bone injury. As part of the physiological process following tissue injury, the wound healing repair process is initiated by the surrounding cells to ensure that tissue regeneration occurs. The wound healing process includes cell proliferation, cell migration, angiogenesis, cell differentiation, and the synthesis of extracellular proteins and the release of growth factors and polypeptides to aid the healing process (Velnar, Bailey and Smrkolj, 2009). PGs can be involved in the wound healing process by activation of various elements such as heparin. Heparin is thought to support the wound healing process via the inflammation process. According to Mcpherson et al. (1988), heparin is released in wounds to support the healing process by increasing vascularization at the wound site, which can attract different types of growth factors, cytokines as well as extracellular proteins such as fibronectin to participate in this process, in addition to thrombocyte degranulation (Kratz et al. 1997). Bernfield et al. (1999) suggested that cell surface PGs such as syndecan can be over-expressed near the wound site, where syndecan-1 and syndecan-4 levels increase in the wound margins of proliferating cells. Syndecan-1 is thought to help newly generated keratinocytes to migrate to the wound site after complete healing. In addition, neutrophils can release heparinase enzymes in the wound site to depolymerise HS chain from its PG, which is required to activate FGFs that is needed for the healing process.

DSPG plays a pivotal role in skin wound healing. During skin wound injury, DSPGs are upregulated through their syndecan-1 and syndecan-4 in keratinocytes to stimulate endothelial leukocyte adhesion molecules and promote FGF-2 to enhance the repair mechanism. In addition, the present of high levels of DSPG as decorin or biglycan might associate with scarring (Trowbridge and Gallo, 2002). Hyaluronan has a very large molecular weight compared with other GAGs. It has various biological roles including in wound healing process. According to John and Giovanni (2002), hyaluronan enhances the cellular inflammatory response via chemotactic pro-inflammatory molecules and increases inflammatory cells' infiltration to the injury site, and Sherman et al. (1994) suggested that hyaluronan enhances cellular migration to the wound healing site.

1.6.4. GAGs' roles in coagulation

The best-studied GAG-type with anticoagulant activities is heparin. Heparin's anticoagulation activity was discovered by Howell & Holt (1918). This discovery has led to an evolution in clinical practise, especially in patients with blood disorders such as myocardial infarction and pulmonary embolism, amongst other disorders that require well-maintained circulation (Shriver et al., 2012).

When normal haemostasis condition is impaired, for instance, by blood vessel injury, this leads to activating primary and secondary haemostasis mechanisms to prevent haemorrhage. The primary haemostasis mechanism activates platelets to prevent haemorrhage via initiating plugging and activating the secondary haemostasis mechanism. The secondary haemostasis mechanism starts by activating coagulation proteins known as coagulation cascade that ultimately form firm blood clots by converting soluble fibrinogen to insoluble fibrin via activated thrombin (Hoffbrand and Moss, 2015) (Figure 27).

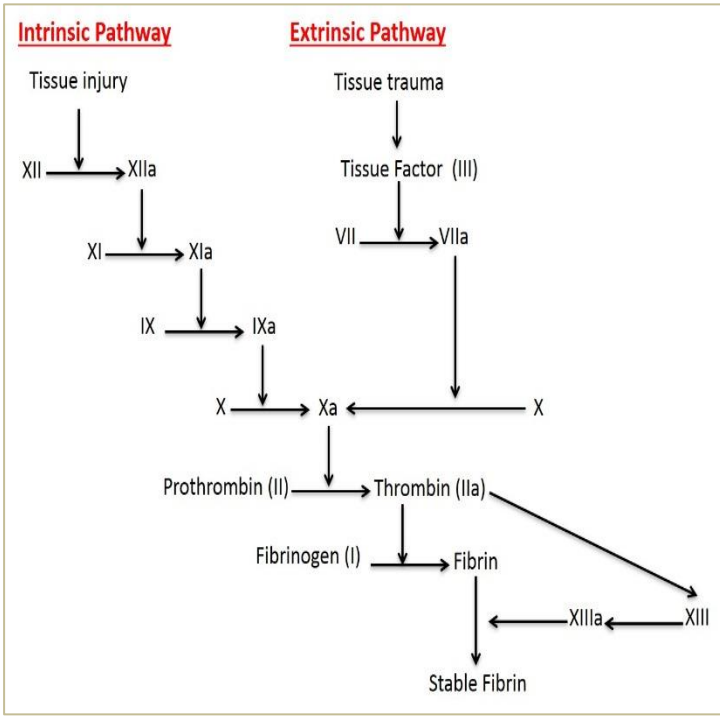

Factor Number	Name	Active form
I	Fibrinogen	Fibrin subunit
II	Prothrombin	Serine protease
III	Tissue factor	Receptor/cofactor
V	Labile factor	Cofactor
VII	Proconvertin	Serine protease
VIII	Antihaemophilic factor	Cofactor
IX	Christmas factor	Serine protease
X	Stuart-Prower factor	Serine protease
XI	Plasma thromboplastin antecedent	Serine protease
XII	Hageman factor	Serine protease
XIII	Fibrin-stabilizing factor	Transglutaminase

Figure 27. Schematic diagram of the coagulation cascade (Hoffbrand and Moss, 2015).

However, blood has a counter-protease that can inhibit this coagulation process known as antithrombin-III, which inhibits the activation of various coagulation proteins, especially factors II and X. Heparin with 15-19 kDa molecular weight has the capability to enhance antithrombin-III activities. The major area of interest in heparin's structure is its

minimal, unique pentasaccharide sequence with a potent anticoagulation role, which is composed of [GlcNAc/S(6S) (1→4) GlcA (1→4) GlcNS(3,6S) (1→4) IdoA(2S) (1→4)GlcNS(6S)] (Figure 28) , however, unfractionated sequence can be as trisulphated-(disaccharides)-pentasaccahride-disulphated(disaccahride) (Onishi et al. 2016).

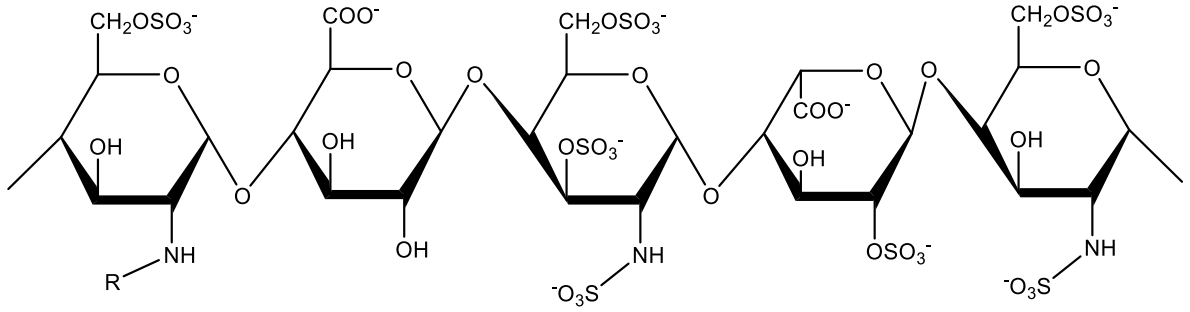

R = SO3- or COCH3

Figure 28. Heparin minimal pentasaccharide structure with unique anticoagulation properties.

This heparin minimal pentasaccharide sequence is required to attach to the antithrombin-III, which interacts with coagulation factor X to inhibit the conversion of pro-thrombin to thrombin. As a result, heparin aids in the deactivation of the coagulation cascade and prevents the formation of blood clots (Rosenberg and Lam, 1979). Furthermore, there is another protease that can enhance thrombin inhibitory process, known as heparin cofactor-II (serpin). This particular protease can inhibit the activated thrombin from activating fibrinogen in the present of several GAGs such as heparin, HS, CS, and DS (Wu, Monroe and Church, 1995).

Although heparin interaction with heparin cofactor-II can result in 1000-folds anti-thrombin activity, oversulphated DS is considered to be a replacement for heparin therapy in patients with heparin side-effects such as thrombocytopenia, as DS's unique hexasaccharides' structure $[(IdoA(2S)\text{-}GalNAc(4S)]_3$ can inhibit the coagulation process by 100-fold through binding to heparin cofactor-II that inhibit thrombin as well as it can inactivate thrombin bound to fibrin (Prabhakar and Sasisekharan, 2006).

1.7. Normal cellular growth

Normal cell division is an essential mechanism to maintain the body's physiological status. Cells divide following a very tight and rigid process known as the cell cycle. The cell cycle is a fundamental component of normal living cells, and it consists of the consecutive

processes of interphase and mitosis. Interphase consists of three phases, namely growth phase 1 (G_1), synthesis phase (S), and growth phase 2 (G_2). In G_1 phase, cells either become prepared entering S phase or it can leave the cell cycle by entering G_0, where cells don't divide, for instance, neurones. During S phase, the most important mechanism is duplication of centrosomes and DNA duplication, where 23 pairs of chromosomes are duplicated resulting in 46 pairs of chromosomes. Then the cell enters G_2 phase, where cells are prepared for mitosis; in this phase cells, for example, initiate microtubules that segregate chromosomes.

Next, cells will enter the mitosis phase, where the cell is divided into daughter cells. Mitosis is divided into different phases, which are prophase, prometaphase, metaphase, anaphase, telophase and cytokinesis. Prophase is the first stage of mitosis, where chromosomes are condensed, and mitotic spindles are formed. Following this, the prometaphase starts by rupture of the nuclear membrane and microtubules attaching to the chromosomes. In the metaphase, all microtubules attached to chromosomes and it all rests in the middle of the cell. During the anaphase, the most important sign is separation of cellular chromatin into two parts. Finally, in the telophase each chromatid is separated from each other, which is the end of mitosis, following which cytokinesis, where the parent cell physically divide into two daughter cells (Park and Lee, 2003).

1.7.1. Cell injury

When cells experience physiological stress like ischemia or potential injury such as infection or exposure to toxins, they can undergo an adaptation process known as reversible injury. However, when the cell injury persists, or the injury is severe, the cellular adaptation mechanism is unable to adapt the physiological status, which makes this injury irreversible, so cell death is established. In addition, cell death can occur in normal status, as in genetic abnormalities of the cell cycle.

After irreversible cellular injury occurs, cell death is proposed to occur by different mechanisms according to the potential cause of cell death, its intensity, and its duration. Rapid and severe disturbances can cause an uncontrolled cell death known as accidental cell death that usually caused by toxins, infections, or trauma, which is morphologically demonstrated as necrosis. In necrosis, all cellular contents leak out, resulting in cellular digestion, which cannot be avoided by cellular adaptation mechanisms, thus, this type of cell death promotes inflammation via the substances released from dead cells in order to start the

repair process. In contrast, when normal cells are forced to die or when cell injury is not severe, cells activate a regulated molecular pathway to facilitate the cellular death process, which is morphologically known as apoptosis. Typically, apoptosis occurs in healthy tissues, and it does not always refer to a pathological event. Cells with intrinsic abnormalities can induce apoptosis by activating certain enzymes that degrade their own DNA and cytoplasmic proteins without causing inflammation; hence, this is called programmed cell death. Programmed cell death can be caused through intrinsic or extrinsic pathways. Both pathways ultimately activate intracellular endoprotease enzymes called caspases. This caspase cascade process cleaves cellular proteins and nucleic acid, resulting in an altered cellular membrane that allows dead cells to be removed by phagocytes (Elmore, 2007).

During the extrinsic apoptotic pathway, cells express death receptors. When cells express their own apoptotic receptors, which can be activated by different ligands such as tumour necrosis factors or T-lymphocytes then the activated receptors activate the cytoplasm domain, resulting in activating further caspases to induce apoptosis. Meanwhile, the intrinsic pathway, which is also known as the mitochondrial pathway, has several proteins that can induce apoptosis. In the mitochondria, there are two families of pro-apoptotic and anti-apoptotic proteins, which are well-balanced during cellular physiological status. When cellular physiological status is altered, the mitochondrial membrane becomes permeable, and the proapoptotic proteins can leak out into the cytoplasm. For instance, cytochrome-c, which is a proapoptotic protein leaks out from the mitochondria into the cytosol, resulting in the activation of the caspase cascade mechanism and eventually apoptosis (Kumar, Abbas and Aster, 2017).

1.8. Cancer progression

Normal cell growth is well regulated by the cell cycle regulator mechanism via the action of cyclin-dependent kinase (CDK) and cell cycle checkpoints. When the cell cycle's function is altered, and the cell cycle repair mechanism is suspended, cancer can develop. There is a wide range of cell cycle alterations that might occur—for example, cell cycle mutation in proto-oncogene, tumour suppressor gene or cell cycle misregulated checkpoints. Each one of these mutations may give rise to tumorigenesis.

Active cyclin and kinases, which have been the subjects of many classic studies on normal cell cycle division and regulation, are responsible for cell cycle progression. Various CDK-inhibitors are released to inhibit the cell cycle progression—for example, *p*53, which is

a tumour suppressor gene. In other words, when the *p*53 tumour suppressor gene mutates/supressed, this can result in the complete absence of CDK, which alters the cell cycle division and leads to the progression unregulated cell division. According to Park and Lee (2003), the development of unregulated cellular division after a point of mutation results in chromosomal abnormalities that eventually increase the probability of cancer progression (Figure 29).

Tumours can be divided into benign or malignant. Benign tumours are made up of differentiated and localised cells and are amenable to surgery without massive fear of metastasis. Malignant tumours are made up of undifferentiated aggressive cells, and have the potential to invade other tissues and spread all over the body; this type of tumour is called a neoplasm, which means "new growth" (Kumar, Abbas and Aster, 2017).

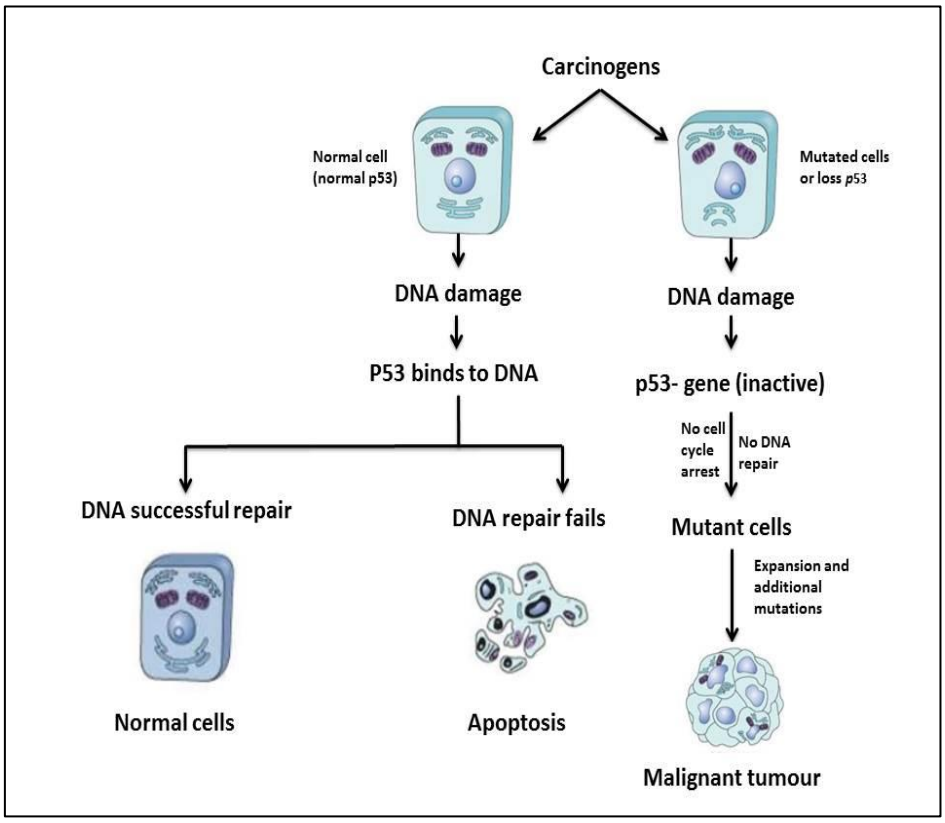

Figure 29. Schematic diagram of cancer progression resulting from inactive tumour suppressor gene *p*53 leading to uncontrolled proliferating cells (Kumar, Abbas and Aster, 2017).

1.9. Cancer epidemiology and incidence

Cancer epidemiological studies have linked some risk factors to cancer progression. Cancer predisposing factors such as age, environment or race can participate in cancer

progression. For instance, cancer risk frequently increases with age, smoking cigarettes increases the risk of lung cancer, and food intake quality and food with less fiber contents might increase the risk of colon cancer. In the United Kingdom, there were over 360,000 new cases of cancer in 2015—that's nearly 990 daily diagnoses with higher incidence of breast, prostate, lung and bowel cancer. In 2015, 8.8 million people died worldwide due to cancer. Leukaemia had 9,900 cases diagnosed in 2015 and 4,712 deaths in 2016. There were 2,697 patients diagnosed with mesothelioma in 2015 and 2,496 deaths were reported in 2016 (Cancer Research UK, 2017).

1.10. Glycosaminoglycans' role in cancer progression

It is well-known that cancer cells' microenvironment has a major role in stimulating tumour growth via interaction with ECM molecules. More recently, there has been great interest in PGs proangiogenic roles. HSPG has significant abilities to bind different growth factors and their splices that occur in the neoplastic area, such as vascular endothelial growth factors (VEGFs) and FGFs. As a result, it could alter the body's physiological status in the case of malignancy, to promote angiogenesis and cancer metastasis (Zhang, 2010).

A tumour's angiogenesis process is stimulated by autocrine cancer clonal growth factors, which in turn stimulate tumour endothelial cell PGs to fine-tune VEGFs to induce tissue remodelling. Ultimately, this process leads to angiogenesis and tumour growth (Stanley et al. 1999). The tumour becomes moderately acidic and hypoxic, so tumour cells express hypoxia-inducible transcription factors (HIFs), which stimulate synthesis of VEGFs, especially VEGF-A to sustain continued growth by increasing the tumour's blood supply. Thereafter, when the neoplastic hypoxic condition is greatly evolved, various types of growth factors bind to HSPGs to fine-tune tumour growth. According to Zhang (2010), when a tumour's hypoxic condition progresses, neoplastic cells alter HSPG's structure, enabling it to bind as much as growth factors, which eventually results in cancer metastasis (Witsch, Sela and Yarden, 2010). As mentioned before, HSPG has two main membrane-bound proteoglycan families, syndecan and glypicans, and one important basement membrane PG known as perlecan; thus, it modulates various functions of the neoplastic cells. For instance, HSPG shows a high ability to bind FGFs, as it is upregulated in angiogenic regions, suggesting HS's role in cancer progression (Blackhall et al., 2001; Zhang, 2010).

The cellular response to different pathological conditions can result in up- or down-regulated CSPGs as it has different roles in cellular proliferation and morphogenesis. CS/DS

role is highly dependent on the sulphation pattern and chain length of their structure (Asimakopoulou et al. 2008; Kalathas et al. 2011). According to Kalathas et al. (2011), CSPGs' synthesising and degrading enzymes have been found in colorectal cancer, which would explain the role of CS in neoplastic cells. In various cancer cells, CSPG has been observed to be abnormally upregulated, which enable it to interact with enormous intracellular and extracellular molecules. Versican and aggrecan, which are extracellular PGs that carry CS as a side chain, might have major roles in cancer metastasis (Asimakopoulou et al., 2008).

Versican has been detected in high concentrations in prostate, brain, breast, and gastric cancer. High concentration of versican promotes tumour cells' growth and metastasis by interaction with various growth factors, especially platelet-derived growth factors (PDGF), which are known to promote cellular growth and division by inducing angiogenesis. In addition, versican has been found upregulated in metastatic melanomas and correlated with poor prognosis in prostate cancer (Asimakopoulou et al., 2008). Furthermore, versican has been found upregulated by the action of transforming growth factor-β in osteosarcoma cells, which indicate a poor prognosis. High levels of CS-E were observed in ovarian adenocarcinoma as it is thought to modulate growth factor function (Afratis et al., 2012).

Cancer cells' migration processes require remodelling of the ECM, which can be induced by depolymerisation of the ECM to promote remodelling and cell migration. For example, cancer cell metastasis can be stimulated by depolymerisation of aggrecan which promotes cancer cell motility by binding to adhesion molecules such as selectins on the endothelial cells via its CS and CD44, resulting in cellular migration. Inhibition of CS formation by treating cells with chondroitinase would result in great inhibition of cellular migration. This result elucidates CS's role in cancer metastasis (Asimakopoulou et al., 2008).

Another extracellular GAG that can promote cancer cell invasion is hyaluronan, which has been found to regulate cancer cell signals during the tumour invasion process (Fuster and Esko, 2005). In addition, high levels of hyaluronan have been found in various malignancies, such as adenocarcinomas, which might indicate its role in cancer morphogenesis and poor prognosis (Heldin et al., 1996).

Overall, common GAG-types have proangiogenic roles, which can promote cancer and cancer metastasis. This is due to their potential capabilities to bind to various lectins such as growth factors and adhesion molecules. Therefore, it is very important to know the role of

GAGs in cancer cells' progression in order to determine the possible therapeutic targets in regard to GAG anticancer therapies.

1.10.1. Cancer treatment related to GAGs' pathological roles

As previously discussed, GAGs have various physiological and pathological roles in cell biology. Targeting GAGs and related products can enhance cancer therapies and inhibit cancer progression in several ways. Firstly, directly targeting growth factors and cell surface receptors that are used by GAGs to promote cancer cell growth by using monoclonal antibodies. As illustrated in certain neoplasms, targeting a tumour's autocrine VEGFs is preferred to inhibit tumour growth and metastasis. This is done by administrating pharmaceutically targeted antibodies against growth factors such as anti-VEGF (Hurwitz et al., 2004). Unfortunately, there are several drawbacks to using this type of treatment. Foremost, this type of specific antibody therapy has a fundamental limitation due to the expression of growth factor splices such as FGF-2, which have a greater capability of inducing tumour metastasis, and in very acidic tumours VEGFs can result in different variants as the tumour progresses. Additionally, antibody-based therapy increases treatment costs (Sandler et al., 2006; Zhang, 2010). Secondly, blocking GAGs' proangiogenic roles, for example, blocking HSPG from fine-tuning growth factors to progress cancer growth and inhibiting heparinases activities that may finally lead to cancer metastasis (Zhang, 2010).

Another selective cancer therapy target is the cell surface transmembrane CD44, which interacts with several adhesion molecules to aid cellular migration. Therefore, its expression is very tightly regulated in normal cells, however, it was found to be highly upregulated in malignant cell surface. CD44 was observed in several tumours as its levels would indicate tumour behaviour and it was thought to be associated with cancer stem cells that would lead to cancer resistance (Liu and Jiang, 2006). According to Zöller (2011), CD44 is associated with tumour biological events such as growth and metastasis, and elevated levels could be related to poor prognosis, which make it a favourable target in cancer selective therapy. *In-vitro* anti-CD44 therapy has successfully inhibited tumour cells' growth and induced apoptosis on undifferentiated leukemic cells, and it could inhibit their progenitor cells (Liu and Jiang, 2006).

Thirdly, targeting the angiogenic factors that are released from neoplastic cells. An example of these tumour angiogenic factors is the epithelial HSPG. Malignant epithelial cells overexpress HSPG in order to increase cancer cells' interaction with the extracellular growth

factor ligands to promote cell growth. Hence, HSPG has great affinity to various growth factors that can lead to cell morphogenesis as well as angiogenesis (Zhang, 2010). Therefore, blocking a tumour cell's HSPG binding sites would decrease its growth factors' binding domains, discontinuing its potential proangiogenic role. Thus, Lamanna (2008), suggested blocking HSPG's proangiogenic activities by using sulphatase enzymes. Sulphatases catalyse the hydrolysis of sulphate groups on GAGs' structure leading to minimising GAGs' biological functions. As an illustration, there are two cell surface HS sulphatase enzymes, known as sulphatase-1 (Sulf-1) and Sulf-2. These sulphatases can contribute to HS structure-activity via endolytic glucosamine 6-O-sulphate from the HSPG chain; these conformational changes would lead to a change in HS's biological function. Furthermore, regarding FGF's crystal structure, FGF's binding to HSPG and its FGFR requires a specific HS sequence with N-sulphated and 6-O-sulphated molecules to increase complex affinity (Yayon et al., 1991). Hence, Sulf-1 and Sulf-2 are determined to be potential tools in cancer therapy, especially in metastatic neoplasms, to minimise cancer cell interaction with extracellular environment as well as to reduce HSPG's angiogenic effectiveness.

Another therapeutic intervention could be done by launching new compounds that have greater affinity for these growth factors than membrane-bound HSPG—for instance, polysulphated-HS-like with a similar sequence to that of the cell membrane HS would have greater affinity for various growth factors than malignant cell HSPG (Rusnati and Urbinati, 2009). Zhang (2010) emphasised that novel compounds such as polysulphated-HS-like can compete with cellular HSPG for growth factors. Johnstone et al. (2010) highlighted that using either a polysulphated pentasaccharide or a polysulphated tetrasaccharide sequence as an HS-imitative compound might become a potential angiogenic antagonist.

Another proangiogenic factor is heparinase enzyme, which digests cell surface HSPG and releases HS unsaturated disaccharides or oligosaccharides. It is physiologically produced from embryonic placenta and lymphoid organs (Vlodavsky and Friedmann, 2001). According to Haimov-Kochman et al. (2002), heparinases are found in large amounts in placenta cells, where their function is thought to involve facilitating growth factors release in the ECM in order to support placental cell development. Contrary to heparinases' physiological function, there is great evidence that suggest heparinases are produced by tumour cells, especially in poorly differentiated carcinomas, promoting cellular invasion and cancer metastasis. As revealed by Koliopanos et al. (2001), a patient's blood test with elevated heparinases would indicate very poor prognosis. It was suggested that after treatment with polysulphated-HS,

tumour cells release heparinases to cleave cell surface HSPG and the extracellular polysulphated-HS-rich in growth factors in order to reactivate the tumour angiogenesis process (Zhang, 2010). Overexpression of heparinases could lead to cleaving HS from its syndecan, which plays a crucial role together with VEGF-A, in facilitating the growth of cancer endothelial cells and accelerates the tumour's growth by activating full-length HSPG activity. Indeed, inhibition of neoplastic heparinase activity would be favoured, since it could reactivate cancer and promote cancer metastasis (Vlodavsky and Friedmann, 2001).

1.11. Blood cancer

Blood cells arise from pluripotent hematopoietic stem cells (HSC) situated in the bone marrow in long bones. HSC have immunological markers that differentiate it from other cell types, however, the exact phenotype is unknown (Hoffbrand and Moss, 2015). Cellular differentiation arises from stem cells to progenitor cells with self-renewal properties, which are capable of producing different blood cell linages. Progenitor cells give rise to either common myeloid lineage or common lymphoid lineage progenitor cells. The term myeloid refers to erythrocytes, megakaryocytes, mast cells, and leukocytes, where leukocytes can be further subdivided into neutrophils, eosinophils, and basophils. The term lymphoid refers to T-lymphocytes, B-lymphocytes, and natural killer cells (Figure 30) (Moore, Knight and Blann, 2016).

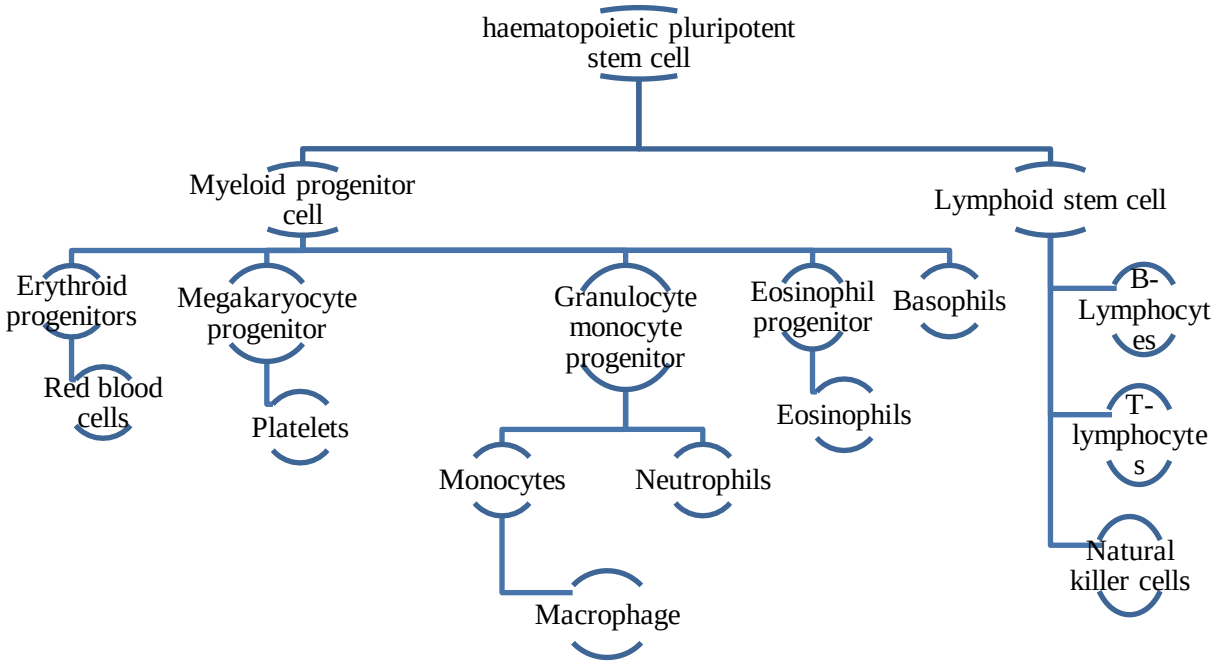

Figure 30. Schematic diagram represents blood cell lines from the bone marrow. Starting from haematopoietic stem cell that is arise from the bone marrow. The common myeloid progenitor cells (left side) that produce red blood cells, platelets, monocytes, neutrophils, eosinophils and basophils. The lymphoid stem cell (right side) can produce B-lymphocytes, T-lymphocytes and natural killer cells.

Haematological malignancies can affect any blood cell lineage from cells situated in the bone marrow to the peripheral lymphoid cells, for instance, leukaemia. Leukaemia is a type of blood cancer, which affects about 3% of the United Kingdom population who are diagnosed with cancer (Cancer Research UK, 2017). The haematological cells can become malignant either due to genetic factors or environmental factors such as radiation and drugs. Genetic mutations can occur due to defects in either tumour-suppressor gene or proto-oncogenes, which would lead to point of mutation. For instance, gain of tyrosine kinase function would affect the secondary messenger resulting in unregulated proliferation of blood cells. Genetic deletion would result in blocking of B-lymphocyte (B-cell) maturation, resulting in enormous number of undifferentiated B-cell clone (Vitanza et al., 2014).

Leukaemia can be classified based on disease progression to either chronic or acute. Chronic leukaemia is characterised by slow development of malignant blood cells with either myeloid or lymphoid linage. In contrast, acute leukaemia is characterised by fast-growing malignant cells with either myeloid or lymphoid linage. It is necessary here to clarify what is

meant by lymphoma in order to differentiate it from leukaemia. Lymphoma is a malignancy of blood lymphocytes with lymphoid organs origin, such as lymph nodes. Lymphoma is diagnosed if there is a link to a primary lymphoid origin (Moore, Knight and Blann, 2016), however, malignant lymphocytes present in the bone marrow is considered as leukaemia. There is a strong possibility of differentiating between leukaemia and lymphoma by studying the bone marrow picture, if more than 25% of bone marrow lymphocytes are affected, it is considered as leukaemia (Ross et al., 2011).

Regarding chronic leukaemia, it can be difficult to cure as it can be divided into chronic myeloid leukaemia (CML) or chronic lymphoid leukaemia (CLL). CML can be subdivided into six-types among the myeloid lineage with 742 new cases in the UK per year; in addition, CLL affect any lymphocytes lineage with 3709 new cases per year in the UK. The most common type of CML is known as CML-Philadelphia positive. This type of malignancy occurs due to abnormal gene translocation between chromosome 9 Abelson proto-oncogene (*ABL*) and chromosome-22 (*BCR* gene), resulting in a fusion protein with tyrosine kinase activity that cause the pluripotent stem cells to proliferate uncontrollably (Hoffbrand and Moss, 2015).

Acute leukaemia is presented as bone marrow proliferation of fast-growing immature blood cells in the blood, which is known to be an aggressive disease, which needs immediate medical intervention (Rocha et al., 2001). According to which progenitor cell type is affected, acute leukaemia is either acute lymphoid leukaemia (ALL) or acute myeloid leukaemia (AML) (Bomken and Josef Vormoor, 2009). ALL incidences are more common than AML. In the United Kingdom, approximately 300 children are diagnosed with ALL annually (Bomken and Josef Vormoor, 2009). According to Raimondi et al. (1988), T-lymphocyte acute lymphoblastic leukaemia (T-ALL) affects about 15% of children with ALL, and it is believed to affect more boys than girls, with a ratio of 3:1. In comparison to T-ALL, B-lymphocyte acute lymphoblastic leukaemia (B-ALL) affects about 85% of children. Nearly 90 children are diagnosed with AML per year in the United Kingdom, with moderately higher incidence in boys than girls (Bomken and Josef Vormoor, 2009). AML incidence is greater during infancy and late adulthood, which affects about 25% of children (Deschler and Lübbert, 2006).

1.12. Malignant mesothelioma

Mesothelium cells are composed of squamous epithelium that lines several body cavities, such as thoracic (pleura cavity), peritoneum (abdominal cavity) and mediastinum (heart sac). Malignant mesothelium cells known as mesothelioma, most frequently occur in the thoracic cavity with asbestos exposure. Cancer has several risk factors that can affect cell growth resulting in uncontrolled proliferation, while mesothelioma is type of cancer which has no definite cause; however, thoracic mesothelioma has a link to asbestos exposure (American Cancer Society, 2018).

Mesothelioma can be divided to three types based on cell morphology as epithelioid, sarcomatoid and biphasic. Epithelioid mesothelioma, according to its cell-type can be treatable with good prognosis. Secondly, sarcomatoid mesothelioma type is uncommon, and is known to be the most aggressive type with poor prognosis, is characterised by spindle shape cells. Sarcomatoid mesothelioma can be subdivided into desmoplastic and lymphohistocytoid mesothelioma. Both subtypes are morphologically similar to other cancer cells, such as lung carcinoma (Klebe et al., 2010). Thirdly, biphasic mesothelioma is composed of mixed type of epithelioid mesothelioma and sarcomatoid mesothelioma, which makes its treatment dependent on the predominant cell type present in the tissues.

1.13. Cancer treatment

There are several types of anticancer treatments such as surgery, chemotherapy, radiotherapy, stem cell therapy, immunotherapy, hormone-therapy, precision medicine and many new approaches in clinical trials. Various new cancer treatment regimens have been launched due to progression of severe forms of cancer that have become more resistant to standard therapies. Growing evidence suggests the presence of cancer stem cells that can lead to drug resistance. Cancer stem cells are defined as a small cell population from a tumour's lineage with self-renewal properties, leading to tumour regrowth and metastasis even after treatment. Therefore, the choice between different types of cancer therapies depends heavily on the disease's severity and the type of malignant cells, aiming to reduce cancer cell resistance, which may result in treatment failure (Prieto-Vila et al., 2017). To this end, various anticancer drugs are used in combination therapy, which defined as using different type of drugs or treatments to minimise drug resistance. Although most anticancer drugs have several side-effects such as anaemia, diarrhoea, constipation, hair loss, infection, nausea, and

fatigue, commonly used anticancer treatments such as chemotherapy, radiotherapy and stem cell transplants have cured 50% of cases in the UK (Cancer Research UK, 2017).

Initially, chemotherapy treatment can be defined as using chemical substances to stop or slow cellular growth, including that of normal and malignant cells, which can make it unpleasant treatment for patients; however, it is very effective. This type of therapy can be used solely or in combination with other therapies. Chemotherapy can be considered to be highly cytotoxic treatment, so its usage may require a specific treatment strategy. For example, treatment of acute leukaemia is largely dependent on which type of leukaemia-cell subtype is affected as well as disease aetiology (Greaves and Wiemels, 2003). Basically, chemotherapy regimens are based on combination chemotherapy, which is been effective on heterogeneous tumours and reduce cellular resistance in comparison to using single-drug (Höök et al., 1984).

Combination therapy in treating leukaemia can be divided to induction therapy followed by post-remission therapy and finally maintenance therapy. Initially, induction therapy is considered to be first line treatment, which is an intermittent chemotherapy injection, as it aims to eliminate as many leukaemia cells from the patient's circulation and the bone marrow. Following successful induction therapy, the post-remission therapy is introduced to ensure eradication of all malignant cells from the body using combination of high-dose chemotherapies, especially with poor prognostic patients. However, patients with good prognosis may receive maintenance therapy regimens instead of post-remission therapy, which is defined as continuous low-dose chemotherapy (Rivera et al., 1991).

The main concern about chemotherapy combination treatment is drug cytotoxicity. Chemotherapy can destroy cells by halting the cell cycle of both normal and malignant cells, which eventually develop various side effects. For example, it would increase the risk of developing chronic disorders for cancer survivals, such as heart disease, renal insufficiency, infertility and myelosuppression (Norris and Adamson, 2012). In addition, most chemotherapy has a small therapeutic window that would allow giving tolerable doses for the shortest period of time that ensures killing of most malignant cells. Although, combination chemotherapy is still the drug regime of choice in childhood leukaemia, chemotherapy-related toxicity is the main issue about this type of therapies.

Secondly, radiotherapy that refers to using high doses of radiation on the area of solid tumours leading to cellular death by DNA damage via an internal or external source of

radiation. Radiotherapy can be used solely or in combination with other therapies; for example, in breast cancer post-operative care, radiotherapy is used to ensure full eradication of all residual malignant cells.

Thirdly, stem cell transplantation therapy is defined as transplanting healthy stem cells to a patient; it can be from the same patient (autologous), from the patient's identical twin (syngeneic), or from someone else (allogeneic). This type of therapy usually indirectly affects cancer cells, which means the newly transplanted stem cells will help the body to recover and produce more normal stem cells after extensive loss of stem cells due to other therapies, as chemotherapy. However, allogeneic stem cell therapy can have direct effects on cancer cells by providing the patient's body with fully functional white blood cells that could attack malignant cells (Copelan, 2006).

Uncommon anti-cancer treatments include immunotherapy and hormone therapy. Immunotherapy is used to treat patients with cancers by enhancing the host's immune system, so it can destroy the cancer cells. Immunotherapy can be achieved either via use synthetic monoclonal antibodies against various cancer cell markers or boost the body's immune system, so it can recognise and attack foreign cells such as malignant cells. Although immunotherapy appears favourable, it is not effective in every patient and it might cause wide-range side-effects (Schuster, Nechansky and Kircheis, 2006).

Hormonal therapy is a type of therapy that controls hormone production to treat a particular cancer. Hormonal therapy is predominantly used to ease cancer symptoms; however, it can slow tumours' growth. For instance, testosterone production can be controlled in order to treat prostate cancer. Finally, precision medicine is a type of medicine that is based on patient's cancer's genetic information, which allows oncologists to select an appropriate personalised therapy. This type of therapy joins several treatments according to disease aetiology and it could target the cause of the disease (Cancer research UK, 2017).

Scientists are trying to overcome these issues by identifying natural products-related compounds with anticancer effects with improved pharmaceutical outcomes. Different anticancer drugs have been discovered from natural products, for instance, L-asparaginase, doxorubicin and cytarabine. Even though, these drugs are derived from natural products, they are classified as chemotherapeutics and it might share some side-effects (Nobili et al., 2009).

Natural products play a pivotal role in biomedical research, especially in cancer research. Agbarya et al. (2014), over the past century nearly 28% of drugs have been

originally derived from natural products or their derivatives, which are widely used as anticancer or antimicrobial agents that are originally extracted from plants and animals (Cragg, Newman and Snader, 1997). Natural products are favoured over other synthetic drugs as they're naturally sourced, so they could be degraded easily by the normal living cells, which decrease unfavourable cytotoxicity (Du and Tang, 2014). Therefore, developing novel anti-cancer drugs that are derived from natural products with minimal side effects would be preferred instead of using chemically synthesised drugs alone. Marine life has potential source of promising anticancer drugs, which could play an important role in anticancer treatments (Nobili et al., 2009).

1.14. Polysaccharides from natural products as pharmaceutical agents

Over the past several years, there has been an increased demand for new cancer pharmaceutical agents from natural products such as plants, bacteria and animals, including marine life. The main advantage of natural product–derived anticancer drugs that it has acceptable side-effects than of other synthetic drugs (Zhang et al., 2013).

There are several drugs either approved by the United State Food and Drug Administration (US-FDA), European Medicines Agency (EMA) or in clinical trial that have been derived from marine sources. For instance, Cytarabin that was the first marine-derived chemotherapeutic drug isolated from a sponge (*Tethya crypta*) (Wlawick, Roberts and Dekker, 1959). Dolastatin which is a polypeptide product from marine mollusc (*Dolabella auricularia*) can inhibit microtubule assembly as well as tubulin polymerisation, resulting in cell apoptosis. Although it was not successfully approved, this drug also progressed to advanced phases in clinical trials and its derivatives are still being considered as anticancer candidates (Hearn, Shaw and Myles, 2007; Han et al., 2018).

Halichondrin is a tubulin inhibitor, which was isolated from Japanese sponge (*Halichondria okadai*). It is synthetic, macrocyclic ketone with enhanced antitumor activities against breast cancer. The US-FDA has approved its synthetic analogue since 2010 (Osgood et al., 2017). Cyclic-peptide drug Kahalalide-F was isolated from the mollusc (*Elysia rubefescens*) has anti-lysosomal properties. It has entered phase-I clinical trials against prostate cancer and phase-II against hepatocellular carcinoma, non-small cell lung cancer and melanoma (Avendaño and Menéndez, 2008; Ning et al., 2018). Didemnin-B isolated from (*Carribean tunicate*) shows inhibition of DNA-synthase that leads to cell cycle arrest (Nobili et al., 2009).

One of the largest phyla in the animal kingdom are known as molluscs, including snails, bivalves, squid, octopuses, oysters, and others. Many molluscs have been used for dietary intake, as they have great nutritional benefits (Celik 2014). Traditionally, molluscs have been used as natural treatments in Chinese traditional medicine; therefore, there has been great interest in investigating their valuable elements to be used as pharmaceutical sources (Cesaretti et al., 2004).

Generally, mollusc soft-body structural investigations have revealed high amounts of carbohydrates with some proteins and lipids, which makes carbohydrates a major area of interest from a pharmaceutical perspective (Amornrut et al., 1999). Polysaccharides from vertebrates and invertebrates have emerged as powerful platforms for medical utilities, as they have various biological activities such as immunostimulatory, antioxidant, and antitumor activities (Liao et al., 2013).

Polysaccharides isolated from invertebrates have shown very different structures to common mammalian polysaccharides in terms of monosaccharide composition, molecular weight, degree of sulphation, type of glycosidic linkages, and branching points. For instance, a novel polysaccharide isolated from the head of a shrimp has a novel combination structure between heparin and HS known as a hybrid hep/HS structure (Brito et al., 2014). This structural diversity in polysaccharides has generated additional features for these novel molecules that could make them potent tools in glycobiology, especially as pharmaceutical agents.

Polysaccharide (including GAGs) structural analysis is very challenging due to their structural heterogeneity and polysaccharide structure vary according to species, season of harvest, and extraction method; accordingly, all these structural differences might interrupt the structural analysis as well as the biological activities of these molecules (Wang et al., 2017). In addition, carbohydrates cannot be visualized using UV or fluorescent as it lacks chromophore, therefore, detection usually requires a derivatization step (Rovio, Yli-Kauhaluoma and Sirén, 2007). For that reason, structural analysis has been heavily dependent on spectroscopic analysis, which is defined as the relationship between light or electromagnetic radiation and matter, such as nuclear magnetic resonance (NMR) and Fourier-transform infrared (FT-IR), in addition to chemical analytical methods in order to allow detection and to determine the final structure of these polysaccharides (Pomin, 2015; Wang et al., 2017).

The high content of uncommon polysaccharides structures in marine organisms make them a favourable source of natural products with various pharmaceutical benefits, including

in cancer therapy. The following section reviews polysaccharides derived from vertebrates and invertebrates with different structures and biological and pharmaceutical properties such as anticoagulation and anti-neoplastic properties.

1.14.1. Head of shrimp—*Litopenaeus vannamei*

A GAG-like structure was isolated from head of the shrimp *Litopenaeus vannamei* with a unique structure of both heparin and HS disaccharides merged together, resulting in an uncommon GAG-like structure known as hybrid heparin/HS (Brito et al., 2014). This hybrid Heparin/HS has both heparin and HS properties in addition to their basic disaccharide structure of glucosamine and iduronic acid/glucuronic acid [→4)-β-D-GlcA/α-L-IdoA (1→4) α-D-GlcNS-(1→] (Figure 31) (Pomin, 2015). The structural analysis was based on both disaccharides and NMR analysis, which has found a high amount of GlcA (77.6%) not epimerized to iduronic acid and only 22.4% IdoA; this finding suggests the influence of the HS chain. On the other hand, there is a high amount of sulphated GlcNS 71.5%, and GlcNAc represents about 22.5%. In addition, 75.5% of GlcNS was found to be GlcNS(6S), and 5% was found to have the rarest GlcN(3,6S) disaccharides, which simulates heparin's structure (Brito et al., 2014).

As this novel structure is related to heparin, its anticoagulation activity was examined and compared with that of the well-known heparin pentasaccharide. This novel structure was found to have anticoagulation activities lower than heparin that facilitate interaction with antithrombin to prolong the clotting time. Pomin (2015) suggested that this potent anticoagulant activity might be due to the pattern of N- and O-sulphation. More surprisingly, this hybrid type has very few side-effects in terms of bleeding.

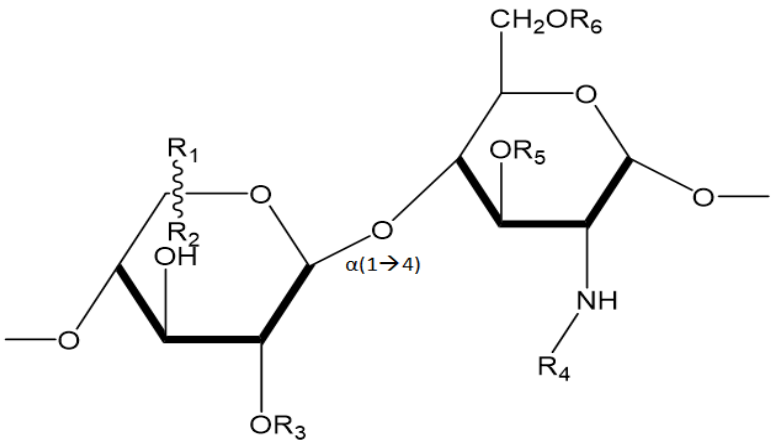

R1= COO-, R2= H (β-D-GlcA >> R1= H, R2= COO- (α-L-IdoA)

HS
When R1=COO- and R2=H
R3=H or SO3- (ocacasionally)
R4=SO3- (frequently) or COCH3 or H (rarely)
R5= SO3- (very rarely), R6=SO3- (freqyently)

Heparin
When R1=H and R2=COO-,
R3-H or SO3- (mostly)
R4=SO3- (mostly) or COCH3 or H (rarely)
R5=SO3- (rarely) and R6= SO3- (mostly)

Figure 31. Structural presentation of novel hybrid heparin-HS structure, which isolated from head of shrimp (*Litopenaeus vannamei*) (Pomin, 2015).

1.14.2. Bivalve mollusc—*Nodipecten nodosus*

A novel HS-like structure was isolated from a marine mollusc bivalve known as *Nodipecten nodosus*. Structural analysis has revealed a unique highly sulphated HS-like structure. Structural analysis using multinuclear-NMR has confirmed the presence of novel structural features of HS-like compound such as α-D-GlcNH$_2$ residues and β-D-GlcA (2,3S) with no IdoA residues detected. The α-D-GlcNH$_2$ residues contain 61% GlcNAc and 39% GlcNS. On the other hand, structural analysis has shown that 50% of the GlcA disaccharides are non-sulphated, 28% are 2-O-sulphated, and 22% 3-O-sulphated. According to Gomes et al. (2010), despite the presence of disulphated 2,3-O-sulphated GlcA, which is very rare in nature, an insignificant amount was determined (Figure 32).

This unique structure suggests the presence of an HS-like structure rather than heparin for several reasons. First, all uronic acids were typically in the β-anomeric configuration, as β-D-GlcA with no resonance for α-L-IdoA. Second, high levels of α-D-GlcNAc were detected, which indicates a more typically HS-like structure. Therefore, this suggests a novel HS structure that is uncommon in mammalian HS, especially with the particular pattern of sulphation on both the GlcA residues (Gomes et al., 2010; Pomin, 2015). Regarding its

pharmaceutical outcomes, this novel HS-like compound showed a six-fold decrease in anticoagulant activity in comparison to porcine heparin; however, this unique HS-like compound has potent anticoagulant activities in the presence of heparin-cofactor-II, which can increase the anticoagulant activities to up to 1,000 times stronger (Gomes et al., 2010).

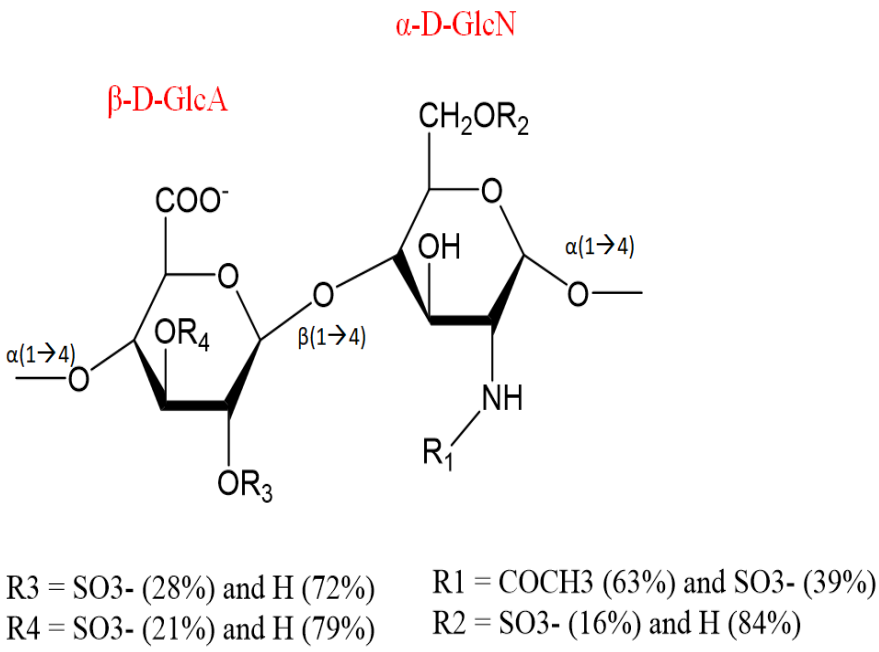

Figure 32. Structural presentation of novel HS-like structure isolated from bivalve mollusc (*Nodipecten nodosus*).

1.14.3. Bivalve mollusc—*Corbicula fluminea*

Corbicula fluminea is an edible bivalve mollusc originating in eastern Asia. This mollusc has various nutritional value, in addition to its valuable pharmacological benefits such as antiproliferative activities, antioxidants, and antihypertensive effects (Qiu, Dai and Li, 2009). Liao et al. (2013) purified three polysaccharide samples from *Corbicula fluminea's* soft body, namely, crude extracts of CFPS and CFPS-2 with anti-tumour activities. CFPS-2 was structurally analysed using various spectroscopic methods including FT-IR and NMR. The FT-IR structural analysis confirmed the presence of β-glycosidic linkages between polysaccharides, pyranose rings, sulphate esters, the N-acetyl functional group, the hydroxyl group, and the carboxyl group. Moreover, NMR structural analysis found pyranoses, β-glucose, β-galactose, α-glucose, and β-fucose. These findings suggest the presence of polysaccharides; however, no definite structure was determined.

Regarding the biological activities, the purified fractions were tested against various human cancer cell lines such as prostate, ovarian, and gastric carcinomas to check their anti-

proliferative activities. All three types of purified polysaccharides showed dose-dependent antiproliferation activities on all cancer cells. Liao et al. (2013) claimed, the presence of highly sulphated contents (8.1%) makes these polysaccharides water-soluble and enhances their anti-proliferative activities.

1.14.4. Sea cucumber—*Ludwigothurea grisea*

GAG-like structures were isolated from a sea cucumber known as a holothurian (*Ludwigothurea grisea*). This unique, highly sulphated structure shares the common mammalian CS-like structure; however, the GlcA C-3 has a branched O-linked fucose unit, so it's known as fucosylated-CS. This sea cucumber's unique structure is composed of sulphated α-L-fucopyranose branch linked to β-D-GlcA and β-D-GalNAc [Fuc*p* α(1→3) GlcA β(1→3) GalNAc β(1→] (Vieira and Mourão, 1988; Pomin, 2015) (Figure 33).

Spectroscopic structural analysis using NMR has confirmed a number of patterns of sulphation on the α-L-fuc*p*, as it can acquire mono-sulphate, 2,4-disulphate, and 3,4-disulphate (Pomin, 2015); in addition, the β-D-GlcA of holothurian-CS can acquire a 3-O-sulphate. The other disaccharides from this sea cucumber are the typical CS chains, which is similar to the mammalian CS in terms of structure and sulphate decorations can also be unsulphated, 4-O-sulphated or 6-O-sulphated (Myron, Siddiquee and Al Azad, 2014). All these different structures made this GAG-like polysaccharide resistant to chondroitinase enzymes (Vieira, Mulloy and Mourão, 1991).

Holothurian fucosylated-CS can participate in various biological activities such as tumour metastasis, coagulation, cellular morphogenesis, inflammation, and angiogenesis (Pomin, 2015). Borsig et al. (2007) suggested that the sea cucumber's fucosylated-CS with di-sulphated fucose-branch plays a role in inhibiting tumour cell metastasis via stopping adhesion molecules such as selectins. Furthermore, fucosylated–CS has a very potent role in inhibiting thrombus formation (Mourão et al., 1998). Depolymerised fucosylated-CS was introduced to reduce the activities of prothrombin, mainly by inhibition of coagulation factor X, which is responsible for conversion of prothrombin to thrombin (Wu et al., 2015).

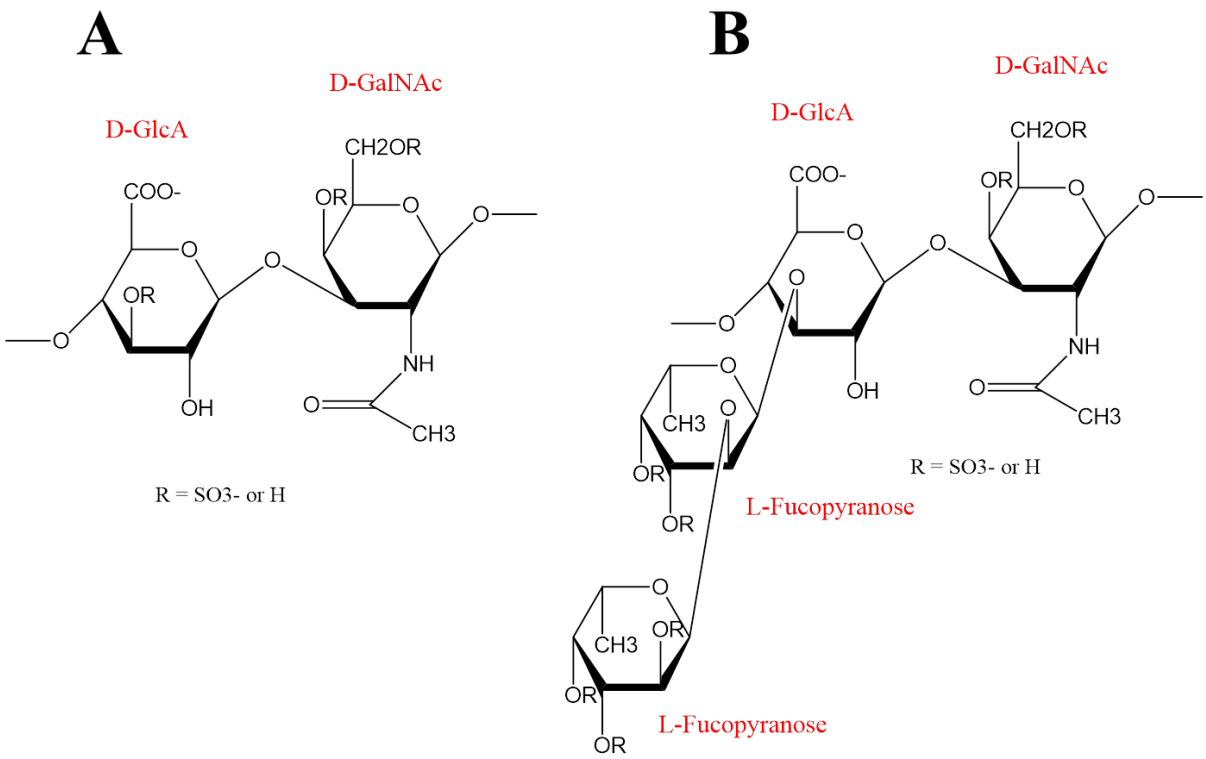

Figure 33. (A) Shows CS-like disaccharides from *Ludwigothurea grisea* as GlcA can acquire 3-O-sulphate group. (B) Shows CS-like disaccharide structure from marine *Ludwigothurea grisea* with fuc*p* attached α(1→3) to GlcA making this novel fucosylated-CS, where fucopyranose are attached via (1→2) glycosidic linkages.

1.14.5. Squid cartilage—*Ommastrephes sloani pacificus*

A novel GAG polysaccharide was purified from squid cartilage (*Ommastrephes sloani pacificus*) (Kawai et al. 1966). Habuchi et al. (1977) reinvestigated the squid cartilage's CS structure and found a large number of glucose branches linked to C-6 of the GalNAc moieties, which could be due to incomplete digestion of the PG residues. In addition, Kinoshita-Toyoda et al. (2004) purified a squid cartilage CS-like polysaccharide with branched hexose structure. Squid cartilage was digested with chondroitinases that resulted in four fractions; one of these fractions (fraction II) contains polysaccharides with glucose branches. Therefore, fraction II was sub-fractionated into 11 fractions. The authors most interesting observations were in subfractions 2 and 6 that both contained extensive glucose branches.

For structural analysis, NMR data proposed two structures from fraction-II, which are fraction-II-2 and fraction-II-6 that have glucose branching structures. Fraction-II-2 proposed unique structure—[GlcA β(1→3) Glc β(1→6) GalNAc(4S)] (Figure 34)—and fraction-II-6 is

characterised by this unique structure—[GlcA β(1→3) Glc β(1→6) GalNAc(4S) β(1→4) GlcA β(1→3) GalNAc(4,6S)] (Figure 35). In addition to these glucose branches, NMR structural analysis detected the presence of the rare 3-O-sulphation on the GlcA residues, thus making this part of the CS-E novel and uncommon to the mammalian CS as [GlcA(3S) β(1→3) GalNAc(4,6S)] (Kinoshita-Toyoda et al., 2004; Lamari and Karamanos, 2006).

Regarding the biological activities of the squid cartilage CS-like polysaccharide, it has anticoagulation activities that are different from those of mammalian CS. CS-like polysaccharide can inhibit the complement pathway through inhibition of the positive regulator of the complement pathway, known as properdin. This anticoagulation activity is highly dependent on squid cartilage CS-like polysaccharide size and structure (Kinoshita et al. 1997).

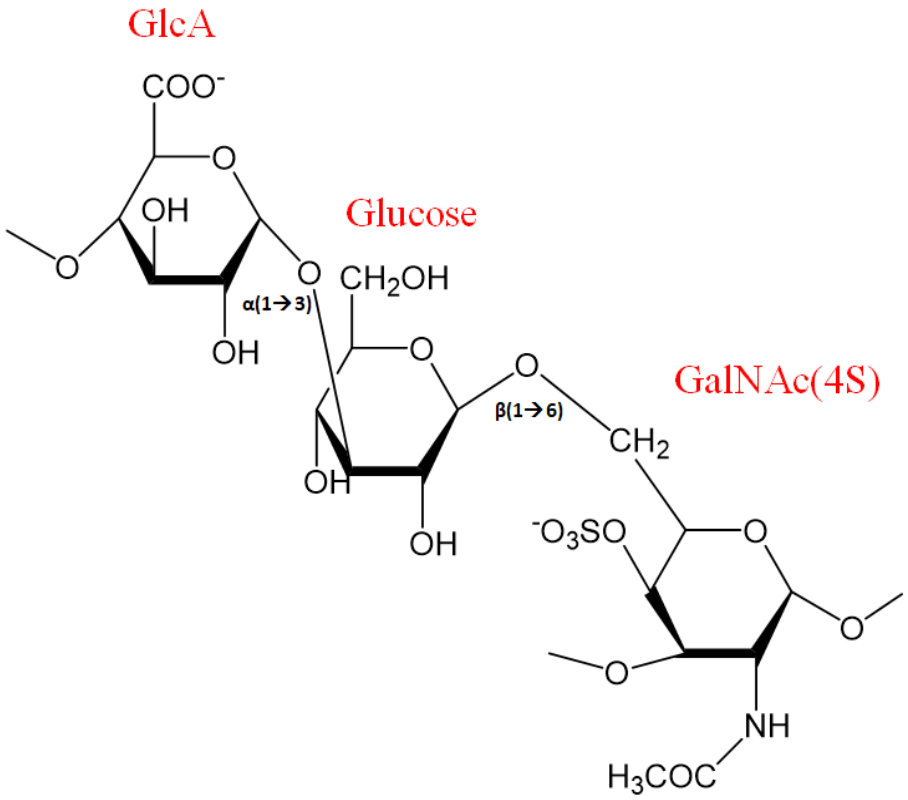

Figure 34. Structural presentation of squid cartilage (*Ommastrephes sloani pacificus*) purified fraction-II-2—[GlcA β(1→3) Glc β(1→6) GalNAc(4S)].

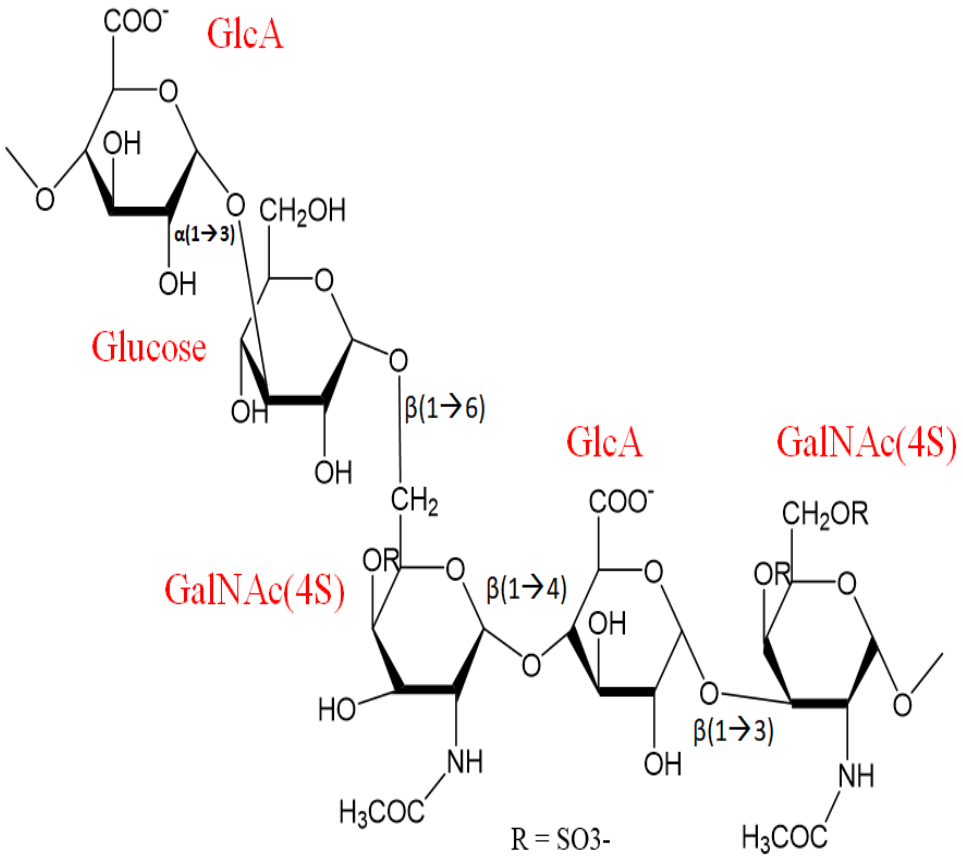

Figure 35. Structural presentation of squid cartilage (*Ommastrephes sloani pacificus*) purified fraction-II-6—[GlcA β(1→3) Glc β(1→6) GalNAc(4S) β(1→4) GlcA β(1→3) GalNAc(4S,6S)].

1.14.6. King Crab Cartilage—*Tachypleus tridentatus*

A GAG-like polysaccharide was isolated from king crab (*Tachypleus tridentatus*), which can be related to CS-like structures (Sugahara et al. 1996). Kitagawa et al. (1997) reinvestigated the structure of king crab CS-like structure by digesting using different enzymes such as hyaluronidase and chondroitinase, then fractionating using gel-filtration chromatography, which resulted in nine different oligosaccharides (fractions 1–9). The structure of each fraction was determined by NMR spectroscopy (Table 4). Most interestingly, king crab CS-like GAG contains 3-O-sulphated GlcA and 3-O-fucosylated-GlcA; thus, the fucosylated-GlcA is located in an inner position as an unsulphated and unbranched.

Table 4. NMR proposed CS-like oligosaccharides isolated from king crab (*Tachypleus tridentatus)*. Fractions 8 and 9 have hexasaccharides with different pattern of sulphation including 3-O-sulphated GlcA. Fraction 2A has pentasaccharides structure, whereas fractions 6 and 7 have octasaccharides, all of them contain both 3-O-sulphated GlcA and 3-O-fucosylated GlcA (Kitagawa et al., 1997).

Fraction	Oligosaccharides proposed structure
Fraction 8	GlcA(3S) β(1→3) GalNAc(4S) β(1→4) GlcA(3S) β(1→3) GalNAc(4S) β(1→4) GlcA β(1-3) GalNAc(4S)
Fraction 9	GlcA(3S) β (1→3) GalNAc(4S) β(1→4) GlcA(3S) β(1→3) GalNAc(4S) β(1→4) GlcA(3S) β(1→3) GalNAc(4S)
Fraction 2A	GlcA(3S) β (1→3) GalNAc(4S) β(1→4) Fuc α(1→3) GlcA β(1→3) GalNAc(4S)
Fraction 6	GlcA(3S) β(1→ 3) GalNAc(4S) β(1→4) Fuc α(1→3) GlcA β(1→3) GalNAc(4S) β(1→4) GlcA β(1→3) GalNAc(4S)
Fraction 7	GlcA(3S) β(1→3) GalNAc(4S) β(1→4) GlcA(3S) β(1→3) GalNAc(4S) β(1→4) Fuc α(1→3) GlcA β(1→3) GalNAc(4S)

1.14.7. African snail—*Achatina fulica*

A novel acharan sulphate (AS), with a molecular weight 29 kDa, was first isolated from an African snail *Achatina fulica* by Kim et al (1996). NMR spectroscopic analysis has demonstrated the presence of a homogenous structure of IdoA and GlcNAc repeated disaccharides, formulated as [→4) α-L-IdoA(2S) (1→4) α-D-GlcNAc (1→] (Figure 36) (Vieira et al., 2004; Pomin, 2015). In addition, NMR structural analysis confirmed that the fully epimerised IdoA has a very low pattern of sulphation. According to Pomin (2015), AS structure is similar to that of mammalian heparin and HS, as the IdoA can acquire 2-O-sulphation; however, the $GlcNH_2$ residues are acetylated, which makes it different from mammalian GAGs.

AS biological activities include the successful inhibition of angiogenesis in fertilised chicken eggs, which represents the antiangiogenic activities of this novel molecule (Lee et al. 2003). AS has very weak anticoagulation activities in comparison to mammalian heparin (Li et al., 2004).

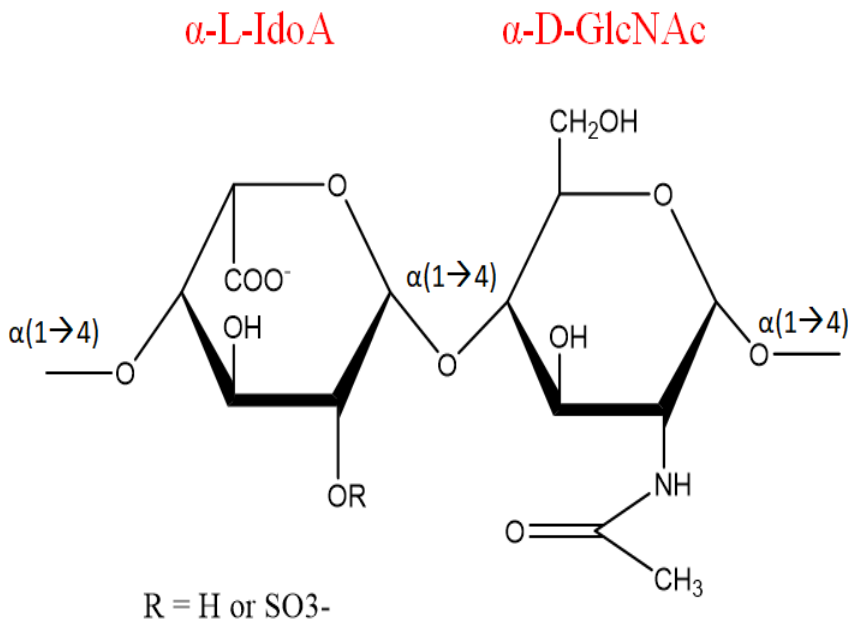

Figure 36. Structural representation of the AS, isolated from African snail (*Achatina fulica)*. IdoA can acquire sulphate group at C-2, whereas, the glucosamine residues are acetylated (Pomin, 2015).

1.14.8. Sea squirt—*Ascidian*

The ascidian is a form of marine life known as the sea squirt that is considered to be a rich source of polysaccharides with unique structure. Ascidians have high amounts of DS-like structures, which are composed of [→4 α-L-IdoA (1→3) β-D-GalNAc 1→] (Figure 37). There are many structural variations on the patterns of sulphation within ascidian species, as the IdoA can be non-sulphated or 2-O-sulphated, and the GalNAc can be 4-O-sulphated and/or 6-O-sulphated. Nearly 70% of the ascidian DS-like disaccharides show highly sulphated structures such as [α-IdoA(2S) (1→3) GalNAc(4S)] in comparison to mammalian DS, which contains lower quantities of di-sulphated disaccharides. This ascidian DS-like polysaccharide has been tested for various medical purposes, including anticoagulant and anti-metastatic agent (Pomin, 2015).

Regardless of inter-species variations, sea squirt DS-like polysaccharides show anticoagulation activities. The DS-like structure [α-IdoA(2S) (1→3) GalNAc(4S)] shows anticoagulation activities, which accelerate the activities of heparin-cofactor-II (Pavão, 2002). Regarding the anti-metastatic role of ascidians' DS-like polysaccharide, two DS-like structures were purified from two different sea squirts known as *Styela plicata* and *Phallusia nigra*, which have the unique structures [IdoA(2S)-GalNAc(4S)] and [IdoA(2S)-

GalNAc(6S)], respectively. Both structures have shown anti-metastatic activities by inhibiting the interaction between cancerous cells and adhesion molecules such as selectins, on endothelial cells (Kozlowski, Pavao and Borsig, 2011).

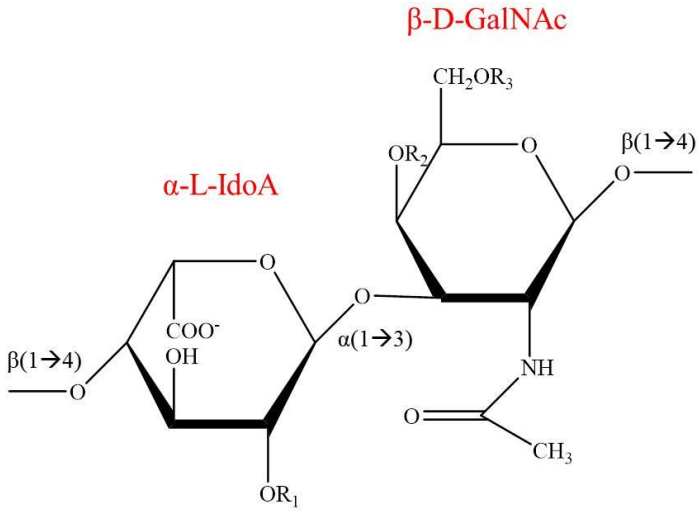

Sulphation %	
Styels picata	R1 = 67%, R2 = 94%, R3 = 6%
Phallusia nigara	R1 = 80%, R2 = <5%, R3 = 100%

Figure 37. Structural representation of the DS-like extracted from two different ascidian species (Pomin, 2015).

1.14.9. Cuttlefish ink—*Sepiella maindroni*

Ink from the cuttlefish ink (*Sepiella maindroni*) was used in Chinese traditional medicine, and has various haemostatic effects and immunomodulatory functions. Liu et al. (2008) successfully isolated and characterised a novel polysaccharide structure from *Sepiella maindroni* ink. After carbohydrate purifications, monosaccharide analysis was carried out using gas chromatography coupled with mass spectroscopy (GC-MS), which identified the presence of fucose, Man, GalNAc, and GlcA with α- and β- linkages. Afterwards, NMR structural analysis confirmed the presence of hexasaccharide repeating sequence within an inner branched GlcA α(1→3), as [→4) L-fucose β(1→4) L-fucose β(1→4) D-GalNAc α(1→6) D-Man α(1→4) GalNAc α(1→], where the GlcA is attached to the Man in α(1→3) linkages (Figure 38).

Sepiella maindroni's hexasaccharide biological activities were assessed on mice with sarcomas using an *in-vivo* analysis. It was found that a combination of chemotherapy and polysaccharides reduced the mutagenic effects caused in the sarcoma blast cells (Liu et al. 2008).

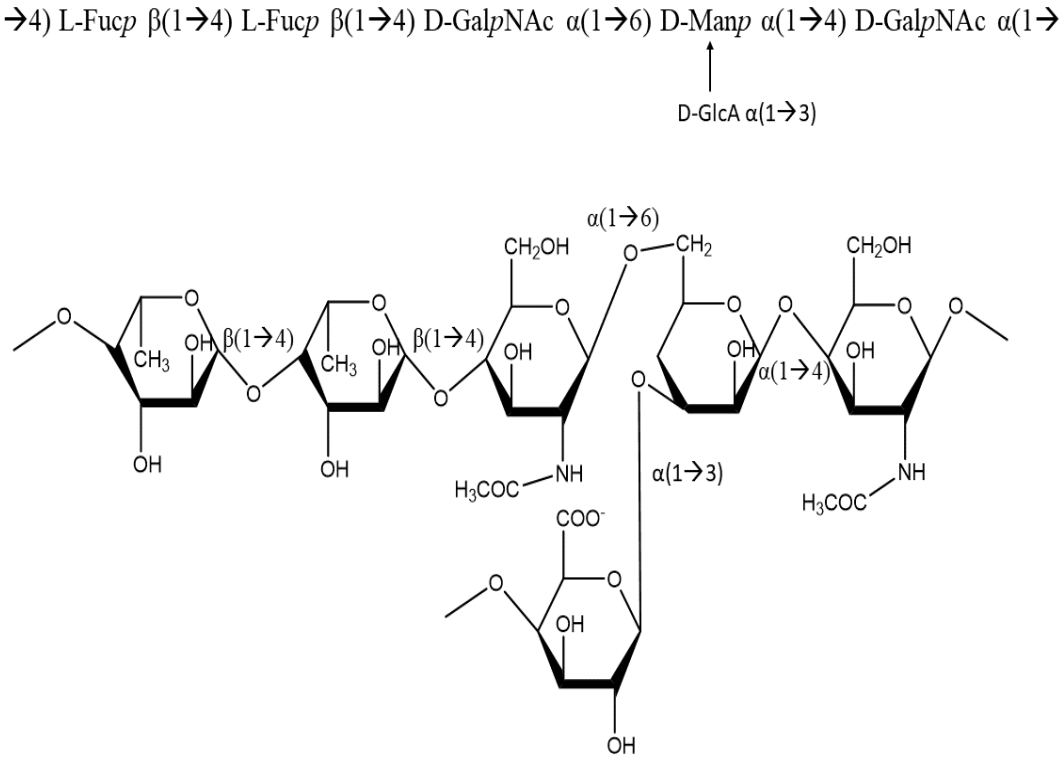

Figure 38. Structural representation of *Sepiella maindroni* ink hexasaccharide repeating structure that is composed of [→4) L-Fuc*p* β(1→4) L-Fuc*p* β(1→4) D-GalNAc α(1→6) D-Man α(1→4) GalNAc α(1→], where the GlcA is attached to the Man in α(1→3) linkages.

1.14.10. Bivalve mollusc—*Ruditapes philippinarum*

Ruditapes philippinarum is a bivalve edible mollusc used in Chinese traditional medicine. Zhang et al. (2008) isolated and purified polysaccharide from *Ruditapes philippinarum*, resulting in a crude extract; further purified using gel filtration, which resulted in sub-fractionated four peaks. All four fractions were assessed for biological function against human hepatoma cancer cell line, fraction-1 the only peak that showed antiproliferative activities. A further purification step was carried out on the purified extract, which successfully separated the PE to two peaks, namely, purified extract fraction-1 (PEF-1) and purified extract fraction-2 (PEF-2).

Structural analysis was performed using FT-IR and NMR, which demonstrated the presence of homo-polysaccharide chains with no uronic acid residues. The PEF-1 chain

consists of α(1→4) glucopyranosyl residues with α(1→6) branching point, while PEF-2 has co-existent α(1→4) and β(1→6) glucopyranosyl residues. In addition, the presence of protein residues has suggested the presence of protein-bound polysaccharides within the sequence.

Only the PE has shown potent inhibitory properties against the human hepatoma cell line in a non-dose-dependent manner, while PEF-1 and PEF-2 have shown lower inhibitory effects. Zhang et al. (2008) concluded that these antiproliferative activities could be due to chemical composition, type of glycosidic linkage, molecular mass, degree of branching and/or the protein-bound polysaccharides, which could be responsible for the antiproliferative activities against the hepatoma cell line.

2. Aims and objectives

The aim of this study is to isolate marine polysaccharides derived from cockle bivalve molluscs (*Cerastoderma edule*), examine their antiproliferative activity on different cancer cell lines, then characterise their structure in order to correlate a structure-activity relationship.

The main objectives of this study

- Polysaccharide isolation from common cockle using cetylpyridinium chloride precipitation methods.
- Assessment of the cockle polysaccharides antiproliferative activities on different cancer cell lines.
- Application of various structural tools to determine the structure of common cockle polysaccharides with antiproliferative activity such as monosaccharide, disaccharide compositional analysis, FT-IR and NMR.

3. Materials and methods

3.1. Outline of experimental work

Common cockle (*Cerastoderma edule*) obtained from the Irish Sea and the British Isles. The extracted polysaccharide was investigated using various biochemical and structural tools to check its *in-vitro* role as an antiproliferative agent against different cancer cell lines, and to characterise their antiproliferative structures. Firstly, common cockle polysaccharide was isolated and purified from cockle's soft body following the cetylpyridinium chloride precipitation method previously described (Kim et al., 1996). The resulted cockle crude extract (CE) polysaccharide was tested to check its antiproliferative activity using two leukaemia cell lines (K-562 and Molt-4) and a mesothelioma cell line (Mero-25). Next, various structural analysis approaches were conducted to assess the cockle CE polysaccharide's structural similarities to mammalian GAGs. Secondly, the cockle CE polysaccharide with confirmed antiproliferative activity was purified using anion-exchange resin coupled with fast performance liquid chromatography system (FPLC). The anion-exchange chromatography successfully separated the cockle CE polysaccharide into six fractions according to their anionic strength. Then, the cockle polysaccharide purified fractions' antiproliferative activity was assessed against the three cancer cell lines to confirm the activity. Finally, structural analysis was conducted using various structural techniques to discover this novel antiproliferative structure of the CE polysaccharides as well as the antiproliferative activity of fraction 5 from the anion-exchange separation.

3.2. Materials

Cockles (Manchester Fish Market, UK), acetone (Sigma-Aldrich, UK), razor blade blender, alcalase enzyme *Bacillus licheniformis* (Merck, Millipore, Watford, UK), tricloroacetic acid (Sigma-Aldrich, UK), cold centrifuge (life sciences, Beckman coulter), potassium acetate (Sigma-Aldrich, UK), ethanol (Fisher Scientific, UK), sodium chloride (Sigma-Aldrich, UK), cetylpyridinium chloride (Sigma-Aldrich, UK), dialysis tubes (Scientific Laboratory Supply, UK), freeze-dryer (Scanvac coolsafe, Labogene, Denmark), Ethylenediaminetetraacetic acid (EDTA) (Sigma-Aldrich, UK), anion exchange resin diethylaminoethanol-sepharose (GE Healthcare, Little shallot, UK), FPLC system (Pharmacia, Stockholm, Sweden), empty column XK 16/20 (GE Healthcare, Little shallot,

UK), sodium phosphate monobasic (Sigma-Aldrich, UK), sodium phosphate dibasic (Sigma-Aldrich, UK), fraction collector (FRAC-100, Pharmacia, Stockholm, Sweden), PD-10 column (GE Healthcare, Little shallot, UK), RPMI-1640 (Lonza group Ltd), DMEM (Fisher Scientific,UK), fetal bovine serum (Labtech International Ltd, UK), L-glutamine (Labtech International Ltd, UK), penicillin and streptomycin (Labtech International Ltd, UK), heparanase from *Flavobacterium Heparinum* (Grampian Enzymes, Aberdeen, UK), Chondritinase-ABC (Grampian enzymes, UK), α-L-fucosidase (Sigma-Aldrich, UK), sodium acetate (Sigma-Aldrich, UK), calcium acetate (Sigma-Aldrich), bovine serum albumin (Thermo fisher scientific, UK), Spectrophotometer (Multiscan, Thermo Fisher, UK), Nanosep 10 kDa spin filter (Pall Laboratory, USA), Tris-HCL (Sigma-Aldrich, UK), sodium citrate (Sigma-Aldrich, UK), MTT powder (Sigma-Aldrich, UK), Cisplatin (Sigma-Aldrich, UK), mammalian HS (Celsus, Cincinnati, OH, USA), heparin (Celsus, Cincinnati, OH, USA), CS (Celsus, Cincinnati, OH, USA), DS (Celsus, Cincinnati, OH, USA), 10 x phosphate buffer saline (Sigma-Aldrich, UK), Dimethyl sulfoxide (Fisher Scientific UK Ltd), 0.22 µM filter (Merck, Millipore, Watford, UK), Apoptosis assay kit (BD biosciences, UK), Flow cytometry (BD FACSVerse, Franklin Lakes, NJ, USA), Dionex ICS-3000 system (Sunnyvale, CA, USA), MilliQ water (Merck, Millipore, Watford, UK), trifluoroacetic acid (Sigma-Aldrich), Isopropanol (Fisher Scientific UK Ltd), Dionex CarboPac PA1 column (Thermo fisher scientific, uk), 4 mm x 50 guard column (Thermo fisher scientific, UK), sodium hydroxide (Sigma-Aldrich, UK), UV detector (Gilson USA), sodium cyanoborohydride (Sigma-Aldrich), HS disaccharides standards (Calbiochem and Sigma-Aldrich), CS disaccharides standards (Oxford Glycosystems), LC/MS (Thermo-Finnigan, San Jose, CA), Dibutylamine (Sigma-Aldrich), C-18 reversed-phase column (0.46 cm X 25 cm, Vydac), methanol (Fisher Scientific, uk), FT-IR spectroscopy system (Bruker, Billerica, Massachusetts, United States), NMR spectroscopy 800 MHz (Bruker, Billerica, Massachusetts, United States), duterum oxide 99.9% (Sigma-Aldrich, UK), tetramethylsilane (Sigma-Aldrich, UK).

3.3. Methods

3.3.1. Extraction of sulphated polysaccharides from common cockle

This extraction procedure, known as the cetylpyridinium chloride precipitation method, was previously used to extract GAG-like polysaccharides from invertebrate soft bodies (Kim et al., 1996). Initially, cockle shells were removed, and 250 g of cockle soft body tissue was soaked in acetone 400 mL for 72 h to ensure fat removal; the acetone was

changed every 24 h. Defatted tissues were left to dry for 24-48 h at room temperature then ground to a fine powder using a razor blade blender. The powder (50 g) was suspended in of 0.05 M sodium carbonate (500 mL) with pH 9.2 and 25 mL of Alcalase enzyme (30 Anson units/g) was added, and then the mixture was incubated at 60 °C for 48 h with constant agitation at 200 rpm.

The mixture was then cooled to 4 °C and 5% trichloroacetic acid (w/v) was added to the mixture and mixed for 10 min. Then, the precipitated peptides were removed by centrifugation (8000 rpm for 25 min). After centrifugation, the supernatant was transferred to a cylinder and three volumes of 5% (w/v) potassium acetate in ethanol were added to one volume of the supernatant and the mixed solution left overnight at 4 °C.

Subsequently, the precipitated cockle polysaccharide was recovered by centrifugation (8000 rpm for 30 min). The recovered precipitate (about 12 g) was then dissolved in of 0.2 M NaCl solution (480 mL) and centrifuged (8000 rpm for 30 min) to remove any insoluble material. Next, cetylpyridinium chloride (6.25 mL of a 5% (w/v) solution) was added to the supernatant and the mixture was centrifuged (8000 rpm for 30 min). The precipitate was subsequently dissolved in of 2.5 M NaCl buffer (125 mL), followed by the addition of 5 volumes of absolute ethanol. The precipitated cockle polysaccharide was recovered by centrifugation (10,000 rpm for 30 min); the precipitated polysaccharides were recovered and dissolved in water (30 mL) in order to be ready for dialysis process.

According to cockle preparation procedure which depends heavily on their negative charge, the dialysis tubing's were treated prior to adding final polysaccharide mixture to remove any charged particles attached to it. Initially, tubes were treated with 30 mM sodium bicarbonate (10 g) and 10 mM EDTA (0.146 g) in distilled water (400 mL) for 10 min. Then, tubes were washed with boiled distilled water for 10 min. Finally, tubes were washed with 10 mM EDTA (0.146 g) in distilled water (250 mL) and absolute ethanol (250 mL). Afterward, the polysaccharide mixture, which was dissolved in water (30 mL), was added to the freshly prepared dialysis tubing with a molecular weight cut-off (MWCO) of 14 kDa against water for 72 h, as dialysis water was changed every 24 h. The dialysate was lyophilized to obtain a white powder containing approximately 24 mg of cockle polysaccharide that was coded as crude extract (CE).

3.3.2. Anion-exchange chromatography

The cockle CE polysaccharide preparations were purified using anion-exchange resin coupled with the fast performance liquid chromatography (FPLC) system. The anion-exchange column (16 X 200 mm) was packed with fast flow diethylaminoethyl-sepharose (DEAE-Sepharose) (10 mL) that is composed of cross-linked agarose 6% (Silva, 2006). Cockle CE polysaccharide was dissolved in distilled water (1 mg/mL) prior to injection into the FPLC system. The column was pre-washed with 1 column volume (10 mL) of 1.5 M NaCl, then 1 mL of cockle CE polysaccharide mixture was injected to the FPLC system and the cockle CE polysaccharide was eluted using a linear gradient 0-1.5 M of NaCl (7.8 g/L) in 50 mM sodium phosphate buffer (7.098 g/L) at pH 7.0 over 75 min at a flow rate of 1 mL/min. Absorbance was monitored at 280 nM (Rovio, Yli-Kauhaluoma and Sirén, 2007), and 1 mL fractions were collected using Pharmacia fraction collector, then pooled as indicated. After each run, the column was washed with 1 column volume (10 mL) of 1.5 M NaCl to ensure removal of any attached materials as well as to recharge the column.

Pooled fractions corresponding to the peaks in the elution profile were dialysed extensively against water using a dialysis tube with MWCO 14 kDa over 3 consecutive days. After the dialysis process, fractions were lyophilised using freeze-drier for 3 days to obtain the final polysaccharide products. A further desalting step was performed to ensure samples are salt-free using a desalting column PD-10. The PD-10 column is a desalting column containing gel filtration sephadex (G-25) resin, using gravity method. The column was washed with of 10% ethanol (30 mL), and then 2.5 mL of the sample was applied. The first 2.5 mL was discarded, as it was the column void volume; the next 3.5 mL was collected, lyophilised, and stored at -20 °C (Kitagawa et al., 1997).

3.3.3. Enzymatic digestion

The extracted cockle polysaccharide was digested using different enzymes, namely heparinase enzymes, chondroitinase-ABC and/or α-L-fucosidase, to be used for further analysis in order to release unsaturated disaccharides from both cockle CE or cockle purified fractions, as follows.

3.3.3.1. Heparinase dilution and working concentration

Heparinases were purchased in international units (IU) as stock concentrations as heparinase-I (2.0 IU), heparinase-II (0.2 IU) and heparinase-III (0.5 IU) (Grampian enzymes, UK). Enzyme dilution was performed following the manufacturer's recommendations, as follows. Initially, the enzyme concentration was adjusted to 1.0 IU/ml on the enzyme stock, by adding 1x heparinase buffer, which is composed of 50 mM sodium acetate and 10 mM calcium acetate at pH 7.0, containing bovine serum albumin (BSA) 0.2-0.4 µg/mL as a stabiliser. Then, the adjusted enzyme stock was split into 100 µL aliquots, in which each 100 µL contains 1.0 IU/ml of enzyme that was stored at -80 °C. For the enzyme working concentration, 400 µL of 1x heparinase buffer was added to one vial (100 µL at 1.0 IU/mL) of enzyme stock, without BSA, to reach a final volume of 500 µL containing about 200 mIU/mL of the enzyme. This 500 µL (200 mIU/mL) was aliquoted into 10 µL in each vial to obtain about 5-10 mIU. All enzyme aliquots were stored at -20 °C (Lamanna, 2008).

For cockle polysaccharides digestion, 100 µg of polysaccharide was dissolved in 200 µL of 1 x heparinase buffer and heparinase-I (30 mIU), heparinase-II (30 mIU), heparinase-III (30 mIU), separately or in combination of all three enzymes. This was incubated at 30 °C for 24 h. The enzyme digests were monitored spectrophotometrically at 232 nM and the reactions were terminated by heating at 100 °C for 5 min. The samples were passed through a 10 kDa spin filter, and then both retained materials and flow through materials were dried prior to further analysis.

3.3.3.2. Chondroitinase-ABC dilution and working concentration

Chondroitinase-ABC was purchased in 5 IU quantities (Grampian enzymes, UK). The enzyme working concentration was adjusted by reconstitution in 5 mL of 50 mM Tris-HCl and 50 mM sodium acetate buffer at pH 8.0 with 0.2% BSA to make 1.0 IU/mL. The enzyme was aliquoted at 1 mL/vial and stored at -80 ºC. Then, 1 mL stock at 1.0 IU/mL was split into 100 µL aliquots, in which each 100 µL at 1.0 IU/mL of enzyme that was stored at -80 °C. For enzyme working concentration, 400 µL of 1 x condroitinase buffer was added to one vial of enzyme stock (100 µL at 1.0 IU/mL), without BSA, to reach a final volume of 500 µL containing 200 mIU/mL of the enzyme. This 500 µL (200 mIU/mL) was aliquoted into 10 µL in each vial to obtain about 5-10 mIU. All aliquots were stored at -20 °C.

For cockle polysaccharides digestion, 100 µg of cockle polysaccharides was dissolved in 200 µL of chondroitinase-ABC buffer and added to 30 mIU of the enzyme. Then, it was incubated for 24 h at 37 °C. The enzyme digests were monitored spectrophotometrically at 232 nM and the reactions were terminated by heating at 100 ºC for 5 min. The samples were passed through a 10 kDa spin filter, and then both retained materials and flow through materials were dried prior to further analysis.

3.3.3.3. Fucosidase enzyme dilution and working concentration

α-L-fucosidase enzyme is a broad-spectrum hydrolase enzyme that cleaves fucose from proteoglycans, extracted from bovine kidney. It has broad substrate properties that can cleave [α-L-fucose 1→ (2,3,4,6)] from both N- or O-linked glycan (Parekh et al., 1987).

The enzyme was purchased in 0.5 IU quantities in a 3.2 M ammonium sulphate solution containing 10 mM sodium phosphate monobasic and 10 mM sodium citrate. Initially, the ammonium sulphate was discarded by centrifugation and the pellet containing the enzyme was recovered. The enzyme working concentration was adjusted by reconstitution in 500 µL of 100 mM sodium citrate buffer at pH 5.6 (0.5 IU/500 µL). The enzyme was aliquot of 100 µL containing 0.1 IU been stored at 2-8 ºC. For the enzyme working concentration, 400 µL of 1 x enzyme buffer was added to one vial of 100 µL stock, as the 500 µL containing about 200 mIU/mL, then 10 µL in each vial to obtain about 5-10 mIU. Enzyme check was determined using spectrophotometer at 400 nM.

For cockle polysaccharide digestion, 100 µg of the cockle polysaccharide was dissolved in 200 µL of α-L-fucosidase buffer and 30 mIU of the enzyme was added. Then, it was incubated for 24 h at 37 °C. The enzyme digests were monitored spectrophotometrically at 400 nM and the reactions were terminated by heating at 100 ºC for 5 min. The samples were passed through a 10 kDa MWCO spin filter, and then both retained materials and flow through materials were dried before further analysis.

3.3.4. Maintenance of cell lines

Cell culture was conducted using two human leukaemia cell lines, CML-derived cell line K-562 and ALL-derived cell line Molt-4, and human malignant mesothelioma with asbestos exposure (pleural cavity) Mero-25 cell line (ECACC 09100102). The human leukaemia cell lines were grown in RPMI-1640 cell culture medium containing 1 g/L glucose

and the Mero-25 cell line was grown in a DMEM cell culture medium containing 3.7 g/L glucose. All culture media were supplemented with 10% (v/v) inactivated fetal bovine serum (FBS), 2 mM L-glutamine, 100 units/mL penicillin and 100 µg/mL streptomycin. All cell lines were maintained in 75 mL flasks under a sterile and humidified atmosphere of 95% air and 5% CO_2 at 37 °C.

3.3.5. Cell proliferation assay

Cell proliferation was assessed using MTT (3-(4,5-dimethylthiazol-2-yl)-2,5-diphenyl tetrazolium bromide) assay, which is an *in-vitro* colorimetric technique that is widely used to assess cell viability and proliferation. Physiologically viable cells' mitochondria produce an enzyme known as nicotinamide adenine dinucleotide (phosphate) (NAD(P)H)-dependent oxidoreductase, which reduces the tetrazolium (MTT-dye) to a compound called formazan (a crystalline product purple in colour) (Gerlier and Thomasset, 1986). In contrast, non-viable cells do not catalyse the reduction of the tetrazolium to produce purple-coloured crystal formazan. Therefore, this assay detects the density of the colour and gives qualitative indications of viable and non-viable cells using half-maximal inhibitory concentration (IC_{50}), which is defined as the quantity of a drug required to inhibit the biological activity by half, thereby illustrating anti-proliferative activity.

Cells were seeded at a density of 5 X 10^3 cells per well in 96-well plates containing 100 µL of culture medium prior to treatment with polysaccharide samples for K-562 and Molt-4 cell lines, however, for Mero-25 cell line, the cells were seeded in 96-well plate and incubated overnight, to allow cells to attach to the plate. Following that the addition of different drugs, such as cockle polysaccharide samples with increased dose (0, 0.78, 1.56, 3.12, 6.25, 12.5, 25, 50 (µg/mL)), mammalian GAGs (0, 0.78, 1.56, 3.12, 6.25, 12.5, 25, 50 (µg/mL)), and cisplatin (0, 0.39, 0.78, 1.56, 3.12, 6.25. 12.5, 25 (µM)) that was used as positive control, in triplicates, then, cells were incubated for 96 h following. Following the incubation period, 50 µL of the MTT solution (5 mg/mL in PBS) was added to each well and plate was further incubated for 3 h at 37 °C, then solution was removed by aspiration. Next, 200 µL of dimethyl sulfoxide (DMSO) was added to each well in order to dissolve the formazan crystal product. The amount of the MTT dye converted to formazan is directly proportionally to the viable cells. The plate was gently agitated until the colour reaction was uniform and the absorbance was measured at 570 nM using a multi-well plate reader.

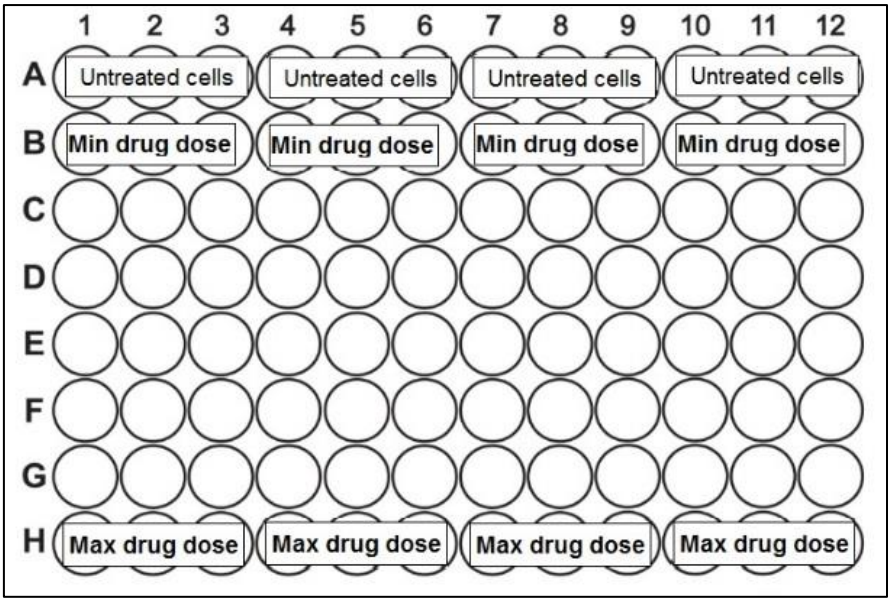

Figure 39. MTT assay 96-well U-shaped wells for suspension cell lines or Flat-shaped wells for adherent cell line. Maximum drug concentration was added in the last row (H), then, drug was diluted until row (B). Row (A) was used for untreated control cells. Every drug concentration was tested in triplicates including control cells.

3.3.5.1. Determination of IC_{50} values

The average cell values were determined from triplicates at each data set in order to obtain IC_{50} values using GraphPad Prism 8.0 (La Jolla, CA, USA). First, the values from untreated cells were considered to have the maximum growth rate and the values from the treated cells were determined according to the untreated control values. Second, in order to plot a dose-response curve, all data values were normalised as the largest value was assigned as 100% growth, and the smallest value was assigned to 0%. Therefore, the y-axis was defined as the growth percentage and the x-axis was defined as the drug concentration. Finally, the IC_{50} values were determined using non-linear regression inhibitor vs normalised response option.

3.3.6. Annexin-V Apoptosis Assay

There are several biochemical techniques to determine the cellular death process. One of these techniques is to determine early apoptotic markers of cell death. One early apoptotic marker is known as phosphatidylserine, which is a phospholipid compound that is part of the inner cell membrane. During early apoptotic conditions, such as hypoxia, phosphatidylserine is translocated to the outer cell membrane, which makes it exposed to antibodies, for example. Phosphatidylserine on the outer cell membrane can bind to a binding protein known as Annexin-V, therefore, Annexin-V was conjugated with a fluorochrome called fluorescein

isothiocyanate (FITC) to visualise this reaction using flow cytometry. In order to differentiate between apoptosis and necrosis, cells were stained with propidium iodide (PI), which binds to the necrotic cells, in addition to FITC-Annexin-V. Hence, using flow cytometry as a quantitative technique to count FITC-Annexin-V and PI-stained cells is very useful to evaluate cellular death progression (Biosciences, 2011).

To perform the apoptosis assay using FITC-Annexin-V and PI stains, cells were seeded into a sterile 6-well plate at 5 X 10^5 / mL at 37 °C. Next, cockle CE polysaccharide or cockle purified active fraction was added to the cells and left for 24 h. Afterwards, treated and untreated cells were washed twice with cold PBS and centrifuged at 2000 X g for 5 min, followed by resuspension in 1 x binding buffer (0.1 M HEPES buffer, 1.4 M NaCl and 25 mM calcium chloride) at a concentration of 1 X 10^6 cells/mL. Cells (100 µL) were then stained with Annexin V-FITC (5 µL) and PI (5 µL). Stained cells were gently vortexed and incubated in the dark for 15 min at room temperature 25 °C. After incubation, 400 µL of 1 x binding buffer was added to cells prior to analysis using a flow cytometer.

3.3.7. Monosaccharide composition analysis

Monosaccharide composition analysis was conducted using high-pH anion-exchange chromatography coupled with pulsed amperometric detection (HPAEC-PAD) using a Dionex ICS-3000 system (Hardy, Townsend and Lee, 1988). This method was favoured for monosaccharides composition analysis as it does not require sample derivatisation, which makes it advantageous for an unknown polysaccharide sample. Because polysaccharides lack a chromophore, an electrochemical detector was chosen which has several advantages. For instance, it has the ability to discriminate between monosaccharides and the mobile phase, and is a qualitative, quantitative, sensitive and non-destructive detector.

For cockle monosaccharide composition analysis, 50 µg of cockle CE polysaccharide or 50 µg of each purified fraction was dissolved in 200 µL MilliQ water. The mixture was then incubated with 1 mL of 4M trifluoroacetic acid at 100 °C for 6 h to ensure the release of both monosaccharides and uronic acids. Then the sample was centrifuged at 2000 rpm for 2 min, followed by the removal of acid using a dry nitrogen flush and 50 µL of 50% (v/v) aqueous isopropyl alcohol as a co-evaporative to remove the remaining acid until the sample was completely dry.

For monosaccharide analysis, 20 µg of the hydrolysed polysaccharide sample was suspended in 100 µL MilliQ water. Then, 50 µL of the sample was injected into a Dionex CarboPac PA1 column (4 mm x 250 mm, 4µm, with 4 mm x 50 mm guard column) at a flow rate of 1 mL/min. Monosaccharides were eluted using gradient elution under strong alkaline conditions formed from three solvents: high purity H_2O as solvent (A); 100 mM sodium hydroxide (NaOH) with 5 mM sodium acetate (NaOAc) as solvent (B); and 100 mM NaOH with 250 mM NaOAc as solvent (C) (Table 5). Peaks were detected using a pulsed amperometric detector with standard quad waveform for carbohydrates and evaluated according to a standard profile.

Table 5: HPAEC solvent gradient setting for monosaccharides and organic acids analysis

Time (minutes)	Solvent A%	Solvent B%	Solvent C%
0	84	16	0
20	84	16	0
21	79	16	5
50	0	16	84
65	0	16	84
66	84	16	0
80	84	16	0

3.3.8. Disaccharides analysis

Cockle CE polysaccharide (5 µg) or cockle purified fraction (5 µg) were incubated with a mixture of 30 mIU for each of heparinases I, II and III in 200 µL heparinase buffer or they were incubated with 30 mIU of chondroitinase-ABC in 200 µL of chondroitinase buffer. Samples were incubated overnight at 37 °C and the reaction was terminated by heating to 100 °C for 5 min. The samples were passed through a 10 kDa spin filter then dried before further analysis.

Glycan reductive isotope labelling (GRIL) using isotopic aniline tagging was used for composition analysis and mass detection of disaccharide yields from heparinase- or chondroitinase-treated cockle polysaccharides (Lawrence et al., 2008). 15 µL (165 μmol) of labelled aniline tagging added to 5 µg of dried heparinase- or chondroitinase-derived disaccharides, then 15 µL of 1M sodium cyanoborohydride, freshly prepared in DMSO/acetic acid (7:3, v/v), were added to the sample. Reactions were carried out at 37 °C for 16 h, and

then dried using centrifugal evaporator, then the sample was spiked with [$^{13}C_6$] of 5 µL (8 *p*mol) of unsaturated disaccharide standards tagged. The dried samples were prepared for liquid chromatography coupled with mass spectrum (LC-MS) analysis by suspension in a running buffer (8 mM acetic acid, 5 mM in ion-pairing agent dibutylamine (DBA)), then disaccharides were separated on a C18 reversed-phase column (0.46 cm X 25 cm).

The solvent system for eluting the samples was 100% buffer (A) (8 mM acetic acid, 5 mM DBA) for 10 min, 17% buffer (B) (70%, methanol 8 mM acetic acid 5 mM DBA) for 15 min, 32% buffer (B) for 15 min, 40% buffer (B) for 15 min, 60% buffer (B) for 15 min, 100% buffer (B) for 10 min and 100% buffer (A). Ions of interest were detected in negative ion mode and the capillary temperature and spray voltage were kept at 140 °C and 4.75 kilo-volt, respectively, with UV detection set at 232 nM, data shown in appendix XII and XIII.

3.3.9. FT-IR

FT-IR is a type of spectroscopic technique that principally uses the infrared spectrum. It is simple, non-destructive, fast technique that can indicate the functional groups present within a sample and can aid in understanding the chemical structure of that sample. The main principle of the technique is the detection of the bonds between atoms, which can undergo stretching, bendingn or wagging rotation. IR radiation can pass through the sample and transmit light to the detector or it can be absorbed by the molecule. Therefore, the IR spectrum can be represented with an x-axis (wave number cm-1) and it's corresponding y-axis (transmittance%) (Movasaghi, Rehman and ur Rehman, 2008).

For the analysis of cockle CE polysaccharide, the sample platform was cleaned using 70% ethanol, followed by 16 scans to resolve any noise prior use. Then, 500 µg of dried cockle CE polysaccharide was placed on the sample platform and full infrared scan was determined in 16 scans. Data was analysed using OMNIC software.

3.3.10. NMR

NMR is a powerful spectroscopic technique that allows identifying the presence of certain physical and chemical properties of a molecule. As a result, it is excellent for providing the structural properties of an unknown molecule. The NMR instruments interacts with the nucleus by applying an external magnetic field. It has the ability to identify more than one nucleus at a time known as multi-dimensional NMR spectroscopy. This technique gathers more information about the presence of selected atoms. For instance, two-

dimensioned NMR can detect the resonance of both ^{1}H and ^{13}C at the same time, resulting in a correlation between the bonds of these two atoms (Friebolin and Becconsall, 1993).

For cockle polysaccharide analysis, one and two-dimensional (2D) ^{1}H and ^{13}C spectra of the cockle polysaccharides were recorded using Bruker 800 MHz machine with a triple resonance probe, and the spectra were analysed using TopSpin software. Approximately 5 mg of the cockle CE polysaccharide or its purified fraction 5 were dissolved in 0.5 mL of 99.9% deuterium oxide. All spectra were recorded at 56 ºC in water peak suppression mode. All chemical shifts were relative to the internal reference tetramethylsilane (TMS) (5 µL).

4. Results—Cockle CE polysaccharide biological and structural analysis

Cockle CE polysaccharide was extracted from marine-source cockle (*Cerastoderma edule)* using a typical cetylpyridinium chloride precipitation method, which resulted in about (24 mg) white fluffy material. Several biological and structural analyses tools were performed on cockle CE polysaccharide in order to assess its role as an antiproliferative agent as well as to assess its related structure. Firstly, cockle's CE polysaccharide pharmaceutical outcome as antiproliferative agent was assessed against two leukaemia cell lines (K-562 and Molt-4) and a mesothelioma (Mero-25) cancer cell line using a cell proliferation assay (MTT), this was followed by an apoptosis assay to determine its role in mediating cell death. Secondly, after confirming the antiproliferative activity against the cancer cell lines, several structural techniques were implemented such as monosaccharide and disaccharide compositional analyses, as well as FT-IR and NMR in order to obtain more structural details about this potent pharmaceutical agent.

4.1. Biological activities of cockle CE polysaccharides

4.1.1. Cockle CE polysaccharides—cell proliferation assay

Numerous studies have shown the potential medicinal properties of marine polysaccharides. In this study, marine polysaccharides isolated from cockle showed antiproliferative effects on cancer cell lines *in-vitro*. Cockle CE polysaccharides antiproliferative activities were assessed against leukaemia cell lines K-562 and Molt-4 and mesothelioma cell line Mero-25, which resulted in considerable inhibitory effects as determined using MTT assay (Figure 40). Some batch-to-batch variability in IC_{50} values was determined due to different cockle preparations as well as because of the complex heterogeneity of the polysaccharide chains present. Cisplatin was used in all assays as a positive control in the comparisons of different preparations. Typical IC_{50} values were around 10 ± 2 μg/mL, 1.2 ± 0.5 μg/mL and 22 ±4 μg/mL for the K-562, Molt-4 and Mero-25 cell lines, respectively.

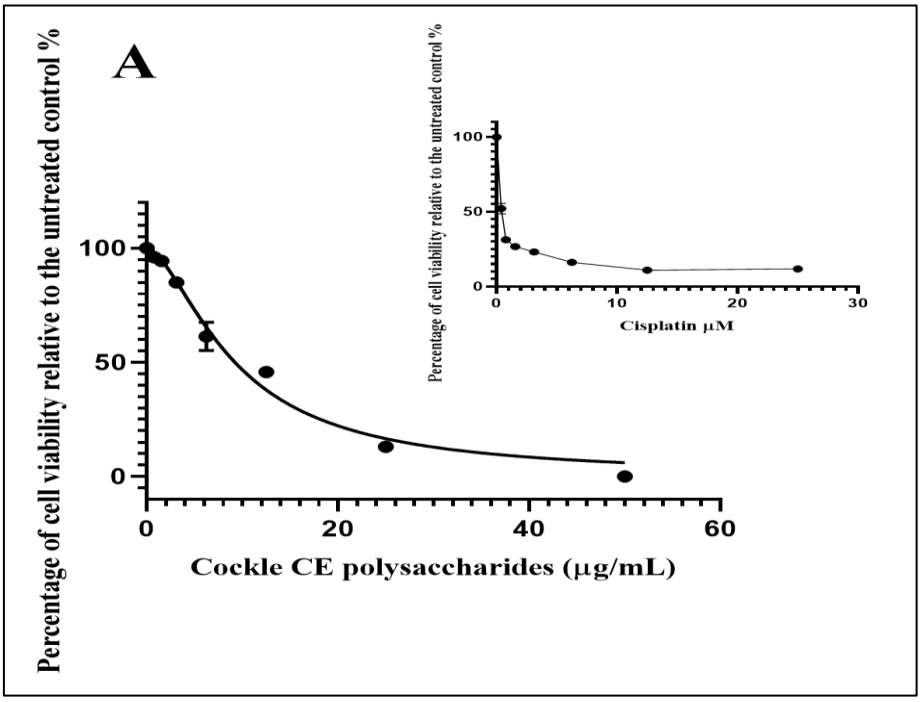
A
Percentage of cell viability relative to the untreated control %
100
50
0
0
20
40
60
Cockle CE polysaccharides (μg/mL)
Percentage of cell viability relative to the untreated control %
100
50
0
0
10
20
30
Cisplatin μM

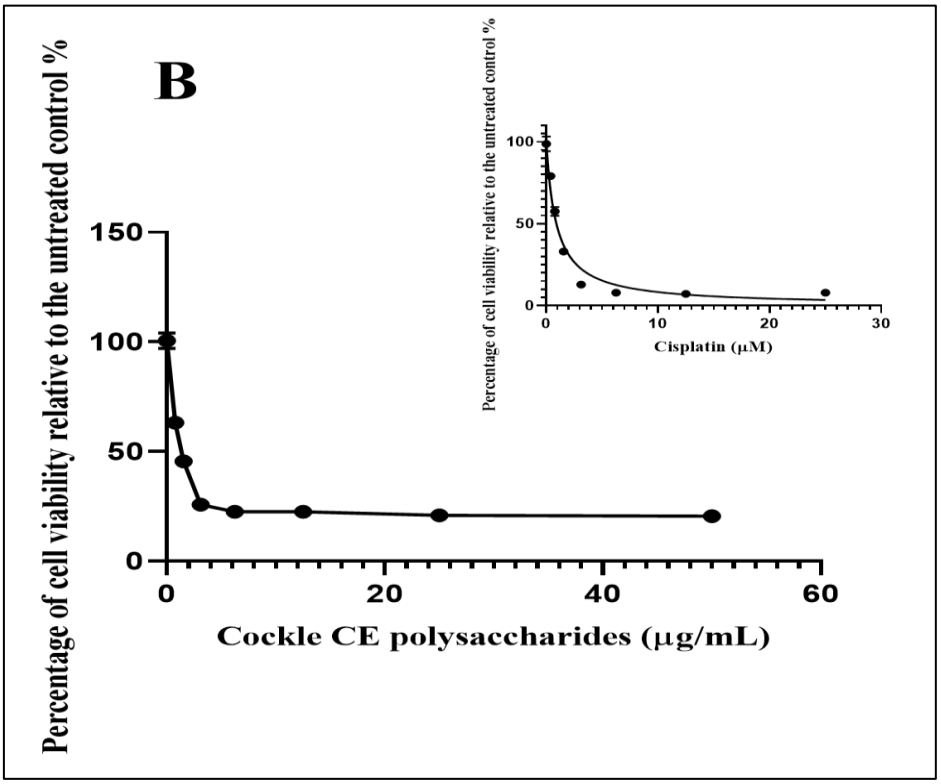
B
Percentage of cell viability relative to the untreated control %
150
100
50
0
0
20
40
60
Cockle CE polysaccharides (μg/mL)
Percentage of cell viability relative to the untreated control %
100
50
0
0
10
20
30
Cisplatin (μM)

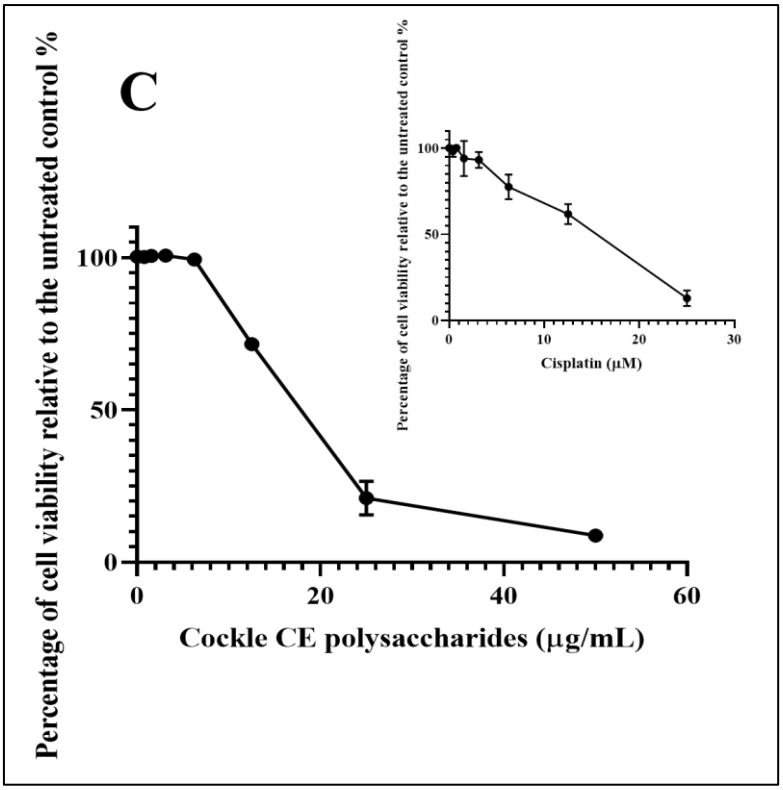

Figure 40. The antiproliferative activity of cockle CE polysaccharides on three cancer cell lines. Cancer cell lines K-562 (A), Molt-4 (B) and Mero-25 (C) were treated with increasing doses of cockle CE polysaccharides (0, 0.78, 1.56, 3.12, 6.25, 12.5, 25, 50 µg/mL) and cell viability was determined using MTT assay, as detailed in section 3.3.4. The inserts show the effects of cisplatin treatment on the number of viable cells. Cell viability is expressed as a percentage relative to the untreated control cells. All experiments were conducted in triplicate and the results are shown as the mean ± the SD. Cells were cultured under standard conditions and maintained at 37 °C in a humidified 5% CO_2 atmosphere.

Table 6. Present list of IC_{50} of cockle CE polysaccharide and cisplatin as positive control on all cell lines. All IC_{50} values were conducted in triplicate and calculated using non-linear regression analysis (GraphPad Prism 8.0).

Drug	List of IC_{50} on each cell line		
	K-562	Molt-4	Mero-25
Cockle CE polysaccharide (µg/mL)	9.23 (µg/mL)	1.5 (µg/mL)	19.33 (µg/mL)
Cisplatin (µM)	0.49 (µM)	0.9 (µM)	14.67 (µM)

4.1.1.1. Comparisons of cockle CE polysaccharide GAG-like antiproliferative activity with mammalian GAGs

Further investigations confirmed that mammalian-derived GAGs (porcine) had no antiproliferative activity on cancer cell lines using MTT assay (Figure 41). Cell proliferation assay showed that no measurable IC_{50} could be determined for mammalian heparin, HS, CS and DS against cancer cell lines; however, the cockle CE polysaccharides continued to show significant antiproliferative activity. In fact, at low concentrations, mammalian HS showed slight stimulatory activity on cell growth. These results suggest that, if HS-like-GAG chains are involved in the antiproliferative activity of cockle CE polysaccharides, then they must have unique structural features not found in typical mammalian GAGs.

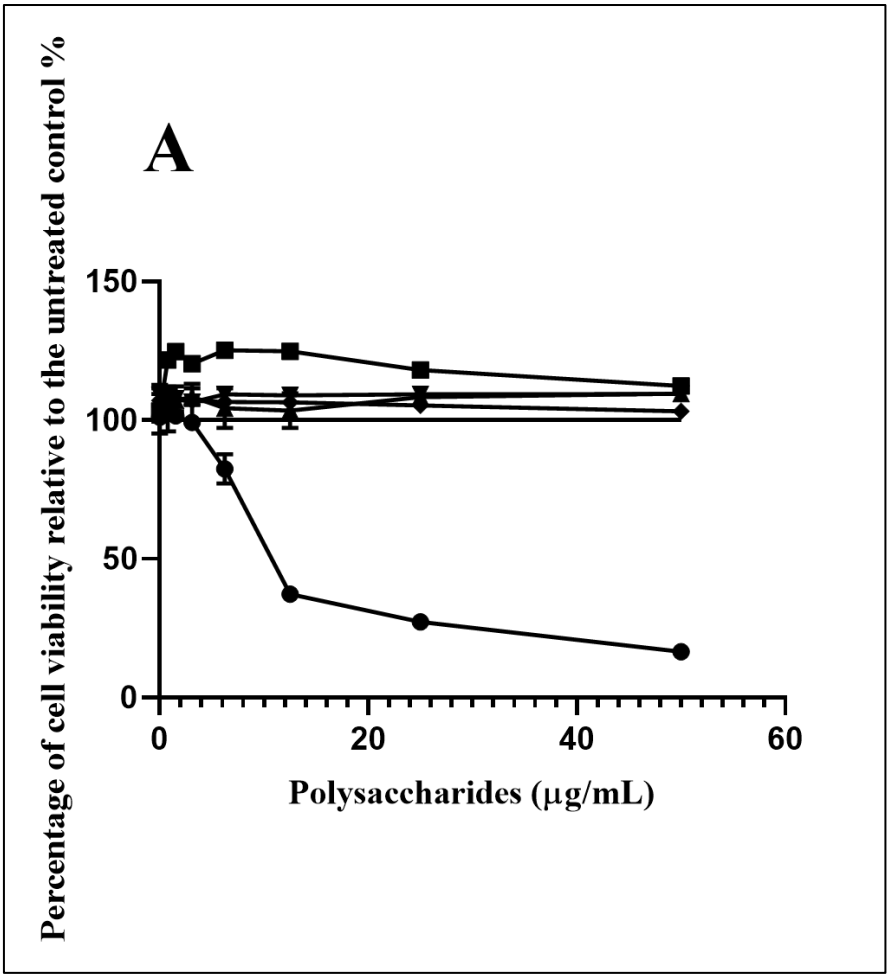

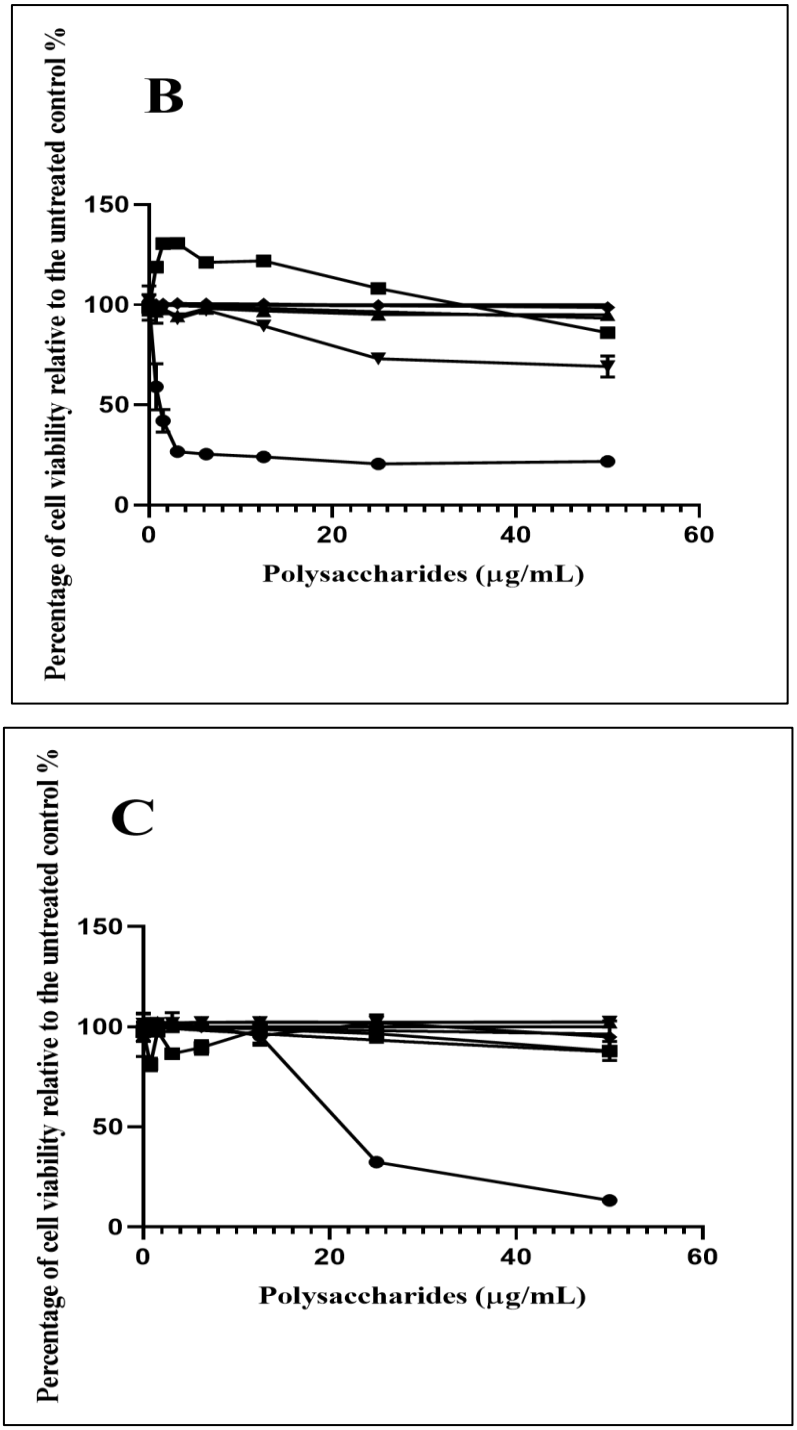

Figure 41. Comparisons between the antiproliferative activity of cockle CE polysaccharides and the common mammalian GAGs on cancer cell lines. The three cancer cell lines, K-562 (A), Molt-4 (B) and Mero-25 (C), were treated with increasing doses of cockle CE polysaccharides (0, 0.78, 1.56, 3.12, 6.25, 12.5, 25, 50 µg/mL) or common mammalian-GAGs (0, 0.78, 1.56, 3.12, 6.25, 12.5, 25, 50 µg). Cockle CE polysaccharides was the only agent that show antiproliferative activity on all cell lines. Cockle CE polysaccharides (●), mammalian-heparin (♦), mammalian-HS (■), mammalian-CS (▲) and mammalian-DS (▼). The data are presented as the percentage of viable cells following treatment with different polysaccharides, relative to the untreated control. All experiments were conducted in triplicate and the results are shown as the mean ± the SD. Cells were cultured and maintained at 37 °C in a humidified 5% CO_2 atmosphere.

Table 7. Present list of IC_{50} of cockle CE polysaccharide (0, 0.78, 1.56, 3.12, 6.25, 12.5, 25, 50 μg/mL) and mammalian GAGs (0, 0.78, 1.56, 3.12, 6.25, 12.5, 25, 50 μg/mL) on all cell lines. IC_{50} was determined when a drug has inhibited the cancer cells growth by 50% at maximum concentration of 50 μg/mL, therefore, if a drug has inhibited less than 50%, then the drug is considered to be inactive. All values were conducted in triplicate and the IC_{50} calculated using non-linear regression analysis (GraphPad Prism 8.0).

Polysaccharides as antiproliferative agent	List of IC_{50} on each cell line		
	K-562	Molt-4	Mero-25
Cockle CE polysaccharide	12.34 (μg/mL)	1.41 (μg/mL)	27.54 (μg/mL)
Mammalian-heparin	Inactive	Inactive	Inactive
Mammalian-HS	Inactive	Inactive	Inactive
Mammalian-CS	Inactive	Inactive	Inactive
Mammalian-DS	Inactive	Inactive	Inactive

4.1.1.2. Effects of enzymatic degradation on cockle CE polysaccharide antiproliferative activity

The extraction procedure designed to enrich the content of sulphated GAGs or sulphated GAG-like structures that also could cause attachment of contamination from other marine polysaccharides. These non-GAG polysaccharides may have contributed, solely or in part, to the observed antiproliferative activity of the cockle CE polysaccharides. Enzymatic treatments of the cockle CE polysaccharides were achieved. Heparinases, chondroitinase-ABC or fucosidase to investigate any link between typical GAG-like structures and the observed antiproliferative activity. After applying the 10 kDa spin filter, each sample has separated into two parts, flow through and retained part. The flow through part contained all the disaccharides, which showed no antiproliferative activity 9.8), while, the retained part has shown the antiproliferative activity. Figure 42 demonstrates that there was no appreciable change in the antiproliferative activity of the retained part when cockle CE polysaccharides were treated with chondroitinase-ABC and fucosidase. Heparinase digestion (individually and in combination), however, did lead to a significant loss of the antiproliferative activity within the retained part, with an approximate decrease in IC_{50} values for combined

heparinases (I, II, III) of around 4-, 8- and 2-fold for the K-562, Molt-4 and Mero-25 cell lines, respectively (Table 8).

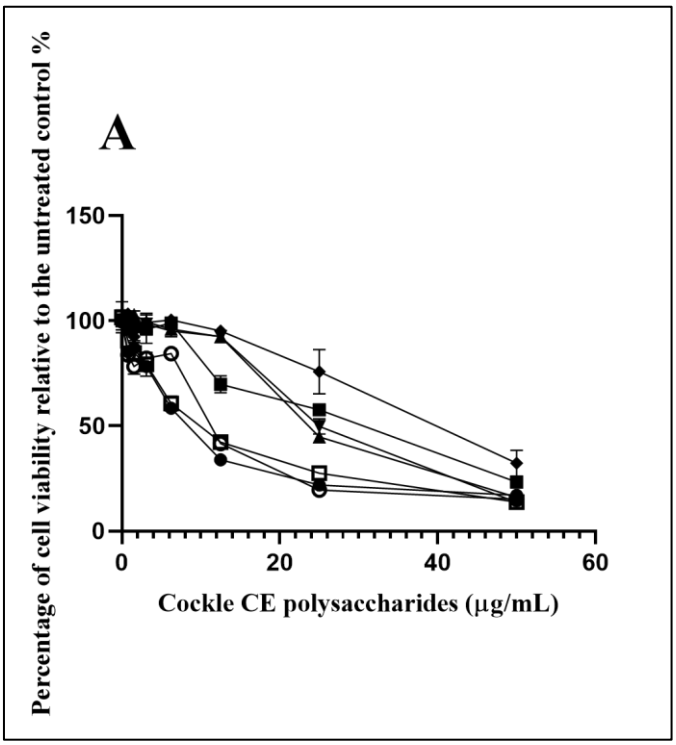

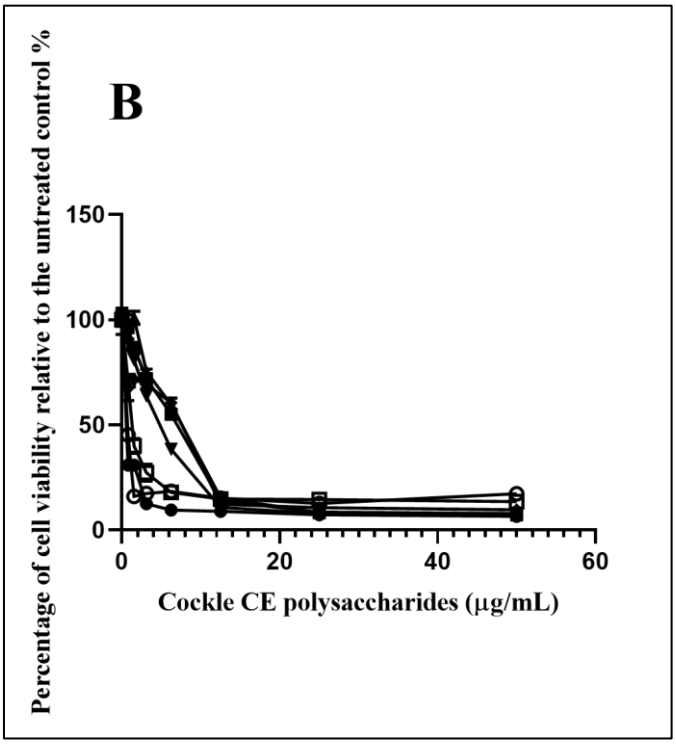

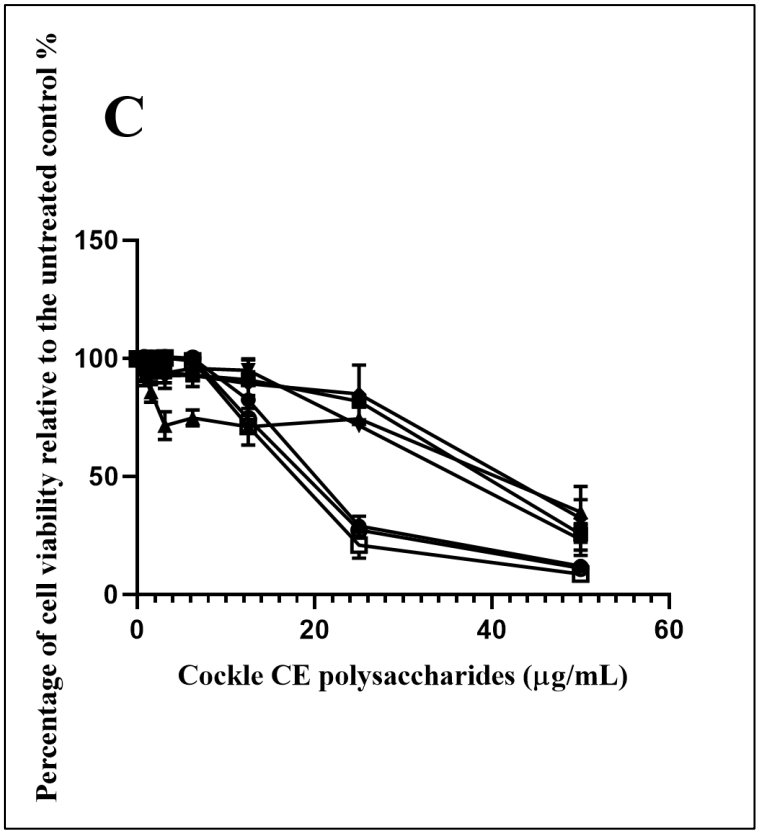

Figure 42. The effect of heparinase (I, II, III), chondroitinase ABC and α-L-fucosidase enzymatic digestion on cockle CE polysaccharide antiproliferative activity. The sensitivity of the cockle CE polysaccharide's antiproliferative activity to the enzymatic degradation was determined using MTT assay. The figure shows the antiproliferative activity of cockle polysaccharides retained part of the 10 kDa spin filter on the K-562 (A), Molt-4 (B) and Mero-25 (C) cell lines, with and without enzymes, as cockle CE polysaccharides (●), cockle CE treated with heparinase-I (■), cockle CE treated with heparinase-II (▲), cockle CE treated with heparinase-III (▼), cockle CE with heparinase-I, II, III treated (♦), cockle CE treated with chondroitinase-ABC (○) and cockle CE treated with fucosidase (□). The data are presented as the percentage of viable cells following treatment with cockle polysaccharides, relative to the untreated control. Cockle CE showed high sensitivity to heparinase enzymes (solely and in combination), while chondroitinase-ABC and fucosidase showed no effect on the antiproliferative activity. All experiments were conducted in triplicate and the results are shown as the mean ± the SD. Cells were cultured in suspension and maintained at 37 °C in a humidified 5% CO_2 atmosphere.

Table 8**.** Present list of IC_{50} of cockle CE polysaccharide (0, 0.78, 1.56, 3.12, 6.25, 12.5, 25, 50 μg/mL) and its digested chains by the action of heparinases, chondroitinase-ABC or fucosidase on cancer cell lines. All IC_{50} values were conducted in triplicate and calculated using non-linear regression analysis (GraphPad Prism 8.0).

Polysaccharide as antiproliferative agent	List of IC_{50} on each cell line (μg/mL)		
	K-562	Molt-4	Mero-25
Cockle CE polysaccharide	8.18	0.5	23.5
Cockle CE polysaccharide with heparinase-I	26.43	5.7	48
Cockle CE polysaccharide with heparinase-II	24.52	6.6	32.04
Cockle CE polysaccharide with heparinase-III	25.52	4.33	43.7
Cockle CE polysaccharide with heparinase-I, II and III	38.06	4.7	50
Cockle CE polysaccharide with chondroitinase-ABC	11.07	0.6	21.4
Cockle CE polysaccharide with α-L-fucosidase	9.5	1.4	19

4.1.2. Apoptosis detection assay—Annexin V

Cell apoptosis detection assay using Annexin-V FITC/PI staining, followed by flow cytometry was used to investigate the mechanism of cell death following treatment with cockle CE polysaccharides. Cell death mechanism of all cell lines treated with cockle CE polysaccharides was potentially mediated via apoptosis. K-562 and Molt-4 cell lines showed a small increase in the late apoptotic phase, Mero-25 cell line did not show any late apoptotic markers (Annexin V+/PI+), when cells were treated with cockle CE polysaccharide. However, early apoptosis (Annexin V+/PI−) showed the biggest change in all cell populations after 24 h incubation. Necrotic cells (Annexin V−/PI+) showed little change over

untreated controls. The results shown in Figure 43 clearly implicate apoptosis as the most likely cause of cellular cytotoxicity following treatment by cockle CE polysaccharides. However, primary necrosis cannot be ruled out.

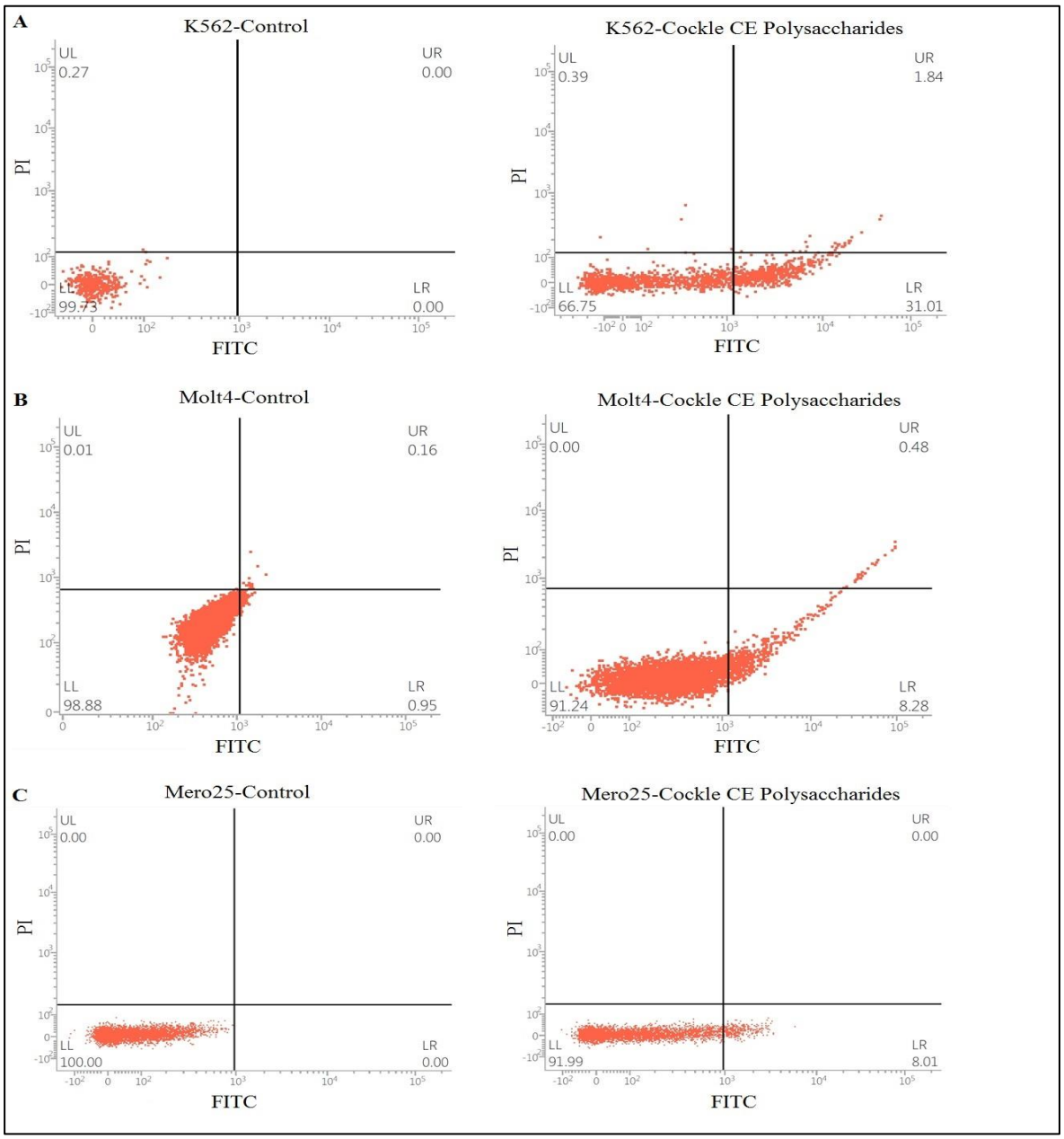

Figure 43. Apoptosis assay Annexin-V FITC/PI. K-562 (A), Molt-4 (B) and Mero-25 (C) cell lines were treated with cockle CE polysaccharides (50 μg) for 24 hours, then cells were stained with Annexin V-FITC and PI stains, in addition to staining the untreated cells, which left as control. A: K-562 scatter plot of Annexin V-FITC/PI stained control cells (left) and scatter plot of cells treated with cockle CE polysaccharides (right). B: Molt-4 scatter plot of Annexin V-FITC/PI stained control cells (left) and scatter plot of cells treated with cockle CE polysaccharides (right). C: Mero-25 scatter plot of Annexin V-FITC/PI stained control cells (left) and scatter plot of cells treated with cockle CE polysaccharides (right).

4.2. Structural analysis of cockle CE polysaccharides

4.2.1. Disaccharide analysis of cockle CE polysaccharides

Disaccharide analysis was used in the first instance to confirm the presence of typical unsaturated HS/heparin and CS/DS disaccharides residues following treatment of the cockle CE polysaccharide with heparinase I, II and III or chondroitinase-ABC. Primary analysis of the HS/heparin unsaturated disaccharide compositions, which were released after digestion of the cockle CE polysaccharides with combined heparinases (I, II, III), showed that susceptible chains within the cockle CE polysaccharide sequence did contain the major disaccharide types found in mammalian HS/heparin. However, the combined digestion of heparinases (I,II and III) is suggested to be incomplete, according to the proliferation activity (Figure 42).

The key differences between cockle CE unsaturated disaccharides and mammalian HS unsaturated disaccharides were the low levels of unsulphated disaccharide of [ΔHexA-GlcNAc] and the high levels of the disulphated disaccharide [ΔHexA-GlcNS(6S)] released from the cockle polysaccharides (Table 9). On the other hand, other unsaturated disaccharides were at similar levels to those seen with typical mammalian HS types. As heparinases treatment of the cockle polysaccharides failed to generate high quantities of this highly sulphated disaccharide [ΔHexA(2S)-GlcNS(6S)], which could indicate the presence of HS-like structure within cockle CE polysaccharides is much closer to mammalian HS than heparin.

Despite the fact that the chondroitinase-ABC treatment of cockle CE polysaccharides failed to show any significant loss of antiproliferative activity, CS/DS disaccharide analysis was performed. The principle unsaturated disaccharides were produced by chondroitinase-ABC digestion as [ΔHexA-GalNAc(4S)], [ΔHexA-GalNAc(6S)] and [ΔHexA-GalNAc(4,6S)]. The results undoubtedly show that CS/DS-like chains also exist within the cockle CE polysaccharide preparations.

Overall, information gathered from the disaccharide analysis data support the initial suggestion that the reduction in the antiproliferative activity, following by treatment of cockle CE polysaccharides with heparinases, was due to breakdown of HS/Heparin-like chain. Since it resulted in the release of unsaturated disaccharides that are found in mammalian HS/heparin types. The presence of heparinase resistant fragments as well as the lack of antiproliferative activity of the mammalian GAGs suggested the presence of an uncommon

HS-like structure, which suggested that active HS-like could be different from the mammalian HS.

Table 9. Disaccharide composition analysis of cockle CE polysaccharide, mammalian HS/heparin and mammalian CS/DS. Data are presented as a percentage of the moles of HS/Heparin[1] and CS/DS[2] unsaturated disaccharides produced by heparinase (I, II, III) and chondroitinase-ABC digestion.

HS/Heparin Disaccharides	**Cockle CE disaccharides produced (mole %)**	**Standard HS disaccharides produced (mole %)**
ΔHexA-GlcNAc	26.6	61.5
ΔHexA(2S)-GlcNAc	0.0	1.9
ΔHexA(2S)-GlcNH2	0.0	0.01
ΔHexA-GlcNAc(6S)	4.1	1.9
ΔHexA(2S)-GlcNAc(6S)	4.0	0
ΔHexA-GlcNS	25.5	17.8
ΔHexA(2S)-GlcNS	9.5	11.5
ΔHexA-GlcNS(6S)	24.7	0.8
ΔHexA-GlcNH2(6S)	0.0	0
ΔHexA(2S)-GlcNS(6S)	5.6	4.6
ΔHexA(2S)-GlcNH2(6S)	0.0	0
Total	100%	100%
Type of sulphation	**Sulphate %**	**Sulphate %**
Unsulphated	26.61	61.51
N-SO_3^-	65.23	34.67
2-O-SO_3^-	19.06	18.04
6-O-SO_3^-	38.47	7.32
Number of Sulphates	**Mole %**	**Mole %**
0-SO_3^-	26.61	61.51
1-SO_3^-	29.60	21.55
2-SO_3^-	38.20	12.35
3-SO_3^-	5.58	4.59
Total GAG disaccharides produced by heparinase digestion (µg)	0.06	0.61
Average sulphate per disaccharides	1.23	0.60

CS/DS Disaccharides[2]	**Cockle CE disaccharides produced (mole %)**	**CS standards disaccharides produced (mole %)**
ΔHexA-GalNAc	3.2	5.08
ΔHexA-GalNAc(4S)	33.5	56.05
ΔHexA-GalNAc(6S)	17.2	37.94
ΔHexA(2S)-GalNAc(4S)	0	0.21
ΔHexA(2S)-GalNAc(6S)	0.7	0.02
ΔHexA-GalNAc(4S)(6S)	45.4	0.7
ΔHexA(2S)-GalNAc(4S)(6S)	0	0
Total	100%	100%
Type of sulphation	**Sulphates %**	**Sulphates %**
Unsulphated	3.22	5.0
2-O-SO_3^-	0.68	0.23
4-O-SO_3^-	78.87	56.9
6-O-SO_3^-	63.29	38.67
Number of Sulphates	**Mole %**	**Mole %**
0-SO_3^-	3.22	5.0
1-SO_3^-	50.73	93.99
2-SO_3^-	46.05	0.94
3-SO_3^-	0.00	0.00
Total GAG disaccharides produced by chondroitinase-ABC digestion (µg)	0.12	1.1
Average sulphate per disaccharides	1.43	0.96

4.2.2. Monosaccharide compositional analysis

The disaccharide analysis employed in this study did not provide adequate information about the identity of the uronic acid as well as missing some information about the non-GAG compounds that could be linked to the cockle CE polysaccharide sequence. These two major issues were resolved by monosaccharide analysis of the cockle CE polysaccharides. Analysis of the cockle CE polysaccharide preparations revealed the

presence of significant quantities of the monosaccharides $GalNH_2$, $GlcNH_2$ and GlcA, which are typically found following acid hydrolysis of mammalian and marine GAG chains (Table 10). Interestingly, the lack of an IdoA component would suggest the presence of HS-like chains, rather than heparin. The neutral sugars such as Glc and Gal were by far the most predominant monosaccharides present in the cockle CE polysaccharide preparations, which are components typically found in marine N- and O-linked glycans, with about 10% fucose residues that can be derived from the original N-linked sequence preparations or fucosylated glycan. The data support the presence of GAG-like chain, as was indicated by both the susceptibility of cockle CE polysaccharides to heparinase/chondroitinase ABC digestion and the production of a range of unsaturated disaccharides typically found in mammalian GAG chains.

Table 10. Monosaccharide composition analysis of the cockle CE polysaccharide. 50 µg of sample was degraded with trifluoroacetic acid prior to HPAEC-PAD analysis. The peaks observed were identified by comparison with the elution positions of known monosaccharide standards. Data are presented as a percentage of the moles of monosaccharide produced by acid hydrolysis.

Monosaccharide	**Cockle CE polysaccharide (mole %)**
Fucose	11.1
$GalNH_2$	16.7
$GlcNH_2$	9.9
Gal	19.1
Glc	35.2
Man	3.7
GlcA	4.3
IdoA	0
Total	100

4.2.3. FT-IR

FT-IR spectroscopic analysis of cockle CE polysaccharides and qualitative analysis of functional groups were carried out. Cockle CE polysaccharide's spectrum is illustrated in Table 11. The table shows peaks ranging from 814.02 to 3351.09 cm^{-1}. Major peaks are at 814.02, 1043.39, 1223.17, 1417.02, 1644.69, 2927.87 and 3351.09 cm^{-1}. Interestingly, a lack of signals around 1700 cm^{-1} confirm the absence of IdoA (Zhang et al., 2008).

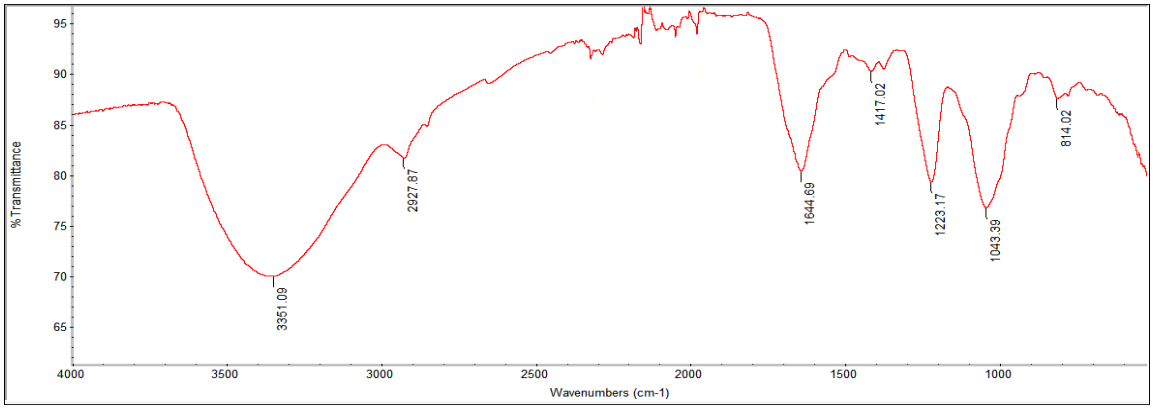

Figure 44. FT-IR spectra of cockle CE polysaccharide with wave number (cm^{-1}).

Table 11. Peak assignment of FT-IR spectrum for cockle CE polysaccharide and standard heparin (bovine).

Wavelength (cm^{-1})		**Assignments**	**Reference**
Standard heparin	Cockle CE polysaccharide		
1020	≈ 1043.39	C-O-C pyranose ring (stretching vibration).	(Charles, Huang and Chang, 2008; Liao et al., 2013).
1220.11	≈ 1223.02	S=O sulfonate stretching vibration.	(Cabassi, Casu and Perlin, 1978).
1417.4	1417.02	Carboxylate stretching of uronic acid at C-6.	(Liao et al., 2013).
1604.44	≈ 1644.69	Antisymmetric vibration of carboxylate of uronic acid C-6.	
2944.95	≈ 2927.87	C-H stretching of hexosamine.	(Zhang et al., 2013).
3404.74	≈ 3351.09	Hydroxyl O-H stretching.	

4.2.4. NMR spectroscopy

Although NMR is a potent structural technique, especially for carbohydrates, it was unable to provide useful structural information about cockle CE polysaccharides. It was clear from disaccharide and monosaccharide analysis that there was considerable heterogeneity in the types of marine polysaccharides in the cockle CE as well as high structural diversity within each polysaccharide. Therefore, the cockle CE polysaccharides with the antiproliferative activity were fractionated according to their anionic charges, by anion-exchange chromatography, in order to allow a more focused structural analysis, while separating the contamination from the antiproliferative activity, which could help in determining the nature of cockle polysaccharides with GAG-like properties.

5. Results—Cockle GAGs purification and polysaccharides fractions analysis

Cockle polysaccharide heterogeneous nature has limited the ability to identify the final structure with antiproliferative activity on cancer cell lines. Therefore, cockle CE polysaccharides were purified using anion-exchange chromatography in order to determine structures and to correlate the structures to the novel antiproliferative activity from the purified fractions. After successful isolation of 6 purified fractions from the anion-exchange chromatography (Figure 45), biological activity was assessed using the cell proliferation assay (MTT assay), followed by an apoptosis assay (for active fractions only), on the K-562, Molt-4 and Mero-25 cell lines. Thereafter, additional structural determinations were to be performed to evaluate the active fraction structure.

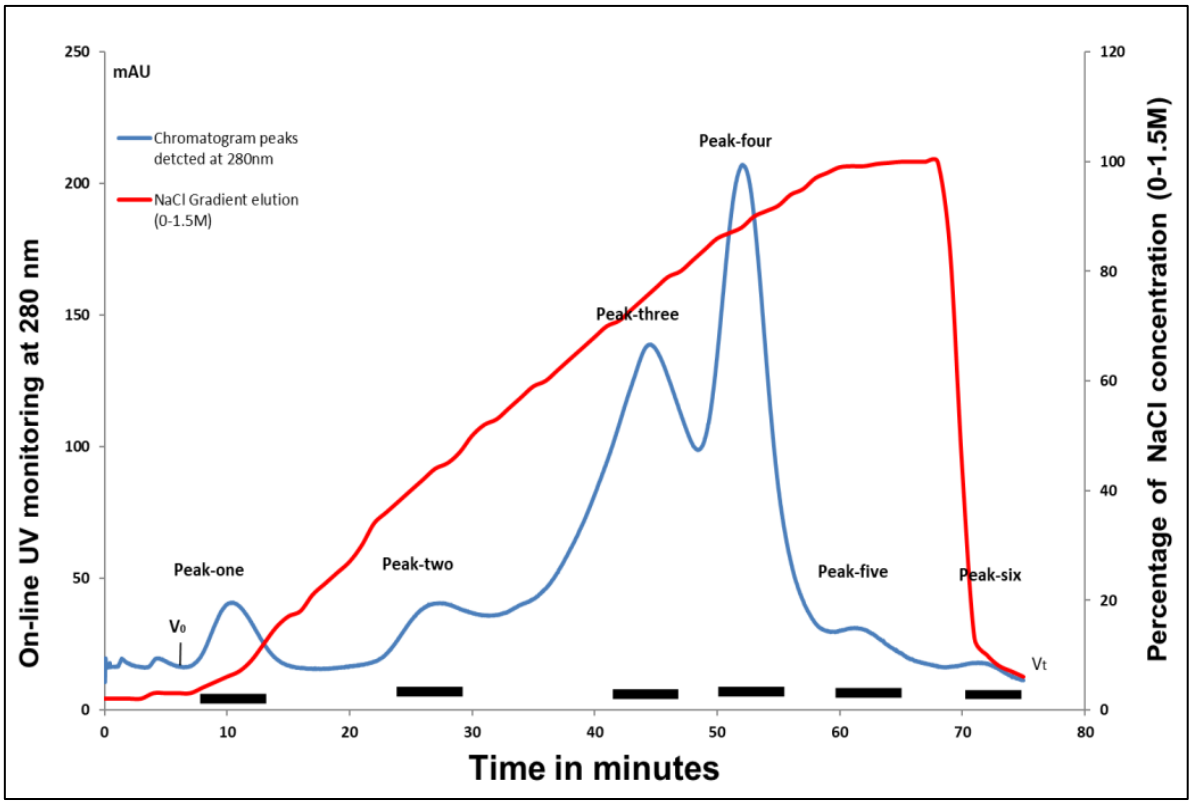

Figure 45. Anion-exchange chromatography of cockle CE polysaccharides. The cockle CE polysaccharide sample was injected to the FPLC system using anion-exchange DEAE-Sepharose resin and it was eluted using linear gradient of 0–1.5 M NaCl over 75 min. Peaks were pooled, as indicated by the bars shown, then, desalted, lyophilised and stored at -20 °C for further analysis.

5.1. Anion-exchange chromatography

Accordingly, cockle CE polysaccharide was purified based on their anionic charge using anion-exchange chromatography as described in section (3.3.2) (Habuchi, Habuchi and Kimata, 1995). The eluent was monitored at 280 nM to detect the peptide fragments still attached to the polysaccharide chains following the initial protease digestion, which resulted in typical elution profile shown in (Table 12) with six generally occurring peaks. The absorbance measured under each peak was broadly comparable to the dry weights of polysaccharides obtained after desalting and lyophilisation.

Table 12. Representation of the anion-exchange chromatography elution peaks of purified cockle CE polysaccharide in minutes and its corresponding NaCl molarity % was assessed by the electroconductivity on-line monitor.

Peak number	NaCl %	Elution time (min)
Peak-one	3-12	7-13
Peak-two	36-52	23-31
Peak-three	71-80	42-47
Peak-four	86-92	50-55
Peak-five	99-100	60-65
Peak-six	44-6	70-75

5.2. Biological activities of cockle polysaccharide purified fractions

5.2.1. Cell proliferation assay—Cockle purified fractions

Following the purification of cockle CE polysaccharide, all fractions were collected, desalted and lyophilised. Cockle polysaccharide fractions' antiproliferative activities were evaluated using a cell proliferation MTT assay on the K-562, Molt-4 and Mero-25 cell lines. Figure 46 shows that most of the antiproliferative activity was due to fraction 5, with negligible antiproliferative activity observed with fractions 1–3. The elution profile from the anion-exchange chromatography suggests that the low levels of activity observed in fractions 4 and 6, which could be due to cross-contamination with fraction 5. The results indicate that

the antiproliferative activity of fraction 5 is relatively due to minor component of the CE polysaccharides (approximately 1-2% of the total dry mass)

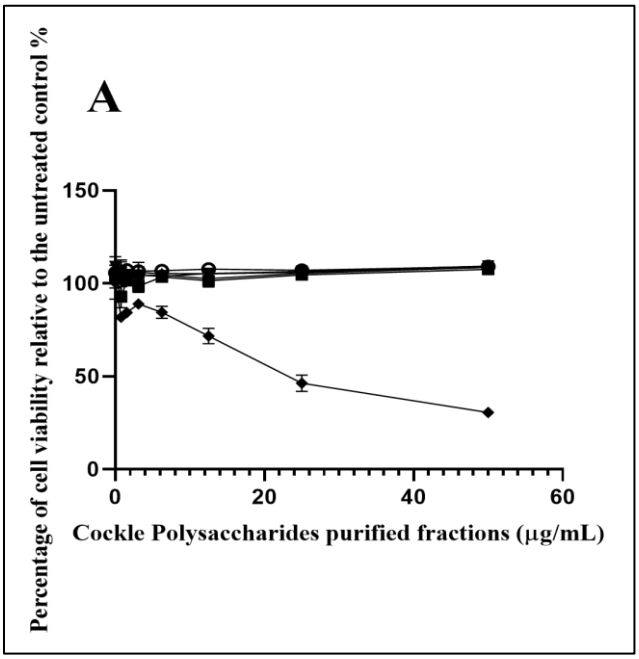

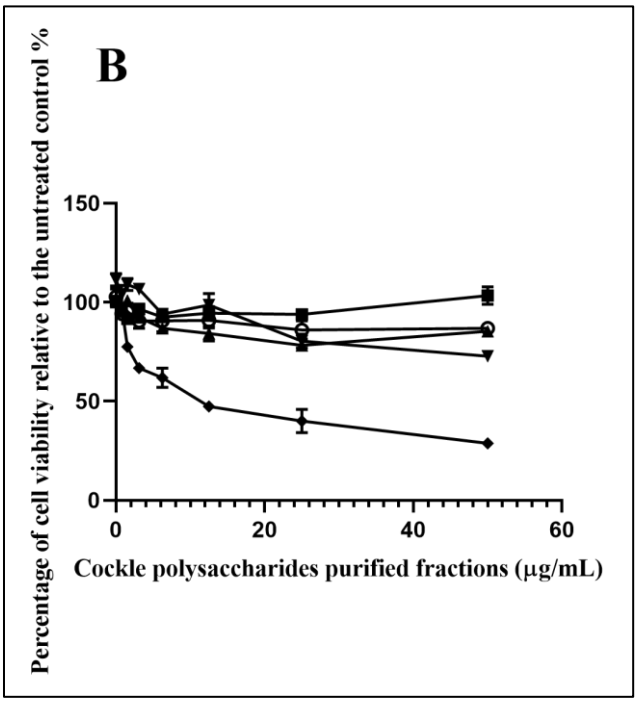

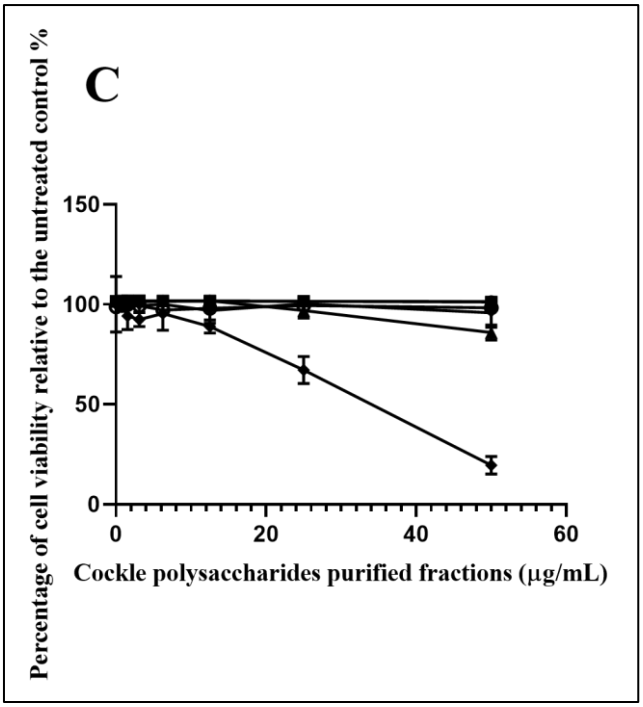

Figure 46. Antiproliferative activity of cockle polysaccharide purified fractions. Assessment of the antiproliferative activity of the purified fractions on K-562 (A), Molt-4 (B) and Mero-25 (C) cell lines that were achieved using MTT assay. Fraction 5 was expressed potent antiproliferative activity, in comparisons to other inactive fractions in terms of IC_{50}. Fraction one (●), fraction two (■), fraction three (▲), fraction four (▼), fraction five (♦) and fraction six (○). The data are presented as the percentage of viable cells following treatment with cockle polysaccharides fractions, relative to untreated control. All experiments were conducted in triplicate and the results are shown as the mean ± the SD and the IC_{50} values were calculated using non-linear regression analysis (GraphPad Prism 8.0). Cells were cultured and maintained at 37 °C in a humidified 5% CO_2 atmosphere.

Table 13. Presents list of IC_{50} of the cockle polysaccharide purified fractions on cancer cell lines. IC_{50} was determined when drug inhibited the cancer cells growth by 50% at maximum concentration of 50 µg/mL, therefore, if the drug has inhibited less than 50%, then the drug is considered to be inactive. All IC_{50} values were conducted in triplicate and calculated using non-linear regression analysis (GraphPad Prism 8.0).

Cockle polysaccharide purified fraction	List of IC_{50} on each cell line (µg/mL)		
	K-562	Molt-4	Mero-25
Fraction-1	Inactive	Inactive	Inactive
Fraction-2	Inactive	Inactive	Inactive
Fraction-3	Inactive	Inactive	Inactive
Fraction-4	Inactive	Inactive	Inactive
Fraction 5	24	11.4	37
Fraction-6	Inactive	Inactive	Inactive

5.2.2. Effects of enzymatic degradation on cockle polysaccharide Fraction 5 antiproliferative activities

Enzymatic treatment of the cockle polysaccharide purified fraction 5 using heparinases (I, II, III) or chondroitinase-ABC was used to investigate any link between GAG-like chains and the observed antiproliferative activity. Cockle polysaccharide fraction 5 treated with chondroitinase-ABC enzyme has shown no appreciable decrease in antiproliferative activity on the retained part of the 10 kDa spin filter on all cell lines. On the other hand, treatment of fraction 5 by heparinase enzymes (individually and in combination) on the K-562 and Mero-25 cell lines showed a considerable reduction in the antiproliferative activities on the retained part of the spin filter. There was little difference between the individual heparinase enzymes on the Molt-4 cell line; however, in replicates heparinase-II significantly destroyed the antiproliferative activity, while the other heparinase treatments led to significantly loss of most the antiproliferative activity, as seen with heparinase-I and III, and in combination with all enzymes including heparinase-II. Taken together, the data suggest that HS/heparin-like-GAG structure probably exists in the active fraction 5, and it could play an important contributing role to the antiproliferative activity of ion-exchange purified cockle polysaccharides (Figure 47).

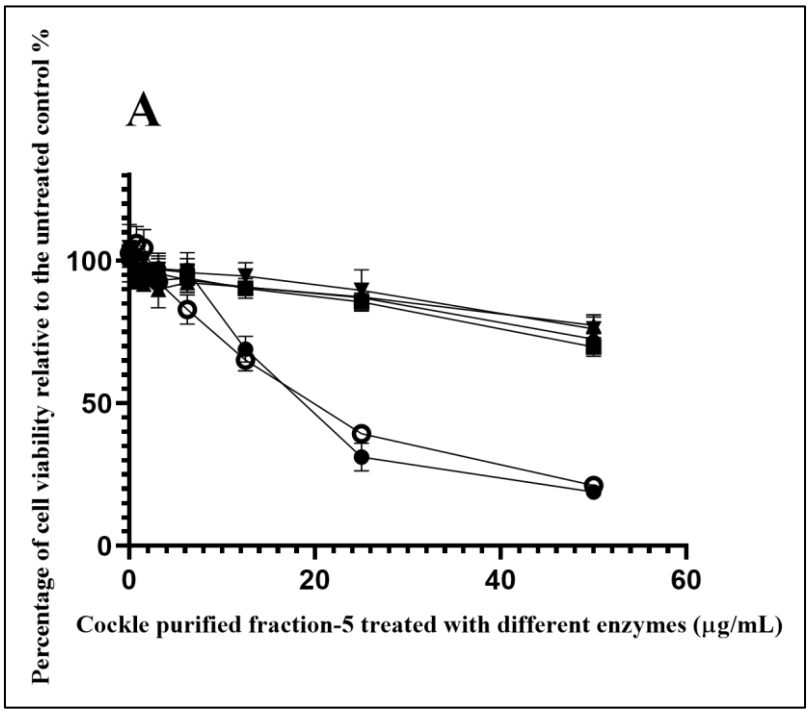

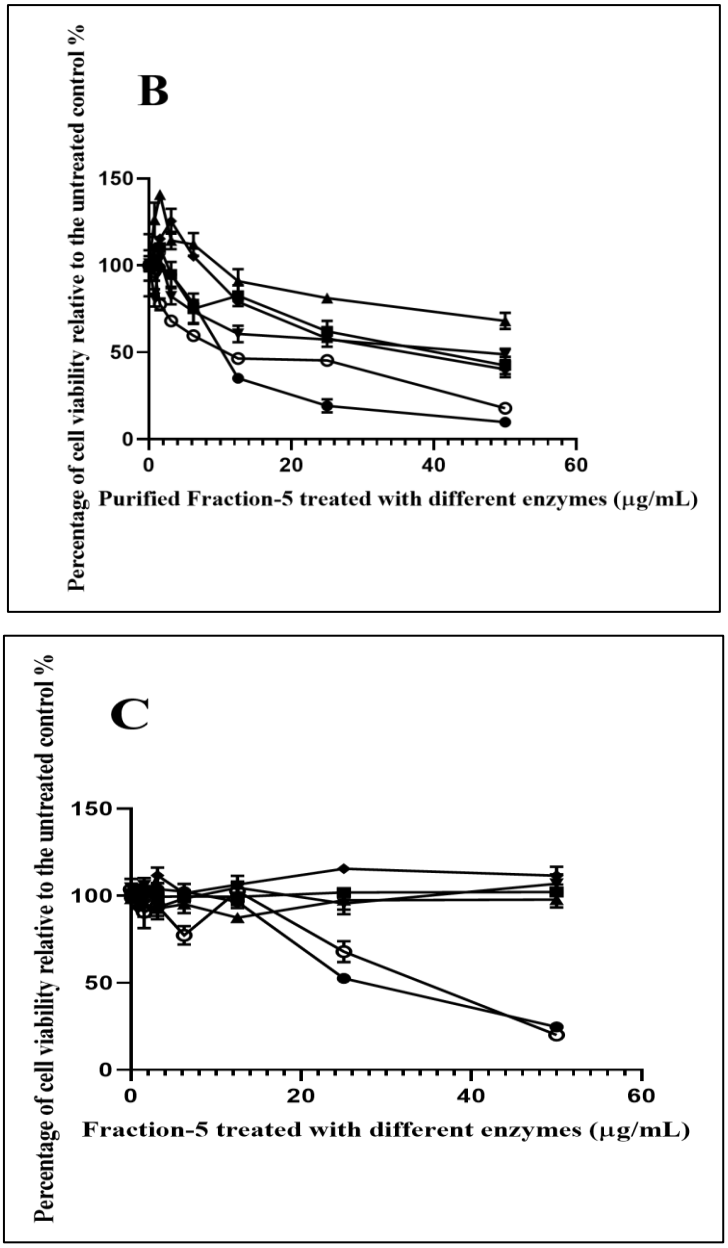

Figure 47. The effect of heparinase enzymes (individually or in combination) (I, II, III) or chondroitinase-ABC enzymatic digestion on the antiproliferative activity of the cockle polysaccharide purified fraction 5. The sensitivity of the cockle polysaccharide's purified fraction 5 to the enzymatic degradation on the antiproliferative activity was determined using MTT assay on the K-562 (A), Molt-4 (B) and Mero-25 (C) cell lines, in addition to assessing the antiproliferative activity of undigested fraction 5 in order to confirm the difference between chains activity. Cockle polysaccharides Fraction 5 (●), cockle polysaccharides Fraction 5 treated with heparinase-I (■), cockle polysaccharides Fraction 5 treated with heparinase-II treated (▲), cockle polysaccharides Fraction 5 treated with heparinase-III treated (▼), cockle polysaccharides Fraction 5 treated with heparinase I, II, III treated (♦) and cockle polysaccharides Fraction 5 treated with chondroitinase-ABC (○). The data is presented as the percentage of viable cells following treatment with cockle polysaccharides fraction 5 and its digests, relative to untreated control. All experiments were conducted in triplicate, the results are shown as the mean ± the SD and the IC_{50} values were calculated using non-linear regression analysis (GraphPad Prism 8.0). Cells were cultured and maintained at 37 °C in humidified 5% CO_2 atmosphere.

Table 14. Represents list of IC_{50} of cockle polysaccharide purified fractions on all cell lines. IC_{50} was determined when drug has inhibited the cancer cells growth by 50% at maximum concentration of 50 μg/mL, therefore, if the drug has inhibited less than 50%, then the drug is considered to be inactive. All IC_{50} values were conducted in triplicate and calculated using non-linear regression analysis (GraphPad Prism 8.0).

Cockle purified fraction 5 treated with different GAG-related enzymes	List of IC50 on each cell line (μg/mL)		
	K-562	Molt-4	Mero-25
Fraction 5	21.42	11.5	37
Fraction 5 treated with heparinase-I	Inactive	40.35	Inactive
Fraction 5 treated with heparinase-II	Inactive	Inactive	Inactive
Fraction 5 treated with heparinase-III	Inactive	28.60	Inactive
Fraction 5 treated with heparinase-I, II and III	Inactive	48.67	Inactive
Fraction 5 treated with chondroitinase-ABC	21	10.70	38.2

5.2.3. Apoptosis detection assay Annexin-V—Cockle polysaccharide purified fraction 5

The antiproliferative activity of cockle polysaccharide fraction 5 was further investigated on cancer cell lines using an apoptosis assay. Cancer cells were treated with cockle polysaccharide purified fraction 5, then, cellular apoptosis was assessed using cellular apoptosis targets Annexin-V FITC/PI, followed by flow cytometry. *In-vitro* treatment with fraction 5 was potentially mediated via apoptosis. Early apoptotic markers (Annexin V+/PI−) showed the biggest change in cell populations after 24 h incubation in all cell lines. However, the K-562 and Molt-4 cell lines showed small increases in the late apoptotic phase (Annexin V+/PI+), while, Mero-25 cell line did not show any increase in the late apoptotic phase. K-562 necrotic cells (Annexin V−/PI+) showed little change over untreated controls. Thus, the results clearly implicate apoptosis as the most likely cause of the cellular cytotoxicity seen following treatment by cockle polysaccharide fraction 5 (Figure 48). However, primary necrosis cannot be ruled out.

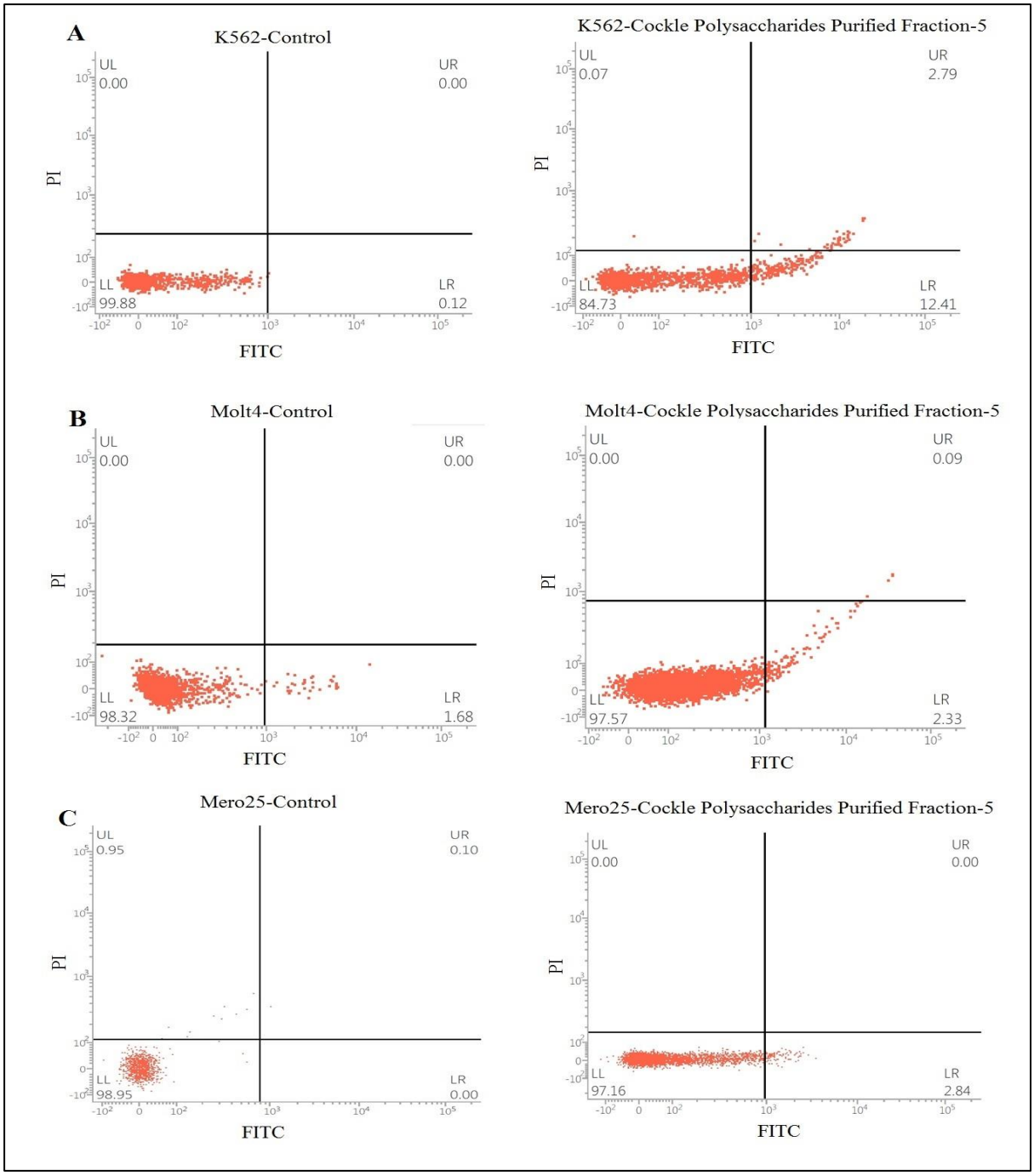

Figure 48. Apoptosis assay Annexin V-FITC/PI. K562 (A), Molt-4 (B) and Mero-25 (C) cell lines, were treated with 50 µg/mL of cockle polysaccharide purified fraction 5 for 24 h, then stained using Annexin V-FITC and propidium iodide (PI). A: K562 scatter plot of Annexin V-FITC/PI stained control cells (left) and scatter plot of cells treated with cockle polysaccharide purified Fraction 5 (right). B: Molt-4 scatter plot of Annexin V-FITC/PI stained control cells (left) and scatter plot of cells treated with cockle polysaccharide purified fraction 5 (right). C: Mero-25 scatter plot of Annexin V-FITC/PI stained control cells (left) and scatter plot of cells treated with cockle polysaccharide fraction 5 (right). Cancer cells treatment with Fraction 5 has led to cellular apotosis. Results are presented as the mean ± of three independent experiments.

5.3. Structural analysis of cockle polysaccharides purified fractions

5.3.1. Disaccharide analysis—anion-exchange purified fractions

Disaccharide composition analysis of the cockle purified polysaccharide fractions was used to identify the nature of the glycan structures presented within the purified fractions in order to correlate its structure to the antiproliferative activity in comparisons to the known marine/mammalian GAGs. Table 15 shows the distribution of unsaturated disaccharides of all purified fractions and the amounts produced in micrograms when each fraction was treated with a combination of all heparinases (I, II, III). The total weight of disaccharides produced from each microgram of sample digested indicated that only fraction 5 produced a significant number of unsaturated disaccharides. Fractions 1, 2, 3 and 4 produced approximately 30-, 150-, 30- and 6- fold less disaccharide than did fraction 5, respectively, suggesting that the early eluting fraction contains mainly non-HS-like chains.

The compositions of fractions 5 and 6 showed the presence of all major disaccharides found within mammalian HS/heparin chains. The enrichment of the trisulphated disaccharide [ΔHexA(2S)-GlcNS(6S)] and the disulphated disaccharide [ΔHexA(2S)-GlcNS] showed approximately four-fold and three-fold increases, respectively, in comparison to the unfractionated cockle polysaccharides (Table 9). These likely contributed significantly to the later elution of these chains from the anion-exchange column.

Fraction 1 appeared to generate the highest proportion of sulphates per disaccharides than any other fractions; however, the quantity, in micrograms of disaccharides produced was very small, compared to the total material digested. In fact, there is little correlation between the increase in the number of sulphates per disaccharide produced from heparinase digestion and the elution positions. This could be linked to the limited digestion of the glycan chains contained within them.

Table 15. HS disaccharide analysis of cockle polysaccharide anion-exchange purified fractions. Data are presented as a percentage of the moles of unsaturated disaccharides produced by heparinases (I, II and III) digestion of all purified fractions 1-6.

HS Disaccharides	**F1 (%)**	**F2 (%)**	**F3 (%)**	**F4 (%)**	**F5 (%)**	**F6 (%)**
ΔHexA-GlcNAc	4.6	28	84.4	31.9	9.8	6.8
ΔHexA(2S)-GlcNAc	0	0	0	0	0.9	0.4
ΔHexA(2S)-$GlcNH_2$	0	0	0	0.1	0.2	0
ΔHexA-GlcNAc(6S)	0.2	2.4	1.6	5.3	4.9	3.3
ΔHexA(2S)-GlcNAc(6S)	30.4	10.9	0	0	3.1	4.6
ΔHexA- GlcNS	0.7	8.6	12.9	28.4	10.4	5.9
ΔHexA(2S)-GlcNS	16.6	25.2	0.5	12.8	24.4	34
ΔHexA-GlcNS(6S)	4.9	10.9	0.6	15.9	19.4	16.4
ΔHexA-$GlcNH_2$(6S)	0	0	0	0.1	0.2	0
ΔHexA2S-GlcNS(6S)	42.7	14	0	5.7	26.3	28.6
ΔHexA2S-$GlcNH_2$(6S)	0	0	0	0	0.3	0.1
Unsulphated	4.6	28	84.4	31.9	9.8	6.8
N-SO_3	64.8	58.8	14	62.6	80.5	84.8
2-O-SO_3	89.6	50.2	0.6	18.5	55.3	67.6
6-O-SO_3	78.1	38.2	2.2	27	54.2	53
Total GAG disaccharides produced by heparinase digestion (μg)	0.01	0.002	0.01	0.05	0.29	0.06
Average sulphate per disaccharide	2.33	1.47	0.17	1.08	1.9	2.05

The relative distribution of unsaturated disaccharides and the amounts produced when each fraction was treated exhaustively with chondroitinase-ABC enzyme are shown in Table 16. Disaccharide analysis of each fraction also showed that early eluting fractions (1, 2 and 3) lack correlation between the sulphate content per disaccharides and the fractions' elution positions. Again, this is likely linked to the incomplete nature of the digests, as confirmed by the quantity, in micrograms, of disaccharides released after digestion. The later eluting fractions (4, 5 and 6) produced disaccharide compositions close to those seen for the

unfractionated cockle polysaccharides (Table 9). The later eluting fractions, 5 and 6, contain a CS-like GAG chain; however, Figure 47 suggests that these chains do not contribute to the antiproliferative activity of Fraction 5.

Table 16. CS/DS Disaccharide analysis of anion-exchange purified cockle polysaccharide fractions. Data are presented as a percentage of the moles of unsaturated disaccharides produced by chondroitinase-ABC digestion of the anion-exchange fractions (F1–F6).

CS/DS Disaccharides	**F1 (%)**	**F2 (%)**	**F3 (%)**	**F4 (%)**	**F5 (%)**	**F6 (%)**
ΔHexA-GalNAc	70.6	72.36	86.446	8.75	3.5	3.6
ΔHexA-GalNAc(4S)	23.1	26.68	13.55	89.85	56.8	35
ΔHexA-GalNAc(6S)	3.8	0.18	0	1.396	3.7	4.3
ΔHexA(2S)-GalNAc(4S)	0	0	0	0	0	0
ΔHexA(2S)-GalNAc(6S)	0	0	0	0	1.8	3.9
ΔHexA-GalNAc(4,6S)	2.5	0.78	0	0	34.2	53.2
ΔHexA(2S)-GalNAc(4,6S)	0	0	0	0	0	0
Unsulphated	70.6	72.4	86.4	8.8	3.5	3.6
2-O-SO3	0.0	0.0	0.0	0.0	1.8	3.9
4-O-SO3	25.6	27.5	13.6	89.9	91.0	88.2
6-O-SO3	6.3	1.0	0.0	1.4	39.7	61.5
Total GAG disaccharides produced by ABC-lyase digestion (µg)	0.002	0.006	0.006	0.026	0.285	0.086
Average sulphate per disaccharide	0.32	0.28	0.14	0.91	1.31	1.51

Taken together, the data indicate the presence of heparinases and chondrotinase-ABC susceptible linkages, therefore, GAG-like structures are present in the cockle purified later eluting fractions. The production of a significant quantity of HS disaccharides, from the active fraction 5 confirms the link between HS-GAG-like structures and the antiproliferative activity of the cockle polysaccharides. However, the retained activity of the heparinase-resistant chains must also be considered when judging on the structure/activity relationships.

5.3.2. Monosaccharide composition analysis—anion-exchange purified fractions

Monosaccharide analysis was carried out on each cockle purified fraction (F1-F6) (Table 17). The anion-exchange purified fractions analysis showed enrichment of the GAG-related monosaccharides such as $GalNH_2$, $GlcNH_2$, and GlcA in the later eluting fractions (Fractions 3–6). The components found in the active fraction 5 showed typical GAG-like contents with the highest amount of GlcA and no detectable IdoA residues, however, this does not, on its own, explain the unique activity of the cockle derived HS-like GAG chains.

Table 17. HPAEC-PAD analysis of monosaccharides derived from anion-exchange purified fractions (F1–F6). Samples were hydrolysed to monosaccharides. The observed peaks were identified by comparison with the elution position of monosaccharide standards. Data are presented as a percentage of the moles of monosaccharides produced by acid hydrolysis.

Monosaccharide	**F1 (%)**	**F2 (%)**	**F3 (%)**	**F4 (%)**	**F5 (%)**	**F6 (%)**
Fucose	5.11	5.8	3.3	3.6	14.2	2.1
$GalNH_2$	3	4	11.7	35.6	21.8	9.5
$GlcNH_2$	3.9	2.1	11.9	10.4	14.5	3.6
Galactose	2.3	3	11	14.4	20.1	8.8
Glucose	73.49	57.4	52.8	30	10.4	50.4
Mannose	5.06	28.1	7.4	2.7	4.9	23.5
Glucuronic acid	1.02	0.7	1.9	3.3	14.1	2.1
Iduronic Acid	0	0	0	0	0	0

5.3.3. NMR—anion-exchange purified fractions

Extensive chromatography separation of the cockle CE polysaccharides using anion-exchange chromatography was inefficient to purify a single polysaccharide chain with antiproliferative activity. In fact, the disaccharide analysis of the fraction 5 indicated the presence of HS-like and CS-like components. In addition, the monosaccharide composition analysis suggested the presence of fucosylated polysaccharides, N-linked and O-linked glycan and HS-like polysaccharides as represented only a minority of the glycan chain. Therefore, in order to further characterize the structure of cockle polysaccharides with antiproliferative activity, an attempt was made to study fraction 5 by NMR spectroscopy.

A number of spectra where recorded at 800 MHz including ^{1}H NMR, ^{13}C NMR, correlation spectroscopy (COSY), total correlation spectroscopy (TOCSY) and heteronuclear single quantum correlation (HSQC). These spectra are shown in the appendices. It was clear from the spectra obtained that it would be extremely difficult to make unambiguous assignments of the various saccharides present due to the complexity of the resonance patterns observed. Consequently, it was even more difficult to obtain fine structure differences between mammalian-HS, which has no antiproliferative activity, and the cockle HS-like structures that had previously, based on heparinase activity, shown to be active at inhibiting the growth of cancer cells. The COSY spectrum in Figure 49, in the appendices, shows three of the spin systems linked to fucosylated-CS (red lines) and the GlcNAc and GlcNS monosaccharides of HS-like cockle glycans (green lines). However, time and complex signal overlap, resulting from contaminating glycan chains did not allow further assignment of spin systems.

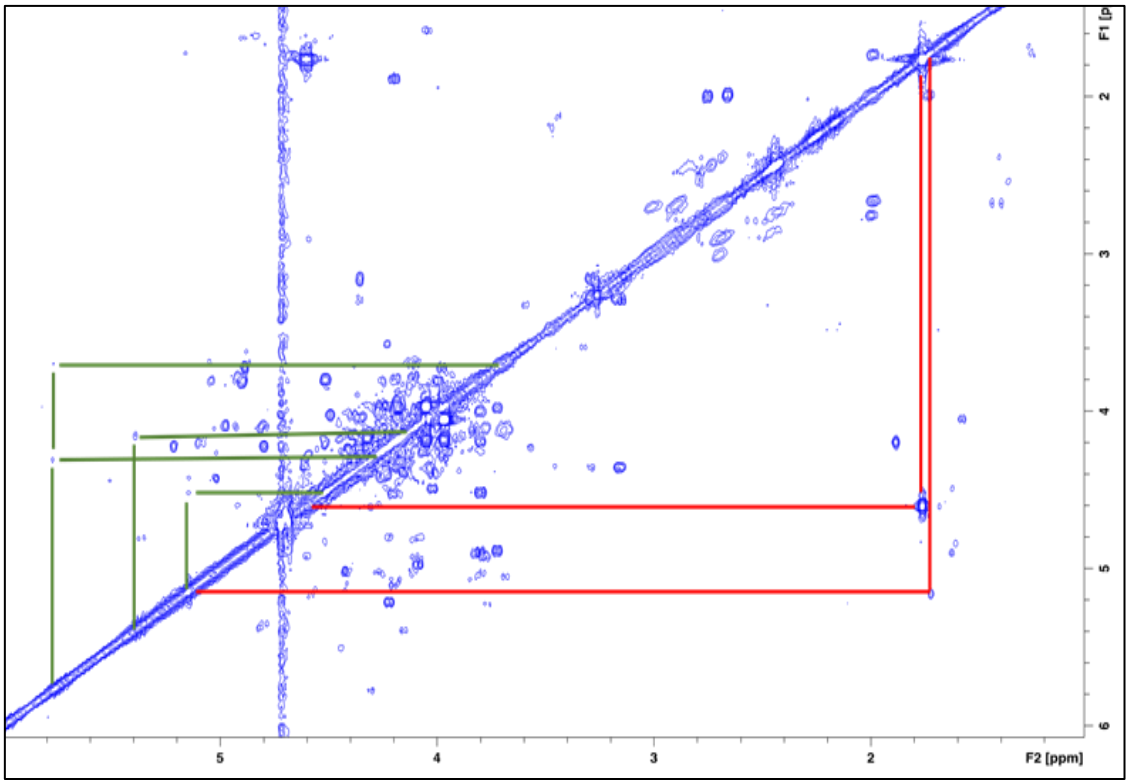

Figure 49. 2D ^{1}H-^{1}H NMR-COSY for cockle purified fraction 5. Red lines CH_3 linked to fucopyranose at 5.2 ppm, and green lines indicate possible spin systems found in mammalian HS. The spectra were recorded at 56.85 °C.

Further analysis of these samples might in the future provide more detail regarding the structural attributes of the cockle GAG-like active structure. However, it is clear that the

analysis would benefit from further purification of the active fraction from other contaminating molecules, such as fucosylated-CS and other N- and O-linked glycans. Problems with further purification system from the relative abundance of fraction 5 in the crude cockle GAG mixture, as it is a very minor component (Figure 45). Other methods for chromatography such as size-exclusion might be useful in removing smaller contaminating N- and O- linked glycan changes but are unlikely to enable separation between HS, CS and fucosylated polysaccharides. Different stationary phases and function groups might be employed along with further ion-exchange chromatography but might be ineffective in the short term in producing samples that could be worked on more effectively by NMR analysis.

6. Discussion

Typical mammalian GAGs chains are composed of long unbranched polysaccharides characterised by repeating disaccharide building blocks of uronic acid and hexose-sugar. GAGs are classified into six types according to their disaccharide building blocks—HS, heparin, CS, DS, KS and hyaluronate (Nelson, Lehninger and Cox, 2008). Each type can acquire different structural modifications on its disaccharide including chain length, type of glycosidic linkage, branching point, the addition of various functional groups and the addition of other saccharides. Chain structural modifications provide GAGs with their unique structures and biological functions (Vlodavsky and Friedmann, 2001). The aim of this study focused on the isolation, purification and characterisation of common cockle (*Cerastoderma edule*) polysaccharides with *in-vitro* novel antiproliferative activity against a cancer cell line.

One of the main objectives of this study was to isolate common cockle polysaccharides and examine their anticancer activity. Therefore, the cockle polysaccharides were successfully isolated using an anionic cetylpyridinium chloride precipitation method, which has been used to target the anionic properties within cockle polysaccharides structure. The antiproliferative activity was assessed *in-vitro* against three cancer cell lines using cell proliferation assays (MTT assay), which resulted in potent antiproliferative activity on all cell lines used (Figure 40) and induced by programmed cell death.

As hypothesised, the cockle polysaccharide is likely to contain GAG-like chain, on the basis of the isolation method used that could be linked to the antiproliferative activity. This antiproliferative activity of GAG-like polysaccharides was unusual given that mammalian GAGs, in this and other studies, failed to show any antiproliferative activities against cancer cell lines (Figure 41). As a consequence, structural analysis was conducted in order to determine cockle polysaccharides structure and to correlate it to that of typical members of the mammalian GAG families, in an attempt to determine the exact structural nature of the observed antiproliferative activity.

Initially, an important structural and biological characteristic of the mammalian GAGs is the pattern of sulphation, which can influence the biological activity of a particular glycan chain. For instance, the highly sulphated heparin pentasaccharide sequence, with potent anticoagulation activity, make it able to prevent blood coagulation by binding to antithrombin-III to inhibit the action of factors X and II, which plays an important role in the coagulation cascade (Rosenberg and Lam, 1979). Besides that HS chains can acquire various forms of structural heterogeneity, including considerable variation in sulphated and non-

sulphated patterns within domains; which are no doubt linked to its important physiological and pathological roles according to its structure (Höök et al., 1984; Yayon et al., 1991; Stanley et al., 1999; Ornitz, 2000). Marine glycans pattern of sulphation, are also highly variable across species. Liao et al. (2013) reported that polysaccharide from bivalve molluscs (*Corbicula fluminea*) with a high level of sulphation have very potent antiproliferative activity against human cancer cell lines, in comparison to other less-sulphated fractions. Hence, the initial isolation and purification methods were performed to explain the highly variable anionic properties of the polysaccharides, and to maximise the chances of linking structural differences with biological activity.

The only clearly defined GAG sequence activity relationship to date continues to be the highly sulphated heparin pentasaccharide antithrombin-III binding sequence chain with confers on heparin its potent anticoagulant activity, as it has been used for a long time in clinical practice (Howell and Holt, 1918). Mammalian heparins have never previously been shown to have any antiproliferative activity in-vitro, however, chemical modification of heparin has been reported to have led to inhibitory effects that cannot destroy 50% of cancer cells (Yu et al. 2010). These results are consistent with the high-molecular-weight porcine mucosal heparin used in this study, which did not show any antiproliferative activity on cancer cell lines (Figure 41). Cockle CE polysaccharides show high sulphate content and it might be argued that this this alone is responsible for the potent antiproliferative activity observed, with no role for fine structural variation in polysaccharide structure. However, the disaccharide analysis results from the cockle purified fraction-6 has the highest overall sulphate content but, with significantly no antiproliferative activity than the earlier eluted fraction 5 and the CE samples (Table 15).

A possible explanation for these results would therefore be that a specific sequence and/or type of linkage within cockle polysaccharides chain is playing a pivotal role in mediating their antiproliferative activity. This difference is also linked to the lack of antiproliferative activity seen with the mammalian GAGs in this study.

In this study we show for the first time, that marine polysaccharides with antiproliferative activity are susceptible to the digestion of three different classes of heparinase enzymes that are typically used to cleave mammalian HS/heparin chains. After the treatment of cockle polysaccharides with heparinase enzymes, the potent antiproliferative activities were dramatically decreased on all cell lines. In other words, the cockle CE polysaccharide treated with combined heparinase enzymes showed an increase of up to 3

times in IC_{50} values, as shown in the K-562 and Mero-25 cell lines, and up to 9 times on the Molt-4 cell line compared to the untreated cockle CE polysaccharide (Figure 42). More surprisingly, the purified cockle polysaccharide active fraction 5 lost all its antiproliferative activity on both K-562 and Mero-25 cell lines, with great loss of activity on the Molt-4 cell line following treatment with heparinases I,II,III (Figure 47).

Although these findings could be viewed as a direct link between the cockle polysaccharide's antiproliferative activity and the presence of a GAG HS-like structure, a potential structural difference from mammalian-HS is still implicated by the lack of antiproliferative activity of the latter. Some antiproliferative activity show some resistant to the heparinase treatment, particularly in the cockle CE, which could be due to structural differences between the cockle HS-GAG-like and mammalian HS. Consequently, it was suggested that a new, atypical, marine polysaccharide has been identified in this study, with GAG-like properties that are linked, at least in part, to the antiproliferative activity observed in the three cell lines tested. In the future, a reductionist assessment of the structural features within these heparinase resistant sequences might be an attractive research approach that could will lead to a more thorough understanding of the precise structural features required to determine the antiproliferative activity seen in this study.

The disaccharide analysis employed in this study aimed to identify compositional differences between mammalian GAGs and cockle-derived polysaccharides with potent antiproliferative activity. The cockle CE polysaccharide or the purified fractions were treated with a combination of heparinase enzymes (I, II and III), which resulted in the most common unsaturated disaccharides typically observed in mammalian HS, apart from the rarest 3-O-sulphated disaccharide, using the method described. The most significant characteristic of the disaccharide analysis is related to the highest levels of the N-sulphated disaccharides produced after heparinase digestion. For example, cockle CE polysaccharide has about 66% of its glycan chain N-sulphated, and the purified fraction 5 has about 80% N-sulphated glycans, as opposed to the much lower amount from the porcine intestinal mucosal, which contains approximately 40% N-sulphated HS (Deakin and Lyon, 2008).

Another notable finding is the differences in the levels of the disaccharides [ΔHexA(2S)-GlcNS] and [ΔHexA(2S)-GlcNS(6S)], which were generated by combined heparinase digestion of the anion-exchange purified active fraction 5, making up 24% and 26% of the disaccharides, respectively, as opposed to the percentage of these disaccharides in porcine mucosal heparin (0.9% and 14.6%, respectively) (Saad et al., 2005), and porcine mucosal HS (11% and 4.59%, respectively). Although fraction 5 showed antiproliferative

activity and an increased level of these disaccharides compared to porcine mucosal HS, it seems unlikely that these disaccharides are solely responsible for the antiproliferative activity, as described in section (4.1.1.2). In fact, disaccharide analysis of cockle CE polysaccharide showed less abundance of these particular disaccharides (9.5% and 5.6%, respectively), which gives no definitive clues about the differences in the biological activity seen in cockle polysaccharides and mammalian GAGs (Table 9). The anion-exchange purified fractions (1, 2, 3, 4 and 6) with no antiproliferative activity were enriched with a significant amount of neutral sugars and comparatively lower GAG-like properties. These findings would suggest that a particular role of the GAG-like structure within the cockle polysaccharide would influence the antiproliferative activity.

To date, invertebrate-derived polysaccharides with different pharmacological outcomes are linked to a non-GAG like structure, as they typically differ from those of mammalian GAGs in terms of monosaccharide composition, disaccharide composition, and/or structural homogeneity. The literature has distinguished various types of polysaccharides isolated from different invertebrates with active pharmaceutical outcomes such as antiproliferative, anti-metastatic and anticoagulation activities. These polysaccharides can differ in several ways from typical mammalian GAGs, as their most dramatic structural differences in the type of linkages, branching, monosaccharide compositions, disaccharides building blocks, chain length, chain modifications and/or homogeneity. As an illustration, a polysaccharide derived from the marine bivalve mollusc (*Corbicula fluminea*) is composed of neutral sugars such as fucose, glucose and galactose and demonstrates anti-tumour, antiproliferative and antioxidant activities; however, its final structure has not yet been determined, and its structural analysis did not confirm any link to mammalian GAGs polysaccharides (Liao et al., 2013).

Moreover, the marine bivalve mollusc (*Ruditapes philippinarum*) polysaccharide-derived chain shows antiproliferative activity against the human hepatoma cell line, but its structure lacks heterogeneity, as its composed of glucose-based polysaccharides with several branches, which means it is not structurally linked to mammalian GAGs that are known to be heterogeneous and unbranched (Zhang et al., 2008). In addition, the unique AS polysaccharides isolated from the African snail (*Achatina fulica*) lack structural heterogeneity, they are composed of IdoA and essentially GlcNAc, which make it different from mammalian GAGs in terms of structural heterogeneity (Vieira et al., 2004; Pomin, 2015). Similarly, the cuttlefish ink (*Sepiella maindroni*) novel hexasaccharide, which is composed of both neutral and acidic sugars. Its structure shows the presence of the

unbranched β-fucose and a branched GlcA, which makes it different from mammalian GAGs in terms of disaccharide building blocks and branching points (Liu et al., 2008).

The highly sulphated DS-like polysaccharide isolated from *Ascidian*, a fucosylated-CS isolated from sea cucumber, hybrid heparin/HS chains isolated from head of shrimp and the highly sulphated GlcA-containing HS chain isolated from bivalve mollusc, have been suggested. However, none of these unique GAG-like polysaccharides have previously been reported to have any direct antiproliferative activity.

Monosaccharide composition analysis of cockle polysaccharides showed no evidence of IdoA residues within the chains; therefore, the presence of the highly sulphated DS-like structure is unlikely to exist within the cockle polysaccharide preparation (Table 10) (Pavão, 2002; Pomin, 2015). Secondly, regarding the novel fucosylated-CS with GAG-like structures extracted from sea cucumber, its CS-like structure has been reported to be insensitive to chondroitinase-ABC without prior removal of the attached fucose chain (Vieira and Mourão, 1988). In contrast, the disaccharide analysis of the cockle GAG-like polysaccharide revealed susceptibility to chondroitinase-ABC, which resulted in the release of typical mammalian CS-related disaccharides (Table 9). According to Vieira et al. (1991), the GlcA chain of the fucosylated-CS either can acquire branched 3-O-fucopyranose or 3-O-sulphate. The rarest 3-O-sulphate was not determined within cockle GAG-like polysaccharides. Although treatment of the cockle GAG-like polysaccharide with chondritinase-ABC did not affect its antiproliferative activity, fucosylated polysaccharide was present in the cockle structure, so its contribution to the antiproliferative activity cannot be ruled out, however it is not known to be sensitive to any of the three heparinase enzymes used in this study.

The literature has identified two marine derived polysaccharides with heparinase sensitive structures, namely hybrid heparin/HS isolated from the head of the shrimp (*Litopenaeus vannamei*) (Brito et al., 2014) and the highly sulphated GlcA containing-HS isolated from bivalve molluscs (*Nodipecten nodosus*) (Gomes et al., 2010). As the cockle polysaccharide lost some of its antiproliferative activity following heparinase digestion, its structure/activity can possibly be linked to the presence of a similar structure to the hybrid heparin/HS or GlcA-rich HS polysaccharides, although no direct link to antiproliferative data have been reported with these polysaccharide structures. Some activity remained after heparinase digestion of the cockle CE polysaccharide, which could suggest the presence of other uncommon GAG structures that are potentially involved in the antiproliferative activity.

The main findings of the monosaccharide composition analysis of cockle polysaccharides provided two main structural insights into the nature of the cockle polysaccharides. Firstly, following monosaccharide analysis of cockle CE and the purified fraction 5, the main monosaccharides identified were closely related to mammalian GAGs. Cockle CE monosaccharide composition with GAG-like structure represented about 42% of the chain as fucose (11%), $GalNH_2$ (16.7%), $GlcNH_2$ (9.9%) and GlcA (4.3%) (Table 10). Likewise, the purified active fraction 5 monosaccharide GAG-like composition represented approximately 65% as fucose (14.2%), $GalNH_2$ (21.8%), $GlcNH_2$ (14.5%) and GlcA (14.3%) (Table 17). As expected, the monosaccharide composition of the cockle polysaccharide represented the main N-linked and O-linked glycan building blocks found in glycan structures.

Secondly, the non-derivatisation-based method used to confirm the nature of all monosaccharides within the sequence with minimal structural modification identified the type of uronic acid in all cockle monosaccharides was 100% GlcA with no detectable epimerisation to IdoA. However, the absence of IdoA does not on its own, explain the antiproliferative activity of the HS-GAG-like chain within cockle polysaccharides, appendices (Figure 58). Overall, the compositional details do not yet represent satisfactory structural evidence to confirm the final structure of the antiproliferative activity and its relation to the glycan structure. Therefore, detailed structural analysis was suggested to assess the nature of the antiproliferative activity that is linked to the cockle polysaccharides, using NMR spectroscopy.

The NMR spectra recorded from the crude GAG mixtures showed the difficulties that would have to be met in order to determined definitive structural characterisation of all the glycan components. The spectra showed complex signal overlap in many key areas, making it impossible to determine essential structural detail on sequence composition and critically linkage types within different families of glycan components. To date, the data obtained from the anion-exchange chromatography indicated that many of the glycan components might be removed from the active fraction 5. As a result, extensive chromatography runs where undertaken to produce enough amount of the active fraction 5 polysaccharides for NMR analysis. This was a challenge as we had already shown that the active fraction 5 was only a minor component of the initial crude cockle polysaccharide extracts (Figure 45).

Heteronuclear and homonuclear 2D NMR experiments were carried out and spectra recorded for both purified cockle Fraction 5 and commercially available porcine mucosal HS. Once again, analysis the spectra of cockle fraction 5 had been achieved considerable

challenges still remained in attributing a unique HS-like structures within fraction 5. The monosaccharide and disaccharide analysis did point the way to identifying a number of spin systems related to HS-like structures rich in GlcA and fucosylated-CS. However, at the present time the contaminating CS-related structures and N- and O-linked glycans that are clearly still present in fraction 5 and in far larger concentrations than the HS like GAG structures have proven to be extremely challenging for NMR assignment. It is possible that further study of the available spectra will yield more detailed structure/activity findings, and perhaps with additional NMR experiments this could allow a meaningful explanation of the polysaccharide activity. However, it is likely that further purification of the active chains will be needed to succeed in an NMR based approach to understanding the structural differences between the cockle HS-like polysaccharides and typical mammalian GAGs such as HS. This will ultimately lead to a structure-based understanding of the structure/activity relationships between the antiproliferative polysaccharides isolated from cockles.

7. Conclusion and future study

This study was conducted to isolate cockle polysaccharide and assess its antiproliferative activity on cancer cell lines using in vitro cell proliferation assay. Cockle polysaccharide has exhibited potent antiproliferative activity against acute lymphoblastic leukaemia, chromic myeloid leukaemia and mesothelioma cell lines, where cell death was induced by apoptosis, which would make this polysaccharide pharmaceutically a candidate for cancer therapies.

Extensive structural analysis confirmed the presence of GAG-like structures within cockle preparations, specifically HS-like structures. For the first time, marine polysaccharides antiproliferative activity was directly affected after treatment with different classes of heparinase enzymes, which have found to be linked to antiproliferative activity, whereas mammalian GAGs did not exhibit antiproliferative activity on cancer cell lines.

This provides insights into a new marine polysaccharide with HS-like structures with influence on a biological activity that is structurally different from its mammalian counterpart, as the literature exclusively correlates the biological activity in marine polysaccharides with that in non-GAG glycans.

Further structural analysis showed a number of sulphates per disaccharide. The results indicated that not only the highly sulphated polysaccharides' structure would be biologically

active, as cockle CE and the purified fraction 5 showed a lower level of sulphation with potent antiproliferative activity in comparison with fraction 6, which represented a higher number of sulphates per disaccharide. The results of this study indicate that the level of sulphation is not a principal reason for biological activity, which depends on various structural modifications, such as chain length, type of linkages, branching points and addition of functional groups (Bertozzi and Rabuka, 2009).

Structural characterisation of cockles' antiproliferative activity, represented in the purified fraction 5, indicated the presence of not only HS-like structures, but also fucosylated polysaccharide, N- and O-linked saccharides, which made the final structural elucidation very difficult because of the complex nature of the sample. Indeed, further purification strategies may be used to remove non-glycan contaminations, followed by treatment with a combination of heparinase enzymes to improve structural elucidations using NMR spectroscopy. This study offers insight into marine polysaccharides with uncommon therapeutic outcomes from a marine source, as they manifested direct antiproliferative effects on cancer cells related to GAG-like polysaccharides.

8. Limitations

Study limitations make the creation of an overall conclusion about the cockle antiproliferative structure extremely difficult. The main limitation of this study was the evaluation of the nature of the cockle polysaccharide, which has an unknown structure and lacks any chromophore that affects adopting an appropriate purification step. For instance, size-exclusion chromatography requires a well-known molecular weight sample, and lectin affinity chromatography requires knowledge of the exact structure of the antiproliferative compound. As a result, anion-exchange chromatography was chosen according to the negatively charged nature of GAG-like structures, which finally resulted in a relatively small fraction several containing polysaccharides instead of only one purified chain.

Also, because of a lack of a non-destructive sequencing method for polysaccharides, a major polysaccharide structural analysis heavily depends on NMR spectroscopy. However, using NMR requires a strong magnetic field to evaluate carbohydrates (over 500 MHz), high costs of the use of a stronger magnetic field and a sensitive probe and a highly concentrated sample. Finally, NMR requires a high level of expertise to interpret the NMR raw data (Mulloy, Hart and Stanley, 2009).

9. Appendices

9.1. Appendix I: Extraction of polysaccharides from common cockle

Common cockle | Cockle powder | Crude cockle final product

9.2. Appendix II: Cockle polysaccharides purification using size-exclusion chromatography.

Cockle CE polysaccharide was attempted to be separated using size-exclusion chromatography coupled with high performance liquid chromatography (HPLC). This chromatography is based on excluding materials larger than the designated molecular weight for column. Superose-12 column (GE healthcare, UK) is composed of highly cross-linked agarose with molecular range 1-300 kDa. 100 µg of cockle CE polysaccharide sample was dissolved in 200 µL of 0.2 M ammonium bicarbonate buffer (mobile phase) injected to the system at flow rate 0.5 ml/minutes. Depending on cockle CE polysaccharides molecular weight, two peaks eluted from the column, the first one has high molecular weight materials and the second peak was a very wide peak (Figure 50). Another size-exclusion column coupled with HPLC system was used known as superdex-75. It is composed of cross-linked agarose and dextran resin with an exclusion range of 3-70 kDa. Superdex-75 column gives better separation properties for lower molecular weight samples. 100 ug of intact GAG dissolved in 200 µL 1x PBS as column mobile phase (Figure **51**). All chromatographic peaks recorded using on-line UV detector at 280 nM.

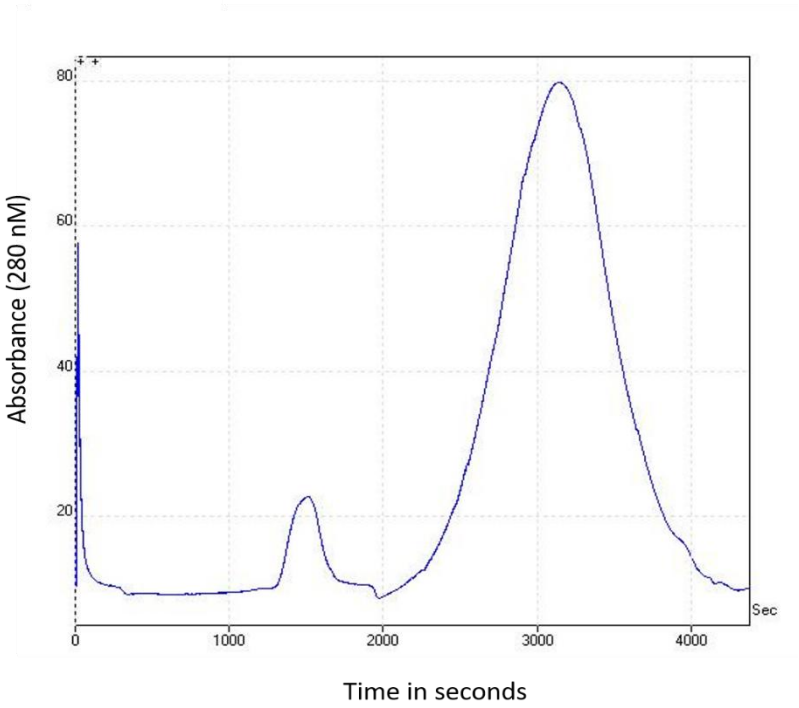

Figure 50. Cockle CE polysaccharide purification using size-exclusion chromatography, superpose-12 column. The figure provides two peaks eluted depending on the materials molecular weight. Namely, high molecular weight and low molecular weight peaks.

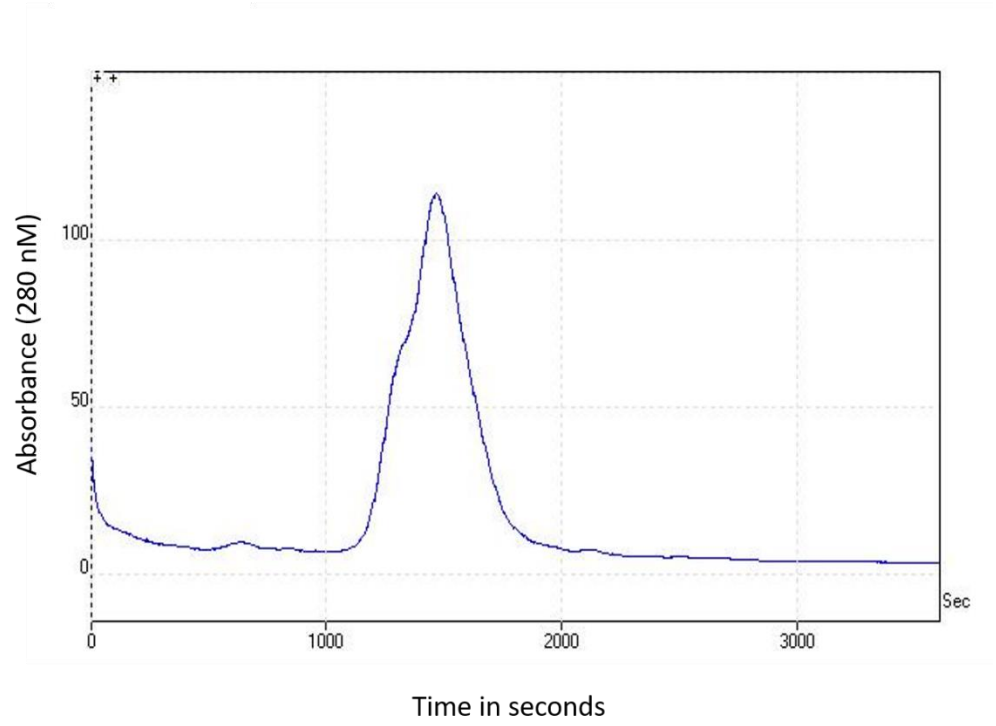

Figure 51. Cockle CE polysaccharides purification using size-exclusion chromatography, superdex-75 column. The figure shows only one peak.

9.3. Appendix III: Anion-exchange optimisation.

Following several unsuccessful purification attempts, cockle polysaccharides were purified based on its charge using anion-chromatography. Anion-exchange column was optimised to separate cockle polysaccharides, using gradient elution profiles ranging from 0-4 M NaCl.

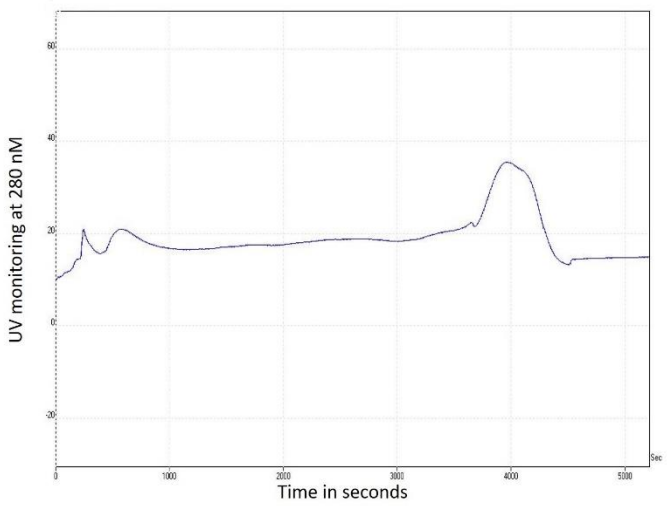

Figure 52. Demonstrate cockle polysaccharide elution profile using anion-exchange chromatography, sephacel-DEAE resin with gradient elution of 0-0.35 M NaCl. It shows from the first attempt that cockle CE can be purified, as figures shows about 4 peaks.

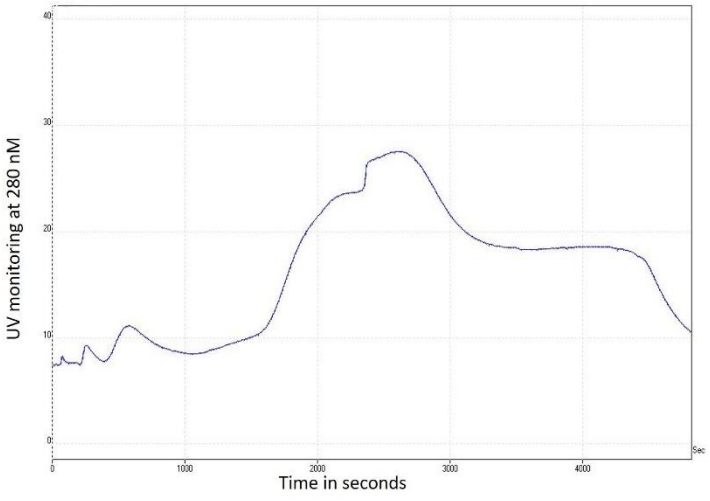

Figure 53. Demonstrate cockle polysaccharide elution profile using anion-exchange chromatography, sephacel-DEAE resin with gradient elution of 0-0.5 M NaCl. It shows better separation of cockle CE, which need more optimisation as still some cross-peaks

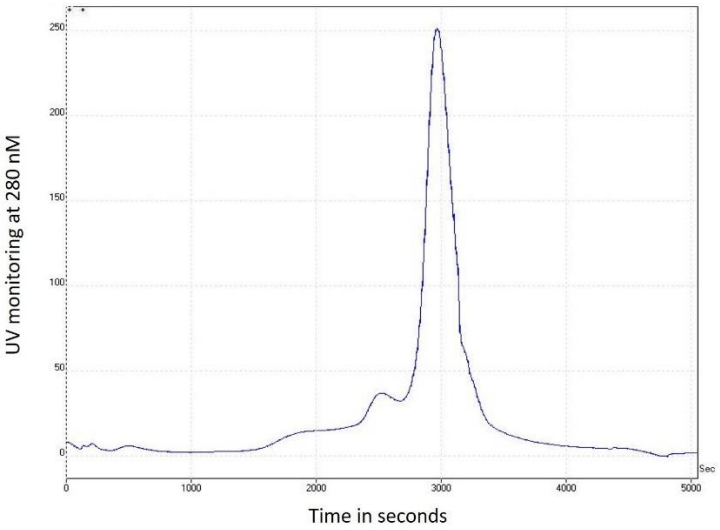

Figure 54. Demonstrate cockle polysaccharide elution profile using anion-exchange chromatography, sephacel-DEAE resin with gradient elution of 0-1 M NaCl. Improved signal of charged materials, however, major eluted materials seems to be eluted in two peaks only.

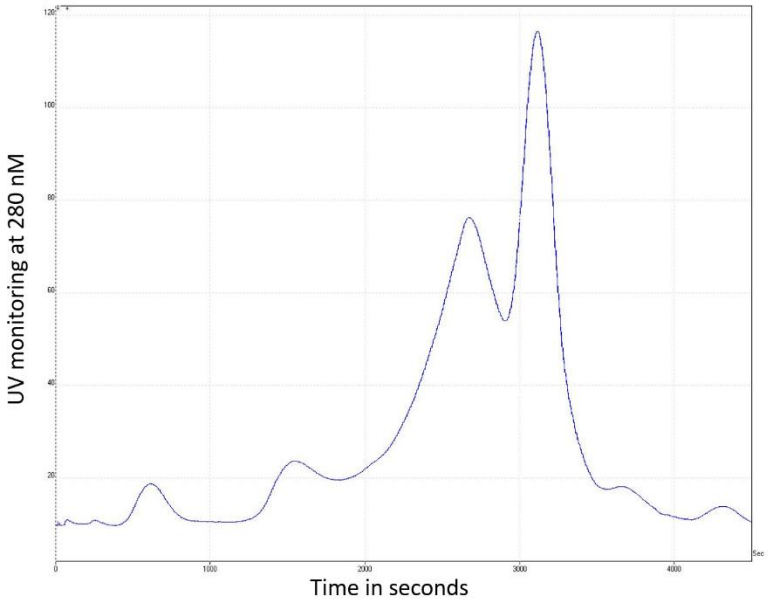

Figure 55. Demonstrate cockle polysaccharide elution profile using anion-exchange chromatography, sephacel-DEAE resin with gradient elution of 0-1.5 M NaCl. It has separated cockle CE into 6 peaks successfully.

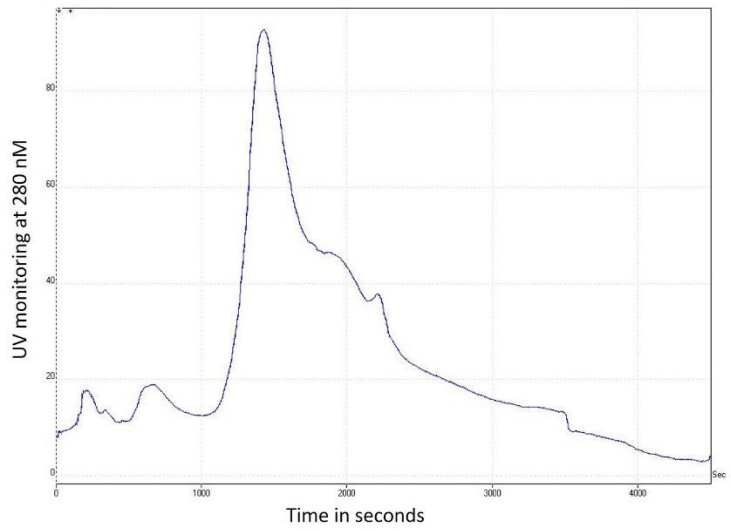

Figure 56. Demonstrate cockle polysaccharide elution profile using anion-exchange chromatography, sephacel-DEAE resin with gradient elution of 0-2 M NaCl. It shown high salts has affected the elution time that resulted in poor purification.

9.4. Appendix IV: Cell proliferation assay using MTS on K-562 cell line.

MTS—[3-(4,5-dimethylthiazol-2-yl)-5-(3-carboxymethoxyphenyl)-2-(4-sulfophenyl)-2H-tetrazolium, inner salt, which is a colorimetric assay that can be used to determined cell viability. Cockle CE polysaccharide (■) with IC_{50} 8.65 (µg/mL), and cockle CE treated with chondroitinase-ABC (▲) with IC_{50} 10.49(µg/mL) were tested in order to check if there are any differences in the IC_{50} results between MTS and MTT. It was shown no difference in the activity prolife when using MTS assay on K-562 cell line (Figure 57).

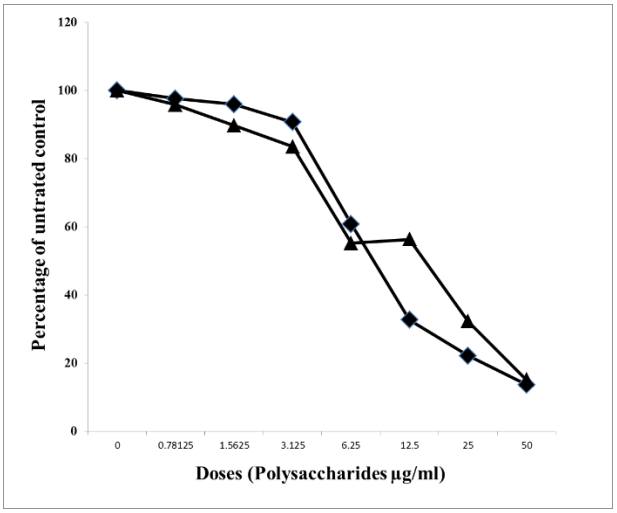

Figure 57. Cell proliferation assay MTS assay. 50 µg of cockle CE polysaccharides was incubated with K562 to check its antiproliferative activity using MTS assay. No great difference in IC_{50} values between MTT and MTS results.

9.5. Appendix V: Monosaccharides cell proliferation assay.

500 µg of cockle CE polysaccharide dissolved in 2 mL of MilliQ water, then added 10 mL of 4M trifluoracetic acid then sample was incubated for 6 h at 100 ºC. Afterwards, sample was cooled on room temperature, then centrifuged at 2000 rpm for 2 minutes. Next, Sample was concentrated by evaporation overnight. Next day, 100 µl of 50% isopropanol, then sample concentrated again. Finally, dried sample was diluted in 2000 µL cell culture media, in order to check the antiproliferative activity using MTT assay using K562, Molt-4 and Mero25 cell lines. As a result, monosaccharide sample shown to be inactive on all cell lines (Figure 58).

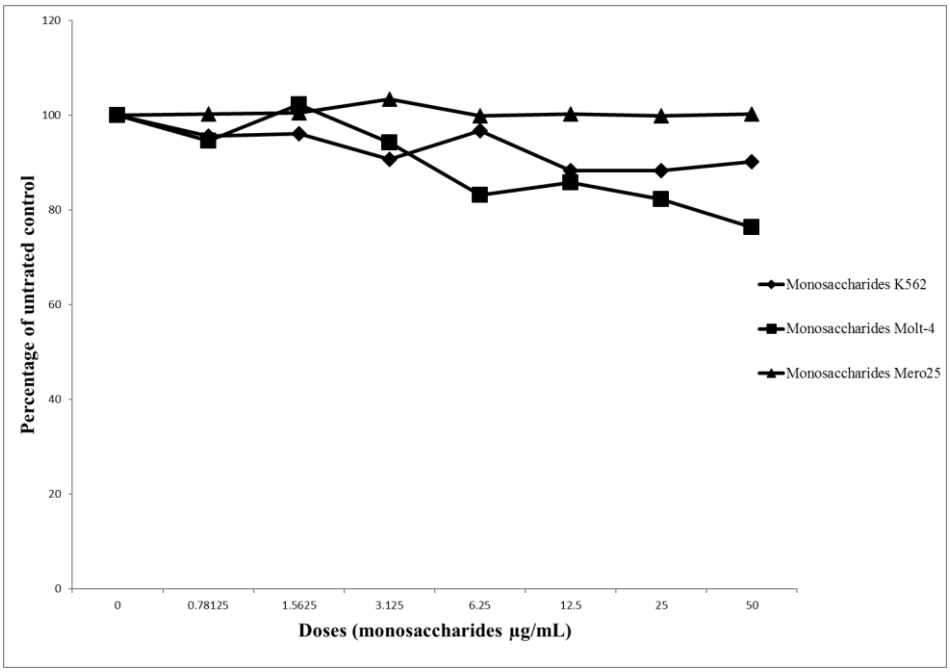

Figure 58. Cell proliferation assay of cockle monosaccharide using K562, Molt-4 and Mero-25 cell lines.

9.6. Appendix VI: Enzymes activity checks using spectrophotometer.

Each heparinase activity was assessed prior use, as 100 µg of standard mammalian HS was dissolved in heparinases buffer then 30 mIU of each enzyme was added. The mixture was incubated at 30 °C for 30 minutes and the enzymes activity were check spectrophotometrically at 232 nm. For chondroitinase-ABC, the enzyme was added to standard mammalian CS.

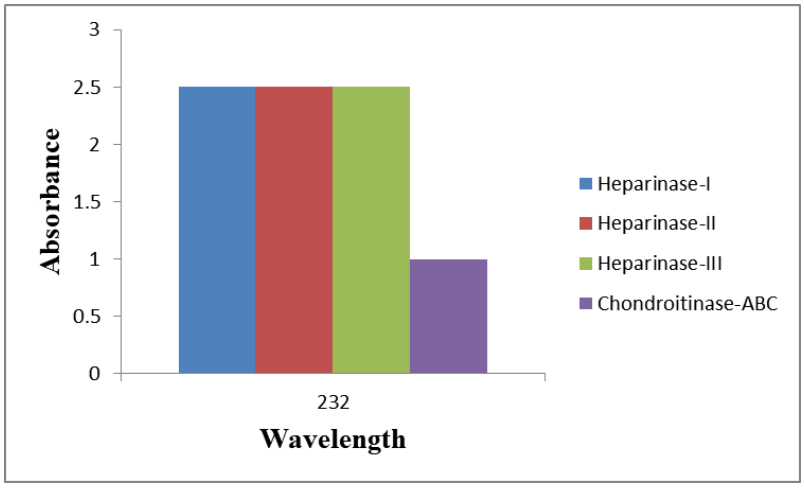

9.7. Appendix VII: α-L-fucosidase activity.

Activity was checked using spectrophotometer. α-L-fucosidase activity was assessed prior use, as 100 µg of cockle CE polysaccharide was dissolved in fucosidase buffer then 30 mIU of the enzyme was added. The mixture was incubated at 30 ○C for 30 minutes and the enzymes activity were check spectrophotometrically at 400 nm**.**

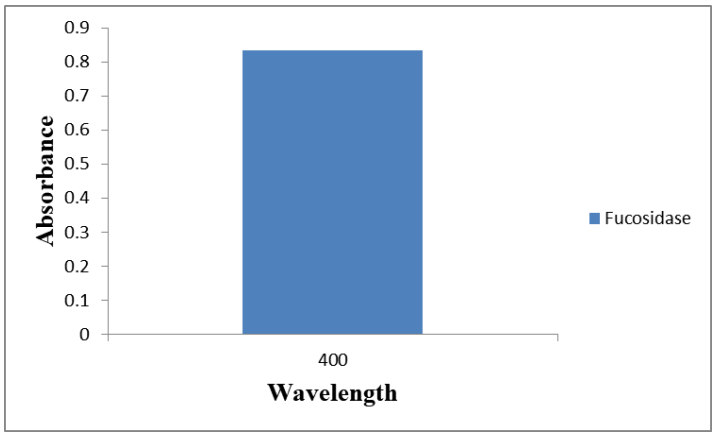

9.8. Appendix VIII: Cell proliferation assay using cockle disaccharides residues from the 10 kDa spin filter.

Cockle CE polysaccharides treated with heparinase (individually or combination), chondroitinase-ABC or fucosidase in order to release disaccharide chains. After incubation period, cockle polysaccharide samples, including CE polysaccharide (Figure 59) and fraction 5 (Figure **60**), were filtered using 10 kDa spin filter in order to separate disaccharides. As disaccharides passed through the filter so it's known as flow through (FT), which was tested to check its antiproliferative activity. 50 µg of each FT samples antiproliferative activity was

assessed using K562 cell line. As a result, the FT sample, which was enriched with disaccharides, it was inactive.

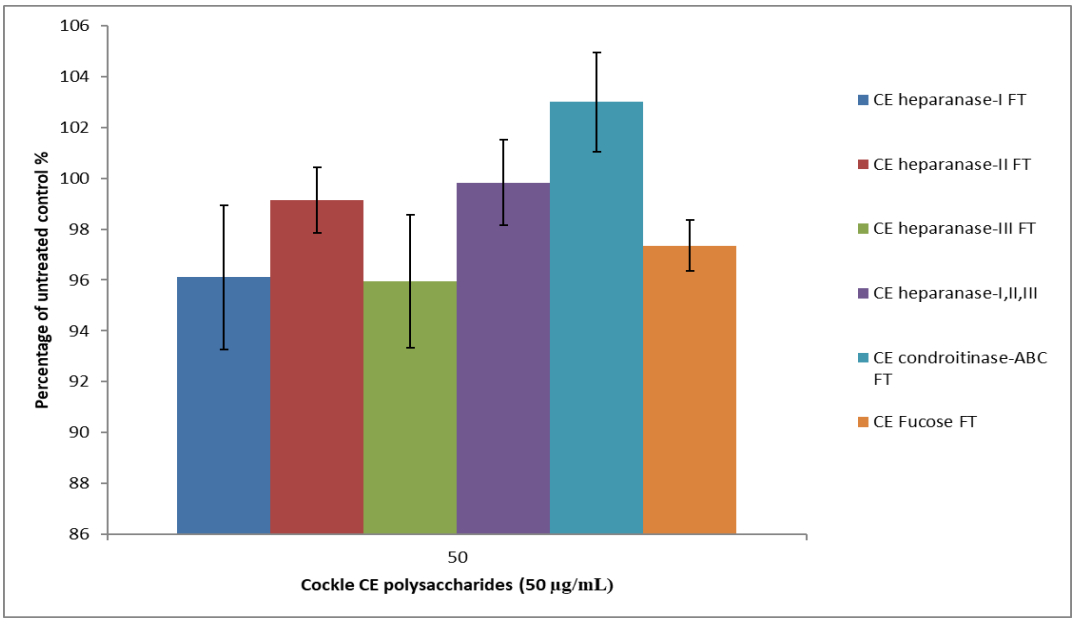

Figure 59. Antiproliferative activity of cockle CE disaccharides on K562 cell line. All disaccharide samples were inactive.

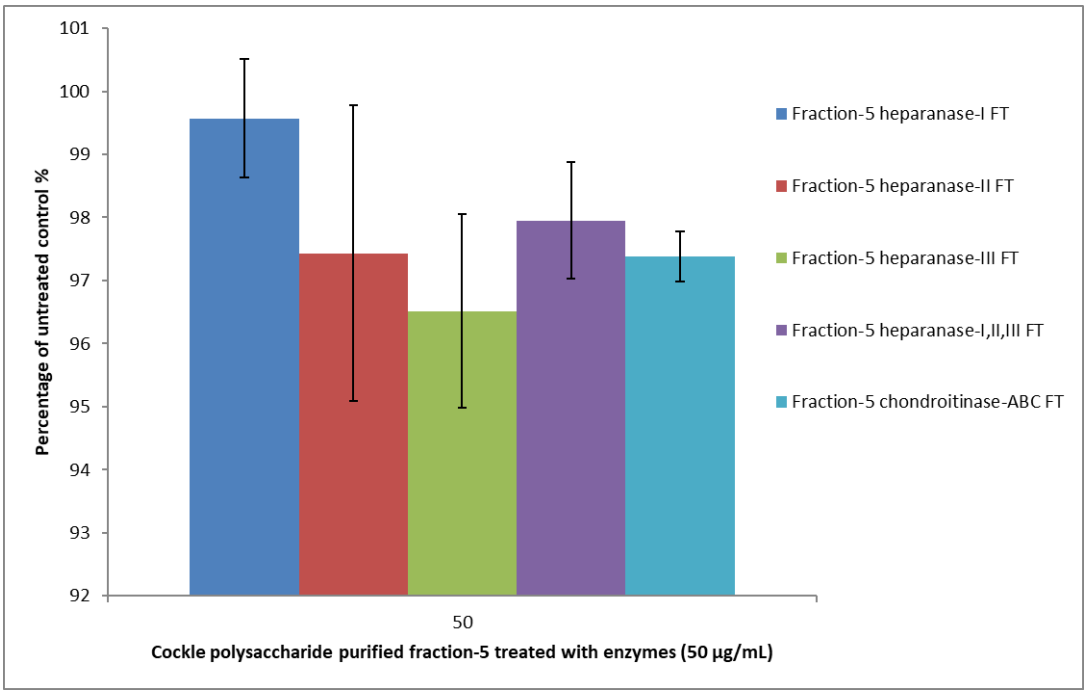

Figure 60. Antiproliferative activity of cockle purified fraction 5 disaccharides on K562 cell line. All disaccharide samples were inactive.

9.9. Appendix IX: Cell proliferation assay using cockle CE polysaccharides treated with different enzymes on Molt-4 cell line.

Cockle CE polysaccharides treated with heparinase (individually or combination), chondroitinase-ABC or fucosidase in order to release disaccharide chains. After incubation period, cockle polysaccharide samples, including CE polysaccharide (Figure 61) and fraction 5 (Figure **62**) were filtered using 10 kDa spin filter in order to separate disaccharides. As disaccharides passed through the filter so it's known as flow through (FT), which was tested to check its antiproliferative activity. 50 µg of each FT samples antiproliferative activity was assessed using Molt-4 cell line. As a result, the FT sample, which was enriched with disaccharides, it was inactive.

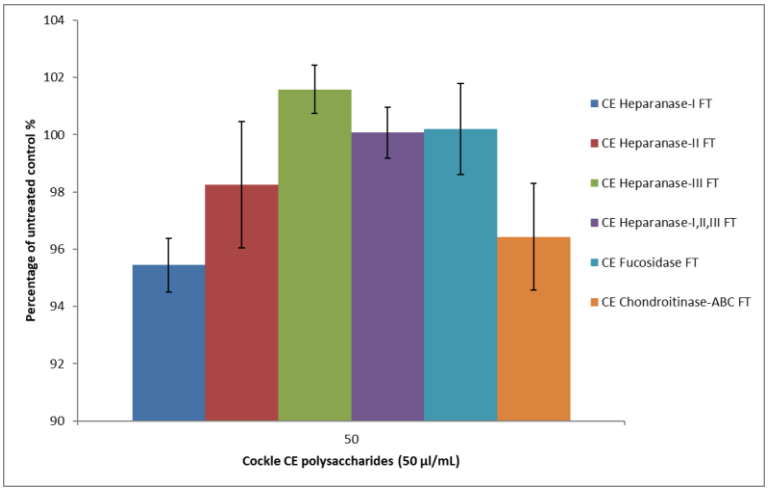

Figure 61. Antiproliferative activity of cockle CE disaccharides on Molt-4 cell line. All disaccharide samples were inactive.

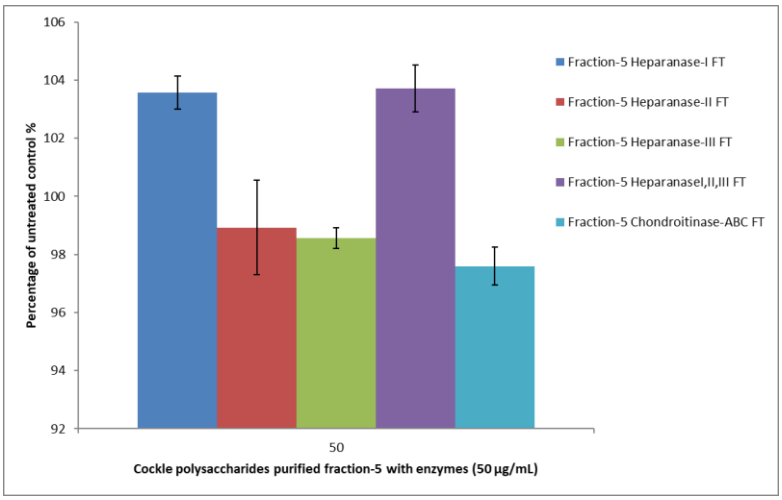

Figure 62. Antiproliferative activity of cockle purified fraction 5 disaccharides on Molt-4 cell line. All disaccharide samples were inactive.

9.10. Appendix X: Cell proliferation assay using cockle CE polysaccharides treated with different enzymes.

Cockle CE polysaccharides treated with heparinase (individually or combination), chondroitinase-ABC or fucosidase in order to release disaccharide chains. After incubation period, cockle polysaccharide samples, including CE polysaccharide (Figure 63) and fraction 5 (Figure **64**), were filtered using 10 kDa spin filter in order to separate disaccharides. As disaccharides passed through the filter so it's known as flow through (FT), which was tested to check its antiproliferative activity. 50 µg of each FT samples antiproliferative activity was assessed using Mero-25 cell line. As a result, the FT sample, which was enriched with disaccharides, it was inactive.

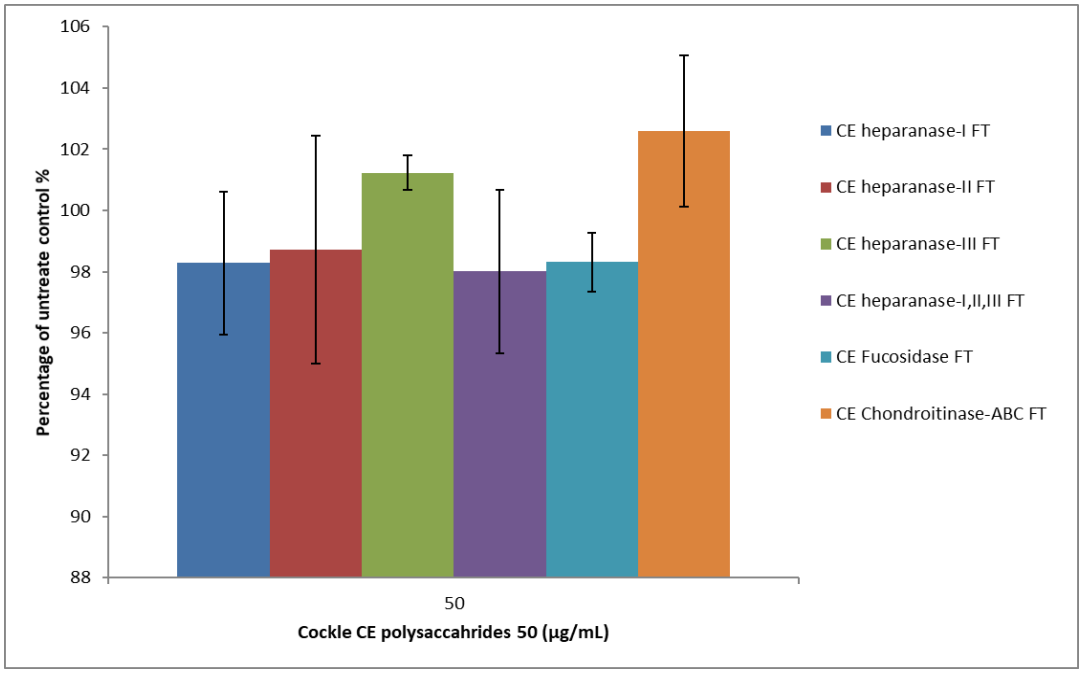

Figure 63. Antiproliferative activity of cockle CE disaccharides on Mero-25 cell line. All disaccharide samples were inactive.

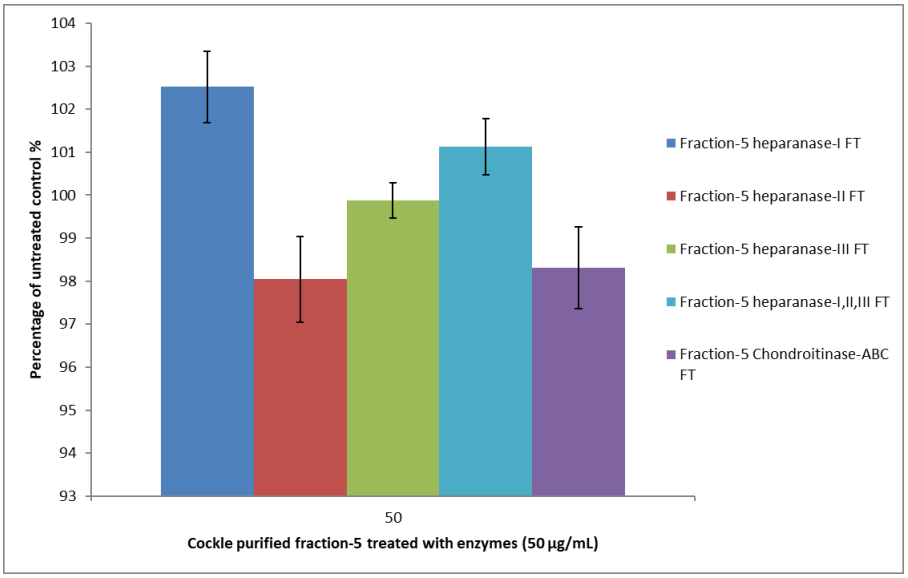

Figure 64. Antiproliferative activity of cockle purified fraction 5 disaccharides on Mero-25 cell line. All disaccharide samples were inactive.

9.11. Appendix XI: Cell proliferation assay of purified cockle polysaccharide samples using 10 mL fractions.

Common cockle polysaccharide was eluted using gradient elution (0-3 M) NaCl and samples were collected in 10 mL fractions over 70 minutes (F10-F70). Afterwards, cell proliferation assay was performed on K562 cell line for each fraction (Figure 65). Surprisingly, no antiproliferative activity was determined and all fractions were inactive.

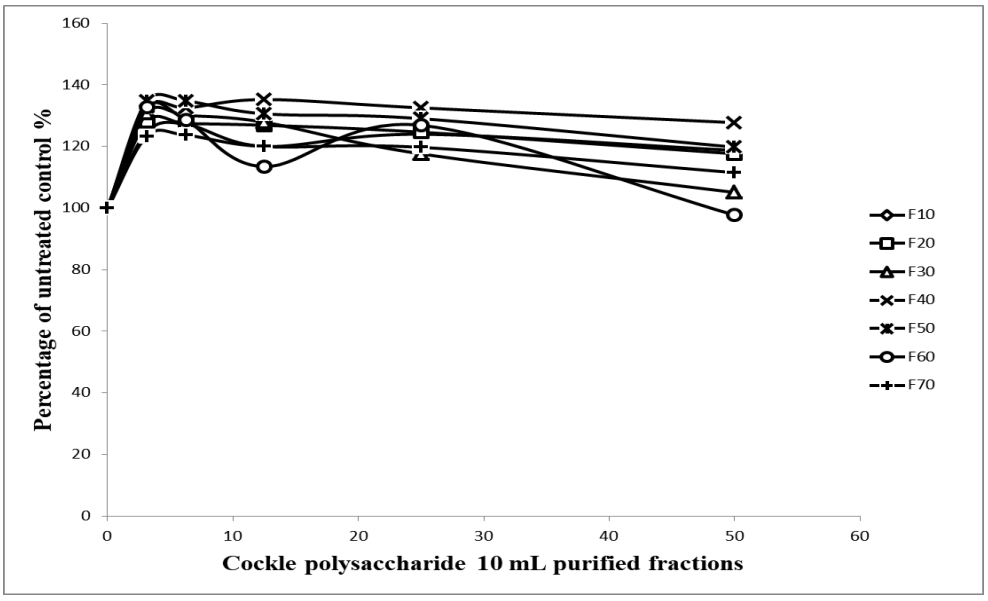

Figure 65. Cell proliferation assay of CE polysaccharides purified fractions using 10 ml fraction of anion-exchange column. 50 µg of cockle CE polysaccharide was incubated with K562 cell line, which enhanced the cancer cells growth instead of inhibiting its proliferation.

Table 18. Cockle CE polysaccharides purification using anion-exchange column. 10 mL fractions were eluted using 0-3 M gradient elution of NaCl.

Fraction number	NaCl % (0-3) M	IC_{50} Maximum drug concentration 50 µg/mL
F-10	0-0.28 (3-9%)	Inactive
F-20	0.36-1.0 (12-33%)	Inactive
F-30	1.1-1.5 (33-50%)	Inactive
F-40	1.6-2.0 (50-66.6)	Inactive
F-50	2.1-2.5 (66.6-83)	Inactive
F-60	2.58-2.9 (83-96)	Inactive
F-70	2.9-3 (96-100)	Inactive

9.12. Appendix XII: HS disaccharide mass spectrum profile.

HS disaccharide analysis of mammalian HS, cockle CE polysaccharides and cockle purified fractions (1-6) using GRIL-LC-MS.

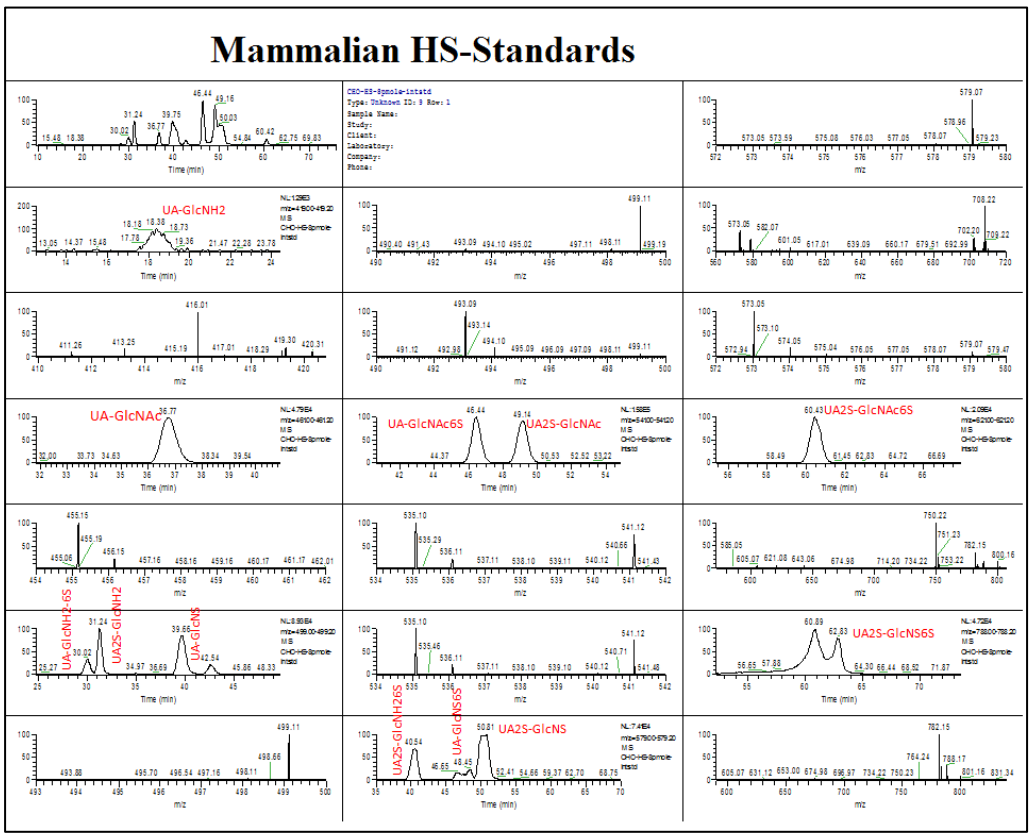

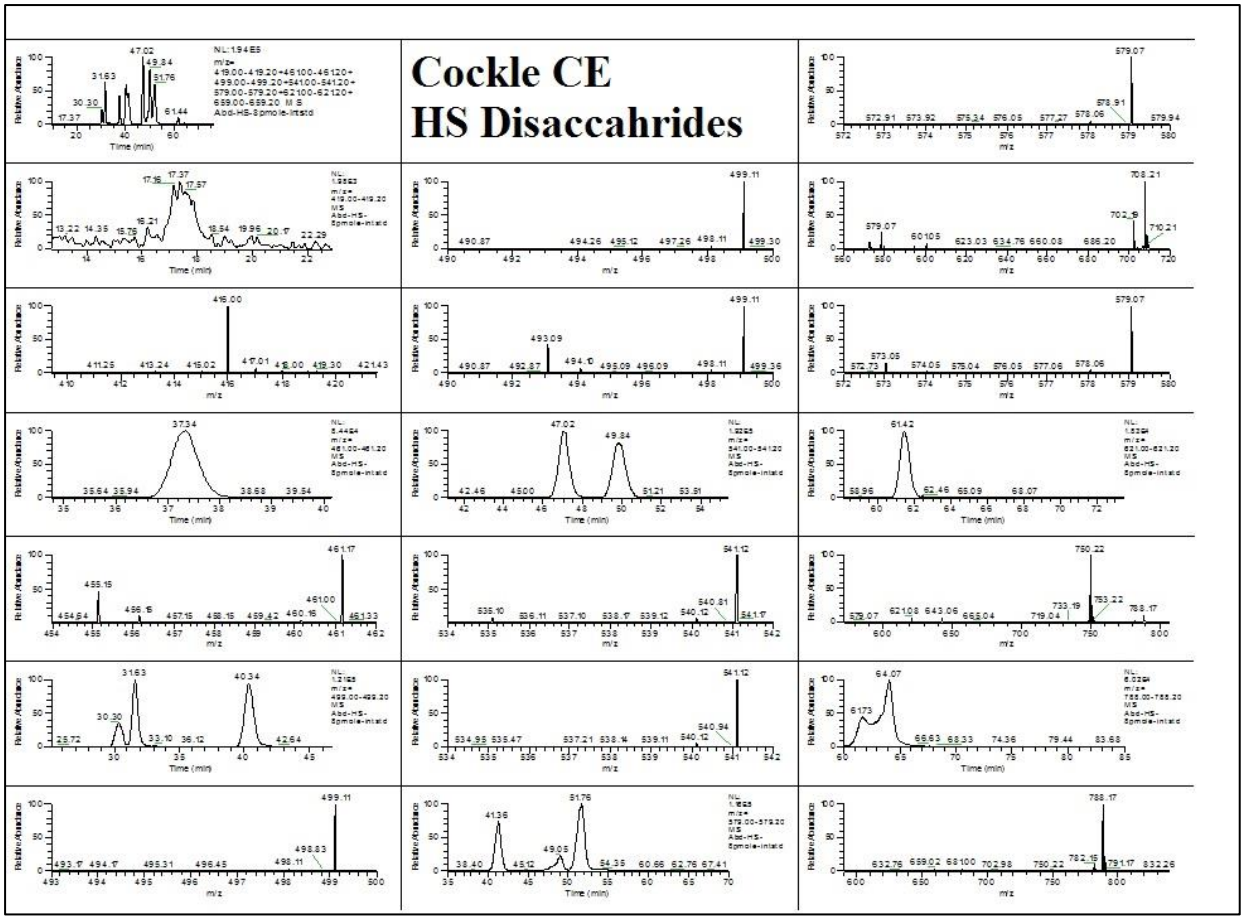
Cockle CE
HS Disaccahrides

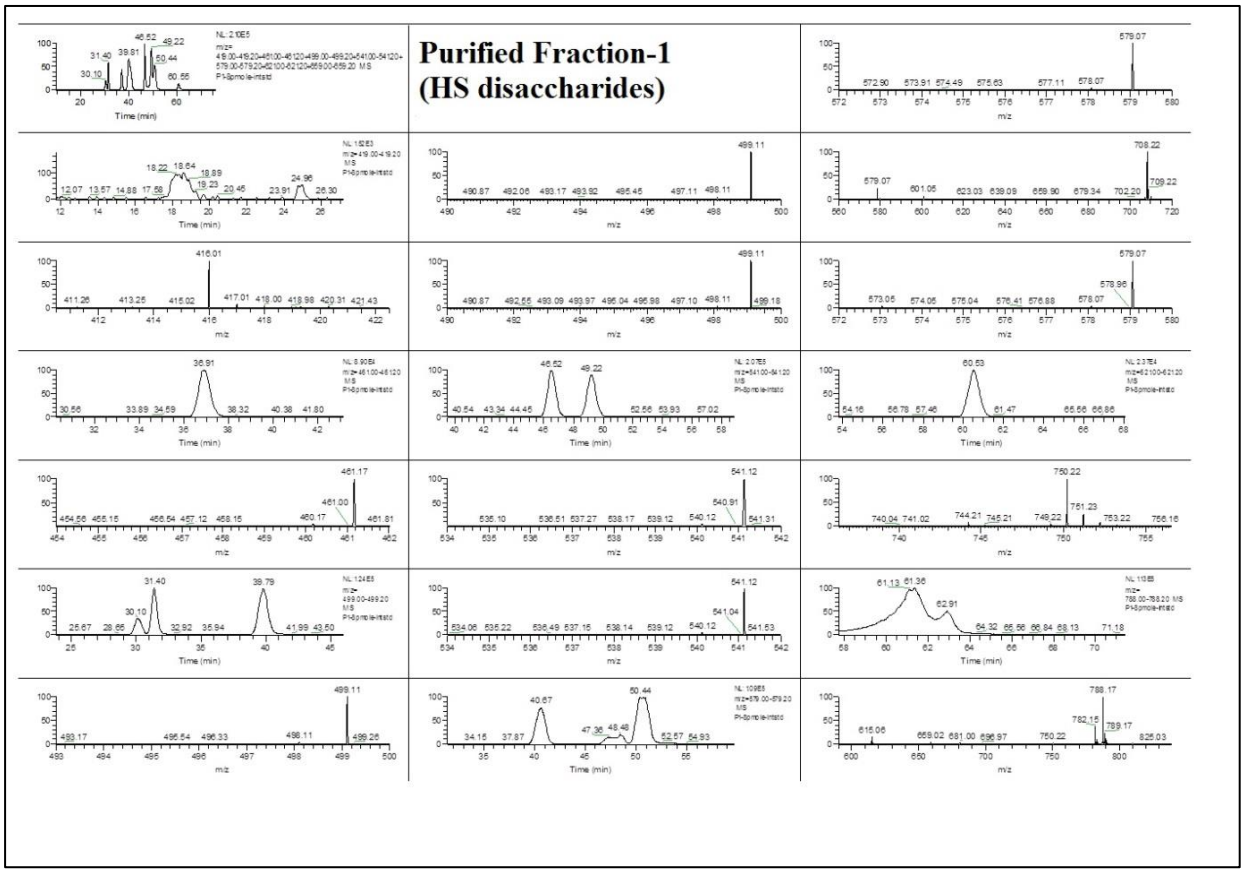
Purified Fraction-1
(HS disaccharides)

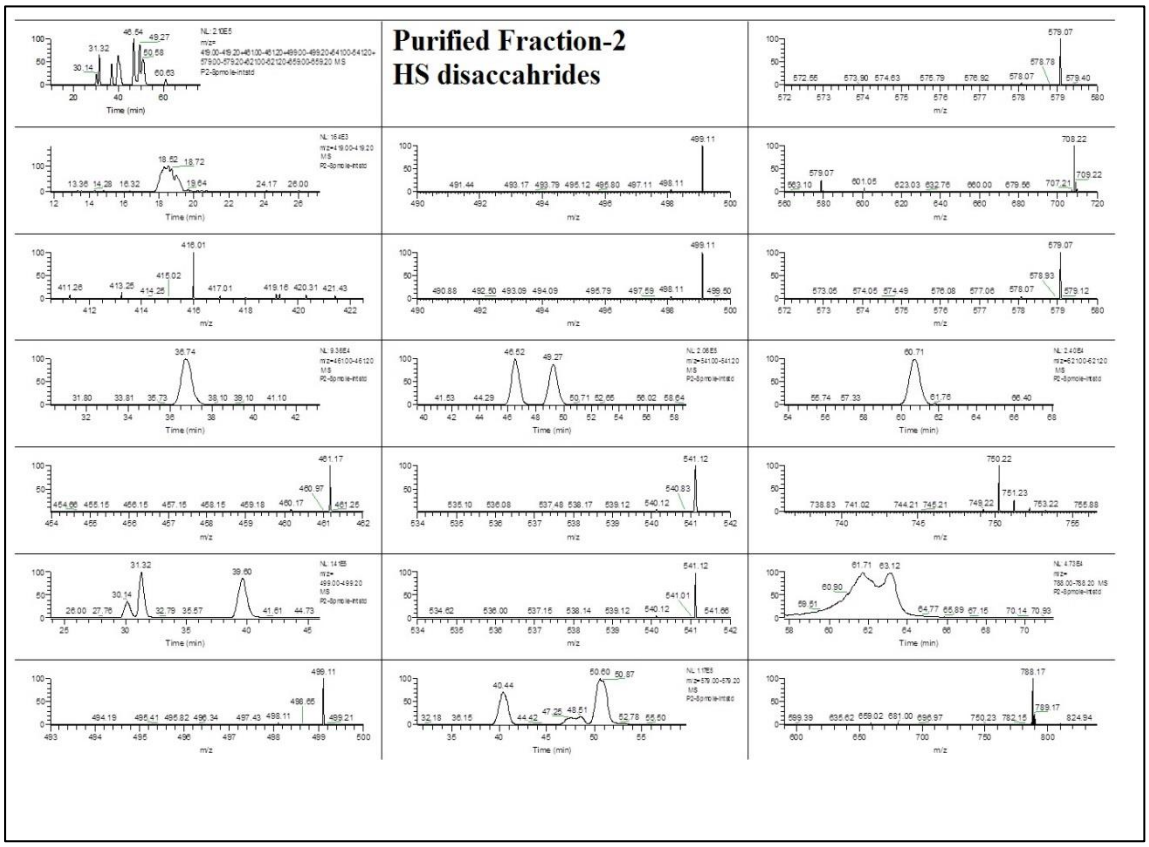
Purified Fraction-2
HS disaccahrides

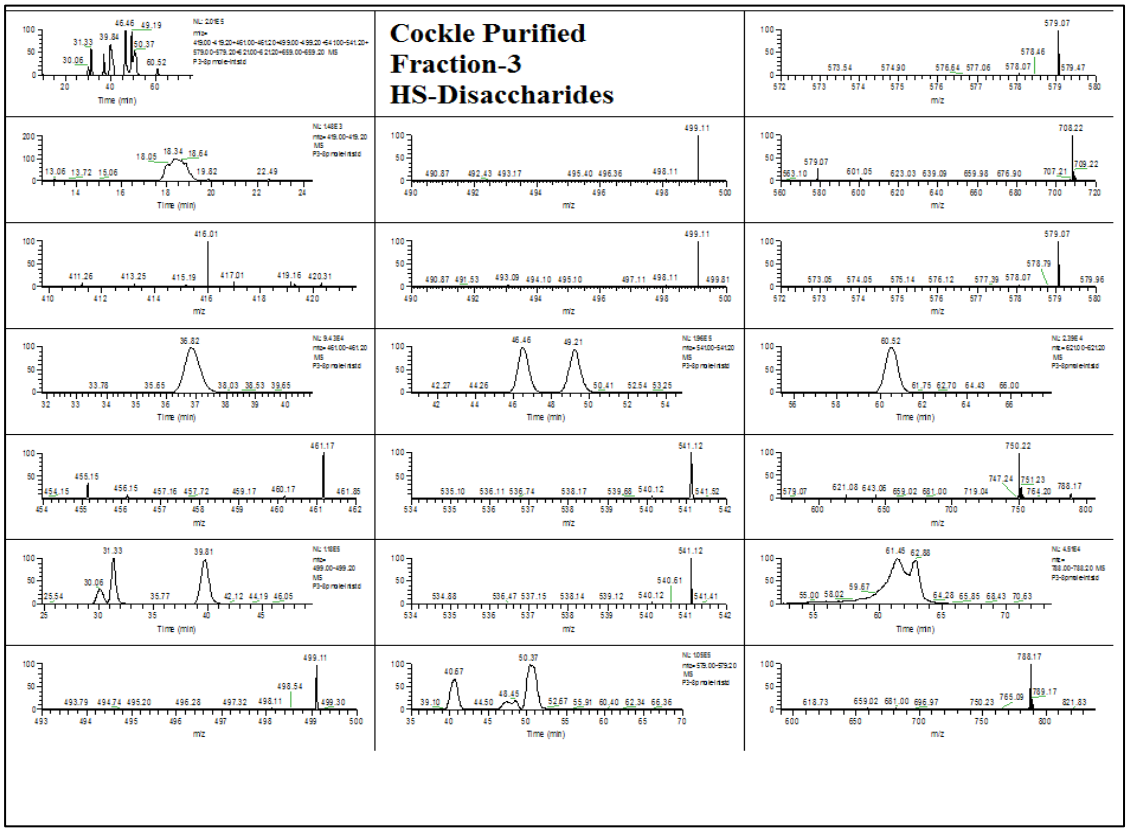
Cockle Purified
Fraction-3
HS-Disaccharides

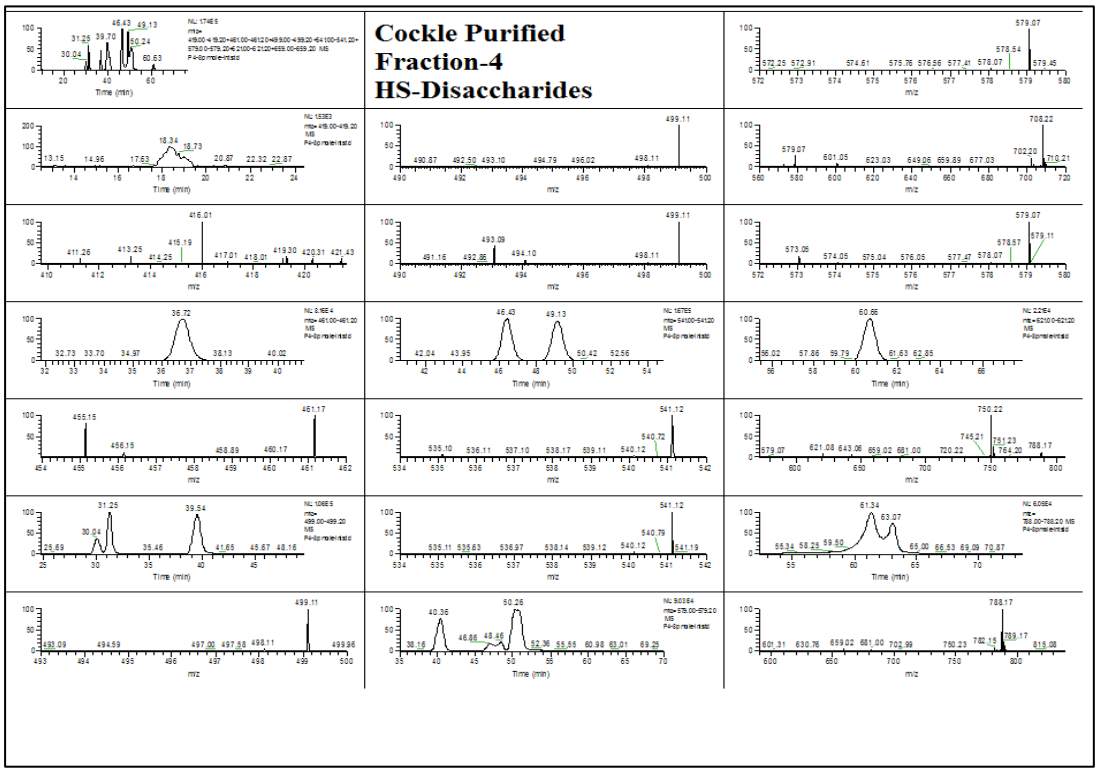
Cockle Purified
Fraction-4
HS-Disaccharides

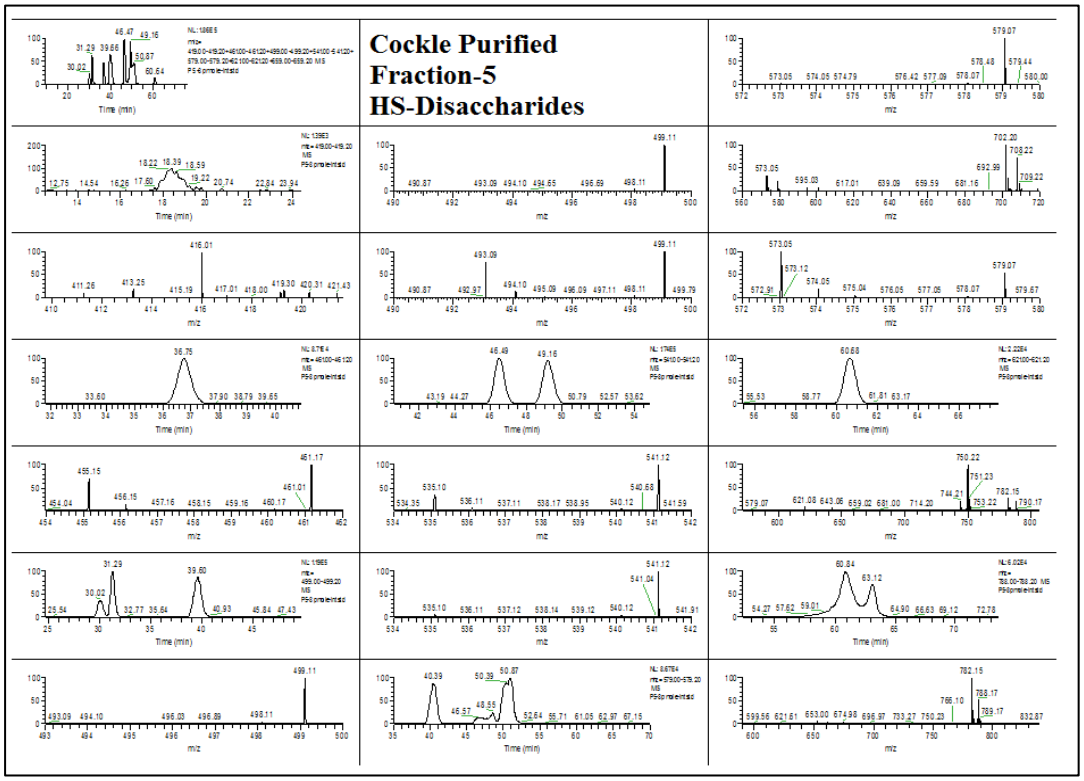
Cockle Purified
Fraction-5
HS-Disaccharides

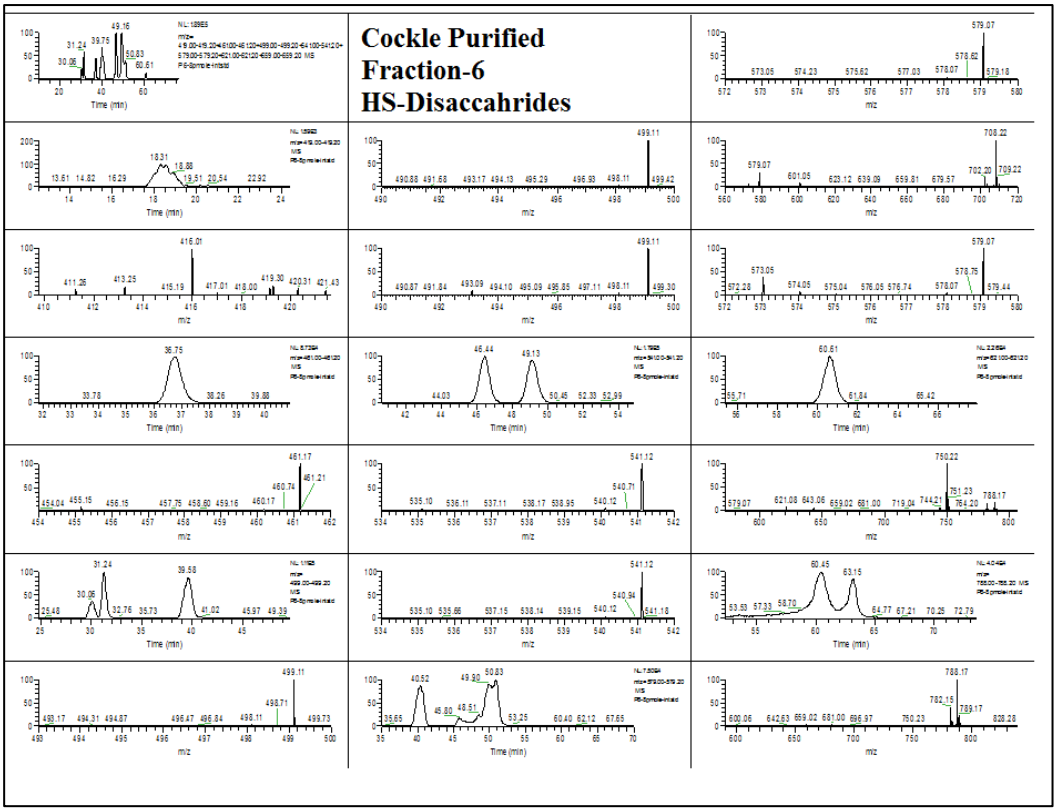
Cockle Purified
Fraction-6
HS-Disaccahrides

9.13. Appendix XIII: CS/DS disaccharide mass spectrum profile.

CS disaccharide analysis of mammalian CS, cockle CE polysaccharides and cockle purified fractions (1-6) using GRIL-LC-MS.

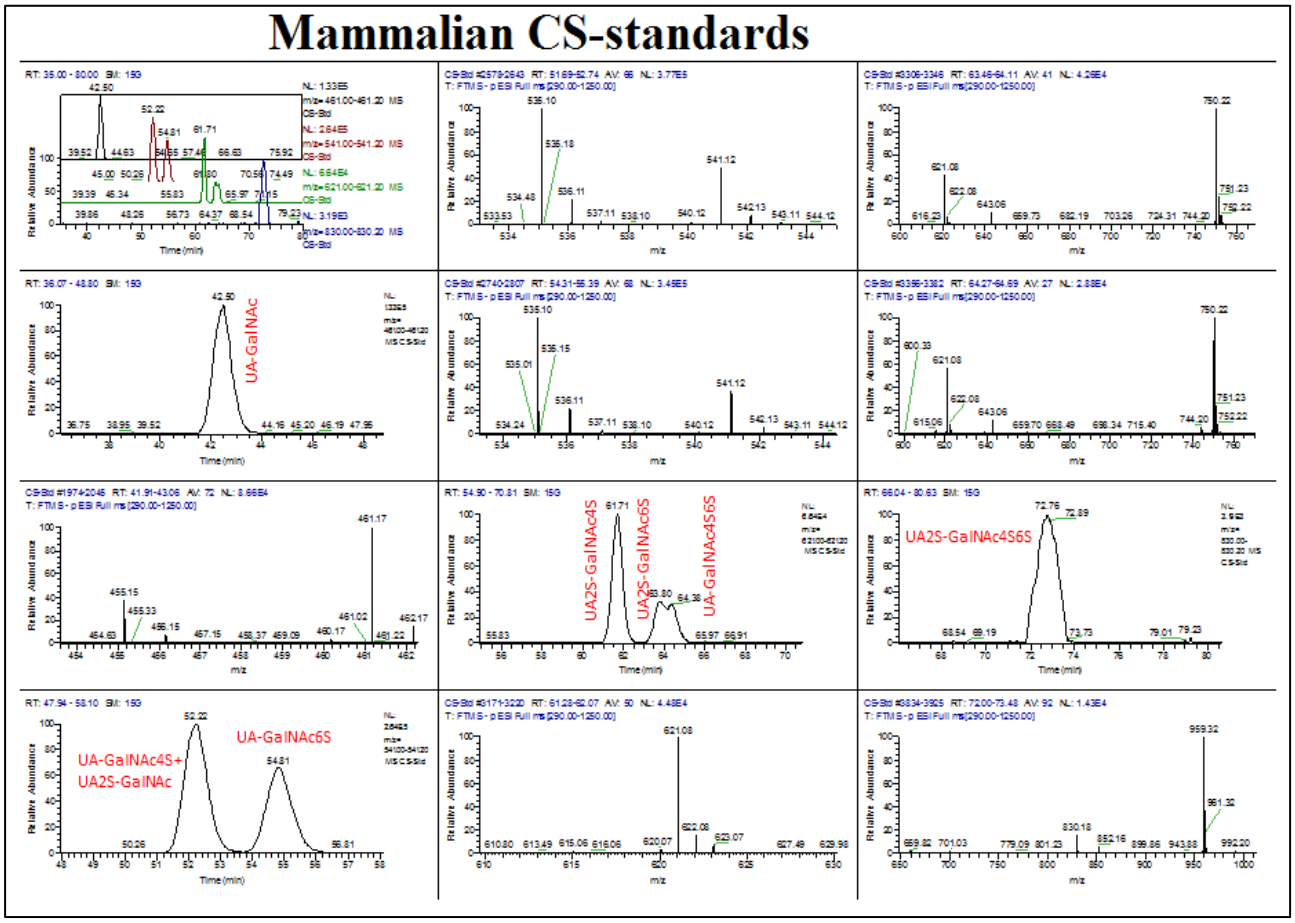

Cockle CE CS-disaccharides

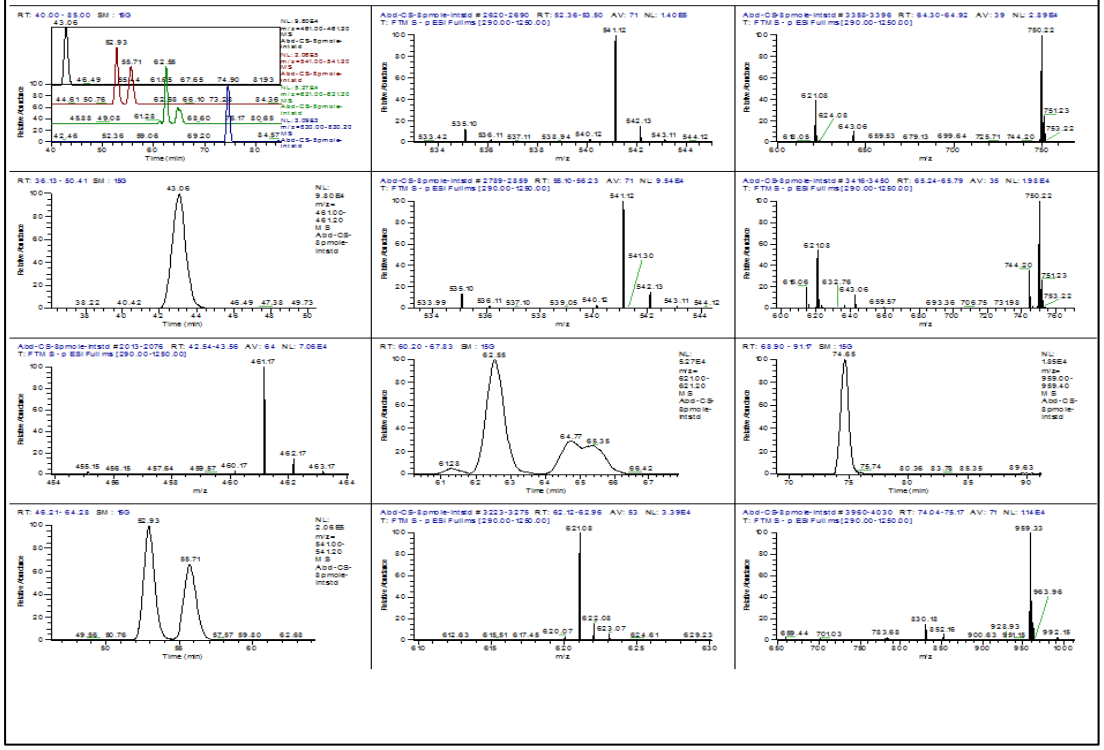

Cockle Purified Fraction-1 CS-Disaccharides

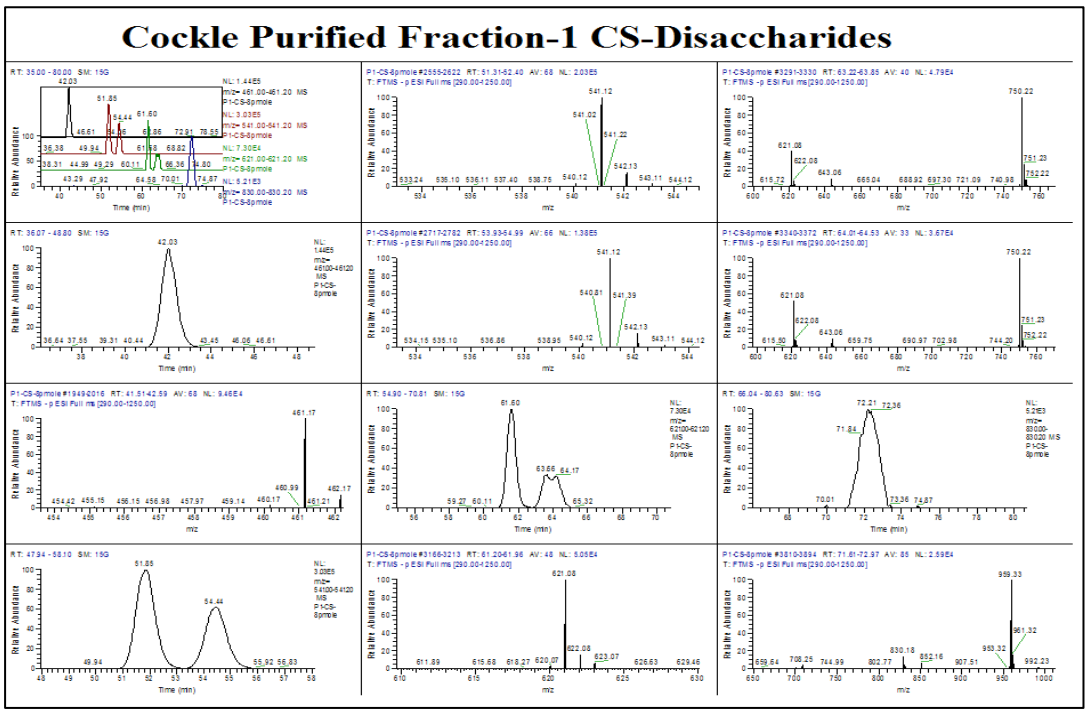

Cockle Purified Fraction-2 CS-Disaccharides

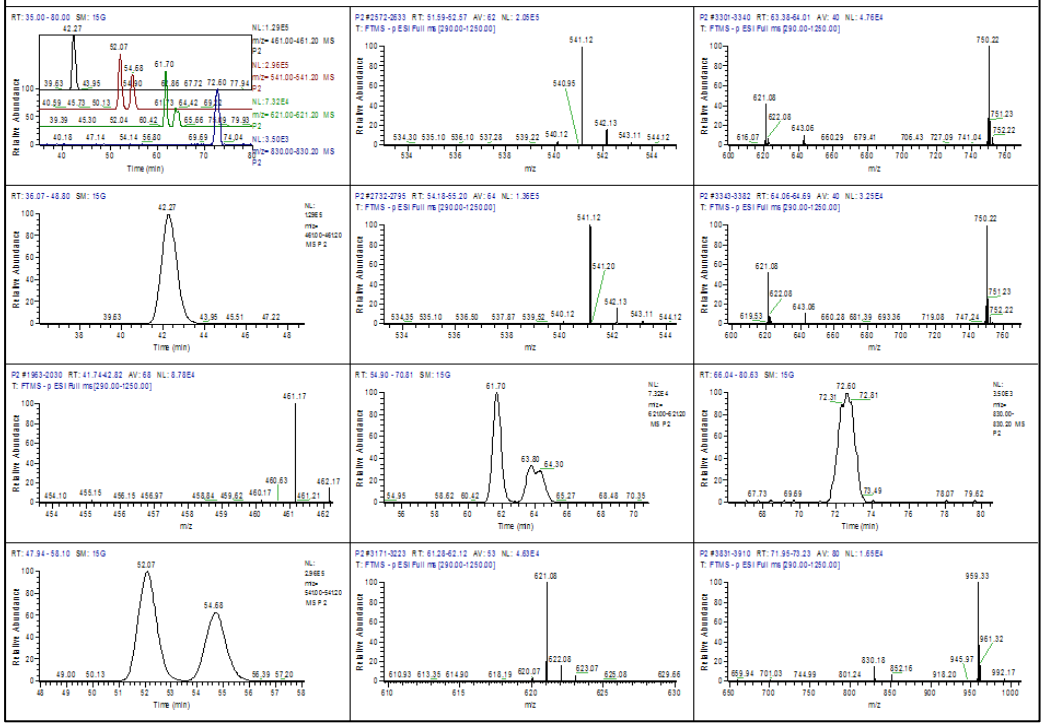

Cockle Purified Fraction-3 CS-Disaccahrides

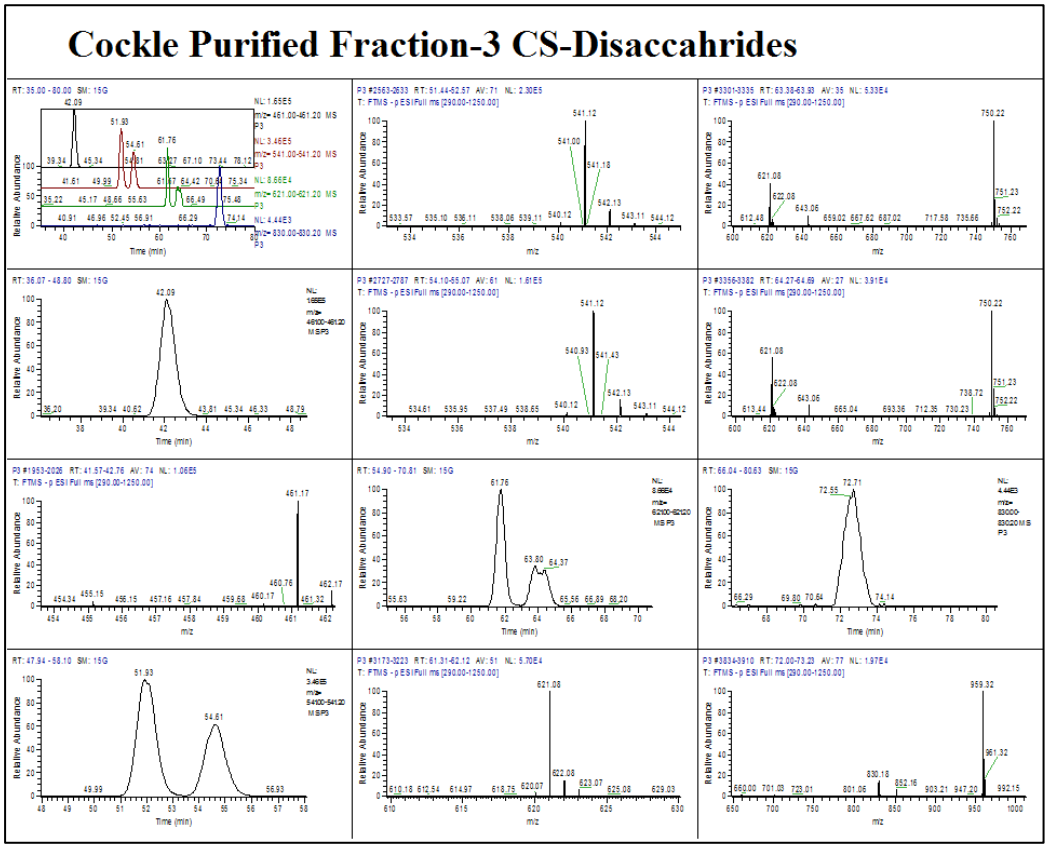

Cockle Purified Fraction-4 CS-Disaccharides

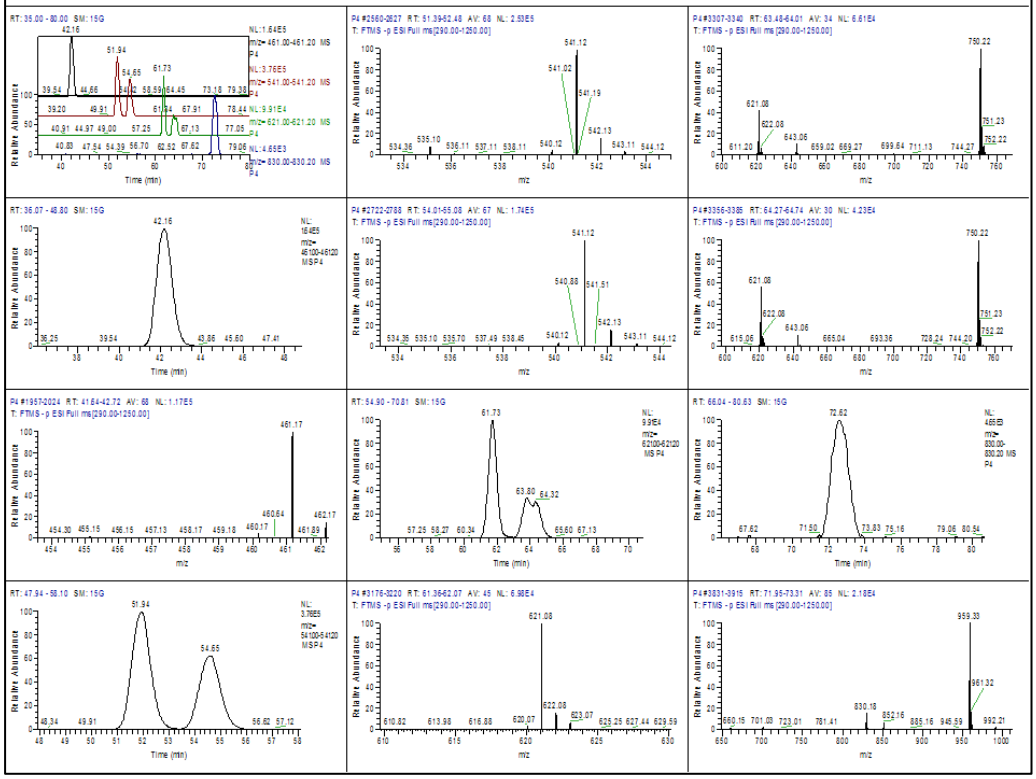

Cockle Purified Fraction-5 CS-Disaccharides

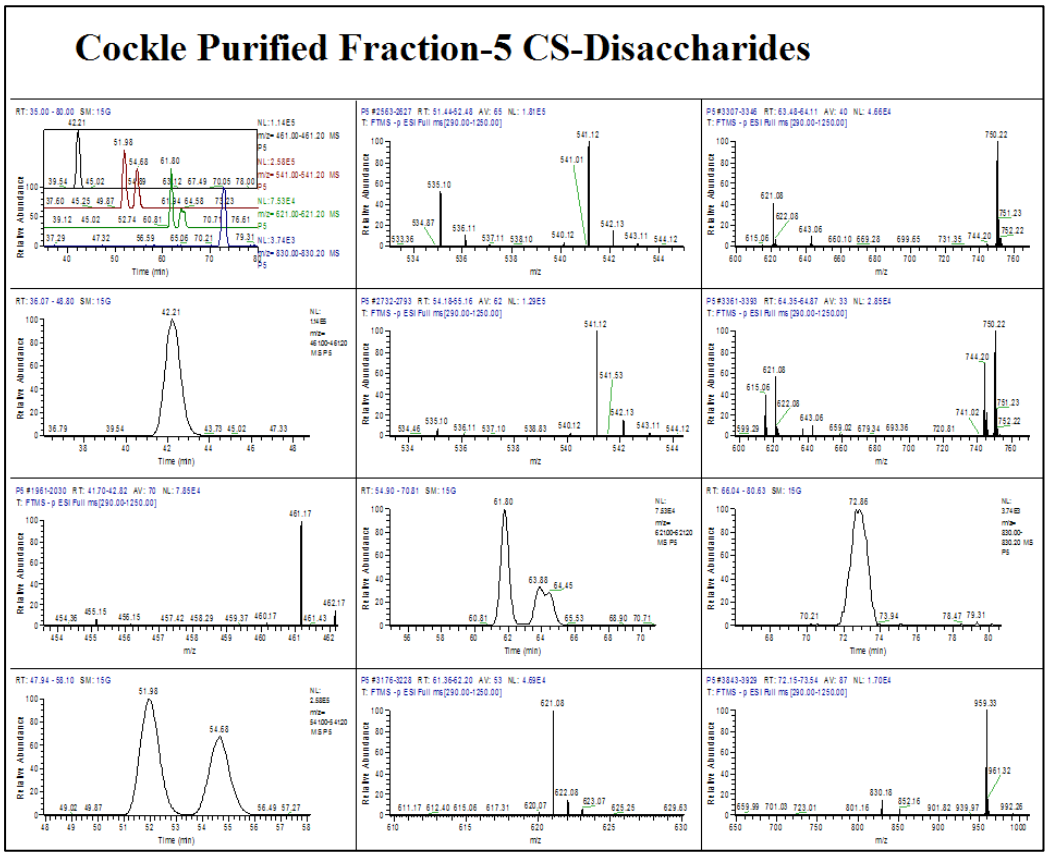

Cockle Purified Fraction-6 CS-Disaccharides

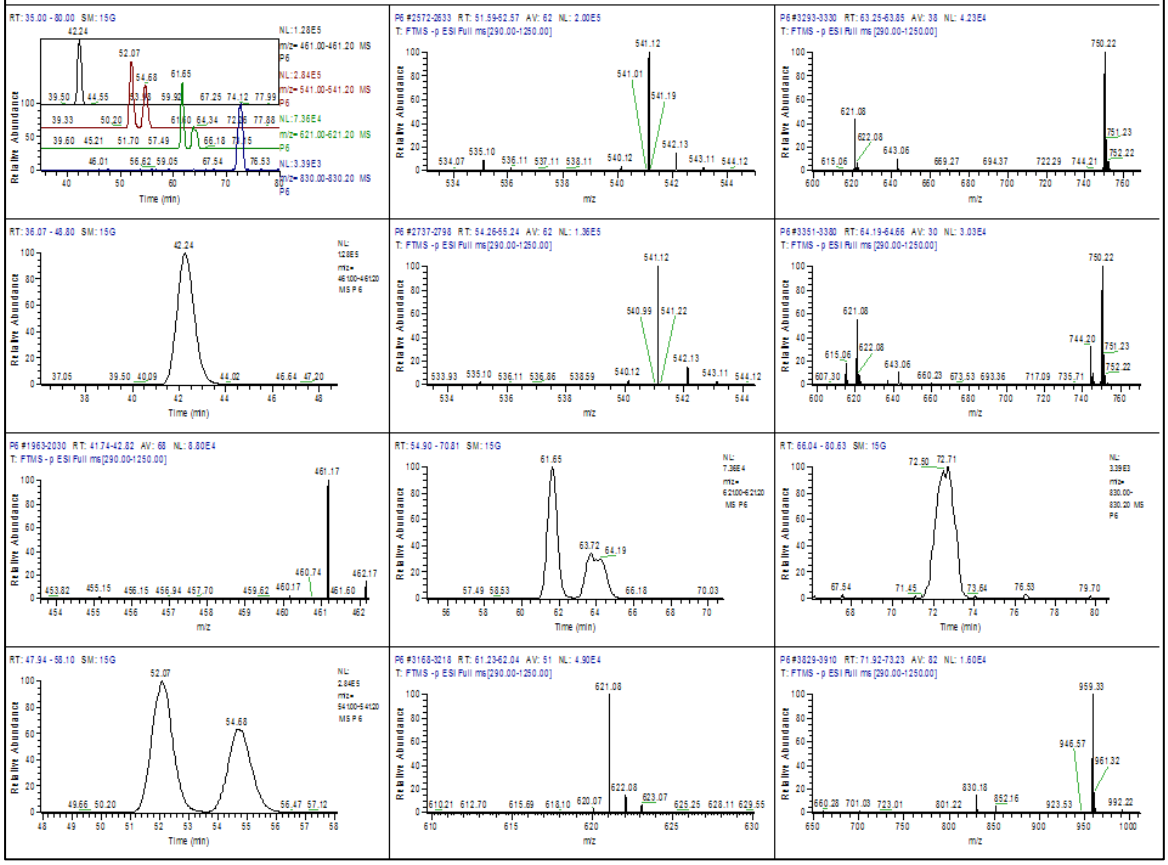

9.14. Appendix XIV: Monosaccharide composition analysis using HPAEC-PAD.

Monosaccharide composition analysis of mammalian HS, cockle CE polysaccharide and cockle purified fractions using HPAEC-PAD. All peaks were referred to the monosaccharide standards.

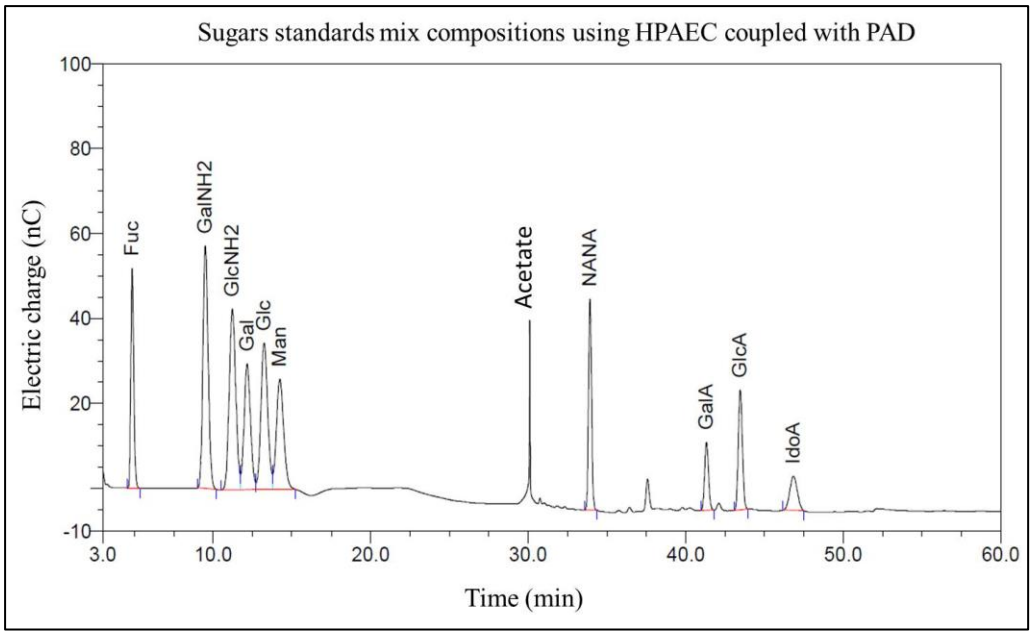

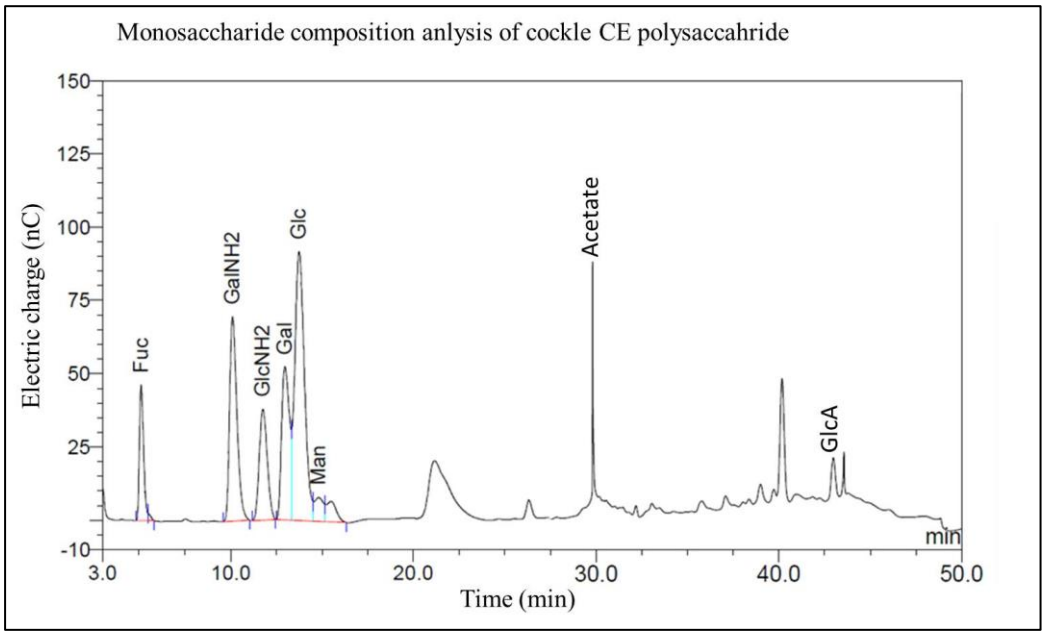

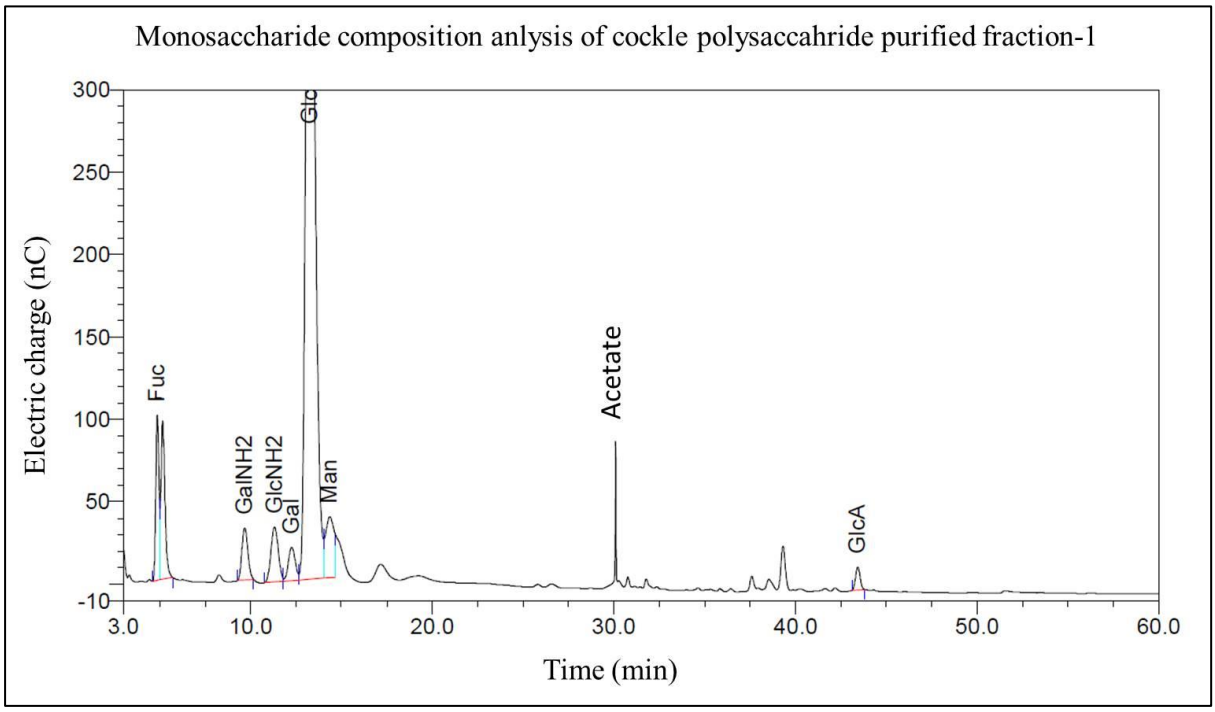
Monosaccharide composition anlysis of cockle polysaccahride purified fraction-1
Electric charge (nC)
Time (min)
Fuc
GalNH2
GlcNH2
Gal
Glc
Man
Acetate
GlcA

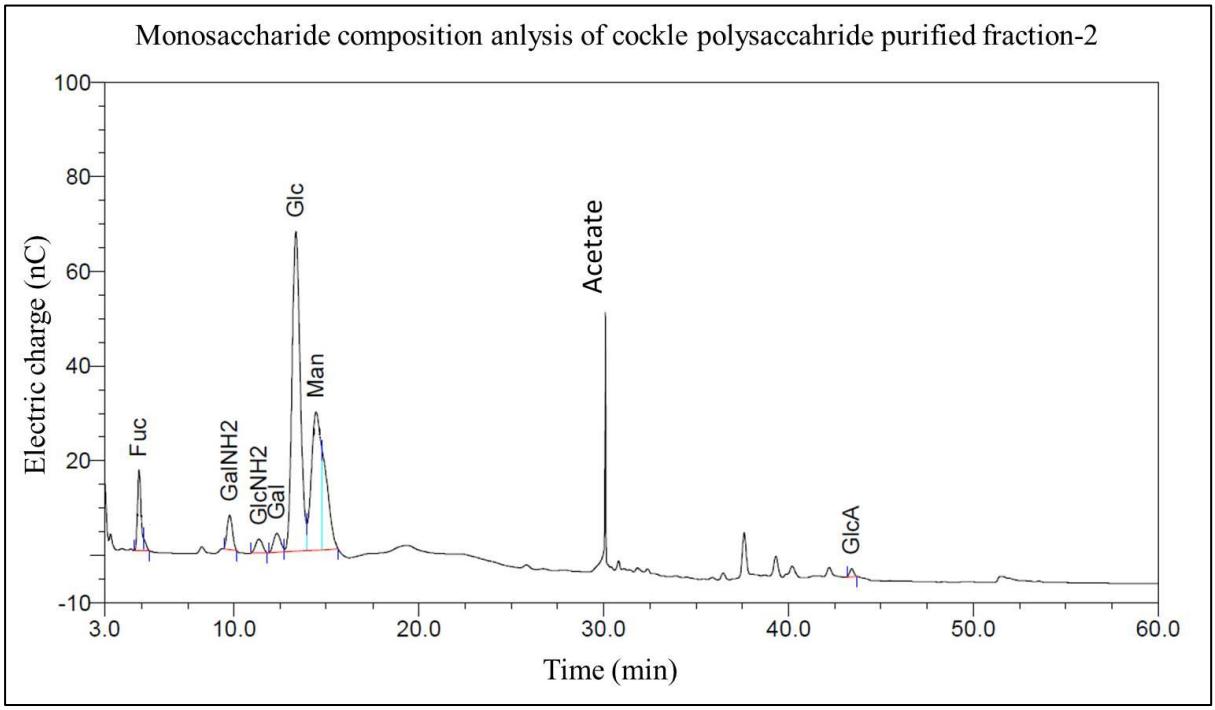
Monosaccharide composition anlysis of cockle polysaccahride purified fraction-2
Electric charge (nC)
Time (min)
Fuc
GalNH2
GlcNH2
Gal
Glc
Man
Acetate
GlcA

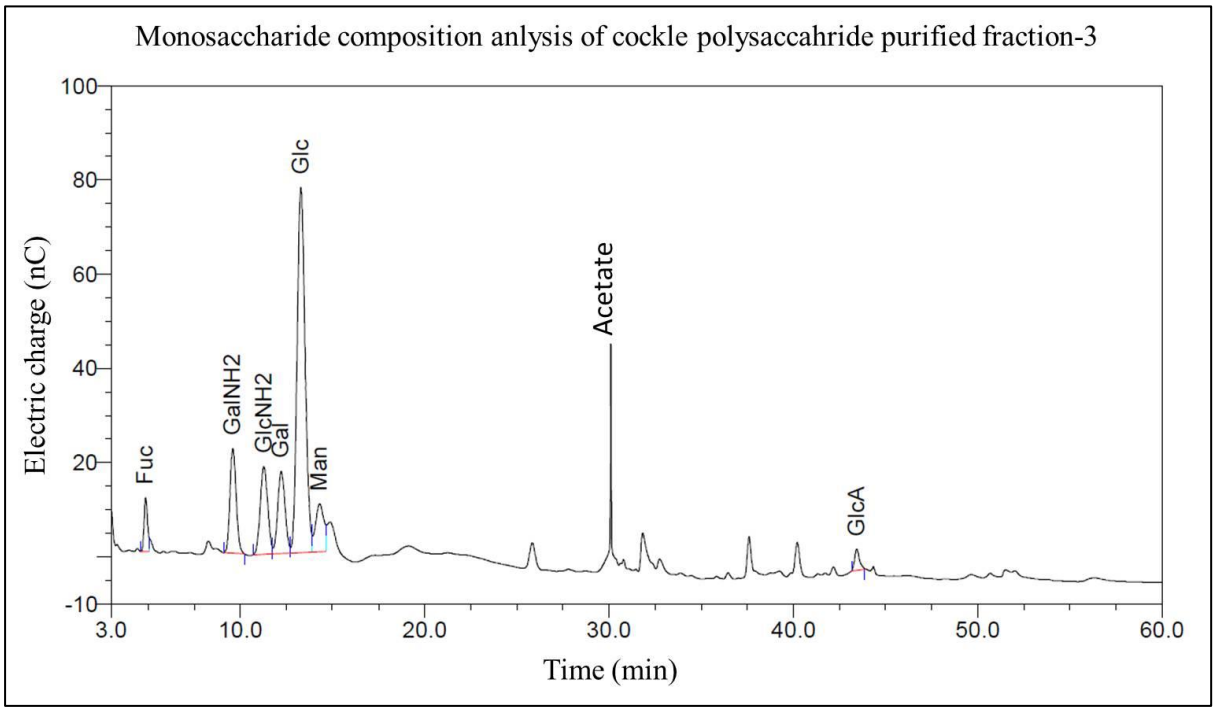
Monosaccharide composition anlysis of cockle polysaccahride purified fraction-3
Electric charge (nC)
Time (min)
Fuc
GalNH2
GlcNH2
Gal
Glc
Man
Acetate
GlcA

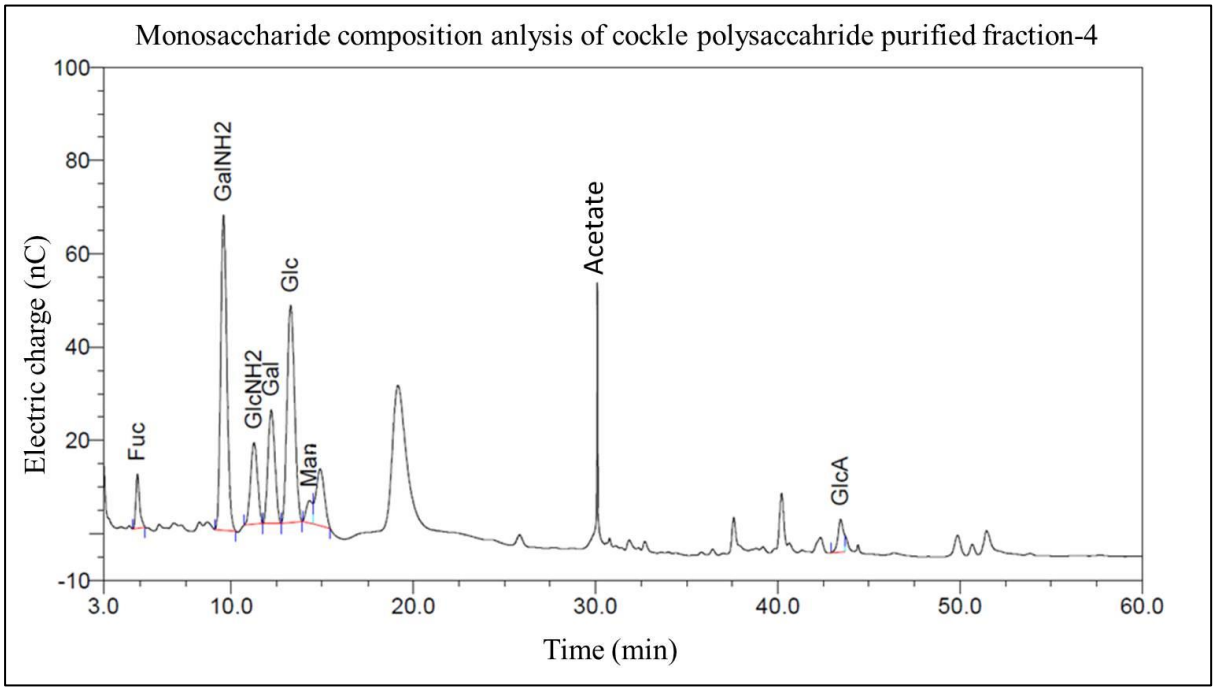
Monosaccharide composition anlysis of cockle polysaccahride purified fraction-4
Electric charge (nC)
Time (min)
Fuc
GalNH2
GlcNH2
Gal
Glc
Man
Acetate
GlcA

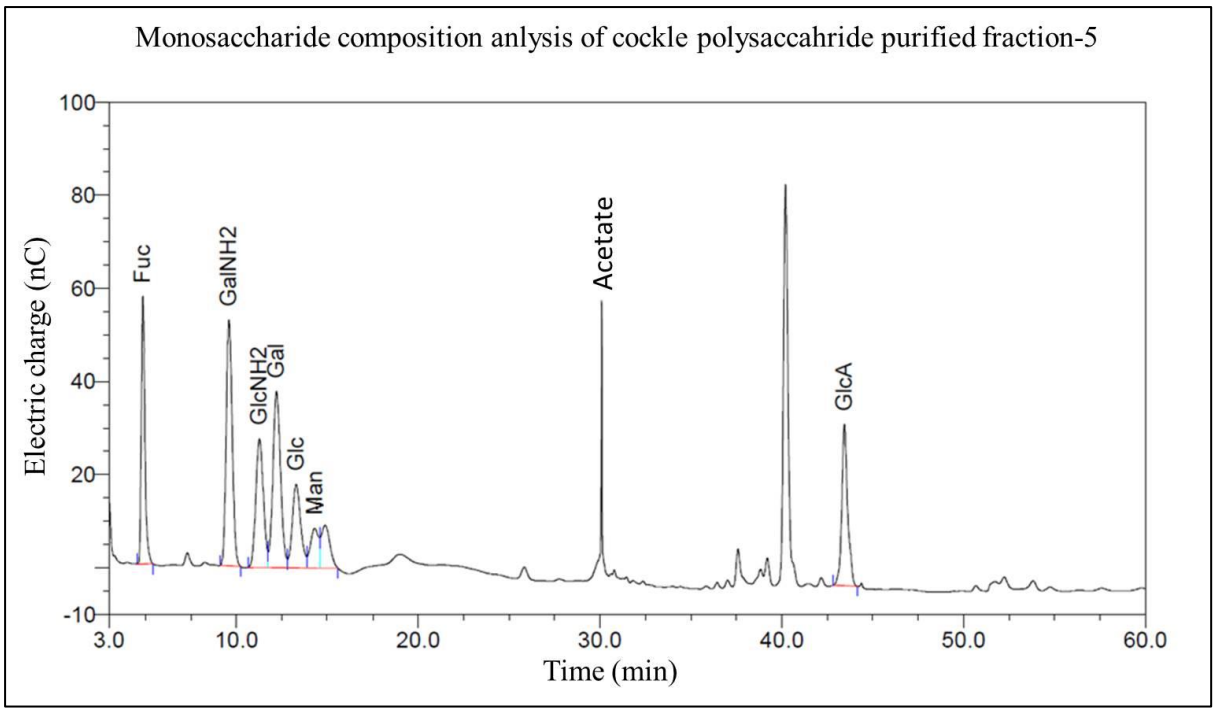
Monosaccharide composition anlysis of cockle polysaccahride purified fraction-5
Electric charge (nC)
Time (min)
Fuc
GalNH2
GlcNH2
Gal
Glc
Man
Acetate
GlcA

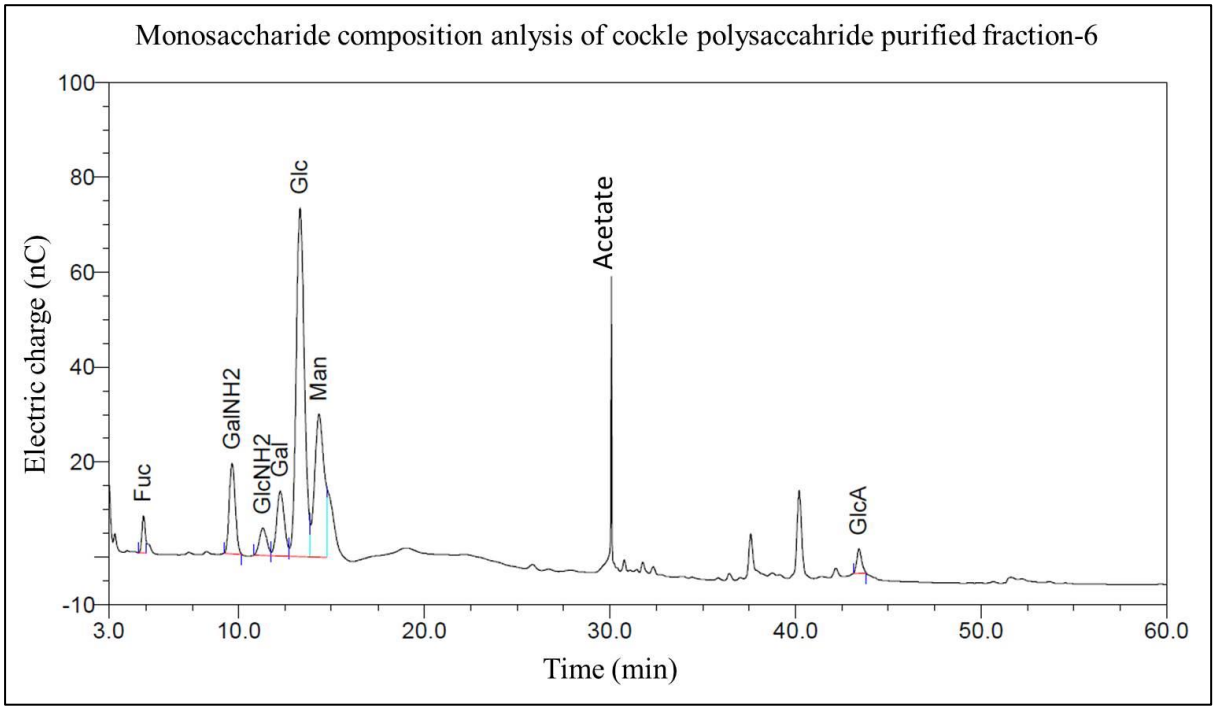
Monosaccharide composition anlysis of cockle polysaccahride purified fraction-6
Electric charge (nC)
Time (min)
Fuc
GalNH2
GlcNH2
Gal
Glc
Man
Acetate
GlcA

9.15. Appendix XV: NMR figures

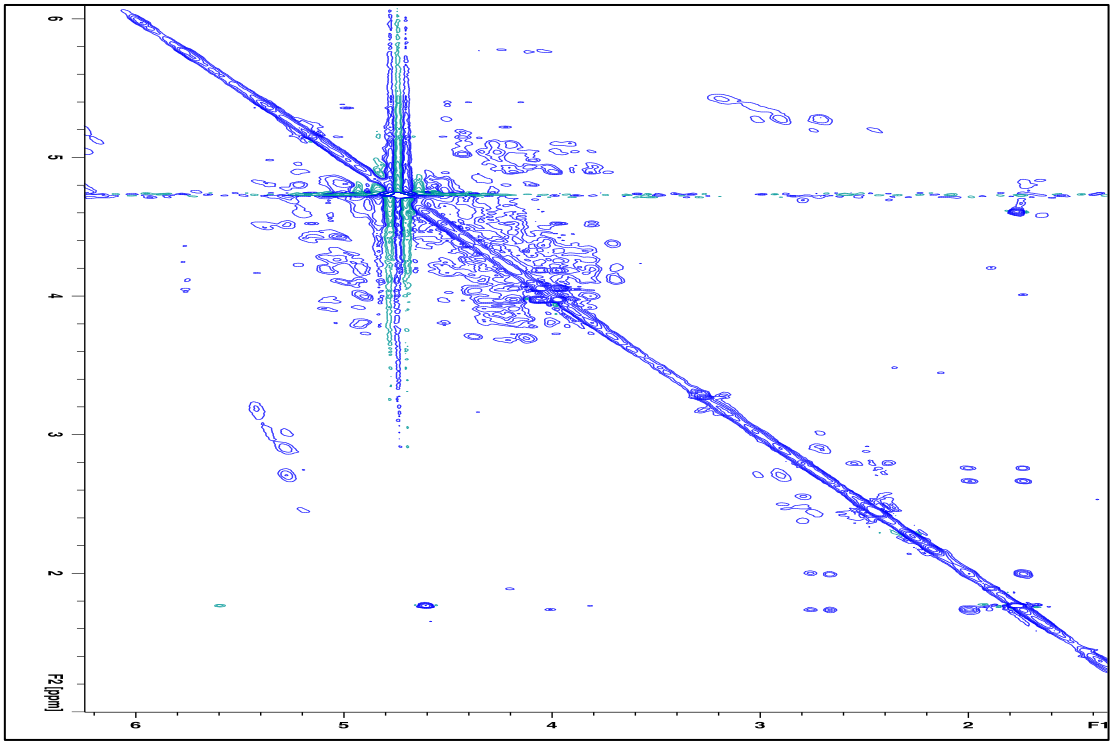

Figure 66. 2D ^{1}H-^{1}H NMR-TOCSY for cockle purified fraction 5. The spectrum was recorded at 56.85 °C.

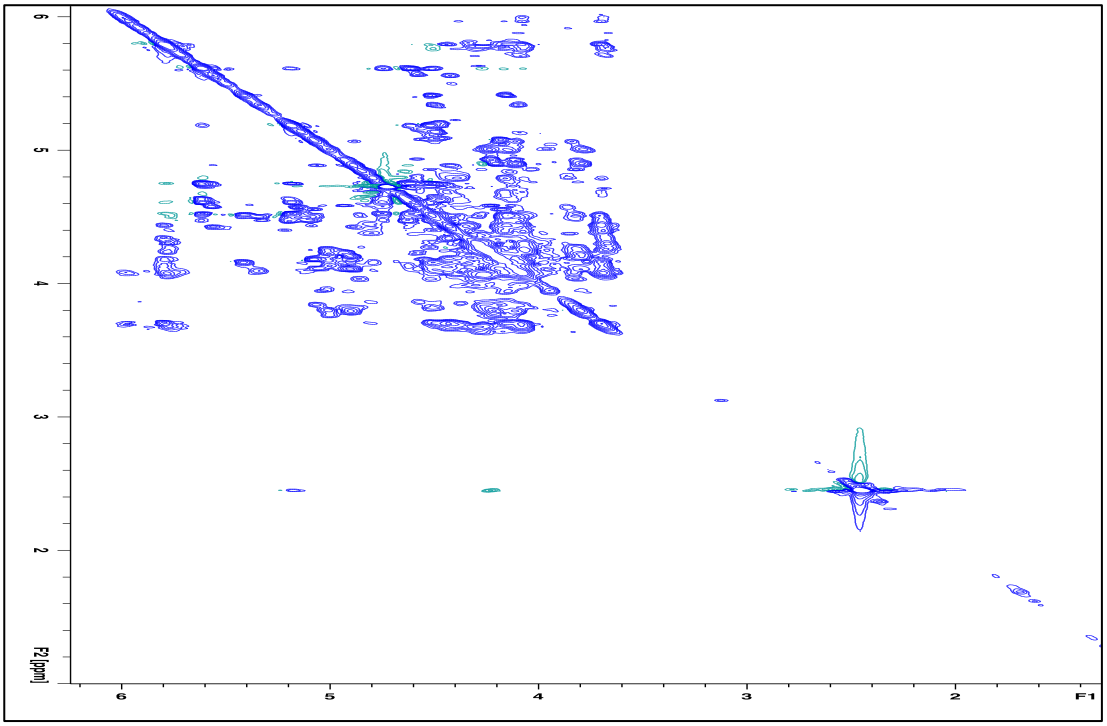

Figure 67. 2D ^{1}H-^{1}H NMR-TOCSY for Mammalian HS. The spectrum was recorded at 56.85 °C.

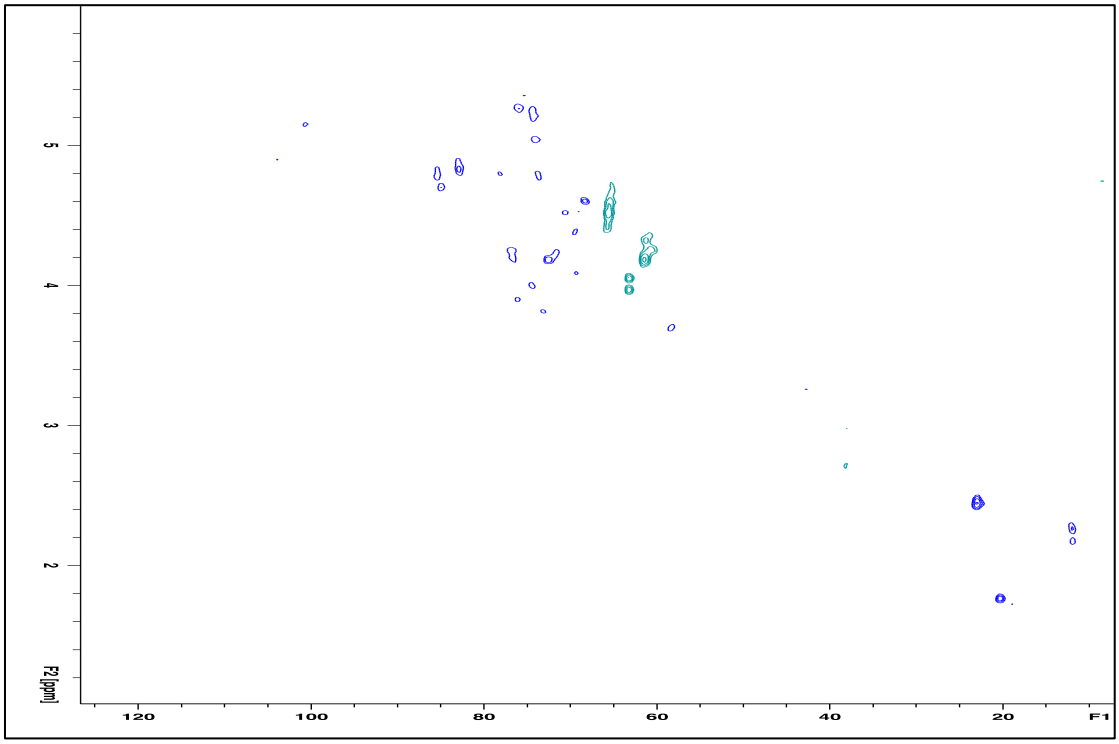

Figure 68. 2D ^{1}H-^{13}C NMR-HSQC for cockle purified fraction 5. The spectrum was recorded at 56.85 °C.

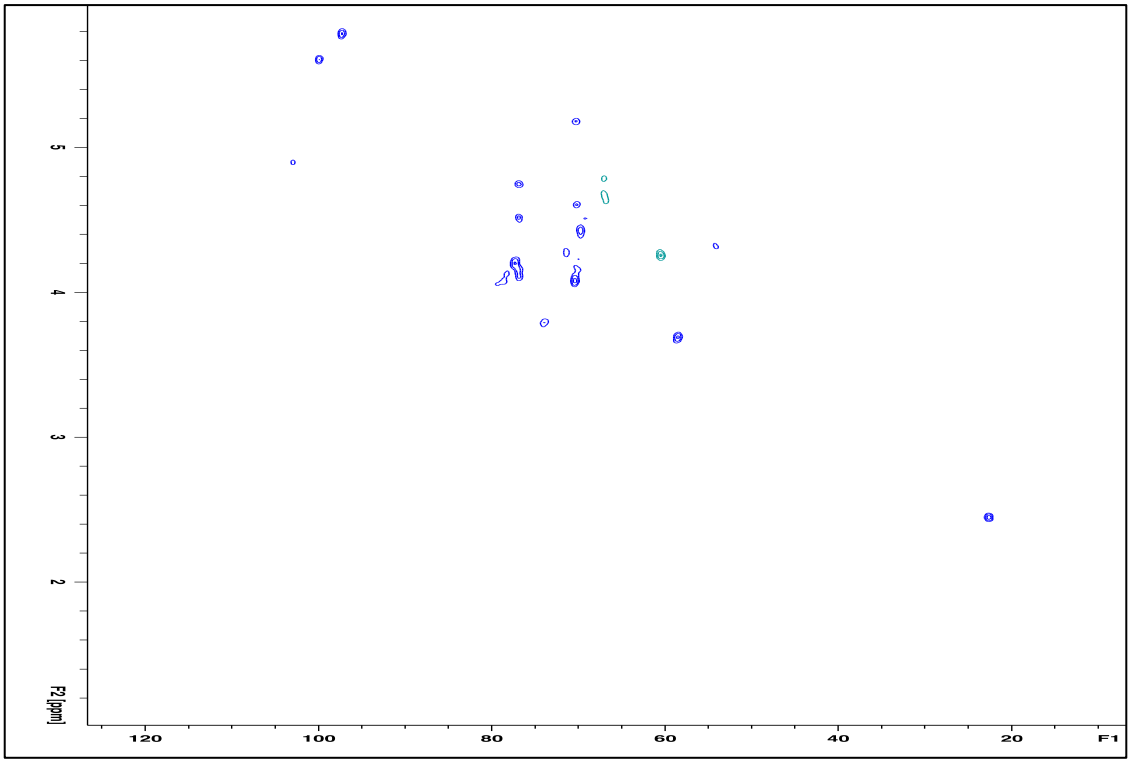

Figure 69. 2D ^{1}H-^{13}C NMR-HSQC for Mammalian HS. The spectrum was recorded at 56.85 °C.

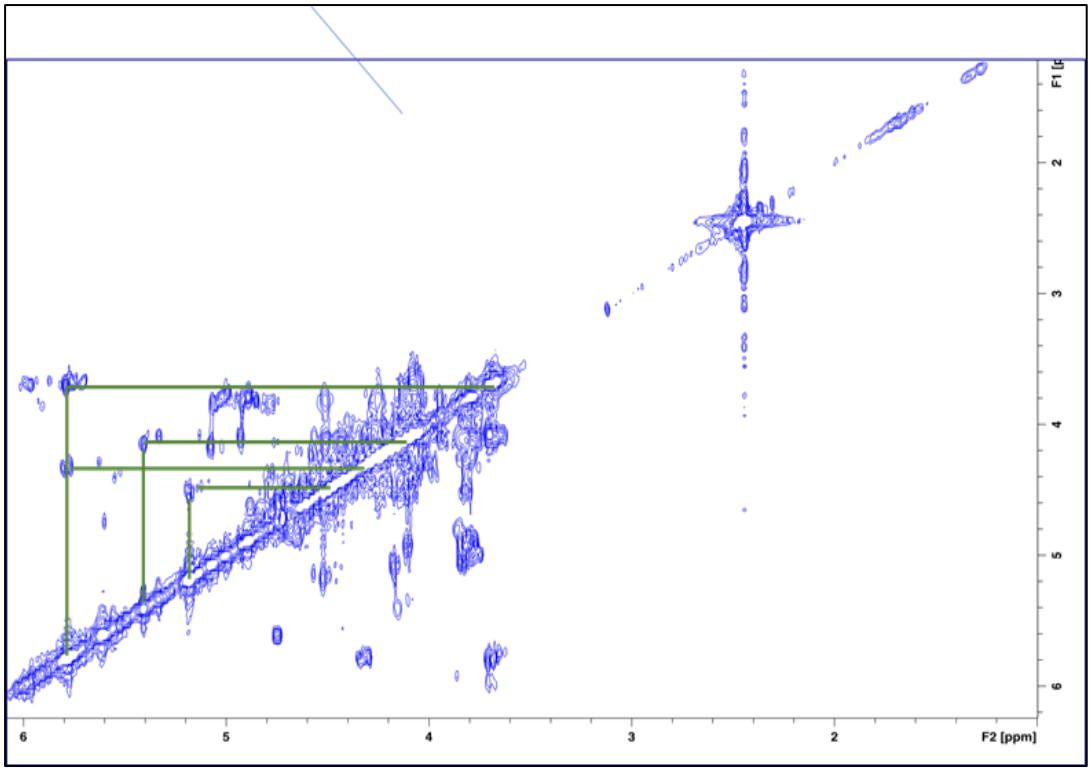

Figure 70. 2D ^{1}H-^{1}H-NMR-COSY for mammalian HS standard. Green lines indicate possible spin systems found in mammalian HS. The spectra were recorded at 56.85 °C.

10. References

Afratis, N. et al. (2012) ‘Glycosaminoglycans: key players in cancer cell biology and treatment’, *The FEBS journal*. Wiley Online Library, 279(7), pp. 1177–1197.

Agbarya, A. et al. (2014) ‘Natural products as potential cancer therapy enhancers: A preclinical update’, *SAGE Open Medicine*. doi: 10.1177/2050312114546924.

Almond, A. (2007) ‘Hyaluronan’, *Cellular and Molecular Life Sciences*. Springer, 64(13), pp. 1591–1596.

Amenta, P. S. et al. (2005) ‘Proteoglycan-Collagen XV in Human Tissues Is Seen Linking Banded Collagen Fibers Subjacent to the Basement Membrane’, *Journal of Histochemistry & Cytochemistry*. Journal of Histochemistry & Cytochemistry, 53(2), pp. 165–176. doi: 10.1369/jhc.4A6376.2005.

American Cancer Society (2018) *What Is Malignant Mesothelioma?, American Cancer Society*. Available at: https://www.cancer.org/cancer/malignant-mesothelioma.html (Accessed: 16 January 2019).

Amornrut, C. et al. (1999) ‘A new sulfated β-galactan from clams with anti-HIV activity’, *Carbohydrate research*. Elsevier, 321(1–2), pp. 121–127.

Asimakopoulou, A. P. et al. (2008) ‘The biological role of chondroitin sulfate in cancer and chondroitin-based anticancer agents’, *In vivo*. International Institute of Anticancer Research, 22(3), pp. 385–389.

Avendaño, C. and Menéndez, J. C. (2008) ‘Chapter 10 - Other Approaches to Targeted Therapy’, in Avendaño, C. and Menéndez, J. C. B. T.-M. C. of A. D. (eds). Amsterdam: Elsevier, pp. 307–349. doi: https://doi.org/10.1016/B978-0-444-52824-7.00010-X.

Bernfield, M. et al. (1999) ‘Functions of cell surface heparan sulfate proteoglycans’, *Annual review of biochemistry*. Annual Reviews 4139 El Camino Way, PO Box 10139, Palo Alto, CA 94303-0139, USA, 68(1), pp. 729–777.

Bertozzi, C. R. and Rabuka, D. (2009) ‘Structural basis of glycan diversity’. Cold Spring Harbor Laboratory Press, Cold Spring Harbor (NY).

Biosciences, B. D. (2011) ‘Detection of Apoptosis Using the BD Annexin V FITC Assay on the BD FACSVerse™ System’.

Bishop, J. R., Schuksz, M. and Esko, J. D. (2007) ‘Heparan sulphate proteoglycans fine-tune mammalian physiology’, *Nature*. Nature Publishing Group, 446(7139), p. 1030.

Blackhall, F. H. et al. (2001) ‘Heparan sulfate proteoglycans and cancer’, *British journal of cancer*. Nature Publishing Group, 85(8), p. 1094.

Bomken, S. N. and Josef Vormoor, H. (2009) ‘Childhood leukaemia’, *Paediatrics and Child Health*. doi: 10.1016/j.paed.2009.04.003.

Bond, C. S. et al. (1997) ‘Structure of a human lysosomal sulfatase’, *Structure*. Elsevier, 5(2), pp. 277–289.

Borsig, L. et al. (2007) ‘Selectin blocking activity of a fucosylated chondroitin sulfate glycosaminoglycan from sea cucumber effect on tumor metastasis and neutrophil recruitment’, *Journal of Biological Chemistry*. ASBMB, 282(20), pp. 14984–14991.

Bosman, F. T. and Stamenkovic, I. (2003) 'Functional structure and composition of the extracellular matrix', *The Journal of Pathology: A Journal of the Pathological Society of Great Britain and Ireland*. Wiley Online Library, 200(4), pp. 423–428.

Bourdon, M. A. et al. (1985) 'Molecular cloning and sequence analysis of a chondroitin sulfate proteoglycan cDNA', *Proceedings of the National Academy of Sciences*, 82(5), pp. 1321 LP – 1325. Available at: http://www.pnas.org/content/82/5/1321.abstract.

Brito, A. S. et al. (2014) 'A non-hemorrhagic hybrid heparin/heparan sulfate with anticoagulant potential', *Carbohydrate Polymers*, 99, pp. 372–378. doi: https://doi.org/10.1016/j.carbpol.2013.08.063.

Brockhausen, I., Schachter, H. and Stanley, P. (2009) 'O-GalNAc glycans', in *Essentials of Glycobiology. 2nd edition*. Cold Spring Harbor Laboratory Press.

Bullock, S. L. et al. (1998) 'Renal agenesis in mice homozygous for a gene trap mutation in the gene encoding heparan sulfate 2-sulfotransferase', *Genes & development*. Cold Spring Harbor Lab, 12(12), pp. 1894–1906.

Bülow, H. E. and Hobert, O. (2006) 'The molecular diversity of glycosaminoglycans shapes animal development', *Annu. Rev. Cell Dev. Biol.* Annual Reviews, 22, pp. 375–407.

Cabassi, F., Casu, B. and Perlin, A. S. (1978) 'Infrared absorption and Raman scattering of sulfate groups of heparin and related glycosaminoglycans in aqueous solution', *Carbohydrate Research*. Elsevier, 63, pp. 1–11.

Cancer research UK (2017) *Treatment for cancer*. Available at: https://www.cancerresearchuk.org/about-cancer/cancer-in-general/treatment.

Cancer Research UK (2017) *Cancer survival statistics for all cancers combined*. Available at: https://www.cancerresearchuk.org/health-professional/cancer-statistics/survival/all-cancers-combined (Accessed: 28 September 2018).

Cesaretti, M. et al. (2004) 'Isolation and characterization of a heparin with high anticoagulant activity from the clam Tapes phylippinarum: evidence for the presence of a high content of antithrombin III binding site', *Glycobiology*. Oxford University Press, 14(12), pp. 1275–1284.

Charles, A. L., Huang, T. C. and Chang, Y. H. (2008) 'Structural analysis and characterization of a mucopolysaccharide isolated from roots of cassava (Manihot esculenta Crantz L.)', *Food hydrocolloids*. Elsevier, 22(1), pp. 184–191.

Copelan, E. A. (2006) 'Hematopoietic stem-cell transplantation', *New England Journal of Medicine*. Mass Medical Soc, 354(17), pp. 1813–1826.

Deakin, J. A. and Lyon, M. (2008) 'A simplified and sensitive fluorescent method for disaccharide analysis of both heparan sulfate and chondroitin/dermatan sulfates from biological samples', *Glycobiology*. Oxford University Press, 18(6), pp. 483–491.

Deschler, B. and Lübbert, M. (2006) 'Acute myeloid leukemia: Epidemiology and etiology', *Cancer*. doi: 10.1002/cncr.22233.

Du, J. and Tang, X. L. (2014) 'Natural products against cancer: A comprehensive bibliometric study of the research projects, publications, patents and drugs', *Journal of cancer research and therapeutics*. Medknow Publications, 10(5), p. 27.

Dutton, G. J. (1966) 'CHAPTER 3 - The Biosynthesis of Glucuronides BT - Glucuronic Acid Free and Combined', in. Academic Press, pp. 185–299. doi: https://doi.org/10.1016/B978-0-12-395501-2.50009-8.

Edgren, G. et al. (1997) ‘Glypican (heparan sulfate proteoglycan) is palmitoylated, deglycanated and reglycanated during recycling in skin fibroblasts’, *Glycobiology*. Oxford University Press, 7(1), pp. 103–112.

Elmore, S. (2007) ‘Apoptosis: a review of programmed cell death’, *Toxicologic pathology*. Sage Publications, 35(4), pp. 495–516.

Esko, J. D. et al. (1987) ‘Inhibition of chondroitin and heparan sulfate biosynthesis in Chinese hamster ovary cell mutants defective in galactosyltransferase I.’, *Journal of Biological Chemistry*. ASBMB, 262(25), pp. 12189–12195.

Esko, J. D. (1991) ‘Genetic analysis of proteoglycan structure, function and metabolism’, *Current opinion in cell biology*. Elsevier, 3(5), pp. 805–816.

Esko, J. D., Kimata, K. and Lindahl, U. (2009) ‘Proteoglycans and sulfated glycosaminoglycans’, in *Essentials of Glycobiology*. Cold Spring Harbor Laboratory Press, pp. 229–248. doi: 10:0-87969-559-5.

Filmus, J., Capurro, M. and Rast, J. (2008) ‘Glypicans’, *Genome biology*. BioMed Central, 9(5), p. 224.

Fraser, J. R. E., Laurent, T. C. and Laurent, U. B. G. (1997) ‘Hyaluronan: its nature, distribution, functions and turnover’, *Journal of internal medicine*. Wiley Online Library, 242(1), pp. 27–33.

Friebolin, H. and Becconsall, J. K. (1993) *Basic one-and two-dimensional NMR spectroscopy*. VCH Weinheim.

Funderburgh, J. L. (2000) ‘MINI REVIEW Keratan sulfate: structure, biosynthesis, and function’, *Glycobiology*. Oxford University Press, 10(10), pp. 951–958.

Fuster, M. M. and Esko, J. D. (2005) ‘The sweet and sour of cancer: glycans as novel therapeutic targets’, *Nature Reviews Cancer*. Nature Publishing Group, 5(7), p. 526.

Gerlier, D. and Thomasset, N. (1986) ‘Use of MTT colorimetric assay to measure cell activation’, *Journal of Immunological Methods*. doi: 10.1016/0022-1759(86)90215-2.

Gomes, A. M. et al. (2010) ‘Unique extracellular matrix heparan sulfate from the bivalve nodipecten nodosus (linnaeus, 1758) safely inhibits arterial thrombosis after photo chemically induced endothelial lesion’, *Journal of Biological Chemistry*. ASBMB, p. jbc-M109.

Greaves, M. F. and Wiemels, J. (2003) ‘Origins of chromosome translocations in childhood leukaemia’, *Nature Reviews Cancer*. Nature Publishing Group, 3(9), p. 639.

Habuchi, H., Habuchi, O. and Kimata, K. (1995) ‘Purification and characterization of heparan sulfate 6-sulfotransferase from the culture medium of Chinese hamster ovary cells’, *Journal of Biological Chemistry*. ASBMB, 270(8), pp. 4172–4179.

Habuchi, O., Sugiura, K. and Kawai, N. (1977) ‘Glucose branches in chondroitin sulfates from squid cartilage.’, *Journal of Biological Chemistry*. ASBMB, 252(13), pp. 4570–4576.

Haimov-Kochman, R. et al. (2002) ‘Localization of heparanase in normal and pathological human placenta’, *MHR: Basic science of reproductive medicine*. European Society of Human Reproduction and Embryology, 8(6), pp. 566–573.

Han, N. et al. (2018) ‘Derivatives of Dolastatin 10 and Uses Thereof’. Google Patents.

Hardy, M. R., Townsend, R. R. and Lee, Y. C. (1988) ‘Monosaccharide analysis of

glycoconjugates by anion exchange chromatography with pulsed amperometric detection', *Analytical biochemistry*. Elsevier, 170(1), pp. 54–62.

Hascall, V. and Esko, J. D. (2015) 'Hyaluronan'. Cold Spring Harbor Laboratory Press, Cold Spring Harbor (NY).

Hassell, J. R., Kimura, J. H. and Hascall, V. C. (1986) 'Proteoglycan core protein families', *Annual review of biochemistry*. Annual Reviews 4139 El Camino Way, PO Box 10139, Palo Alto, CA 94303-0139, USA, 55(1), pp. 539–567.

Hearn, B. R., Shaw, S. J. and Myles, D. C. (2007) '7.04 - Microtubule Targeting Agents', in Taylor, J. B. and Triggle, D. J. B. T.-C. M. C. I. I. (eds). Oxford: Elsevier, pp. 81–110. doi: https://doi.org/10.1016/B0-08-045044-X/00205-4.

Heldin, P. et al. (1996) 'Differential synthesis and binding of hyaluronan by human breast cancer cell lines', *Oncology reports*. Spandidos Publications, 3(6), pp. 1011–1016.

Hirschberg, C. B., Robbins, P. W. and Abeijon, C. (1998) 'Transporters of nucleotide sugars, ATP, and nucleotide sulfate in the endoplasmic reticulum and Golgi apparatus'. Annual Reviews 4139 El Camino Way, PO Box 10139, Palo Alto, CA 94303-0139, USA.

Hoffbrand, V. and Moss, P. A. H. (2015) *Hoffbrand's essential haematology*. John Wiley & Sons.

Höök, M. et al. (1984) 'Cell-surface glycosaminoglycans', *Annual review of biochemistry*. Annual Reviews 4139 El Camino Way, PO Box 10139, Palo Alto, CA 94303-0139, USA, 53(1), pp. 847–869.

Howell, W. H. and Holt, E. (1918) 'Two new factors in blood coagulation—heparin and pro-antithrombin', *American Journal of Physiology--Legacy Content*. Am Physiological Soc, 47(3), pp. 328–341.

Huang, W. et al. (2003) 'Crystal structure of Proteus vulgaris chondroitin sulfate ABC lyase I at 1.9 Å resolution', *Journal of molecular biology*. Elsevier, 328(3), pp. 623–634.

Hurwitz, H. et al. (2004) 'Bevacizumab plus irinotecan, fluorouracil, and leucovorin for metastatic colorectal cancer', *New England journal of medicine*. Mass Medical Soc, 350(23), pp. 2335–2342.

Iozzo, R. V (2005) 'Basement membrane proteoglycans: from cellar to ceiling', *Nature reviews Molecular cell biology*. Nature Publishing Group, 6(8), p. 646.

Iozzo, R. V and Schaefer, L. (2015) 'Proteoglycan form and function: a comprehensive nomenclature of proteoglycans', *Matrix Biology*. Elsevier, 42, pp. 11–55.

Iwata, H. (1969) 'Determination and microstructure of chondroitin sulfate isomers of human cartilage and the pathological cartilage and tissue', *Nihon Seikeigeka Gakkai zasshi*, 43(6), pp. 455–473.

JOHN, C. W. Y. and GIOVANNI, A. (2002) 'Functions of hyaluronan in wound repair', *Wound Repair and Regeneration*. Wiley/Blackwell (10.1111), 7(2), pp. 79–89. doi: 10.1046/j.1524-475X.1999.00079.x.

Johnstone, K. D. et al. (2010) 'Synthesis and biological evaluation of polysulfated oligosaccharide glycosides as inhibitors of angiogenesis and tumor growth', *Journal of medicinal chemistry*. ACS Publications, 53(4), pp. 1686–1699.

KAlATHAS, Di. et al. (2011) 'Chondroitin synthases I, II, III and chondroitin sulfate glucuronyltransferase expression in colorectal cancer', *Molecular medicine reports*.

Spandidos Publications, 4(2), pp. 363–368.

KAWAI, Y., SENO, N. and ANNO, K. (1966) 'Chondroitin polysulfate of squid cartilage', *The Journal of Biochemistry*. The Japanese Biochemical Society, 60(3), pp. 317–321.

Kim, Y. S. et al. (1996) 'A new glycosaminoglycan from the giant African snail Achatina fulica', *Journal of Biological Chemistry*. ASBMB, 271(20), pp. 11750–11755.

Kinoshita-Toyoda, A. et al. (2004) 'Structural determination of five novel tetrasaccharides containing 3-O-sulfated D-glucuronic acid and two rare oligosaccharides containing a β-D-glucose branch isolated from squid cartilage chondroitin sulfate E', *Biochemistry*. ACS Publications, 43(34), pp. 11063–11074.

Kinoshita, A. et al. (1997) 'Novel tetrasaccharides isolated from squid cartilage chondroitin sulfate E contain unusual sulfated disaccharide units GlcA (3-O-sulfate) β1–3GalNAc (6-O-sulfate) or GlcA (3-O-sulfate) β1–3GalNAc (4, 6-O-disulfate)', *Journal of Biological Chemistry*. ASBMB, 272(32), pp. 19656–19665.

Kinsella, M. G. and Wight, T. N. (1986) 'Modulation of sulfated proteoglycan synthesis by bovine aortic endothelial cells during migration.', *The Journal of cell biology*. Rockefeller University Press, 102(3), pp. 679–687.

Kitagawa, H. et al. (1997) 'A Novel Pentasaccharide Sequence GlcA (3-sulfate)(β1-3) GalNAc (4-sulfate)(β1-4)(Fucα1-3) GlcA (β1-3) GalNAc (4-sulfate) in the Oligosaccharides Isolated from King Crab Cartilage Chondroitin Sulfate K and Its Differential Susceptibility to Chondroitinases', *Biochemistry*. ACS Publications, 36(13), pp. 3998–4008.

Klebe, S. et al. (2010) 'Sarcomatoid mesothelioma: a clinical–pathologic correlation of 326 cases', *Modern Pathology*. Nature Publishing Group, 23(3), p. 470.

Koliopanos, A. et al. (2001) 'Heparanase expression in primary and metastatic pancreatic cancer', *Cancer Research*. AACR, 61(12), pp. 4655–4659.

Kolset, S. O. and Tveit, H. (2008) 'Serglycin – Structure and biology', *Cellular and Molecular Life Sciences*, 65(7), pp. 1073–1085. doi: 10.1007/s00018-007-7455-6.

Köwitsch, A., Zhou, G. and Groth, T. (2018) 'Medical application of glycosaminoglycans: a review', *Journal of tissue engineering and regenerative medicine*. Wiley Online Library, 12(1), pp. e23–e41.

Kozlowski, E. O., Pavao, M. S. G. and Borsig, L. (2011) 'Ascidian dermatan sulfates attenuate metastasis, inflammation and thrombosis by inhibition of P-selectin', *Journal of Thrombosis and Haemostasis*. Wiley Online Library, 9(9), pp. 1807–1815.

Kratz, G. et al. (1997) 'Heparin-chitosan complexes stimulate wound healing in human skin', *Scandinavian journal of plastic and reconstructive surgery and hand surgery*. Taylor & Francis, 31(2), pp. 119–123.

Krusius, T. et al. (1986) 'Identification of an O-glycosidic mannose-linked sialylated tetrasaccharide and keratan sulfate oligosaccharides in the chondroitin sulfate proteoglycan of brain.', *Journal of Biological Chemistry*. ASBMB, 261(18), pp. 8237–8242.

Kumar, V., Abbas, A. K. and Aster, J. C. (2017) *Robbins basic pathology e-book*. Elsevier Health Sciences.

Laabs, T. et al. (2005) 'Chondroitin sulfate proteoglycans in neural development and regeneration', *Current Opinion in Neurobiology*, 15(1), pp. 116–120. doi: https://doi.org/10.1016/j.conb.2005.01.014.

Lamanna, W. C. (2008) *Functional characterization of the novel heparan sulfate 6O-endosulfatases Sulf1 and Sulf2*. Cuvillier Verlag.

Lamari, F. N. and Karamanos, N. K. B. T.-A. in P. (2006) 'Structure of Chondroitin Sulfate', in *Chondroitin Sulfate: Structure, Role and Pharmacological Activity*. Academic Press, pp. 33–48. doi: https://doi.org/10.1016/S1054-3589(05)53003-5.

Laurent, T. C., Laurent, U. B. and Fraser, J. R. (1995) 'Functions of hyaluronan.', *Annals of the rheumatic diseases*. BMJ Publishing Group, 54(5), p. 429.

Lawrence, R. et al. (2008) 'Evolutionary differences in glycosaminoglycan fine structure detected by quantitative glycan reductive isotope labeling', *Journal of Biological Chemistry*, 283(48), pp. 33674–33684. doi: 10.1074/jbc.M804288200.

Lee, Y. et al. (2018) 'Testican-1, as a novel diagnosis of sepsis', *Journal of cellular biochemistry*. Wiley Online Library, 119(5), pp. 4216–4223.

Lee, Y. S. et al. (2003) 'Suppression of tumor growth by a new glycosaminoglycan isolated from the African giant snail Achatina fulica', *European Journal of Pharmacology*, 465(1), pp. 191–198. doi: https://doi.org/10.1016/S0014-2999(03)01458-4.

Li, D.-W. et al. (2004) 'Long duration of anticoagulant activity and protective effects of acharan sulfate in vivo', *Thrombosis Research*, 113(1), pp. 67–73. doi: https://doi.org/10.1016/j.thromres.2004.02.003.

Li, J. (2010) 'Glucuronyl C5-Epimerase: An Enzyme Converting Glucuronic Acid to Iduronic Acid in Heparan Sulfate/Heparin Biosynthesis', in Zhang, L. B. T.-P. in M. B. and T. S. (ed.) *Glycosaminoglycans in Development, Health and Disease*. Academic Press, pp. 59–78. doi: https://doi.org/10.1016/S1877-1173(10)93004-4.

Liao, N. et al. (2013) 'Antioxidant and anti-tumor activity of a polysaccharide from freshwater clam, Corbicula fluminea', *Food & function*. Royal Society of Chemistry, 4(4), pp. 539–548.

Lin, X. (2004) 'Functions of heparan sulfate proteoglycans in cell signaling during development', *Development*. The Company of Biologists Ltd, 131(24), pp. 6009–6021.

Linhardt, R. J. et al. (1990) 'Examination of the substrate specificity of heparin and heparan sulfate lyases', *Biochemistry*. ACS Publications, 29(10), pp. 2611–2617. doi: 10.1021/bi00462a026.

Linhardt, R. J. et al. (2006) 'CS Lyases: Structure, Activity, and Applications in Analysis and the Treatment of Diseases', in *Chondroitin Sulfate: Structure, Role and Pharmacological Activity*. Academic Press, pp. 187–215. doi: https://doi.org/10.1016/S1054-3589(05)53009-6.

Liu, C. et al. (2008) 'Structural characterisation and antimutagenic activity of a novel polysaccharide isolated from Sepiella maindroni ink', *Food Chemistry*. Elsevier, 110(4), pp. 807–813.

Liu, J. and Jiang, G. (2006) 'CD44 and hematologic malignancies.', *Cellular & molecular immunology*, 3(5), pp. 359–365. Available at: https://www.scopus.com/inward/record.uri?eid=2-s2.0-34848816366&partnerID=40&md5=20f11cfb9575a1ace6a7280e4f4182bb.

M Cragg, G., J Newman, D. and M Snader, K. (1997) 'Natural products in drug discovery and development.', *Journal of Natural Products*, 60(1), pp. 52–60. Available at: http://www.mendeley.com/research/natural-products-in-drug-discovery-and-development-1/.

Magee, C., Nurminskaya, M. and Linsenmayer, T. F. (2001) 'UDP-glucose pyrophosphorylase: up-regulation in hypertrophic cartilage and role in hyaluronan synthesis', *Biochemical Journal*, 360(3), pp. 667 LP – 674. Available at: http://www.biochemj.org/content/360/3/667.abstract.

Mcpherson, J. M. et al. (1988) 'The Influence of Heparin on the Wound Healing Response to Collagen Implants in vivo', *Collagen and Related Research*, 8(1), pp. 83–100. doi: https://doi.org/10.1016/S0174-173X(88)80037-2.

Meininger, M. et al. (2016) 'Sialic acid-specific affinity chromatography for the separation of erythropoietin glycoforms using serotonin as a ligand', *Journal of Chromatography B*, 1012–1013, pp. 193–203. doi: https://doi.org/10.1016/j.jchromb.2016.01.005.

Meyer, K. et al. (1953) 'The mucopolysaccharides of bovine cornea', *J Biol Chem*, 205(2), pp. 611–616.

Meyer, K. and Palmer, J. W. (1934) 'The polysaccharide of the vitreous humor', *Journal of Biological Chemistry*. ASBMB, 107(3), pp. 629–634.

Mikami, T. and Kitagawa, H. (2013) 'Biosynthesis and function of chondroitin sulfate', *Biochimica et Biophysica Acta (BBA) - General Subjects*, 1830(10), pp. 4719–4733. doi: https://doi.org/10.1016/j.bbagen.2013.06.006.

Mizumoto, S., Yamada, S. and Sugahara, K. (2015) 'Molecular interactions between chondroitin–dermatan sulfate and growth factors/receptors/matrix proteins', *Current opinion in structural biology*. Elsevier, 34, pp. 35–42.

Moore, G., Knight, G. and Blann, A. (2016) *Haematology*. Oxford University Press.

Mourão, P. A. S. et al. (1998) 'Antithrombotic activity of a fucosylated chondroitin sulphate from echinoderm: sulphated fucose branches on the polysaccharide account for its antithrombotic action', *British journal of haematology*. Wiley Online Library, 101(4), pp. 647–652.

Movasaghi, Z., Rehman, S. and ur Rehman, D. I. (2008) 'Fourier transform infrared (FTIR) spectroscopy of biological tissues', *Applied Spectroscopy Reviews*. Taylor & Francis, 43(2), pp. 134–179.

Mulloy, B., Hart, G. W. and Stanley, P. (2009) 'Structural analysis of glycans'. Cold Spring Harbor Laboratory Press.

Myron, P., Siddiquee, S. and Al Azad, S. (2014) 'Fucosylated chondroitin sulfate diversity in sea cucumbers: A review', *Carbohydrate Polymers*, 112, pp. 173–178. doi: https://doi.org/10.1016/j.carbpol.2014.05.091.

Mythreye, K. and Blobe, G. C. (2009) 'Proteoglycan signaling co-receptors: roles in cell adhesion, migration and invasion', *Cellular signalling*. Elsevier, 21(11), pp. 1548–1558.

Nadanaka, S. et al. (1998) 'Characteristic hexasaccharide sequences in octasaccharides derived from shark cartilage chondroitin sulfate D with a neurite outgrowth promoting activity', *Journal of Biological Chemistry*. ASBMB, 273(6), pp. 3296–3307.

Nelson, D. L., Lehninger, A. L. and Cox, M. M. (2008) *Lehninger principles of biochemistry*. Macmillan.

Ning, C. et al. (2018) 'Marine-derived protein kinase inhibitors for neuroinflammatory diseases', *Biomedical engineering online*. BioMed Central, 17(1), p. 46.

Nobili, S. et al. (2009) ‘Natural compounds for cancer treatment and prevention’, *Pharmacological Research*, 59(6), pp. 365–378. doi: 10.1016/j.phrs.2009.01.017.

Norris, R. E. and Adamson, P. C. (2012) ‘Challenges and opportunities in childhood cancer drug development’, *Nature Reviews Cancer*. Nature Publishing Group, 12(11), pp. 776–782. doi: 10.1038/nrc3370.

Onishi, A. et al. (2016) ‘Heparin and anticoagulation’, *Front Biosci (Landmark Ed)*, 21, pp. 1372–1392.

Ornitz, D. M. (2000) ‘FGFs, heparan sulfate and FGFRs: complex interactions essential for development’, *Bioessays*, 22(2), pp. 108–112.

Osgood, C. L. et al. (2017) ‘FDA approval summary: eribulin for patients with unresectable or metastatic liposarcoma who have received a prior anthracycline-containing regimen’, *Clinical Cancer Research*. AACR, p. clincanres-2422.

Parekh, R. B. et al. (1987) ‘Tissue-specific N-glycosylation, site-specific oligosaccharide patterns and lentil lectin recognition of rat Thy-1.’, *The EMBO journal*, 6(5), pp. 1233–1244.

Park, M.-T. and Lee, S.-J. (2003) ‘Cell cycle and cancer’, *Journal of biochemistry and molecular biology*, 36(1), pp. 60–65.

Pastrana, L. and Jauregi, P. (2017) ‘Basic Biochemistry’, in *Current Developments in Biotechnology and Bioengineering*. Elsevier, pp. 33–58.

Pavão, M. S. G. (2002) ‘Structure and anticoagulant properties of sulfated glycosaminoglycans from primitive Chordates’, *Anais da Academia Brasileira de Ciências*. SciELO Brasil, 74(1), pp. 105–112.

Pavasant, P., Shizari, T. M. and Underhill, C. B. (1994) ‘Distribution of hyaluronan in the epiphysial growth plate: turnover by CD44-expressing osteoprogenitor cells’, *Journal of cell science*. The Company of Biologists Ltd, 107(10), pp. 2669–2677.

Pocock, G. et al. (2013) *Human physiology*. Oxford university press.

Pomin, V. H. (2015) ‘NMR structural determination of unique invertebrate glycosaminoglycans endowed with medical properties’, *Carbohydrate research*. Elsevier, 413, pp. 41–50.

Prabhakar, V. and Sasisekharan, R. B. T.-A. in P. (2006) ‘The Biosynthesis and Catabolism of Galactosaminoglycans’, in *Chondroitin Sulfate: Structure, Role and Pharmacological Activity*. Academic Press, pp. 69–115. doi: https://doi.org/10.1016/S1054-3589(05)53005-9.

Prieto-Vila, M. et al. (2017) ‘Drug resistance driven by cancer stem cells and their niche’, *International journal of molecular sciences*. Multidisciplinary Digital Publishing Institute, 18(12), p. 2574.

Prydz, K. and Dalen, K. T. (2000) ‘Synthesis and sorting of proteoglycans’, *J Cell Sci*. The Company of Biologists Ltd, 113(2), pp. 193–205.

Qiu, P. P., Dai, Y. Y. and Li, H. L. (2009) ‘Inhibition effect of Corbicula fluminea extract on human hepatocarcinoma SMMC–7721 cell’, *Journal of Xiamen University (Natural Science)*, 48, pp. 406–409.

Rabenstein, D. L. (2002) ‘Heparin and heparan sulfate: structure and function’, *Natural product reports*. Royal Society of Chemistry, 19(3), pp. 312–331.

Raimondi, S. C. et al. (1988) ‘Cytogenetics of childhood T-cell leukemia’, *Blood*. Am Soc Hematology, 72(5), pp. 1560–1566.

Rivera, G. K. et al. (1991) ‘Improved outcome in childhood acute lymphoblastic leukaemia with reinforced early treatment and rotational combination chemotherapy’, *The Lancet*. Elsevier, 337(8733), pp. 61–66.

Rocha, V. et al. (2001) ‘Comparison of outcomes of unrelated bone marrow and umbilical cord blood transplants in children with acute leukemia’, *Blood*. Am Soc Hematology, 97(10), pp. 2962–2971.

Rosenberg, R. D. and Lam, L. (1979) ‘Correlation between structure and function of heparin’, *Proceedings of the National Academy of Sciences*. National Acad Sciences, 76(3), pp. 1218–1222.

Ross, J. A. et al. (2011) ‘Epidemiology of acute childhood leukemia’, in *Childhood leukemia*. Springer, pp. 3–26.

Rovio, S., Yli-Kauhaluoma, J. and Sirén, H. (2007) ‘Determination of neutral carbohydrates by CZE with direct UV detection’, *Electrophoresis*. Wiley Online Library, 28(17), pp. 3129–3135.

Rusnati, M. and Urbinati, C. (2009) ‘Polysulfated/sulfonated compounds for the development of drugs at the crossroad of viral infection and oncogenesis’, *Current pharmaceutical design*. Bentham Science Publishers, 15(25), pp. 2946–2957.

Saad, O. M. et al. (2005) ‘Compositional profiling of heparin/heparan sulfate using mass spectrometry: Assay for specificity of a novel extracellular human endosulfatase’, *Glycobiology*, 15(8), pp. 818–826. doi: 10.1093/glycob/cwi064.

Sage, E. H. and Bornstein, P. (1991) ‘Extracellular proteins that modulate cell-matrix interactions. SPARC, tenascin, and thrombospondin’, *J Biol Chem*. ASBMB, 266(23), pp. 14831–14834.

Salyers, A. A. and O’Brien, M. (1980) ‘Cellular location of enzymes involved in chondroitin sulfate breakdown by Bacteroides thetaiotaomicron.’, *Journal of bacteriology*. Am Soc Microbiol, 143(2), pp. 772–780.

Sandler, A. et al. (2006) ‘Paclitaxel–carboplatin alone or with bevacizumab for non–small-cell lung cancer’, *New England Journal of Medicine*. Mass Medical Soc, 355(24), pp. 2542–2550.

Sarrazin, S., Lamanna, W. C. and Esko, J. D. (2011) ‘Heparan sulfate proteoglycans’, *Cold Spring Harbor perspectives in biology*. Cold Spring Harbor Lab, 3(7), p. a004952.

Sasisekharan, R. et al. (2002) ‘Roles of heparan-sulphate glycosaminoglycans in cancer’, *Nature Reviews Cancer*. Nature Publishing Group, 2(7), p. 521.

Sasisekharan, R. and Venkataraman, G. (2000) ‘Heparin and heparan sulfate: biosynthesis, structure and function’, *Current opinion in chemical biology*. Elsevier, 4(6), pp. 626–631.

Schleicher, E. D. and Weigert, C. (2000) ‘Role of the hexosamine biosynthetic pathway in diabetic nephropathy’, *Kidney international*. Elsevier, 58, pp. S13–S18.

Schuster, M., Nechansky, A. and Kircheis, R. (2006) ‘Cancer immunotherapy’, *Biotechnology Journal: Healthcare Nutrition Technology*. Wiley Online Library, 1(2), pp. 138–147.

Shannon, J. M. et al. (2003) ‘Chondroitin sulfate proteoglycans are required for lung growth and morphogenesis in vitro’, *American Journal of Physiology-Lung Cellular and Molecular Physiology*. American Physiological Society, 285(6), pp. L1323–L1336.

Sherman, L. et al. (1994) ‘Hyaluronate receptors: key players in growth, differentiation, migration and tumor progression’, *Current opinion in cell biology*. Elsevier, 6(5), pp. 726–733.

Shriver, Z. et al. (2012) ‘Heparin and heparan sulfate: analyzing structure and microheterogeneity’, in *Heparin-A Century of Progress*. Springer, pp. 159–176.

Silbert, J. E. (1966) ‘CHAPTER 6 - Metabolism of Polysaccharides Containing Glucuronic Acid A2 - DUTTON, GEOFFREY J. BT - Glucuronic Acid Free and Combined’, in. Academic Press, pp. 385–453. doi: https://doi.org/10.1016/B978-0-12-395501-2.50012-8.

Silva, L. F. B. T.-A. in P. (2006) ‘Isolation and Purification of Chondroitin Sulfate’, in *Chondroitin Sulfate: Structure, Role and Pharmacological Activity*. Academic Press, pp. 21–31. doi: https://doi.org/10.1016/S1054-3589(05)53002-3.

Spooncer, E. et al. (1983) ‘Regulation of haemopoiesis in long-term bone marrow cultures. IV. Glycosaminoglycan synthesis and the stimulation of haemopoiesis by beta-D-xylosides.’, *The Journal of cell biology*. Rockefeller University Press, 96(2), pp. 510–514.

Stanley, M. J. et al. (1999) ‘Syndecan-1 expression is induced in the stroma of infiltrating breast carcinoma’, *American journal of clinical pathology*. Oxford University Press Oxford, UK, 112(3), pp. 377–383.

Stanley, P., Schachter, H. and Taniguchi, N. (2009) ‘N-Glycans’, in Varki, A. et al. (eds). Cold Spring Harbor (NY), Cold Spring Harbor (NY).

Steen, P. Van den et al. (1998) ‘Concepts and principles of O-linked glycosylation’, *Critical reviews in biochemistry and molecular biology*. Taylor & Francis, 33(3), pp. 151–208.

Stringer, S. E. (2006) ‘The role of heparan sulphate proteoglycans in angiogenesis’. Portland Press Limited.

Sugahara, K. et al. (1996) ‘Novel sulfated oligosaccharides containing 3-o-sulfated glucuronic acid from king crab cartilage chondroitin sulfate K unexpected degradation by chondroitinase ABC’, *Journal of Biological Chemistry*. ASBMB, 271(43), pp. 26745–26754.

Sugahara, K. et al. (2003) ‘Recent advances in the structural biology of chondroitin sulfate and dermatan sulfate’, *Current opinion in structural biology*. Elsevier, 13(5), pp. 612–620.

Sugahara, K. and Kitagawa, H. (2002) ‘Heparin and heparan sulfate biosynthesis’, *IUBMB life*. Wiley Online Library, 54(4), pp. 163–175.

Suzuki, M. (1939) ‘Biochemical studies on carbohydrates’, *The Journal of biochemistry*. The Japanese Biochemical Society, 30(2), pp. 185–191.

Thiele, H. et al. (2004) ‘Loss of chondroitin 6-O-sulfotransferase-1 function results in severe human chondrodysplasia with progressive spinal involvement’, *Proceedings of the National Academy of Sciences*. National Acad Sciences, 101(27), pp. 10155–10160.

Toole, B. P. (1997) ‘Hyaluronan in morphogenesis’, *Journal of internal medicine*. Wiley Online Library, 242(1), pp. 35–40.

Trowbridge, J. M. and Gallo, R. L. (2002) ‘Dermatan sulfate: new functions from an old glycosaminoglycan’, *Glycobiology*. Oxford University Press, 12(9), pp. 117R-125R.

Ustyuzhanina, N. E. et al. (2015) ‘Structure and biological activity of a fucosylated chondroitin sulfate from the sea cucumber Cucumaria japonica’, *Glycobiology*. Oxford University Press, 26(5), pp. 449–459.

Varki, A. and Gagneux, P. (2017) ‘Biological functions of glycans’. Cold Spring Harbor Laboratory Press.

Varki, A. and Sharon, N. (2009) ‘Historical background and overview’, in *Essentials of Glycobiology. 2nd edition*. Cold Spring Harbor Laboratory Press.

Velnar, T., Bailey, T. and Smrkolj, V. (2009) ‘The wound healing process: an overview of the cellular and molecular mechanisms’, *Journal of International Medical Research*. Sage Publications Sage UK: London, England, 37(5), pp. 1528–1542.

Vieira, R. P. and Mourão, P. A. (1988) ‘Occurrence of a unique fucose-branched chondroitin sulfate in the body wall of a sea cucumber.’, *Journal of Biological Chemistry*. ASBMB, 263(34), pp. 18176–18183.

Vieira, R. P., Mulloy, B. and Mourão, P. A. (1991) ‘Structure of a fucose-branched chondroitin sulfate from sea cucumber. Evidence for the presence of 3-O-sulfo-beta-D-glucuronosyl residues.’, *Journal of Biological Chemistry*. ASBMB, 266(21), pp. 13530–13536.

Vieira, T. C. R. G. et al. (2004) ‘Acharan sulfate, the new glycosaminoglycan from Achatina fulica Bowdich 1822’, *The FEBS Journal*. Wiley Online Library, 271(4), pp. 845–854.

Vigetti, D. et al. (2014) ‘Hyaluronan: biosynthesis and signaling’, *Biochimica et Biophysica Acta (BBA)-General Subjects*. Elsevier, 1840(8), pp. 2452–2459.

Vitanza, N. A. et al. (2014) ‘Ikaros deletions in BCR–ABL-negative childhood acute lymphoblastic leukemia are associated with a distinct gene expression signature but do not result in intrinsic chemoresistance’, *Pediatric blood & cancer*. Wiley Online Library, 61(10), pp. 1779–1785.

Vlodavsky, I. and Friedmann, Y. (2001) ‘Molecular properties and involvement of heparanase in cancer metastasis and angiogenesis’, *The Journal of clinical investigation*. Am Soc Clin Investig, 108(3), pp. 341–347.

Volpi, N. et al. (2014) ‘Analysis of glycosaminoglycan-derived, precolumn, 2-aminoacridone–labeled disaccharides with LC-fluorescence and LC-MS detection’, *Nature protocols*. Nature Publishing Group, 9(3), p. 541.

Wang, L. C. et al. (2017) ‘Elaboration in type, primary structure, and bioactivity of polysaccharides derived from mollusks’, *Critical reviews in food science and nutrition*. Taylor & Francis, pp. 1–24.

Wight, T. N., Heinegård, D. K. and Hascall, V. C. (1991) ‘Proteoglycans’, in *Cell biology of extracellular matrix*. Springer, pp. 45–78.

Wight, T. N., Kinsella, M. G. and Qwarnström, E. E. (1992) ‘The role of proteoglycans in cell adhesion, migration and proliferation’, *Current opinion in cell biology*. Elsevier, 4(5), pp. 793–801.

Witsch, E., Sela, M. and Yarden, Y. (2010) ‘Roles for growth factors in cancer progression’, *Physiology*. Am Physiological Soc, 25(2), pp. 85–101.

Wlawick, R., Roberts, W. and Dekker, C. (1959) 'Cyclization during phosphorylation of uridine and cytidine', *Proc. Chem. Soc.*, (84).

Wu, H. F., Monroe, D. M. and Church, F. C. (1995) 'Characterization of the glycosaminoglycan-binding region of lactoferrin', *Archives of biochemistry and biophysics*. Elsevier, 317(1), pp. 85–92.

Wu, M. et al. (2015) 'Anticoagulant and antithrombotic evaluation of native fucosylated chondroitin sulfates and their derivatives as selective inhibitors of intrinsic factor Xase', *European Journal of Medicinal Chemistry*, 92, pp. 257–269. doi: https://doi.org/10.1016/j.ejmech.2014.12.054.

Yanagishita, M. (1993) 'Function of proteoglycans in the extracellular matrix', *Pathology International*. Wiley Online Library, 43(6), pp. 283–293.

Yayon, A. et al. (1991) 'Cell surface, heparin-like molecules are required for binding of basic fibroblast growth factor to its high affinity receptor', *Cell*. Elsevier, 64(4), pp. 841–848.

Ye, S. et al. (2001) 'Structural Basis for Interaction of FGF-1, FGF-2, and FGF-7 with Different Heparan Sulfate Motifs', *Biochemistry*. American Chemical Society, 40(48), pp. 14429–14439. doi: 10.1021/bi011000u.

Yu, C.-J. et al. (2010) 'Effect of Fraxiparine, a type of low molecular weight heparin, on the invasion and metastasis of lung adenocarcinoma A549 cells', *Oncology letters*. Spandidos Publications, 1(4), pp. 755–760.

Zhang, D. et al. (2013) 'Three sulphated polysaccharides isolated from the mucilage of mud snail, Bullacta exarata philippi: Characterization and antitumour activity', *Food chemistry*. Elsevier, 138(1), pp. 306–314.

Zhang, L. et al. (2008) 'Isolation and characterization of antitumor polysaccharides from the marine mollusk Ruditapes philippinarum', *European Food Research and Technology*. Springer, 227(1), p. 103.

Zhang, L. (2010) *Glycosaminoglycans in development, health and disease*. Academic Press.

Zhang, Y. et al. (2010) 'Focus on Molecules: Heparanase', *Experimental Eye Research*, 91(4), pp. 476–477. doi: https://doi.org/10.1016/j.exer.2010.05.004.

Zöller, M. (2011) 'CD44: can a cancer-initiating cell profit from an abundantly expressed molecule?', *Nature Reviews Cancer*. Nature Publishing Group, a division of Macmillan Publishers Limited. All Rights Reserved., 11, p. 254. Available at: http://dx.doi.org/10.1038/nrc3023.